UNIVERSITÀ DEGLI STUDI DI PADOVA

Centro Interdipartimentale di Studi e Attività Spaziali (CISAS)
"G.Colombo"

DOTTORATO DI RICERCA IN: SCIENZE TECNOLOGIE E MISURE SPAZIALI
INDIRIZZO: ASTRONAUTICA E SCIENZE DA SATELLITE
CICLO XX

NUMERICAL ALGORITHMS FOR THE SEARCHING OF EXTRASOLAR PLANETS FROM PHOTOMETRIC DATA

ALGORITMI NUMERICI PER LA RICERCA DEI PIANETI EXTRASOLARI DA DATI FOTOMETRICI

Direttore della Scuola: Ch.mo Prof. Pier Luigi Bernacca
Supervisore: Dott. Francesco Marzari
Co-supervisore: Dott. Riccardo Claudi

Dottoranda: Valentina Granata

31 Gennaio 2008

A Me e Nicola

Ai miei Genitori

«E lucean le stelle ... » (*Tosca, G.Puccini – III.2*)

Contents

List of Figures XII

List of Tables XIV

List of Acronyms XV

Abstract XVII

Riassunto XXI

Introduction XXXI

I Photometric Reduction and analysis software 1

1 The physical context 3

1.1 The Exoplanets . . . 3
1.1.1 Working definitions . . . 3
1.1.2 Exoplanets around pulsars . . . 4
1.1.3 The Radial Velocity Searches . . . 5
1.1.4 Characteristics of the known exoplanets, derived from the RV surveys . . . 7
1.1.5 Microlensing . . . 8
1.1.6 Direct imaging . . . 9
1.1.7 Astrometry . . . 10
1.2 The transit method . . . 12
1.2.1 The measurable parameters . . . 14
1.2.2 The false positives . . . 15
1.2.3 White and red noise . . . 17
1.2.4 Analysis of the lightcurves . . . 19
1.2.4.1 Inspection of the lightcurves parts without transits . . . 19
1.2.4.2 Inspection of the lightcurves transits part . . . 20
1.3 HD 209458b . . . 21
1.4 On the radii of the transiting planets . . . 23
1.5 Formation models of giant planets . . . 25
1.6 Motivation for the following study . . . 26

2 The RATS project **29**
2.1 The RATS project 29
2.2 The RATS instruments 30
2.2.1 The Schmidt telescope and the CCD cameras 30
2.2.1.1 The telescope 30
2.2.1.2 The CCD cameras 31
2.2.1.3 The ITANET camera 32
2.2.1.4 The SITe camera 32
2.2.1.5 The Eddington camera 33
2.2.1.6 The CCD controllers 34
2.2.2 The Copernico telescope and Echelle spectrograph 35
2.2.2.1 The telescope 35
2.2.2.2 The Echelle spectrograph 37
2.2.2.3 The optical fiber feeding project 38
2.3 RATS stellar fields selection 40
2.4 Magnitude interval selection 43
2.5 RATS observing strategy 44
2.6 RATS hardware and software environment 45
2.6.1 Hardware dataflow 45
2.6.2 Software dataflow 48
2.7 RATS Users 49

3 RATS headerfits **51**
3.1 What is FITS? 51
3.2 The FITS's philosophy 52
3.3 The ASCII Tables 53
3.4 Basic FITS 54
3.4.1 Primary header 55
3.4.1.1 Required keywords 56
3.4.1.2 Reserved keywords 57
3.5 World Coordinate Systems (WCS) 59
3.5.1 Coordinate Keywords 60
3.6 RATS headerfits: an example 60

4 RATS–ARP: Automatic Reduction Pipeline for RATS **65**
4.1 Photometric reduction background and introduction to the software development . . 66
4.1.1 Shell script programming 66
4.1.1.1 Debugging 68
4.1.2 DAOPHOT 68
4.2 Data analysis 71
4.2.1 Images calibrations 71
4.2.2 Building a stars list 72
4.3 Analysis and pipeline requirements definition 73
4.3.1 The pipeline model 73
4.3.2 Software environment 76

4.3.3 System design and architecture 76
4.3.4 Functional requirements for the pipeline 79

5 The RATS–ARP implementation 81
5.1 Pre-reduction algorithm of astrophysical images 81
5.1.1 Bias 81
5.1.2 Dark current 83
5.1.3 Flat Fielding 83
5.1.4 Bad pixels and cosmic rays 86
5.1.4.1 Bad pixels 86
5.1.4.2 Cosmic rays 86
5.1.5 Implementation of the pre-reduction algorithm 87
5.2 Reduction algorithm of astrophysical images 88
5.2.1 Implementation of the reduction algorithm 88
5.2.2 DAOPHOT modified 89
5.3 Fortran, IRAF and shell script programs: the components description 89
5.3.1 [ADDC1]: calibration.csh 90
5.3.2 [ADDC2]: calibra.cl 90
5.3.3 [ADDC3]: 91
5.3.4 [ADDC4]: 91
5.3.5 [ADDC5]: centring.f 92
5.3.6 [ADDC6]: matchframe.csh 92
5.3.7 [ADDC7]: daomatch.f 93
5.3.8 [ADDC8]: masterframe.csh 93
5.3.9 [ADDC9]: daomaster.f 94
5.3.10 [ADDC10]: transformer_coo.f 94
5.3.11 [ADDC9]: lightcurve_creation 95

6 Software testing and results 97
6.1 Focused images 97
6.1.1 The introductive data 97
6.1.2 The master images for calibration 97
6.1.2.1 Masterbias 98
6.1.2.2 Masterflat 99
6.1.3 The lightcurves 99
6.2 Defocused images 101
6.2.1 The introductive data 101
6.2.2 The master images for calibration 101
6.2.2.1 Masterbias 103
6.2.2.2 Masterflat 103
6.2.3 The lightcurves 103

7 The RATS database: analysis 107
7.1 The database key concepts . . . 107
7.1.1 Database models . . . 108
7.1.1.1 Hierarchical model . . . 108
7.1.1.2 Network model . . . 108
7.1.1.3 Relational model . . . 109
7.1.2 Storage and physical database design . . . 110
7.2 Database management system (DBMS) . . . 111
7.2.1 DBMS description . . . 111
7.2.2 Features and abilities of DBMS . . . 112
7.3 RATS–DB . . . 114
7.3.1 Technical specifications . . . 115
7.3.2 RATS–DB language: `Oracle` . . . 117
7.3.2.1 Physical and logical structuring . . . 117
7.3.2.2 Memory and process architecture . . . 117
7.3.3 Analysis of the storage of RATS data . . . 118
7.3.3.1 Storage performance requirements . . . 118
7.3.4 Analysis of the management of RATS data: access and tools . . . 121
7.3.5 Analysis of the testing of RATS–DB . . . 122
7.3.5.1 Acceptance test procedures . . . 123
7.3.6 DB filling . . . 123
7.3.7 RATS–DB User interface . . . 124
7.3.7.1 Action buttons . . . 124
7.3.7.2 Query fields . . . 125
7.3.7.3 Additional (non query-able) parameters . . . 126
7.3.7.4 Output control . . . 126

II Dynamical simulations 129

8 Planets in binaries: transitional members of multiple star systems 131
8.1 Introduction . . . 131
8.2 Binary stars . . . 132
8.3 Planets in binaries . . . 132
8.3.1 Circumstellar and circumbinary disks . . . 134
8.3.2 Planet formation in binaries . . . 134
8.3.3 Binary planet stability . . . 136
8.4 The "jumping stars model": the co-planar case . . . 136
8.4.1 The numerical algorithm for the co-planar case . . . 137
8.4.2 The onset of instability in the co-planar case . . . 137
8.4.3 Statistical outcome for the co-planar case . . . 140
8.5 The "jumping stars model": the inclined case . . . 142
8.5.1 The numerical algorithm for the inclined case . . . 143
8.5.2 The onset of instability in the inclined case . . . 144
8.5.3 Statistical outcome for the inclined case . . . 146

III Conclusions **151**

9 Conclusions and future works **153**
9.1 Conclusions . . . 153
9.1.1 Part I: Photometric reduction and analysis software . . . 153
9.1.2 Part II: Dynamical simulations . . . 154
9.1.2.1 The co-planar case . . . 154
9.1.2.2 The inclined case . . . 155
9.2 Future works . . . 155

IV Appendix: Software documentation **157**

A RATS journal of observations **159**
A.1 Journal of observations (February 2005) . . . 159
A.2 Journal of observations (April 2006) . . . 162

B RATS Automatic Reduction Pipeline: User Requirement Document (URD) **169**
B.1 Introduction . . . 169
B.1.1 Purpose of the document . . . 169
B.1.2 Scope of the software . . . 169
B.1.3 Definitions, acronyms and abbreviations . . . 170
B.1.4 References . . . 171
B.1.4.1 Referenced documents . . . 171
B.1.4.2 Applicable documents . . . 171
B.1.5 Overview of the document . . . 171
B.2 General description . . . 171
B.2.1 Product perspectives . . . 172
B.2.2 Relation to the current projects . . . 172
B.2.3 General capabilities . . . 172
B.2.4 General constraints . . . 172
B.2.5 User characteristic . . . 173
B.2.6 Relation with the environment . . . 173
B.3 Specific requirements . . . 173
B.3.1 Notation . . . 173
B.3.2 Capability requirements . . . 174
B.3.2.1 Observational strategy . . . 175
B.3.2.2 Data pre-processing parameters . . . 175
B.3.2.3 Data post-processing parameters . . . 176
B.3.2.4 User interface . . . 176
B.3.2.5 Performance . . . 177
B.3.2.6 Accuracy . . . 178
B.3.2.7 Constraints requirements . . . 178

C RATS Automatic Reduction Pipeline: Software Requirement Document (SRD) 181
C.1 Introduction . . . 181
C.1.1 Purpose of the document . . . 181
C.1.2 Scope of the software . . . 181
C.1.3 Definitions, acronyms and abbreviations . . . 182
C.1.4 References . . . 183
C.1.4.1 Referenced documents . . . 183
C.1.4.2 Applicable documents . . . 183
C.1.5 Overview of the document . . . 183
C.2 General description . . . 184
C.2.1 Relation to the current projects . . . 184
C.2.2 Relation to predecessor and successor projects . . . 184
C.2.3 Function and purpose . . . 184
C.2.4 User characteristic . . . 185
C.2.5 Relation with the environment . . . 185
C.2.6 General constraints . . . 185
C.2.7 Model description . . . 186
C.3 Specific requirements . . . 186
C.3.1 Notation . . . 186
C.3.2 Functional requirements: . . . 187
C.3.3 Performance requirements . . . 189
C.3.4 Interface requirements . . . 189
C.3.4.1 Software interface requirements . . . 189
C.3.4.2 Hardware interface requirements . . . 189
C.3.4.3 Communications interface requirements . . . 189
C.3.5 Operational requirements . . . 189
C.3.5.1 Operation mode . . . 189
C.3.5.2 Man/machine interface . . . 189
C.3.5.3 Operator skill profile . . . 189
C.4 Resource requirements . . . 190
C.4.0.4 Processing power . . . 190
C.4.0.5 RAM memory . . . 190
C.4.0.6 Disk space . . . 190
C.4.0.7 Disk access time . . . 190
C.4.0.8 Screen resolution . . . 190
C.4.1 Verification and validation requirements . . . 190
C.4.1.1 Unit Tests . . . 190
C.4.1.2 Integration Test . . . 190
C.4.2 Acceptance tests requirements . . . 191
C.4.3 Documentation requirements . . . 191
C.4.4 Security requirements . . . 191
C.4.5 Portability requirements . . . 191
C.4.6 Quality requirements . . . 191
C.4.7 Reliability requirements . . . 191
C.4.8 Maintainability requirements . . . 192

C.4.9 Safety requirement . . . 192
C.5 UR vs. SR TRACEABILITY MATRIX . . . 192

D RATS Automatic Reduction Pipeline: Architectural Design Document (ADD) 197
D.1 Introduction . . . 197
D.1.1 Purpose of the document . . . 197
D.1.2 Scope of the software . . . 197
D.1.3 Definitions, acronyms and abbreviations . . . 198
D.1.4 References . . . 199
D.1.4.1 Referenced documents . . . 199
D.1.4.2 Applicable documents . . . 199
D.1.5 Overview of the document . . . 199
D.2 System overview . . . 200
D.3 System context . . . 200
D.4 System design . . . 200
D.4.1 Design method . . . 200
D.4.2 System architecture . . . 200
D.4.2.1 H/W layer . . . 200
D.4.2.2 Off-line analysis layer . . . 201
D.4.2.3 Application layer . . . 201
D.4.2.4 User Interface layer . . . 202
D.4.2.5 Decomposition description . . . 202
D.5 Components description . . . 204
D.5.1 [ADDC1]: calibration.csh . . . 204
D.5.1.1 Type . . . 204
D.5.1.2 Purpose . . . 204
D.5.1.3 Function . . . 204
D.5.1.4 Subordinates . . . 204
D.5.1.5 Dependencies . . . 204
D.5.1.6 Interfaces . . . 204
D.5.1.7 Resources . . . 204
D.5.1.8 References . . . 204
D.5.1.9 Processing . . . 204
D.5.1.10 Data . . . 204
D.5.2 [ADDC2]: calibra.cl . . . 205
D.5.2.1 Type . . . 205
D.5.2.2 Purpose . . . 205
D.5.2.3 Function . . . 205
D.5.2.4 Subordinates . . . 205
D.5.2.5 Dependencies . . . 205
D.5.2.6 Interfaces . . . 205
D.5.2.7 Resources . . . 205
D.5.2.8 References . . . 205
D.5.2.9 Processing . . . 205
D.5.2.10 Data . . . 205

D.5.3 [ADDC3]: procedura.csh . . . 206
D.5.3.1 Type . . . 206
D.5.3.2 Purpose . . . 206
D.5.3.3 Function . . . 206
D.5.3.4 Subordinates . . . 206
D.5.3.5 Dependencies . . . 206
D.5.3.6 Interfaces . . . 206
D.5.3.7 Resources . . . 206
D.5.3.8 References . . . 206
D.5.3.9 Processing . . . 206
D.5.3.10 Data . . . 206
D.5.4 [ADDC4]: daophot.f . . . 207
D.5.4.1 Type . . . 207
D.5.4.2 Purpose . . . 207
D.5.4.3 Function . . . 207
D.5.4.4 Subordinates . . . 207
D.5.4.5 Dependencies . . . 207
D.5.4.6 Interfaces . . . 207
D.5.4.7 Resources . . . 207
D.5.4.8 References . . . 207
D.5.4.9 Processing . . . 207
D.5.4.10 Data . . . 207
D.5.5 [ADDC5]: centring.f . . . 208
D.5.5.1 Type . . . 208
D.5.5.2 Purpose . . . 208
D.5.5.3 Function . . . 208
D.5.5.4 Subordinates . . . 208
D.5.5.5 Dependencies . . . 208
D.5.5.6 Interfaces . . . 208
D.5.5.7 Resources . . . 208
D.5.5.8 References . . . 208
D.5.5.9 Processing . . . 208
D.5.5.10 Data . . . 208
D.5.6 [ADDC6]: matchframe.csh . . . 208
D.5.6.1 Type . . . 208
D.5.6.2 Purpose . . . 208
D.5.6.3 Function . . . 209
D.5.6.4 Subordinates . . . 209
D.5.6.5 Dependencies . . . 209
D.5.6.6 Interfaces . . . 209
D.5.6.7 Resources . . . 209
D.5.6.8 References . . . 209
D.5.6.9 Processing . . . 209
D.5.6.10 Data . . . 209
D.5.7 [ADDC7]: daomatch.f . . . 209

D.5.7.1 Type . . . 209
D.5.7.2 Purpose . . . 209
D.5.7.3 Function . . . 209
D.5.7.4 Subordinates . . . 210
D.5.7.5 Dependencies . . . 210
D.5.7.6 Interfaces . . . 210
D.5.7.7 Resources . . . 210
D.5.7.8 References . . . 210
D.5.7.9 Processing . . . 210
D.5.7.10 Data . . . 210
D.5.8 [ADDC8]: masterframe.csh . . . 210
D.5.8.1 Type . . . 210
D.5.8.2 Purpose . . . 210
D.5.8.3 Function . . . 210
D.5.8.4 Subordinates . . . 210
D.5.8.5 Dependencies . . . 210
D.5.8.6 Interfaces . . . 211
D.5.8.7 Resources . . . 211
D.5.8.8 References . . . 211
D.5.8.9 Processing . . . 211
D.5.8.10 Data . . . 211
D.5.9 [ADDC9]: daomaster.f . . . 211
D.5.9.1 Type . . . 211
D.5.9.2 Purpose . . . 211
D.5.9.3 Function . . . 211
D.5.9.4 Subordinates . . . 211
D.5.9.5 Dependencies . . . 211
D.5.9.6 Interfaces . . . 211
D.5.9.7 Resources . . . 211
D.5.9.8 References . . . 212
D.5.9.9 Processing . . . 212
D.5.9.10 Data . . . 212
D.5.10 [ADDC10]: transformer-coo.f . . . 212
D.5.10.1 Type . . . 212
D.5.10.2 Purpose . . . 212
D.5.10.3 Function . . . 212
D.5.10.4 Subordinates . . . 212
D.5.10.5 Dependencies . . . 212
D.5.10.6 Interfaces . . . 212
D.5.10.7 Resources . . . 212
D.5.10.8 References . . . 212
D.5.10.9 Processing . . . 212
D.5.10.10 Data . . . 213
D.5.11 [ADDC11]: lightcurve-creation . . . 213
D.5.11.1 Type . . . 213

D.5.11.2 Purpose . . . 213
D.5.11.3 Function . . . 213
D.5.11.4 Subordinates . . . 213
D.5.11.5 Dependencies . . . 213
D.5.11.6 Interfaces . . . 213
D.5.11.7 Resources . . . 213
D.5.11.8 References . . . 213
D.5.11.9 Processing . . . 213
D.5.11.10 Data . . . 213
D.6 Feasibility and resource estimates . . . 213
D.7 SR vs. components traceability matrix . . . 214

E RATS Automatic Reduction Pipeline: Software User Manual (SUM) 217
E.1 Introduction . . . 217
E.1.1 Intended readership . . . 217
E.1.2 Applicability statement . . . 217
E.1.3 Purpose . . . 218
E.1.4 How to use this document . . . 218
E.1.5 Related documents . . . 218
E.1.6 Definitions, acronyms and abbreviations . . . 218
E.1.7 Problem reporting instructions . . . 218
E.1.8 Contacts . . . 218
E.2 Overview of the document . . . 218
E.2.1 Hardware requirements . . . 219
E.2.2 Software requirements . . . 219
E.3 Installation . . . 219
E.4 Instruction . . . 220
E.4.1 Functional description . . . 220
E.4.2 Procedures . . . 220
E.5 References . . . 220
E.5.1 Functional description . . . 220
E.5.2 Formal description . . . 222
E.5.3 Examples . . . 222
E.5.4 Input files . . . 222
E.5.5 Output file . . . 223
E.6 Warnings and errors: possible causes . . . 223

F RATS Automatic Reduction Pipeline: code documentation 225
F.1 Introduction . . . 225
F.2 Program description . . . 225
F.2.1 Pre-reduction: calibration.csh . . . 226
F.2.2 Reduction: reduction.csh . . . 226

Bibliography 235

List of Figures

1 Diagramma di flusso della fase di pre-riduzione. XXIV
2 Diagramma di flusso della fase di pre-riduzione. XXV
3 Curve di luce di $RATS\_V_1$ e $RATS\_V_2$ XXVI
4 Serie temporali delle immagini defocate XXVII
5 Evoluzione dei parametri orbitali nelle simulazioni di dinamica XXVIII
6 Frazioni dei pianeti che sopravvivono XXIX
7 Istogramma della separazione della binaria e del semiasse planetario XXIX

1.1 Schematic view of the main orbital definitions 6
1.2 Lightcurve with best-fitting and single-lens models of O235/M53 9
1.3 The possible first exoplanet detected by direct imaging 11
1.4 Schematic view of the main transit definitions 12
1.5 Same as Figure 1.4 13
1.6 Duration of a central transit 15
1.7 Example of radial velocity data for transit false positives 17
1.8 Time series with noise 19
1.9 Transit of HD 209458*b* 22
1.10 HST observations of transits of HD 209458*b* 22
1.11 Evolution of the planetary radii of OGLE-TR-56*b* and HD 209458*b* 25
1.12 Mass-radius relation for the known extrasolar transiting planets 27

2.1 The 92/67 cm schmidt telescope 30
2.2 ITANET camera showing the filter system and CCD dewar 32
2.3 The B–V color–magnitude diagram for one of the RATS fields 33
2.4 The quantum efficiency curve of the SITe CCD 33
2.5 The SITe CCD 34
2.6 The e2v 42-C0 Eddington CCD 34
2.7 The "Copernico" telescope at Cima Ekar 35
2.8 The secondary mirror at the "Copernico" telescope 36
2.9 The "Copernico" Cassegrain focus 37
2.10 Echelle overview scheme at the "Copernico" telescope 38
2.11 The *Reosc* Echelle spectrograph 38
2.12 Decker for the Echelle spectrograph 39
2.13 The propagation of light through a multi-mode optical fiber 40
2.14 A typical single-mode optical fiber 40
2.15 The sky fraction limited by "geographical" field selection requisites 41

2.16 The fields distribution related to the quality factor QF 42
2.17 The relation between defocus for a star of $m_V = 9$ and the exposure time 44
2.18 The percentage of necessary spectroscopic follow up time 45
2.19 H/W interfaces and S/W relationship with external environment 46
2.20 Scheme for the software dataflow for the RATS project 48

4.1 Dataflow pre-reduction diagram 74
4.2 Dataflow reduction diagram 75
4.3 Hardware layer scheme for the software architecture 77
4.4 Off-line analysis scheme 77
4.5 Application layer scheme 78
4.6 User interface relationship scheme 78

6.1 `SAOImage DS9` screen-shot of a portion of RATS_10 field in focus 98
6.2 Screen-shots displaying the masterbias and masterflat relative to RATS_10 100
6.3 Lightcurves for $RATS\_V_1$ and $RATS\_V_2$ 101
6.4 `SAOImage DS9` screen-shot of a portion of RATS_4 defocused field 102
6.5 Screen-shots displaying the masterbias and masterflat relative to RATS_4 104
6.6 Lightcurves for RATS_4 field 105

7.1 Logical, physical, and recovery-related structures of the `Oracle` database 119

8.1 Time of the first close encounter between the binary and the singleton *vs.* a_s . . 138
8.2 Distribution of the final binary orbital elements 139
8.3 Histogram of a_b 139
8.4 Distribution of the final eccentricity and inclination of the binary system 141
8.5 Final semimajor axis a_p of the outer planetary orbit 142
8.6 Semimajor axis evolution of the planets around the primary star for $i_m = 90°$ . . 145
8.7 Same as in Fig.8.6 but for $i_m = 30°$ 146
8.8 Orbital parameters evolution 147
8.9 Fraction of binaries retaining at least one of the planets in a stable orbit *vs.* i_m . 148
8.10 Fraction of binaries retaining at least one of the planets in a stable orbit *vs.* a_b . 148

B.1 S/W relationship with the external environment 174

C.1 S/W relationship with the external environment 186
C.2 General dataflow pre-calibration and calibration diagram 194
C.3 General dataflow reduction diagram 195

D.1 S/W relationship with the external environment 201
D.2 Hardware layer for the software architecture 202
D.3 Off-line analysis with ISIS 2.2 package 202
D.4 Application layer: the calibration pipeline 202
D.5 Application layer: the reduction pipeline 203
D.6 User interface relationship 203

F.1 Data flow for the main reduction program `reduction.csh` 230

List of Tables

1 Units of measurement XXXIII

1.1 Data for the known planets candidates detected by transit 28

2.1 Coordinates of the central pillar of schmidt telescope at Cima Ekar 31
2.2 Characteristics of the RATS CCD cameras 31
2.3 The main characteristics of the Copernico's mirrors 36
2.4 Central coordinates for the seven best selected RATS stellar fields 43
2.5 Counting of occupied space by RATS images 49

3.1 Identification of sky coordinate systems 58
3.2 Reference frames for equatorial coordinate systems 60
3.3 Example of RATS header FITS image 61

5.1 Parameters file for `zerocombine` `IRAF` task, setted for RATS images 82
5.2 Parameters file for `imcombine` `IRAF` task, setted for RATS images 84
5.3 Parameters file for `fixpix` `IRAF` task, setted for RATS images 86
5.4 Parameters file for `cosmicrays` `IRAF` task, setted for RATS images 87

6.1 RATS_10 stellar field parameters 98
6.2 RATS_4 stellar field parameters 102

7.1 List of operands that can be used wherever a search string is required . . . 125

A.1 Journal of observations for February 18th 2005 159
A.2 Journal of observations for April 22th–26th 2006 162

B.1 Change record for RATS–*ARP* URD document 169

C.1 Change record for RATS–*ARP* SRD document 181
C.2 User Requirements *vs.* Software Requirements traceability matrix 192

D.1 Change record for RATS–*ARP* ADD document 197
D.2 Software Requirements *vs.* Architectural Components traceability matrix 214

E.1 Change record for RATS–*ARP* SUM document 217
E.2 RATS–*ARP* warnings: messages and meaning 224
E.3 RATS–*ARP* errors: messages and meaning 224

F.1 Change record for RATS–*ARP* code documentation 225
F.2 `calibra.cl` `IRAF` script 231
F.3 `juliandate.csh` shell script 231
F.4 `idlist.f` `FORTRAN77` executable 231
F.5 `centring.f` `FORTRAN77` executable 232
F.6 `matchframe.csh` and `masterframe.csh` shell scripts 232
F.7 `transformer_coo.f` `FORTRAN77` executable 232
F.8 `print_phot.f` `FORTRAN77` executable 233
F.9 `lightcurve.f` and `lightcurve.f` `FORTRAN77` executables 233
F.10 `bestlightcurve.f` and `bestlightcurve1.f` `FORTRAN77` executables 234

List of Acronyms

AD Applicable Document

ADD Architectural and Design Document

CCD Charge Coupled Device

CPU Central Processing Unit

DB Database

ESA European Space Agency

ESP Extrasolar Planet

ESPs Extrasolar Planets

FA False Alarms

FCU Field Camera Unit

FF Flat Field

FoV Field of view

FWHM Full Width Half Maximum

H/W Hardware

IDL Interface Description Language

JD Julian Day

NA Not Available/Not Applicable

OS Operative System

PC Personal Computer

PSF Point Spread Function

RAM Random Access Memory

RATS Radial Velocities and Transit Search

RATS–ARP RATS–Automatic Reduction Pipeline

RD Reference Document

RV Radial Velocity

SRD Software Requirements Document

SS Solar System

SUM Software User Manual

S/W Software

TBD To Be Defined

TBW To Be Written

URD User Requirements Document

UT Universal Time

VSs Variable Stars

WSO-UV World Space Observatory UV

Abstract

THE aim of this research project was twofold: on one hand, we have developed an automatic photometric pipeline with a real time images reduction, which directly provide lightcurves of objects observed in the field. The lightcurves themselves are analyzed in order to catch light diming due to a transit.
On the other hand, we contribute to investigate the dynamical and physical structure of the planetary systems hosted in multiple stellar systems and to compare the results with the current knowledge both of the planetary and stellar formation in order to gain a new insight on the evolution of extrasolar systems.

Even if this PhD Thesis is made up of these two different but complementary aspects, however the final aim of both converges: it contributes to the comprehension of the planetary formation mechanism in order to identify both the environment conditions where these objects could form and some clues on their physical properties. Moreover, the results may be applied to the future space missions: the reduction pipeline could be exploited in whatever surveys of transit search thanks to its automatic nature while the theoretical results could be the starting point for the future investigations from space.

Part I: Photometric reduction and analysis software

An exoplanetary transit occurs when it crosses the line of sight between the observer and the star around which it is orbiting. The flux decrease that it provokes allows us to find out certain orbital parameters and some physical characteristics of the planet that are inaccessible through other techniques. The diversity of the performed studies and the acquired knowledge after the detection of HD 209458b's transits motivated the use of this technique as a tool for exoplanet discoveries.

In this thesis, we describe the reduction algorithm developed in the RATS (RAdial velocities and Transit Search) project context in order to automatically achieve the lightcurves of photometric stars devoted to the search for exoplanets using the transit method. The main aim of the RATS project is twofold. The detection of extra solar planets that transit the disk of their parent star is the main scientific drive of the whole project. We have planned to observe simultaneously thousands of stars (magnitude range between 9^{th} to 14^{th}) in selected star fields for five years since the beginning of 2005. In this manner we are confident to find new transiting planets. The second aim of the project is to use its observing strategy and the scientific data management as a bench work for future planetary transits search mission in order to value it effectiveness. In particular, RATS projects seeks high precision photometric results performed

with stellar images which have been purposely defocused in order to avoid saturation of brighter stars because of the size of Schmidt FoV. Moreover, to maximize the transit probability, each RATS field has been partitioned in seven adjacent sub-fields sequentially pointed.
Up to now, two missions already plan to exploit this untypical strategy: the French CoRoT mission devoted to extrasolar planets search and asteroseismology is planning to collect CCD images which are slightly de-focused; the same observational approach has also been proposed for the Kepler extrasolar space mission as well.

Originally, this research project foresaw many observations from the Cima Ekar Schmidt telescope equipped with a frame transfer CCD lended from INAF−OACT (Istituto Nazionale di AstroFisica−Osservatorio Astronomico di Catania) in concomitance to the very beginning of RATS project. For reasons out of my hands, some months ago INAF−OACT unexpectedly demand it back and the observations were stopped for a considerable amount of time. This aspect, added to the bad weather conditions of the most of 2006, has lessened images acquisition relative to initial expectations. However, in order to automatically reduce the images obtained so far, we have developed an automatic reduction algorithm RATS–*ARP* (*Automatic Reduction Pipeline*) which directly provides light curves of objects in the pre-selected RATS fields. The light curves themselves are analyzed in order to catch light diming due to a planetary transit. This software is based on different modules all called from a main program shell script, each being deputy to an individual step for photometric reduction of images, like:

- *Masterframes setting-up:* these frames are generated from an IRAF script based on some tasks already available calculating the median from initial bias and flats images in order to reduce the noise contribution.

- *Images calibration:* through an IRAF script, these frames are bias reduced and flat normalized.

- *Photometry:* exploiting both available algorithms (*i.e.*, `daophot`) and FORTRAN programs developed *ad hoc*, the values of magnitude for good stars are determined; the conditions to identify stars as "good" are principally to have a magnitude $9 \leq m_V \leq 13$ out crowding regions.

- *Lightcurve files:* some FORTRAN programs generate ASCII file text containing the magnitude value of each selected star varying with time. These time series, if plotted, provide the lightcurves.

- *Database population:* the previous mentioned ASCII files are used to create the tables that will be feed in the project archive.

The described procedure has been applied both to the images in focus and to defocused ones, in particular two stellar fields have been analyzed among those chosen for the project. RATS–*ARP* has shown its robustness in managing both kind of images, performing all its tasks till lightcurve files creation with satisfactory time consuming: it has taken 90 seconds for each image in focus and 180 seconds for each defocused frame, depending on the crowding of the field.

➢ In RATS_10 field, observed in focus on February 18$^{\text{th}}$ 2005, we find the lightcurves of two interesting objects:

A. a V-shaped lightcurve: this object, called $RATS\_V_1$, could be a variable star Mira-like (*i.e.*, giant star χCyg) or a primary star of a eclipse binary system;

B. a lightcurve of a pulsating variable star shape: this object, called $RATS\_V_2$, could be the primary star of a contact variable W UMa system-like as it shows a secondary minimum peculiar of this class of objects.

Up to now, we are not yet able to unveil the nature of $RATS\_V_1$ and $RATS\_V_2$: we need more observations to investigate inside out.

➢ In RATS_4 field, observed in defocus mode in on April $22^{\text{th}} - 26^{\text{th}}$ 2006, we find the some lightcurves but the bad weather conditions make the most observations useless; all the time series of this surveys lacks in data.

Therefore, the pipeline can manage different kind of images and it fulfills all its task. Thereby, we can say that RATS–*ARP* can be exported to projects different from RATS thanks to its pliability. In particular, thanks to its automatic development approach, it could be easily applicable to future space missions which intend to search exoplanets with the transit method with small adjustments.

A detailed analysis for the future implementation of RATS database has been, finally, performed. Requirements and structure of this archive have been identified in order to help in developing a database that can be offered both to scientific community and to non-specialists.

Part II: Dynamical simulations

The present dynamical configuration of planets in binary star systems may not reflect their formation process since the binary orbit may have changed in the past after the planet formation process was completed. An observed binary system may have been part of a former hierarchical triple that became unstable after the planets completed their growth around the primary star. Alternatively, in a dense stellar environment even a single stellar encounter between the star pair and a singleton may significantly alter the binary orbit. In both cases the planets we observe at present would have formed when the dynamical environment was different from the presently observed one.

We have numerically integrated the trajectories of the stars (binary plus singleton) and of test planets, hosted around the primary star of the inner binary, to investigate the above mentioned mechanisms. Different values of mutual inclination, binary separation and singleton initial semimajor axis are explored in a statistical way.

Our simulations show that the circumstellar environment during planetary formation around the primary was gravitationally less perturbed when the binary was part of a hierarchical triple because the binary was necessarily wider and, possibly, less eccentric. We find that a significant mutual inclination between the singleton and the binary is a key factor for instability of the planetary system in terms of orbital spacing, eccentricity, and mass of the individual planets. Infact, from our integration we have found that when the mutual inclination is larger than $\sim 40°$, the fraction of planets in the binary surviving the chaotic phase of the triple declines dramatically. and for an inclination around 90°, the percentage of surviving planets is lower than 20% for all binaries with a semimajor axis smaller than 200 AU. The combination of eccentricity and inclination oscillations of the binary companion induced by the secular perturbations of the

singleton and the sequence of close encounters preceding the ejection of one star fully destabilize a planetary system extending beyond 1 AU from the star.
Even in the case of a single stellar encounter the present appearance of a planetary system in a binary may significantly differ from what it had while planet formation was ongoing.
However, while in the case of instability of a triple the trend is always towards a tighter and more eccentric binary system, when a single stellar encounter affects the system the orbit of the binary can become wider and be circularized.
We can conclude that the frequency of planets in binaries with low separation may be strongly reduced by the residence of the pair in the past in a temporary inclined hierarchical triple.

Riassunto

Un *esopianeta* o *pianeta extrasolare* è per definizione un oggetto avente un valore della massa inferiore al limite di 13 masse gioviane, necessario affinché si inneschi la fusione termonucleare del Deuterio, e ospite di una stella diversa dal nostro Sole.

La scoperta del primo esopianeta (Wolszczan & Frail, 1992) attorno ad una pulsar si basò sulla misura della media dei tempi di arrivo degli impulsi della pulsar. Analoghe misurazioni sono state eseguite anche su altre stelle di questo tipo ma ad oggi, nessun ulteriore risultato è stato ottenuto rivelando che le stelle pulsar ad oggi note non possiedono alcun compagno planetario (Lorimer, 2001). Da questo primo risultato se ne sono succeduti molti altri e, oggi, sono noti più di 270 pianeti, scoperti con diversi metodi osservativi (*velocità radiali*, *transiti fotometrici*, *microlensing*, *osservazione diretta*).
Tra questi, il metodo che ha permesso di ottenere maggiori risultati è quello basato sulla misurazione dell'effetto Doppler sulle righe spettrali della stella indotto dalla presenza di un compagno, da cui si può ricavare la sua massa minima. È stato grazie a queste misurazioni che Mayor & Queloz (1995) scoprirono il primo esopianeta attorno ad una stella di tipo solare, 51 Peg *b*. Solo pochi anni dopo, Charbonneau et al. (2000) scoprirono il primo pianeta extrasolare transitante davanti al disco della sua stella. Da allora, questa tecnica osservativa ha fornito un nuovo grande impulso nella ricerca di tali oggetti permettendone l'osservazione di più di 30. In più, questo metodo consente di determinare il raggio planetario e, accoppiato a quello delle velocità radiali di cui risulta complementare, la densità dell'oggetto.

Lo scopo di questa Tesi di dottorato è stato, per la maggior parte, quello di scrivere un software automatico che permettesse di ottenere le curve di luce di stelle in campi precedentemente selezionati in modo da rivelare, dalla diminuzione del flusso stellare, la presenza di compagno planetario in transito.
Accanto a questo lavoro osservativo, ho contribuito anche a sviluppare un algoritmo numerico che investigasse l'evoluzione dinamica di sistemi stellari (gerarchici) tripli la cui stella primaria ospita un pianeta.

Pur comprendendo due analisi così diverse ma complementari tra loro, lo scopo di entrambe è comunque convergente: contribuire alla comprensione del meccanismo di formazione dei pianeti in modo da identificare sia le condizioni ambientali in cui questi oggetti si formano che gli indizi sulle loro proprietà fisiche. I risultati potranno essere applicati alle future missioni spaziali: la pipeline di riduzione, per la sua stessa natura automatica, potrà essere sfruttata in una qualsiasi campagna osservativa spaziale mentre i risultati teorici saranno la base per lo studio di future indagini dallo spazio.

Parte I: Software per la riduzione e l'analisi fotometrica

La pipeline di riduzione automatica, alla cui scrittura mi sono dedicata soprattutto nei primi anni del Dottorato, si inserisce all'interno del progetto RATS che ne costituisce l'ambiente e la ragione di sviluppo pur non reclamandone l'esclusività.

Il progetto italiano RATS

Il progetto RATS (RAdial velocities and Transit Search, `http://www.pd.astro.it/rats/it/home.php`) nasce da una collaborazione italiana fra diversi Osservatori INAF (Padova, Catania, Napoli e Palermo), i Dipartimenti di Astronomia e Fisica dell'Università di Padova e l'ESA. Lo scopo del progetto è duplice. Da una parte, si prefigge di osservare per mezzo del telescopio Schmidt, regioni selezionate di cielo allo scopo di trovare pianeti di tipo gioviano con il metodo dei transiti e di caratterizzare gli eventuali candidati transiti per mezzo dello spettrografo ad alta risoluzione montato al telescopio Copernico da 182 cm. Entrambi gli strumenti sono dell'Osservatorio Astronomico di Padova (INAF) e sono situati a Cima Ekar presso Asiago (VI). Dall'altra si propone di essere un banco di prova per la strategia di osservazione basata sul defocamento delle immagini e la gestione dei dati, valutandone l'operatività sul campo e sperimentandole al suolo, come in un test di laboratorio, in modo da poterlo poi applicare in future missioni spaziali.

La strategia osservativa, infatti, prevede sia il defocamento delle immagini, in modo da sfruttare il grande campo di vista dello Schmidt e, parimenti, evitare di saturare le immagini spettroscopiche al telescopio Copernico durante la successiva fase di follow-up. Oltre a ciò, per aumentare la probabilità di osservare un transito planetario, uno stesso campo viene suddiviso in sette sottocampi adiacenti soggetti a puntamenti sequenziali.

Fino ad oggi, già due missioni spaziali hanno progettato di sfruttare questa strategia osservativa: la missione francese CoRoT sta osservando immagini defocate sia per il programma di ricerca di esopianeti che per quello asterosismologico; lo stesso approccio osservativo è stato proposto anche per la missione Kepler, dedicata alla ricerca di pianeti extrasolari.

Il software: RATS–ARP

Le immagini ottenute al telescopio Schmidt di campi pre-selezionati sono state sottoposte ad un processo di riduzione automatico, chiamato RATS–*ARP* (Automatic Reduction Pipeline) in modo da avere, come prodotto finito, direttamente le curve di luce degli oggetti giudicati interessanti. Lo scopo è quello di cercare le diminuzioni di luminosità relative ad un transito planetario. È fondamentale tenere in considerazione che tale diminuzione può essere causata da fenomeni astronomici capaci di mimare dei transiti planetari come, per esempio, binarie ad eclisse. Questi fenomeni, che costituiscono una scienza parallela rispetto a quella che si prefigge il progetto, possono essere individuati attraverso un'analisi spettroscopica con osservazioni dedicate.

L'acquisizione delle immagini da CCD viene fatta tramite il PC denominato `cold60` con sistema operativo WinNT, collegato tramite una rete locale al telescopio Schmidt. La mattina successiva alle osservazioni le immagini vengono trasferite attraverso al PC `dolce` su cui è installato un sistema operativo Linux a cui sono connessi un hard disk da 300 Gb ed un masterizzatore DVD per copie di back-up delle immagini. In questo secondo PC risiedono i processi per il controllo e l'attivazione della pipeline di riduzione e delle procedura di archiviazione. Grazie al fatto

che la rete locale di Cima Ekar è connessa direttamente alla rete di Padova, i dati ridotti possono essere trasferiti per mezzo del protocollo FTP al server `serizawa` a cui è connessa un'unità RAID da 2.5 Tb su cui risiederà anche l'archivio delle immagini ridotte di RATS. Per archiviare i dati fotometrici di RATS si opera su due livelli distinti: nel primo vengono salvati i dati rozzi su DVD. Un secondo livello consiste nell' attivare RATS–*ARP*.
Il software, costituito shell script che funziona da main program, è costituito da diversi moduli che, in successione, sono deputati allo svolgimento dei seguenti compiti:

- *Costruzione delle immagini di calibrazione per bias e flat field:* questi masterframes sono generati da uno script di IRAF che sfrutta tasks già disponibili e si ottengono mediando le immagini di bias e flat acquisiti durante le osservazioni in modo da diminuire il contributo del rumore.

- *Calibrazione delle immagini:* tramite uno script di IRAF, le immagini scientifiche vengono calibrate per bias e flat.

- *Fotometria delle immagini:* sfruttando sia algoritmi già noti (`daophot`) che programmi scritti *ad hoc* in FORTRAN, vengono determinate le magnitudini delle stelle considerate "fotometriche", cioè che soddisfano a criteri quali avere una magnitudine $9 \leq m_V \leq 13$ e risiedere in una regione a basso crowding.

- *Costruzione dei file per le curve di luce:* tramite programmi in FORTRAN, vengono generati file di testo contenenti il valore della magnitudine di ciascuna stella, selezionata al variare del tempo. Queste serie temporali forniscono, se inserite in un grafico, la curva di luce richiesta.

- *Popolazione del database:* questi files ASCII vengono utilizzati per la costruzione delle tabelle che andranno a costituire l'archivio del progetto.

Il diagramma di flusso di RATS–*ARP* è illustrato alle Figure 1 e 2: il flusso del *main program* è stato suddiviso in due parti sia per maggiore chiarezza del grafico stesso che per riflettere le due fasi successive del processo di riduzione.

La procedura descritta è stata applicata sia alle immagini a fuoco che defocate; in particolare, sono stati analizzati due campi stellari tra quelli selezionati per RATS. RATS–*ARP* ha dimostrato la sua robustezza nella capacità di gestire entrambi i tipi di immagini, producendo le curve di luce in tempi ragionevoli: $90''$ per un immagine a fuoco e circa $180''$ per un defocata, in dipendenza ovviamente dal numero di oggetti che sono oltre la soglia della bontà fotometrica.

➢ Nel campo RATS_10, osservato a fuoco nella notte del 18 Febbraio 2005, abbiamo rivelato le curve di luce di due oggetti interessanti:

A. una curva di luce V-shaped (Fig. 3, a sinistra): questo oggetto, che abbiamo chiamato $RATS\_V_1$, potrebbe essere un stella variabile di tipo Mira (tipo la gigante χCyg) oppure la stella primaria di una binaria ad eclisse;

B. una curva di luce il cui andamento è tipico di una stella variabile pulsante (Fig. 3, a destra): questo oggetto che abbiamo chiamato $RATS\_V_2$, potrebbe essere un stella variabile "a contatto" tipo la stella primaria del sistema W UMa poiché la curva mostra un secondo minimo tipico di questa classe di oggetti.

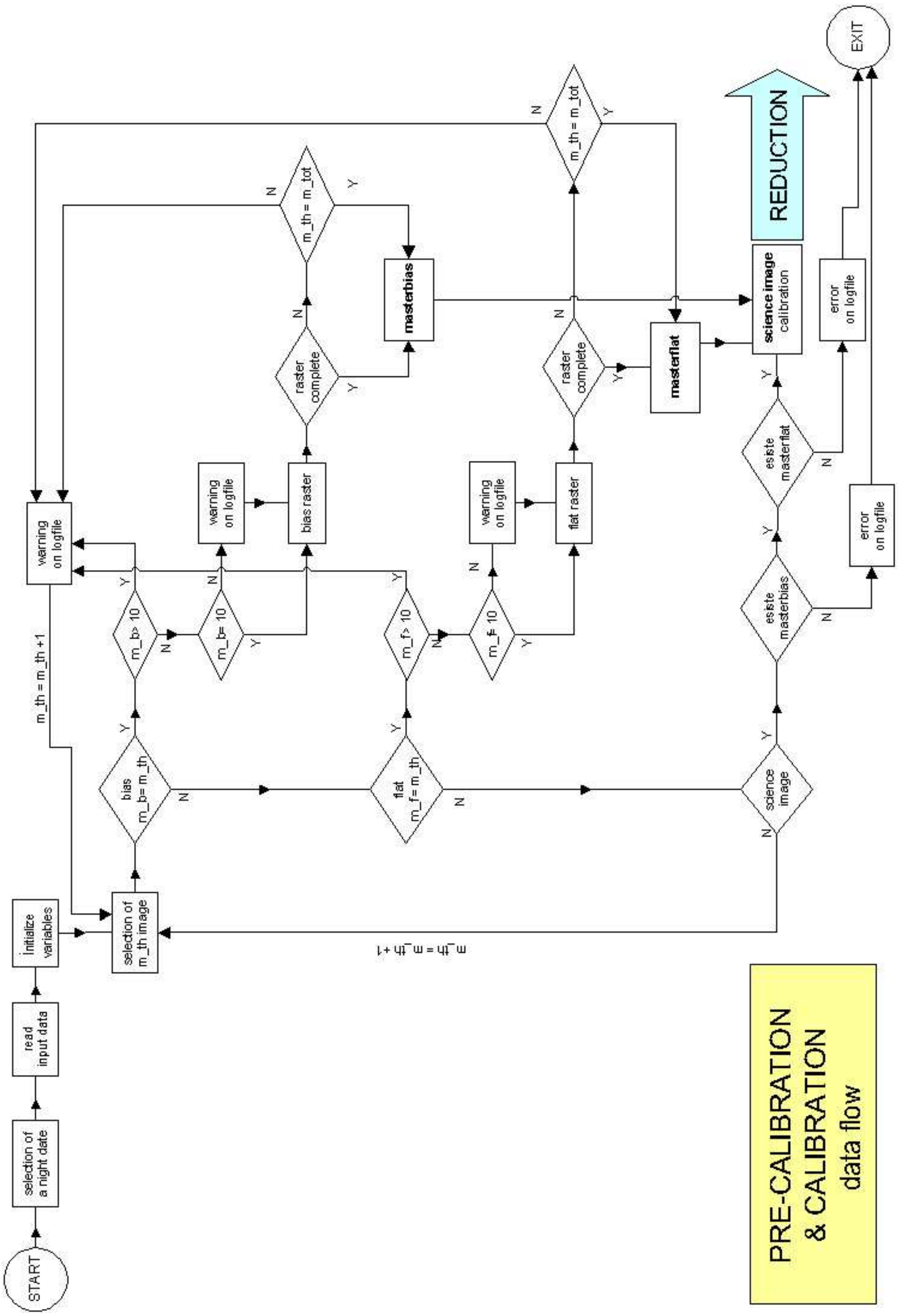

Figure 1: Diagramma di flusso della fase di pre-riduzione.

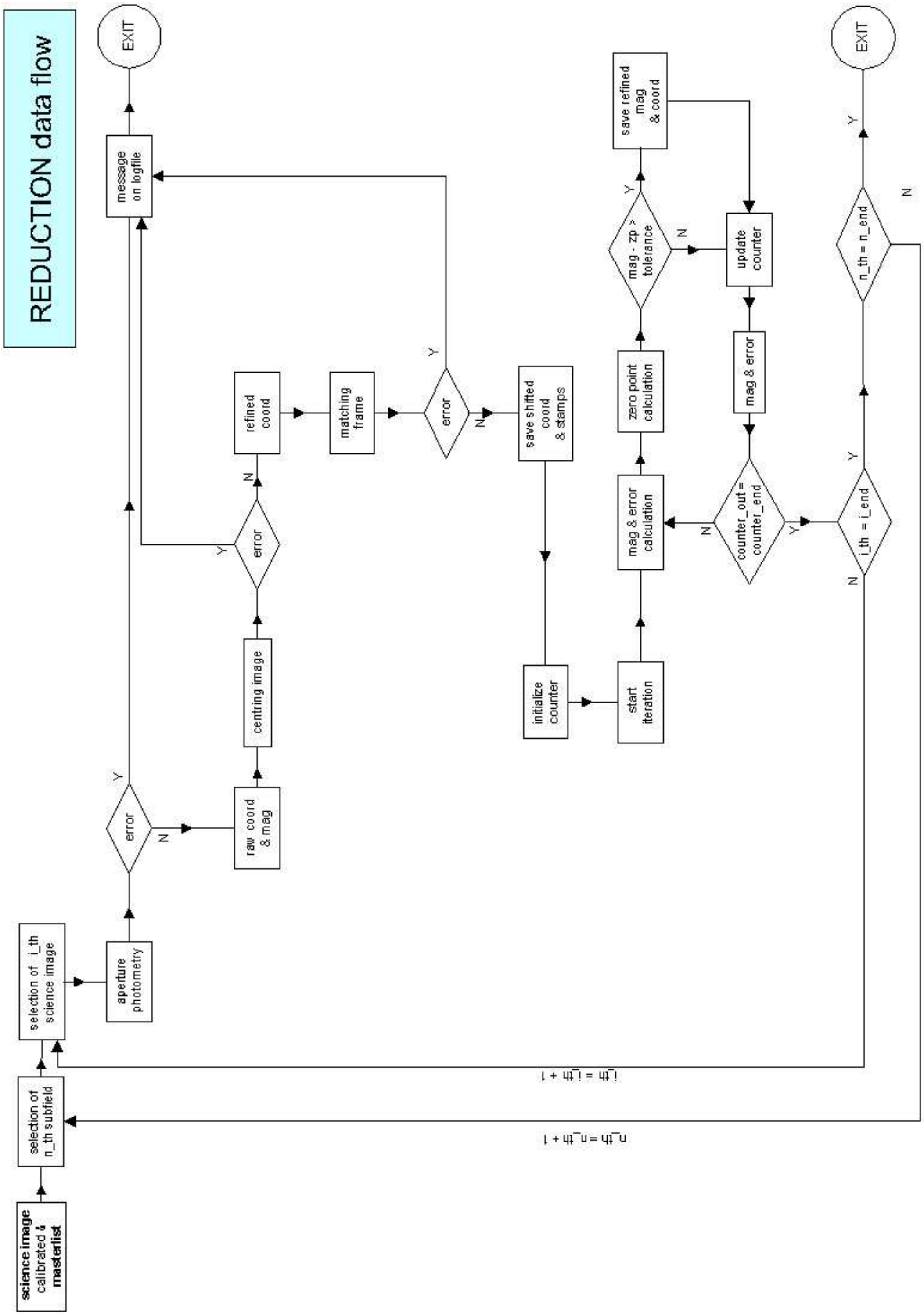

Figure 2: Diagramma di flusso della fase di riduzione.

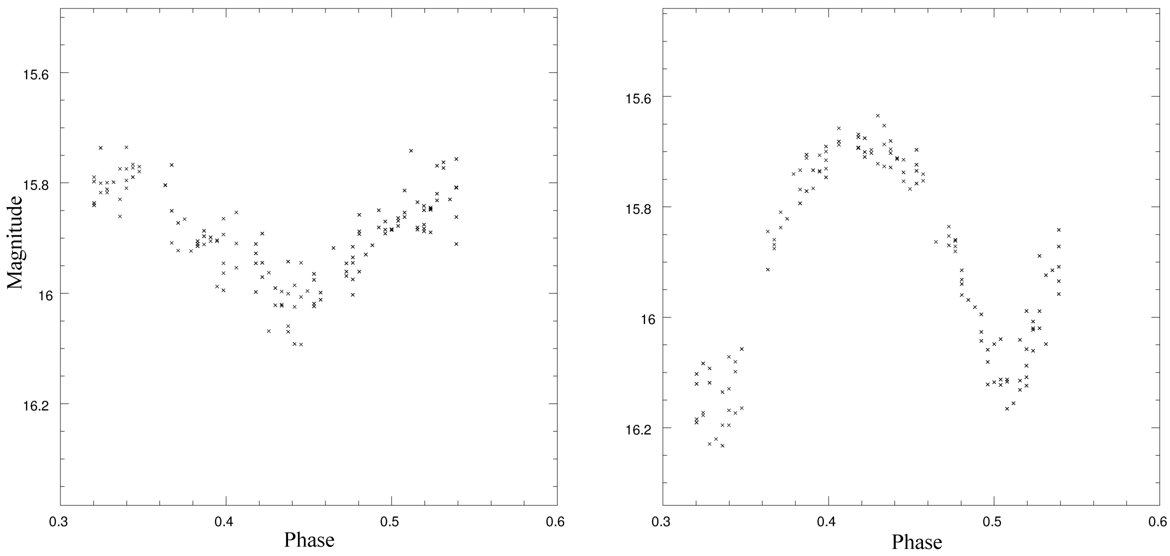

(a) $RATS\_V_1$ (b) $RATS\_V_2$

Figure 3: *A sinistra*: Curva di luce V-shaped di un oggetto chiamato $RATS\_V_1$. In accordo con la teoria, questo oggetto potrebbe avere una stella compagna che transita sopra il suo disco oppure potrebbe essere una stella variabile tipo Mira. *A destra*: Curva di luce tipica di una stella variabile "a contatto", simile alla primaria del sistema W UMa. Questo oggetto è stato classificato col nome $RATS\_V_2$.

Non siamo, per ora, in grado di svelare la vera natura di questi oggetti ma potremmo averne un'idea più chiara avendo a disposizione un maggior numero di osservazioni.

➢ Nel campo RATS_4, osservato defocato nelle notti tra il 22 e il 26 Aprile 2006, abbiamo rivelato le curve di luce di alcuni oggetti ma le cattive condizioni metereologiche hanno reso inutilizzabili la maggior parte delle immagini col risultato che le serie temporali che abbiamo ottenuto mancano di molti dati. Riportiamo in Figura 4 una tipica curva di luce per il campo in questione.

Purtroppo, ad impedire in generale le osservazioni, oltre le cattive condizioni metereologiche verificatesi soprattutto durante il 2006, è stata l'inaspettata richiesta di restituzione del CCD in uso, prestatoci dall'Osservatorio di Catania, che ha interrotto la campagna osservativa per un periodo considerevole. Questa interruzione ha impedito non solo di acquisire immagini degli altri campi selezionati per RATS, ma anche di testare il software scritto su più campioni, in particolare su $RATS\_V_1$ e $RATS\_V_2$.

L'archivio delle immagini di RATS–ARP

Le immagini rozze e ridotte così come i file ASCII e i grafici in formato *.ps* e *.jpeg* relative alle curve di luce ottenute con RATS–*ARP* saranno messe a disposizione della comunità scientifica e amatoriale grazie ad un archivio on-line di futuro sviluppo. L'accesso avverrà tramite

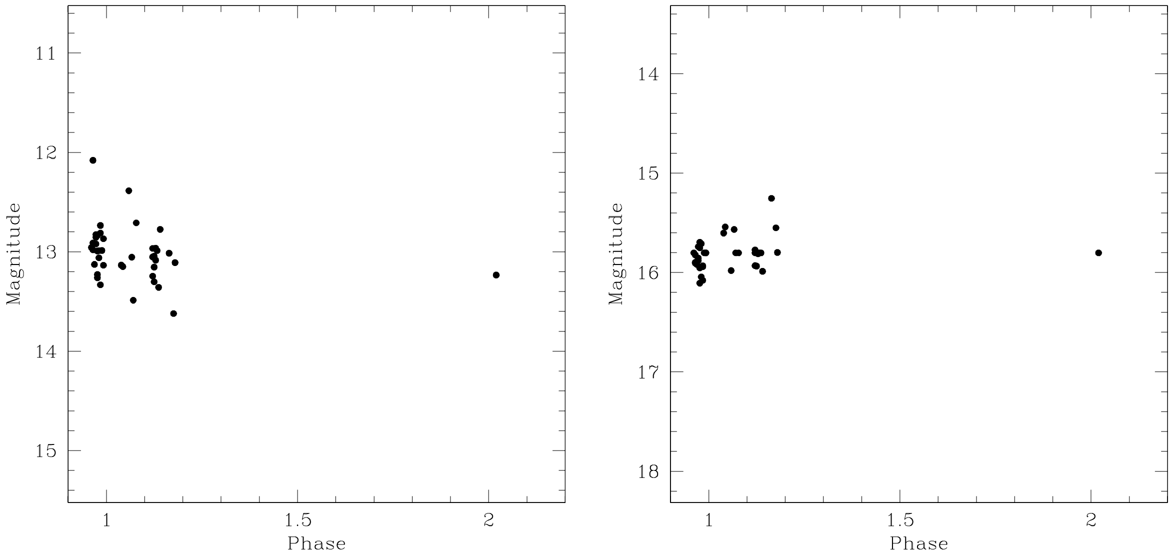

Figure 4: Serie temporali di due oggetti-campione. Le cattive condizioni metereologiche sono la causa evidente della mancanza della maggior parte dati.

un'interfaccia web che verrà sviluppata allo scopo. In questo lavoro di tesi, abbiamo individuato le linee guida per lo sviluppo dell'archivio.

Il database sarà di tipo relazionale e si comporrà di tre tabelle: una relativa alle immagini grezze ed un'altra, connessa alla prima da opportune chiavi, contenente le immagini calibrate. Una terza tabella, a sua volta collegata alla precedente, conterrà i files delle curve di luce.

La costruzione delle diverse tabelle conclude la fase di riduzione. La fase successiva comprende il trasferimento delle tabelle e la popolazione del database che risiederà sulla macchina chiamata `serizawa`, collocata a Padova. Al termine, si inizierà con il processo di aggiornamento sia dell'archivio stesso che della sessione on-line.

Parte II: Simulazioni di dinamica

L'attuale configurazione dinamica dei pianeti in sistemi stellari binari non riflette il loro processo di formazione poiché l'orbita della binaria potrebbe aver subito modifiche nelle epoche precendenti a quella in cui la formazione planetaria si è completata. In particolare, un sistema binario osservato potrebbe essere stato parte di un progenitore sistema gerarchico triplo che è diventato instabile dopo che i pianeti hanno completato la loro formazione attorno alla stella primaria. Alternativamente, in un ambiente densamente popolato di stelle, anche un singolo incontro ravvicinato tra la coppia di stelle e un stella singola isolata potrebbe alterare significativamente l'orbita della binaria stessa. Qualsiasi sia lo scenario che effettivamente si verifica, in entrambi i casi i pianeti che noi osserviamo ora potrebbero essersi formati quanto l'ambiente era molto diverso dal punto di vista dinamico rispetto a quanto possiamo osservare ora.

In un tale contesto, ho contribuito allo sviluppo di un algoritmo numerico che integra le traiettorie delle stelle (sia quelle formanti il sistema binario, sia la stella isolata) e di 10 oggetti planetari di test orbitanti attorno alla stella primaria del sistema binario. Lo scopo è quello di

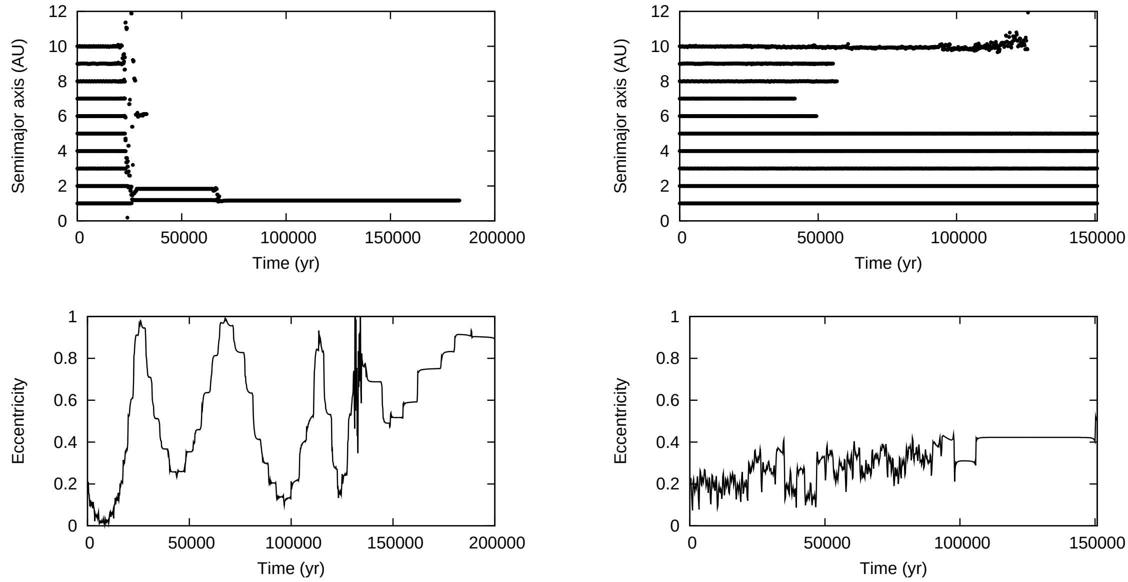

(a) $i_m = 90°$ (b) $i_m = 30°$

Figure 5: *In alto*: Evoluzione temporale dei semiassi maggiori dei pianeti attorno alla stella primaria di un sistema binario per effetto delle perturbazioni della secondaria, a sua volta influenzata dall'attrazione gravitazionale della stella singola per $i_m = 90°$ (*a sinistra*) e per $i_m = 30°$ (*a destra*). *In basso*: Oscillazioni dell'eccentricità della secondaria, perturbata dalla stella singola per $i_m = 90°$ (*a sinistra*) e per $i_m = 30°$ (*a destra*). Il semiasse maggiore iniziale della binaria è 70 AU, l'eccentricità è 0.2 sia per la binaria che per la stella singola.

investigare i meccanismi sopra menzionati tramite uno studio statistico al variare delle mutue inclinazioni, separazione tra le stelle della coppia e del semiasse maggiore della stella singola.

Le nostre simulazioni mostrano che l'ambiente circumstellare instauratosi durante la formazione planetaria attorno alla primaria viene gravitazionalmente perturbato meno quando la coppia di stelle è parte di un sistema gerarchico triplo: in un tale scenario, infatti, la binaria risulta tipicamente più larga e, possibilmente, meno eccentrica cosicché le mutue interazioni gravitazionali sono meno intense. I nostri risultati mostrano che un valore significativo dell'inclinazione mutua tra la stella singola e la coppia è un fattore chiave per l'instabilità del sistema planetario in termini di elementi orbitali quali il semiasse maggiore, l'eccentricità e la massa dei singoli pianeti presenti (Fig. 5). Infatti, dalle nostre integrazioni abbiamo trovato che quando le mutue inclinazioni sono maggiori di $\sim 40°$, la frazione di pianeti nella binaria che sopravvivono alla fase caotica del sistema triplo diminuiscono drammaticamente e, per un valore dell' inclinazione attorno a 90°, la percentuale dei pianeti sopravvissuti risulta inferiore al 20% per tutti i sistemi in cui la binaria ha una separazione minore di 200 AU (Fig. 6). Le oscillazioni combinate di eccentricità e inclinazione della secondaria indotte dalle perturbazioni secolari dovute alla stella singola e la successione di incontri ravvicinati che precedono l'espulsione della secondaria stella tendono a destabilizzare completamente la parte del sistema planetario che si estende oltre 1 AU.

Anche nel caso in cui si verifichi un solo incontro ravvicinato, l'attuale aspetto di un sistema

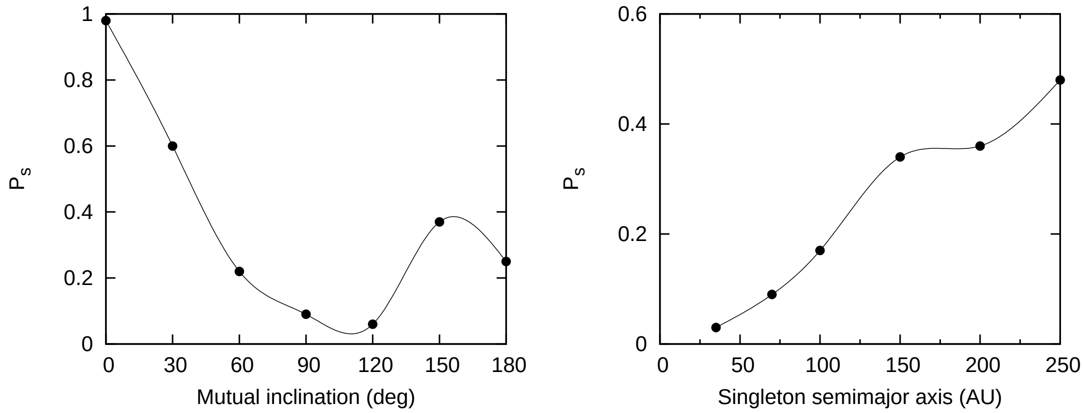

Figure 6: *A sinistra*: Frazione P_s dei sistemi binari che, al termine della fase caotica, trattiene almeno un pianeta in orbita stabile attorno alla stella primaria *vs.* i_m, la mutua inclinazione iniziale tra la coppia e la stella singola. *A destra*: Frazione P_s analoga al pannello sopra *vs.* a_b, la separazione della binaria, per un'inclinazione mutua $i_m = 90°$ corrispondente al caso peggiore in termini di stabilità planetaria.

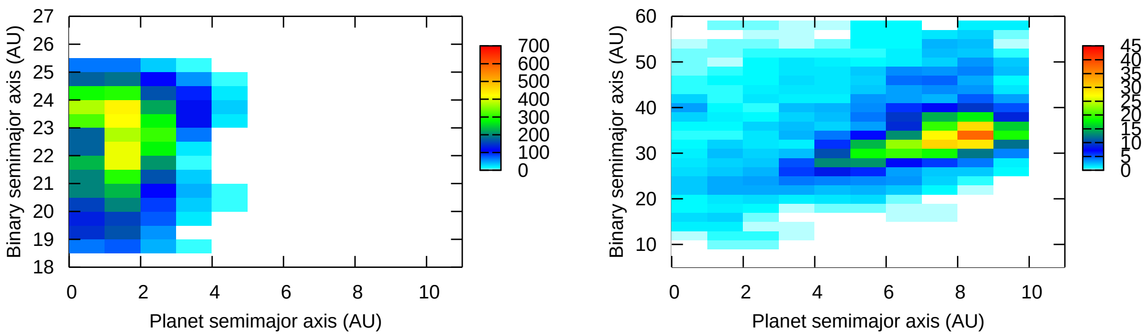

(a) Stella singola legata alla binaria

(b) Stella singola in orbita iperbolica

Figure 7: Istogramma che illustra, per le nostre simulazioni, il numero di sistemi che, alla fine della fase caotica, cade in un certo bin di separazione della binaria a_b in funzione del semiasse maggiore del pianeta più esterno a_p che sopravvive alla fase caotica in cui la stella singola è legata gravitazionalmente alla binaria (*a destra*) e ad un incontro ravvicinato con una stella singola in orbita iperbolica (*a sinistra*).

planetario ospite di un sistema stellare binario può essere significativamente differente rispetto a quanto poteva essere all'epoca in cui la formazione planetaria era in atto. Tuttavia, mentre nel caso di una instabilità a seguito di una fase caotica di un sistema stellare triplo la tendenza è sempre verso una configurazione in cui il sistema binario è più stretto ed eccentrico, nel caso in cui un solo incontro ravvicinato con una stella su orbita iperbolica perturba il sistema, l'orbita della binaria può diventare più larga ed essere circolarizzata (Fig. 7).

Possiamo concludere che la frequenza dei pianeti in sistemi stellari binari che attualmente mostrano piccole separazioni potrebbero, in verità, essere state ridimensionate rispetto al passato perché allora membri di sistema gerarchico triplo e inclinato.

Introduction

THE astrophysics of planetary systems is a good example of a branch of science in which theory is mostly driven by observations and space missions.

The unexpected properties of extrasolar planets have sparked new enthusiasm among theorists, who have engaged in fruitful intellectual confrontations, with the aim of moving from a set of models separately describing different aspects of the physics of the formation and evolution of planetary systems to a plausible, unified theory capable of making robust and testable predictions. Furthermore, a number of new and old techniques of astronomy observations, both from ground and space, have been energized by the new discoveries, with the twin goals of following up and better characterizing the extrasolar planet sample, and covering new areas of the discovery space. The result is an ongoing, positive, creative tension between theory and observation that will put to the test the most basic ideas of how planets form and evolve.

The radial velocity technique has been highly successful in finding planets with more than a hundred detected up to the present. Despite this enormous success, due to the degeneracy between the orbiting mass and the inclination angle, only a minimal mass $m_p * \sin i$ for the planet can be determined.

Planetary transits yield many properties, namely mass and radius of the host star, along with the radius and inclination angle i of the planet. The transit technique has come to fruition in recent years, with the detection of more than 30 Jupiter-mass extrasolar transiting planets (Extrasolar Planet Encyclopedia Web site, `http://www.obspm.fr/encycl/encycl.html` in close-in orbits (< 0.05 AU). The radius of planets can only be determined from transiting planets, representing the principal motivation and strength of the transit technique. A radius measurement is an important quantity, since it allows to constrain the evolutionary and migration history of the planet and to infer its composition and atmosphere through evolutionary models. The diversity of the performed studies and the acquired knowledge after the detection of many transit events motivated the use of this technique as a tool for exoplanet discoveries.

Over 20 ground-based experiments using the transit technique are being undertaken world wide. This technique is also the preferred one for space missions devoted to search of exoplanets: several missions from space with this target have been launched or are to be launched in the near future, such as MOST, Corot, and Kepler. In this scenario, the ground based missions – like Ogle, TReS, RATS, etc. – represent benchmarks for the observation strategy applied in the future space missions. In particular, RATS projects seeks high precision photometric results performed with stellar images which have been purposely de-focused. The French Corot mission search for extrasolar planets and their asteroseismology program are planning to collect ccd images which are slightly de-focused. The same observational approach has also been proposed for the Kepler extrasolar space mission as well.

In this thesis, I describe the RATS–*ARP* software developed in order to produce in a non-interactive mode the stellar lightcurves of images taken at Schmidt Telescope in searching for exoplanets using the transit method.

At the time, I have cooperate in studying the dynamical interaction between multiple stellar systems hosting planetary systems. We have numerically integrated the trajectories of the stars (binary plus singleton) and of test planets to investigate the above mentioned mechanisms. Our simulations show that the circumstellar environment during planetary formation around the primary was gravitationally less perturbed when the binary was part of a hierarchical triple because the binary was necessarily wider and, possibly, less eccentric. This circumstance has consequences for the planetary system in terms of orbital spacing, eccentricity, and mass of the individual planets.

All these arguments are treated and organized in the following structure:

- **Chapter 1**: description of the basic knowledge about the extrasolar planets, a review of the most prominent detection techniques, with particular attention to the method of transits;
- **Chapter 2**: description of RAdial velocities and Transit Search project, which is the context for the developing of the algorithm;
- **Chapter 3**: description of headerfits chosen *ad hoc* for the RATS images;
- **Chapter 4**: description of the photometric reduction background in which the RATS–*ARP* algorithm has been develop;
- **Chapter 5**: description of the implementation of different modules of RATS–*ARP*;
- **Chapter 6**: description of the results obtained from pipeline performance;
- **Chapter 7**: analysis of the main properties required in order to develop the future RATS images database;
- **Chapter 8**: description of the model and simulations describing the dynamical interaction among planets in multiple stellar systems;
- **Chapter 9**: conclusions with discussion of results and future work;
- **Appendix A**: RATS–*ARP* User Requirements Document (URD);
- **Appendix B**: RATS–*ARP* Software Requirements Document (SRD);
- **Appendix C**: RATS–*ARP* Architectural and Design Document (ADD);
- **Appendix D**: RATS–*ARP* Software User Manual (SUM);
- **Appendix E**: RATS–*ARP* Code Documentation.

We report, here below, a table containing the masses of some planets of our Solar System recalled in the next chapters.

	g	$N_{M_\odot}$	N_{M_J}	$N_{M_\oplus}$
$M_\odot$	$2 \cdot 10^{33}$	1	$\simeq 10^3$	$333 \cdot 10^3$
M_J	$2 \cdot 10^{30}$	$\simeq 10^{-3}$	1	318
$M_\oplus$	$6 \cdot 10^{27}$	$3 \cdot 10^{-6}$	$3 \cdot 10^{-3}$	1
M_S	$5.7 \cdot 10^{29}$	$2.8 \cdot 10^{-4}$	$2.8 \cdot 10^{-1}$	95
M_U	$8.7 \cdot 10^{28}$	$4.5 \cdot 10^{-5}$	$4.5 \cdot 10^{-2}$	14.5
M_N	$\simeq 10^{29}$	$0.5 \cdot 10^{-4}$	$0.5 \cdot 10^{-1}$	17

Table 1: In the first column are recorded the masses' symbols of, respectively: Sun ($M_\odot$), Jupiter (M_J), Earth ($M_\oplus$), Saturn (M_S), Uranus (M_U) e Neptune (M_N). In other columns there are the values of these masses given in grams (g), in mass solar number ($N_{M_\odot}$), in Jovian mass number (N_{M_J}), in terrestrial mass number ($N_{M_\oplus}$). The values are taken from *NASA Astrophysics Data System*.

Part I

Photometric Reduction and analysis software

Chapter 1

The physical context

During the last decade, we have witnessed the birth of a new branch of astronomy: the study of planets orbiting stars other than the Sun. Three years after the discovery of the first planets around pulsars (Wolszczan & Frail, 1992), Mayor & Queloz (1995) announced the first exoplanet orbiting around a Sun-like star, 51 Peg *b*. These surprising first results were just the beginning of a whole set of questions that arose almost at the same cadence as planets were detected. One important consequence of these questions was the necessity to find more systems, in order to try to distinguish between regularity and peculiarity in these exo-worlds. As a consequence, and as the refinement of the detection techniques evolved, more and more planets have been detected, providing clues to the planetary formation in other stellar systems.

Most of the more 200[1] up to now known planets have been detected using the same technique, based on the precise Radial Velocity (RV) measurements of the host star.

In this section, we briefly review this and other techniques used to detect exoplanets, paying special attention to their major findings and the current status (§1.1). After that, we will concentrate on the transit method (§1.2), providing the planetary parameters that can be known and reviewing the measurable parameters, the false positives events, the different kind of noises that can affect the measures, and the analysis approach of light curves. The first planet that exhibited transits, HD209458b which is also currently the best known planet outside our Solar System, is treated in more detail in §1.3. This object, according to some authors, turned out to be bigger in size than expected, and several interesting discussions arose from this fact, summarized in §1.4. Then, we outline the current theories for the formation of these objects (§1.5). We conclude this chapter with a hint at the motivations for this study (§1.6).

1.1 The Exoplanets

1.1.1 Working definitions

In this work, we will use the definition of *Extrasolar Planet*[2] given by the Working Group on Extrasolar Planets (WGESP) of the International Astronomical Union (IAU), which states:

[1]Extra Solar Planets Encyclopaedia, by J. Schneider: `http://www.obspm.fr/encycl/encycl.html`
[2]`http://www.ciw.edu/boss/IAU/div3/wgesp/denition.html`

1. Objects with true masses below the limiting mass for thermonuclear fusion of deuterium (currently calculated to be 13 Jupiter masses for objects of solar metallicity) that orbit stars or stellar remnants are *planets* (no matter how they formed). The minimum mass/size required for an extrasolar object to be considered a planet should be the same as that used in our Solar System.

2. Sub-stellar objects with true masses above the limiting mass for thermonuclear fusion of deuterium are *brown dwarfs*, no matter how they formed nor where they are located.

3. Free-floating objects in young star clusters with masses below the limiting mass for thermonuclear fusion of deuterium are not planets, but are *sub-brown dwarfs*.

As pointed out by this group, this constitutes a reasonable working definition of a planet, which is a compromise between definition based on the deuterium-burning mass and the formation mechanism. A better definition will have to wait until more knowledge is acquired.

We will use the term exoplanet as a synonym of the previous concept, as it is also widely used in the community.

The term *Hot Jupiter* will be used throughout this work to mean the planets with masses $m_p \sin i \leq 13 M_J$ (m_p is the planetary mass; i the inclination of the orbital plane respect to the line of sight; M_J is the Jupiter Mass, quoted in Table 1) orbiting close to a parent solar-like star (semimajor axis $a < 0.1$ AU). They are also referred to in the literature as *51Peg b like-objects* or *Close-in Extrasolar Giant Planets (CEGP)*. Some authors (Bouchy et al., 2004) have suggested the term *Very Hot Jupiter* or *Extremely Close-in Extrasolar Giant Planets* for the planets with periods much lower than 3 days (implying typically orbits with $a < 0.025$ AU). As there is no clear consensus in the division among these two classification, we will adopt the more general *Hot Jupiter* denomination as defined above, but we emphasize that it constitutes a working definition throughout this work.

1.1.2 Exoplanets around pulsars

Pulsars are the cores that remain after a Supernova explosion of a star with a mass between 15 and 30 $M_\odot$. These cores are neutron stars, which host strong magnetic fields. If the spin axis of the star and its magnetic field are not aligned, then a beam of radio waves hits the Earth at extremely regular intervals, which range between 2 milliseconds and 2 seconds. The typical rate of change of the period of these objects is thought to be one second every ten million years (Van Straten et al., 2001). Thus, changes in the period faster than this are the effect of orbiting companions to the pulsar. The precision in the pulsar timing is such as to detect objects with Earth masses or even lower. For a detailed review of these concepts and pulsar astronomy in general, we recommend the book by Lorimer & Kramer (2005).

The first indirect detection of an exoplanet was made by Wolszczan & Frail (1992), and in later works (Wolszczan, 1994; Wolszczan et al., 2000) the model was refined, in order to establish, respectively, the existence of one Mercury-sized planet (b), two Earth-sized planets (c & d), and an asteroid-mass object (e,Wolszczan & Konacki, 2005), with masses of 0.020, 4.3, 3.9, and 0.15 M_{Pluto} orbiting at distances of 0.19, 0.36, 0.46 and 2.7 AU respectively from the 6.2-millisecond pulsar PSR B1257+12.

The pulsar planets have also provided the first demonstration of orbital resonances between exoplanets (Wolszczan, 1994; Wolszczan et al., 1999), as planets c and d exhibit a near 3:2 mean motion resonance. The gravitational perturbations between the two planets have been detected by the same authors, and used to estimate the masses and inclinations of the orbits of the two most massive planets (Wolszczan et al., 2003b). The almost coplanar measured inclinations, and the near 3:2 resonance, strongly support the hypothesis of a disk origin for these planetary system.

It is currently thought that these objects formed in a massive circum-pulsar disk, instead of being remains of an original planetary system of the pulsar parent star that survived the Supernova explosion. Miller & Hamilton (2001) and Hansen (2002) examined the conditions of survival and evolution of these pulsar protoplanetary disks, concluding that these planets should grow in a typical 10^7 yr timescale, if the initial disk is sufficiently massive (greater than 10^{25} kg). A smaller disk would not survive the evaporation caused by the pulsar accretion flux. There are some proposed schemes for the quick formation of such a massive disk, for instance by tidal disruption of a stellar companion (Stevens, Rees & Podsiadlowski, 1992; Phinney & Hansen, 1993) or in the process of a white dwarf merger (Podsiadlowski, Pringle & Rees , 1991; Livio, Pringle, & Saer, 1992). These processes would not be very common. That would explain the lack of planetary companions in the vast majority of millisecond pulsars (48 Galactic pulsars studied by Lorimer, 2001).

1.1.3 The Radial Velocity Searches

The precise study of the radial velocity behavior of nearby dwarf stars has been the most successful method to detect exoplanets to date.

Since the first detection of a companion to 51 Peg *b* (Mayor & Queloz, 1995), most of the known planets up to now have been found as a result of velocity oscillations in the host star induced by the presence of a planetary mass companion. The companion pushes the star back and forth along our line of sight at a velocity with an amplitude of K_s; if we assume that $M_p \ll M_s$, and the eccentricity of the planet's orbit is e, then the minimum mass of the planet is given by the expression:

$$M_p \sin i \simeq \left(\frac{P}{2\pi G}\right)^{1/3} K_s M_s^{2/3} (1-e^2)^{1/2} \tag{1.1}$$

and, from the Kepler's laws:

$$a_p \sin i \simeq \left(\frac{GM_s}{4\pi^2}\right)^{1/3} P^{2/3} \tag{1.2}$$

where M_p is the mass of the planet, a_p is the orbital semimajor axis, M_s is the mass of the star and i is the orbital inclination (see Figure 1.1). Using various identities leads to the following expression for the amplitude of the movement:

$$K(\mathrm{m/s}) = \frac{30 M_p \sin i}{(a_p M_s)^{1/2}} \tag{1.3}$$

where the M_p is now given in Jupiter masses, M_s in Solar masses and a_p in AU. This movement of the star can be accurately measured using the Doppler effect. The shift produced by a planetary object is of the order of tens or hundreds of m/s (the amplitude of the Sun's movement due to Jupiter is $\sim$ 12.5 m/s, due to Saturn $\sim$ 4 m/s, and due to the Earth $\sim$ 8 cm/s; 51 Peg *b* moves the

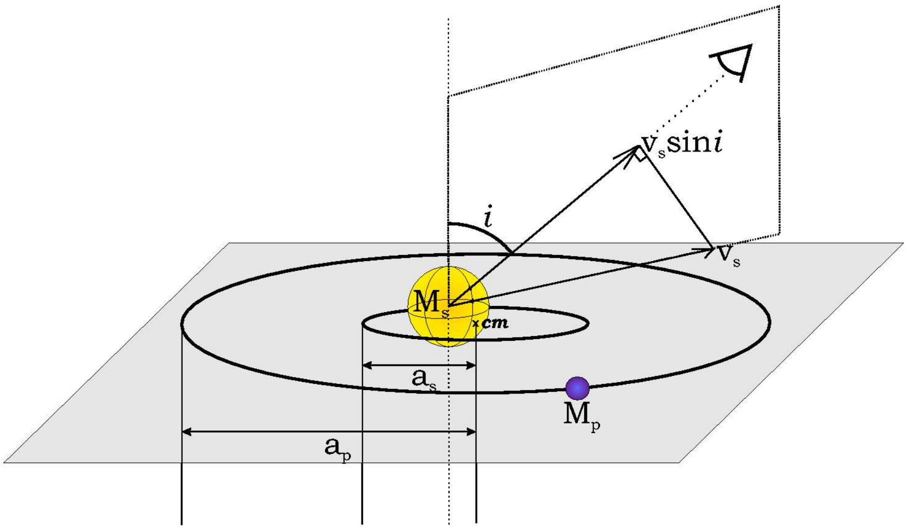

Figure 1.1: Schematic view of the main orbital definitions. The star s and the planet p orbit their center of mass cm, in circular orbits with a radius of a_s and a_p respectively. The orbital plane is plotted in gray, and the inclination of the orbit i is defined as the angle between the normal to this plane and the observer's line of sight. The observer is located in the upper right part of the diagram. An edge-on orbit corresponds to an angle of 90°. The reflex motion of the star v_s, when measured along the line of sight, is affected by the sine of this angle.

host star by $\sim$ 59 m/s), which translates to the necessity to measure shifts in the spectral lines with a precision of roughly 1/1000 of the spectral line width. To achieve this, the radial velocity surveys[3] observe typically sun-like stars (because many spectral lines are needed to improve the measurements) and slow rotators (because fast rotation causes the lines to be broader, and thus the precision is decreased). The information on the radial velocity of the star contained in all spectral lines needs to be concentrated to achieve the required precisions. This is done by computing the cross-correlation between each observed spectrum and a reference spectrum. This reference may be the spectrum of a standard star with well-established radial velocity, or one spectrum of the program star itself. The technique of the cross-correlation function was firstly applied to astronomy by Simkin (1974).

The spectrograph behavior has also to be kept under control, to achieve the required precisions, and a radial-velocity reference serves to accomplish this. There are currently two different techniques to establish this reference: a simultaneous thorium-argon lamp observation (see, e.g. Konacki et al., 2003c) and an Iodine absorption cell (see, e.g. Cumming et al., 1999, and references therein). While the Iodine cell is placed into the path of the star signal, before entering the spectrograph (and thus reducing the signal of the star), the thorium lamp is observed simultaneously as the object (with optical fibers). On the other hand, the advantage of an Iodine cell is the more precision of wavelength calibration. This technique is applied at TNG with the SARG cross disperser spectrograph. SARG (Gratton et al., 2001) offers both single object and long slit (up to 26 arcsec) observing modes, covering a spectral range from $\lambda = 0.37$ up to 1μm and with a resolution ranging from $R = 29000$ up to $R = 164000$. Cross dispersion is provided

[3] see, for instance, `http://www.obspm.fr/encycl/searches.html`

by a means of selection of four grisms. SARG was designed as a multi-purpose instrument, in order to satisfy the scientific needs of a rather wide community, working on a variety of themes, ranging from stellar abundance analysis or extended objects, to line profile studies and accurate radial velocity measurements. Early results showed that, among others, that SARG works with a radial velocities accuracy of ~ 3 m/s using the Iodine cell and ± 150 m/s without the Iodine cell.

Another difficulty with the radial velocity technique is the necessity to maintain good tracking on the star, as its slight movements in and out of the slit can produce spurious radial variations of the star.

At the state of art instruments, such as HARPS (Pepe et al., 2002), working at the 3.6 m ESO telescope at La Silla Observatory (Chile), are beginning to obtain precisions of order of 1 m/s. These allow the detection of objects with roughly Neptune's size or even smaller ones (Santos et al., 2004b; McArthur et al., 2004; Butler et al., 2004).

Despite the unquestionable success of this technique in the last decade, there are a few drawbacks. Below 1 m/s, the precision in the radial velocities is not longer determined by the instrument, but by the intrinsic pulsations of the star (*asteroseismology*), which can have amplitudes of several cm/s, and by the magnetic features on the atmosphere, such as spots, faculae and flares. Even if some of these effects can be modelled and removed (Saar et al., 2003; Kürster et al., 2003), the difficulty increases when trying to reach lower detection thresholds. Thus, it seems difficult for this technique to reach the detection threshold of Earth-sized exoplanets.

Another mayor drawback of the radial velocity searches is that the orbital inclination cannot be known, and thus the exact mass of the planet remains unknown. Actually, only lower limits on the mass can be provided. There are at least two ways to solve the inclination degeneration: astrometric measurements (need to be taken from space to achieve the required precisions) with just one successful case: GJ 876 (Benedict et al., 2002), and the transit method, which will be discussed deeply in this work.

1.1.4 Characteristics of the known exoplanets, derived from the RV surveys

From the sample of planets detected up to now, using mainly the radial velocity technique, a few trends and characteristics of the objects found so far and their host stars are worth mentioning:

- The **fraction of stars** whose planets have masses $M_p > 0.47 M_J$, determined from the Elodie survey is:
  - ▷ $0.70 \pm 0.5\%$ of the surveyed stars have planets with periods below 5 days;
  - ▷ $4.0 \pm 1.1\%$ with periods below 1500 days (4.1 yrs);
  - ▷ $7.3 \pm 1.5\%$ with periods below 3900 days (10.7 yrs).
- The **secondary mass function** is increasing towards low-massive planets, while it also increases toward stellar companions with masses $\gtrsim 0.1 M_\odot$ (see, e.g. Halbwachs et al., 2003). There is a noticeable lack of brown dwarf companions orbiting close to their host star, which is commonly referred as the *brown dwarf desert*. This might point towards a different formation mechanism for the stellar and the planetary companions.
- The **eccentricities** of most of the planets with semimajor axis above 0.06 AU are distributed almost uniformly between 0 and 0.7. All planets with lower semimajor axis re-

side in circular orbits (Goldreich & Soter, 1966, for an estimation of the circularization timescales). The origin of the eccentricities for single planets is not well understood (Marcy et al., 2003, and references therein for plausible mechanisms).

- The **stellar metallicity** of the host stars seems higher for stars with detected planets than for those without detected planets (Santos et al., 2003; Israelian, 2003, for reviews on studies on the iron content, and on other metals, respectively). For instance, Fisher & Valenti (2005) have quantified the planet-metallicity relation for stars with extrasolar planets that have velocity amplitudes $K > 30$ m s^{-1} and orbital periods shorter than 4 yr. In a sample of 850 selected stars, fewer than 3% of stars with sub-solar metallicity have detected planets. However, above solar metallicity, there is a smooth and rapid rise in the occurrence of detected gas giant planets as a function of increasing metallicity. In the highest metallicity bins ($[Fe/H] > +0.3$ dex), 25% of the stars have detected gas giant planets. The authors also find that the high metallicity may play a role in the fraction of stars with multiple-planet systems. Among stars with planets, only 1 of 22 stars (4.5%) with sub-solar metallicity has a multiple-planet system, compared to 13 of 98 stars (13%) with $[Fe/H] > 0.0$. There is also a tendency for the total detected planet mass to increase with increasing metallicity. Fisher & Valenti (2005) conclude that high stellar metallicity appears to be the best predictor for the presence of a gas giant planet.

- The **period-mass distribution** reveals a lack of massive planets in short period orbits (Udry et al., 2002; Zucher & Mazeh, 2002). Furthermore, there seems to be a shortage of planets in the $10 - 100$ days period range, and a lack of light planets ($M_p \sin i < 0.75 M_J$) in orbits with periods larger than 100 days (Udry, Mayor & Santos, 2003). These authors provided possible implications in the distribution of these effects, which seem to be in agreement with the current migration scenarios. Another characteristic of this distribution is an apparent *pile-up* of planets with periods in the $3 - 3.5$ days range. Roughly half of the planets with periods below 10 days have periods in this short range, which may also be providing clues for the migration history of these objects (Gaudi, Seager & Mallen-Ornelas, 2005).

1.1.5 Microlensing

Planets orbiting around other stars can also be detected with the gravitational microlensing effect (Mao & Paczyǹski, 1991; Gould & Loeb, 1992).

When a star (the lens) passes in front of a background source, this effect causes a magnification with a well known symmetrical lightcurve profile. If the star is orbited by a planet, it will also leave a signature on the lightcurve, which can even potentially serve to discover earth-sized planets (Bennet & Rhie, 1996). Several projects have followed this approach:

- MACHO, Alcock et al. (1993);
- PLANET, Kubas et al. (2005) and references therein;
- OGLE, Udalski (2003);
- MOA, Bond et al. (2001);

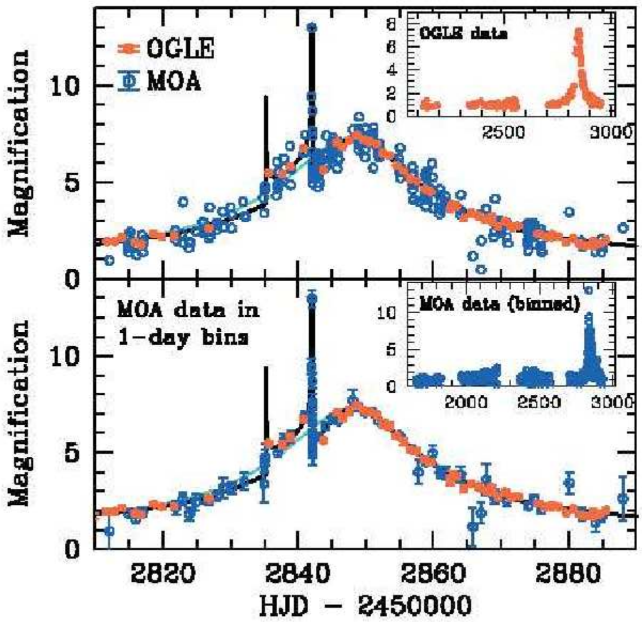

Figure 1.2: Lightcurve with best-fitting and single-lens models of O235/M53 (from Bond et al., 2004).

- MPS, Rhie (2001).

Bond et al. (2004) claim the first confirmed detection of a planetary microlensing event (Figure 1.2) detected from two different sites (the event was named OGLE 2003-BLG-235/MOA 2003-BLG-53, O235/M53 hereafter). The shape of the event can provide the mass ratio between the star and the planet, and the distance of the planet to the star at the moment of the event. Unfortunately, these events are unique, and almost impossible to be observed repeatedly. Also, the blend between the source and the lens (which is the system star-planet) makes it difficult to measure the characteristics of the star, and thus to determine the planetary mass. In the case of O235/M53, the proper motion of the star (lens) should allow resolving lens and star in about 10 years, if adaptative optics are used (Bond et al., 2004). Only at that time the assumed main sequence nature of the lens star will be proven.

Apparently, the power of this method resides in its ability to detect planets in many different systems (Bennet & Rhie, 2002), which include planets in very wide orbits, low mass planets, and even planets in other galaxies. A space mission proposed by these authors, using a $1-2m$ aperture space telescope to monitor $\sim 10^8$ Galactic Bulge main sequence stars, should allow the determination of the average number of planets per star down to $0.1 M_\oplus$ at separations from ~ 0.7 AU to ∞ for terrestrial planets and from 0 AU to ∞ for giant planets, among other scientific outputs.

1.1.6 Direct imaging

Direct observations of exoplanets face the difficulty of the high contrast between the light coming from the star and from the planet, which is of the order of $\sim 10^9$ in the optical and $\sim 10^6$ above

$\sim 10\mu m$, for a Jupiter-like planet in a Jupiter-like orbit. Coronography and interferometry are planned at the different largest telescopes, both from ground and space. The most sensitive cases are young big planets orbiting far out from the parent star ($d > 50$ AU), around nearby stars. These detections, are thus complementary to those of the radial velocity and transit searches, which are more sensitive to planets close to the central star.

A promising candidate for the first detection of a exoplanet with direct imaging techniques is the candidate planetary companion to 2MASS1207334-393254 (hereafter 2M1207, Chauvin et al., 2004). It was detected using the VLT/NACO adaptative optics system. It is apparently orbiting at a distance of ~ 55 AU of the $\sim 25M_J$ brown dwarf 2M1207. Near Infrared photometry (Figure 1.3, left) and spectroscopy are compatible with a spectral type of the companion of L5-L9.5, which places the object in the planetary regime with a mass of $M = 5 \pm 2M_J$, according to different evolutionary models, and a temperature of $T_{eff} = 1250 \pm 200K$ (Chauvin et al., 2004). A later study with the *Hubble Space Telescope* (*HST*) seems to confirm the planetary nature of this candidate (see Figure 1.3, right, by Schneider, 2005).

New observations with the same optical configuration, taken at three different epochs, show that the candidate shares the same proper motion as the brown dwarf, and thus it is not, with a high confidence level, a stationary background object (Chauvin et al., 2005).

Another massive planet or minimum mass brown dwarf has been reported recently by the same investigation group, around the young nearby star AB Pic (Chauvin et al. 2005b, accepted). It was detected as a faint, red source located 5.5" South of the AB *Pic* star, and apparently it also shares the same proper motion. The evolutionary models predictions, based on the JHK photometry, indicate a mass of 13 to 14 M_J for this object, if its age is ~ 30 Myr.

The masses and sizes of these directly detected objects rely on predictions from evolutionary models (Burrows et al., 1997; Chabrier et al., 2000; Baraffe et al., 2002), which depend on hard-to-measure estimates of the age of the system. Thus, these mass measurements of the planets do not achieve the precision obtained by the radial velocity surveys.

A project which aims at the direct detection is SPHERE planet finder at VLT. SPHERE (Spectro-Polarimetric High-contrast Exoplanets REsearch) is a second generation instrument for VLT optimized for high contrast imaging at the Nasmyth focus of one of the VLT units. For this reason, it is optimized for direct observations of faint sources near bright stars. The instruments is optimized for the detection of reflected light of old planets and for the detection of the thermal radiation of young planets in extrasolar systems. A large telescope and special techniques are required to make direct detection of extrasolar planets possible. The challenge consists in the very large contrast between the host star and the planet, at very small angular separations, typically inside the seeing halo. Thus the planet finder instrument consists of an extreme adaptive optics system to restore partly the smearing caused by Earth's atmosphere, a stellar coronagraphs which efficiently block the light from the bright star (Claudi et al., 2006).

1.1.7 Astrometry

As in the case of the radial velocity searches, this method relies in the gravitational wobble induced by a planet in its star. If D is the distance to the star (in parsecs) and a is given in AU, then the observed wobble is:

$$r(\text{mas}) \sim 1000\frac{M_p a}{M_s D} \tag{1.4}$$

It should be noticed that this technique then favors the detection of massive planets in large

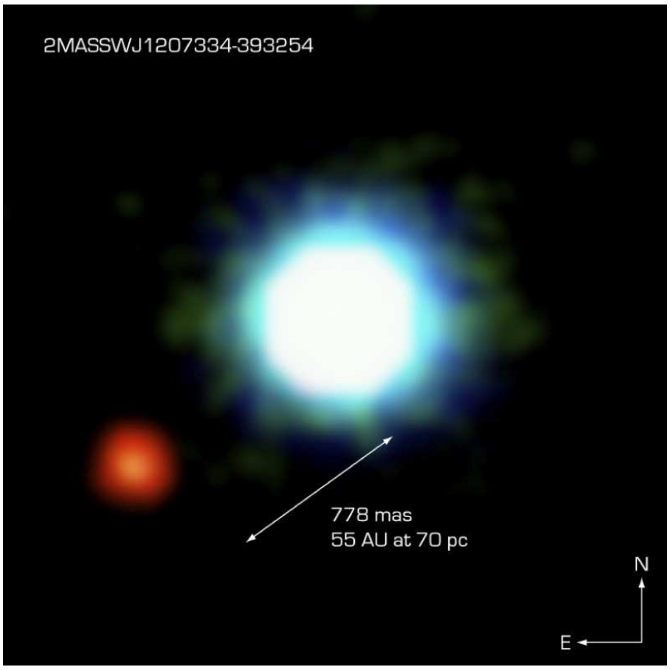

Figure 1.3: The possible first exoplanet detected by direct imaging (*in red*), around the brown dwarf 2M1207 (*in blue*) (Chauvin et al., 2004).

orbits around nearby stars. If we were observing our Solar System at a distance of 10 pc, then the wobble induced by Jupiter would have a maximum amplitude of $r = 500$ μas; Uranus would move the Sun by $r = 100$ μas, and the Earth only $r = 0.3$ μas.

In this technique, the movement of the star is measured directly from the center of the stellar profile in one image, and thus needs systems with superb resolving power. This implies the use of interferometry, of space-borne telescopes, or both. For this reason, this technique will provide excellent tests and technology for the future space interferometric missions, such as Darwin-TPF (Fridlund, Henning & Lacoste, 2003), aimed to take images and spectra of Earth-like planets around nearby stars. But, it seems that it will be very difficult to measure the center of a star with an accuracy better than 1 μas, because of distortions in the star's image created by stellar spots.

As these lines are written, there has been only one important published success of the astrometric method, when it was used to estimate the inclination of the planet around the M4V star GJ 876 (Benedict et al., 2002). To study the perturbation on the star caused by the most massive planet ($1.89M_J$) in the system, GJ 876b, the Fine Guidance Sensors (FGS) on-board *HST* were used to estimate the amplitude of the astrometric perturbation of the planet as $r = 250 \pm 60\mu$as. As a direct consequence, and knowing the orbital parameters ($P = 61$ d, $a = 0.21$ AU, $e = 0.1$, *minimum mass* $= 1.89M_J$) from radial velocity measurements (Delfosse et al., 1998; Marcy et al., 1998) the orbital inclination of the planetary companion was estimated as $84 \pm 6°$, which, together with the minimum mass determination, resulted in a measured mass of the object of $M_p = 1.9 \pm 0.5M_J$.

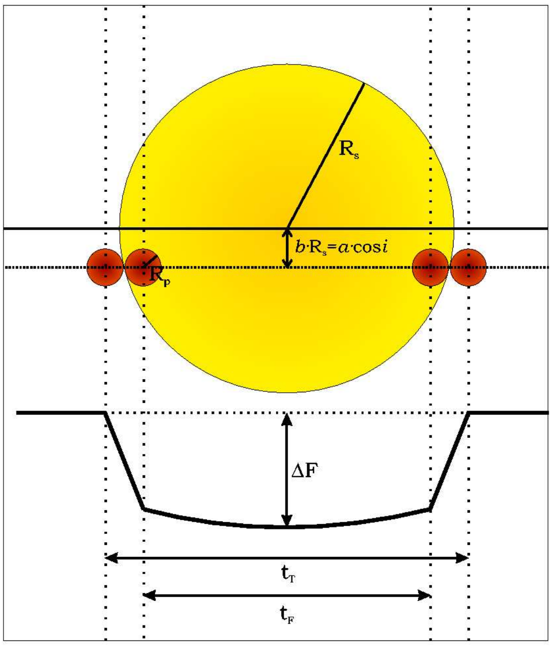

Figure 1.4: Schematic view of the main transit definitions. *Top:* The planet is plotted in four different positions (first to fourth contact). *Bottom:* The flux of the star (solid line) is reduced by an amount ΔF during a transit with a total duration of t_T; the duration between ingress and egress is t_F, and it is also referred as the *flat part* of the transit. The slight curvature of this part is a consequence of the star's limb darkening. Also plotted is the *impact parameter* b, where the definition of the inclination angle i is represented in Figure 1.1.

1.2 The transit method

The first reference about the transit method is given in Struve (1952). If a planet with a radius R_p is seen (from a far enough place, such that the perspective effects are negligible) crossing the disk of a star with radius $R_\star$, causing an event called *transit*, then the flux of the star will decrease by:

$$\Delta F_\star = \frac{R_p^2}{R_\star^2} \tag{1.5}$$

In the case of Jupiter passing in front of the Sun, this $\Delta F_\star$ would be $\sim 1\%$, that is easily detectable with ground-based photometry. The Earth would produce an $\sim 0.0084\%$ transit, which can be detected with space telescopes (Brown et al., 2001), but is not currently possible from ground. Assuming a circular orbit, the transit would last (Seager & Mallen-Ornelas, 2003):

$$t_T = \frac{P}{\pi} \arcsin\left(\frac{R_\star}{a \sin i}\left\{[1 + R_p/R_\star]^2 - [(a/R_\star)\cos i]^2\right\}^{1/2}\right) \tag{1.6}$$

where P, a and i are the period, radius and inclination of the planet's orbit respectively. The inclination is the angle between the normal of the orbital plane and the line of sight. This means that $i = 90°$ is for a planet crossing the star through the middle (solid lightcurve in Figures 1.4 and 1.5). The typical transit durations for Hot Jupiters are 2-3 hours. Assuming circular orbits

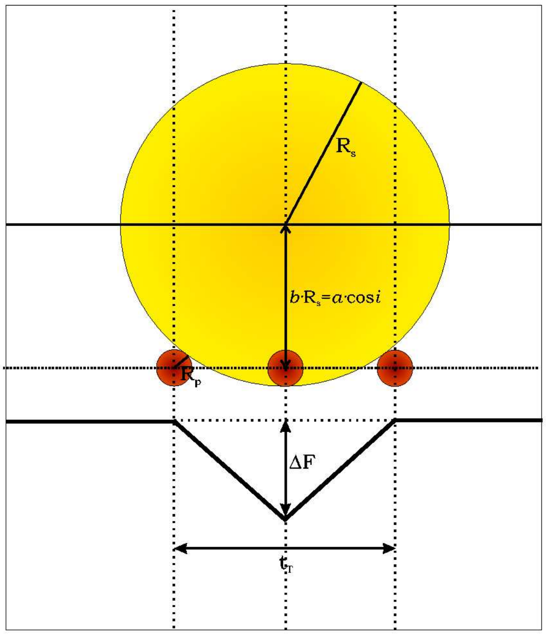

Figure 1.5: Same as Figure 1.4, for the case in which the planet is never projected completely on the stellar disk is plotted in the bottom part. In this case, there are no second nor third contacts, an thus there is no flat part of the transit (i.e., $t_F = 0$).

for the planets, and with a first order approximation $M_\star = M_\odot$, $R_\star = R_\odot$ (in Solar units), Figure 1.6 plots the maximum duration of a $1R_J$ planetary transit as a function of the mass of the star and the period of the planet. This maximum duration can be used as a tool to discard false positives in transit searches.

For such an effect to be observable, the orbit of the planet must cross the line of sight of the star. The probability for this to happen is:

$$P_{\rm tran} = \arctan \frac{R_\star + R_p}{a_p} \sim \frac{R_\star + R_p}{a_p} \quad (1.7)$$

which is low for planets such as Jupiter in our Solar System ($P_{\rm trans} = 0.089\%$), but can be as high as 10% for the Hot Jupiter class objects. The existence of this kind of objects, orbiting $\sim 0.7\%$ of the main sequence stars in the solar neighborhood (see §1.1.4), and the relatively high probability of transits, have motivated a number of transit searches for exoplanets (see Horne et al., 2001, for a review).

The first transiting planet, HD 209458b, was discovered in 2000 (Charbonneau et al., 2000; Henry et al., 2000), but it had been previously detected with the RV method (Mazeh et al., 2000) Mazeh et al. 2000 . We will treat this object in detail in §1.3. The success of these transit searches (discovering planets with the transit method, not previously known from any other technique) came from the OGLEIII team (Udalski et al., 2002a,b,c; Udalski, 2003; Udalski et al., 2004),who have at this time published a list of 177 transiting planet candidates. This project uses a 1.3m telescope placed at the Observatorio de La Silla in Chile, to monitor dense fields for long period of times, with I magnitudes ranging from 13.5 to 17. This places the bulk of the stars at typical distances of 1000 pc. Further follow up works demonstrated that the vast majority of these candidates turned out to be false positives, but 5 planets have been detected to date:

- OGLE-TR-56b (Konacki et al., 2003a);
- OGLE-TR-113b, independent confirmation by (Konacki et al., 2004);
- OGLE-TR-132b (Bouchy et al., 2004);
- OGLE-TR-111b (Pont et al., 2004);
- OGLE-TR-10b (Konacki et al., 2005).

Three of these planets, (OGLE-TR-56b, OGLE-TR-113b, OGLE-TR-132b), apparently orbit their stars with shorter periods than had ever been observed with the radial velocity surveys. This fact led to several authors to group these objects under the terminology of *Extremely Hot Jupiters*. As can be seen in Eq. 1.7, the probability of observing transits from Earth is bigger as the planet is closer to its host star.

The advantages of these deep-field transit searches are that the population of main sequence stars is constituted of smaller stars on average, which can lead to the discovery of smaller planets. Also, differential atmospheric extinction problems are less important as the field of view gets narrower. The major drawbacks are the difficulty of the follow-up observations and thus the precision with which the planet's parameters can be known. The kind of studies performed in HD 209458 are difficult, if not impossible, to repeat in these much fainter stars.

1.2.1 *The measurable parameters*

From the shape and period of the photometric transit (depth of the transit F, total duration t_T, duration of the flat part of the transit t_F, period P), four measurable parameters can be calculated (Seager & Mallen-Ornelas, 2003).

The planet to star radius ratio:

$$\frac{R_p}{R_\star} = \sqrt{\Delta F} \tag{1.8}$$

The impact parameter b:

$$b = \frac{a}{R_\star}\cos i = \left\{ \frac{(1-\sqrt{\Delta F})^2 - [\sin^2(t_F\pi/P)/\sin^2(t_T\pi/P)](1+\sqrt{\Delta F})^2}{1-[\sin^2(t_F\pi/P)/\sin^2(t_T\pi/P)]} \right\}^{1/2} \tag{1.9}$$

The ratio $a/R_\star$:

$$\frac{a}{R_\star} = \left\{ \frac{(1+\sqrt{\Delta F})^2 - b^2[1-\sin^2(t_T\pi/P)]}{\sin^2(t_T\pi/P)} \right\}^{1/2} \tag{1.10}$$

And the stellar density, assuming $Mp \ll M_\star$:

$$\rho_\star \equiv \frac{M_\star}{R_\star^3} = \left(\frac{4\pi^2}{P^2G}\right)\left(\frac{a}{R_\star}\right)^3 = \left(\frac{4\pi^2}{P^2G}\right)\left\{ \frac{(1+\sqrt{\Delta F})^2 - b^2[1-\sin^2(t_T\pi/P)]}{\sin^2(t_T\pi/P)} \right\}^{3/2} \tag{1.11}$$

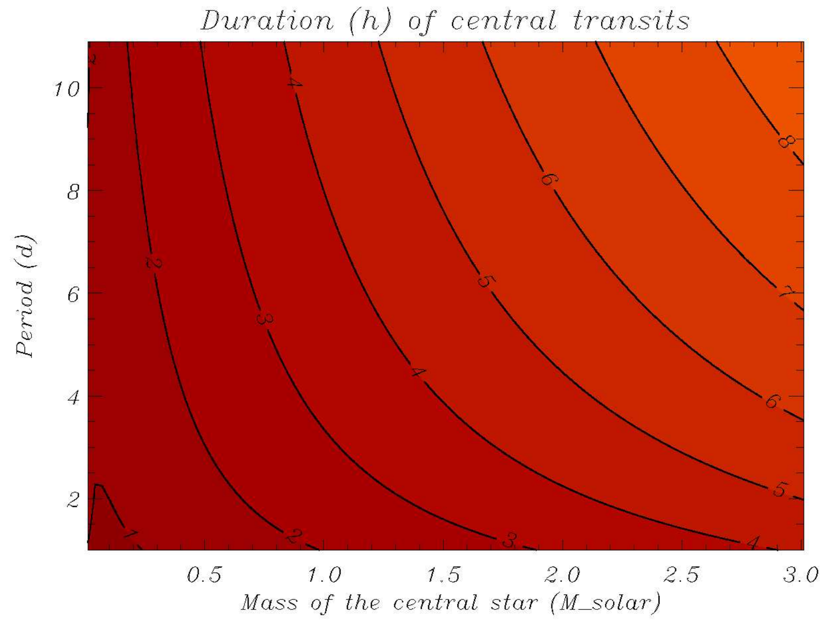

Figure 1.6: Maximum duration (in hours) of a central ($i = 90°$) transit, as a function of the star's mass (in Solar units) and the planet's period (in days). Circular orbits and $M_\star = M_\odot$, $R_\star = R_\odot$ (main sequence stars) have been assumed.

In these formulas limb darkening has not been considered and circular orbits have been assumed. Combining the measured inclination i (which can be extracted from Eqs. 1.9 and 1.10), with information on the orbit that results from radial velocity measurements (Eq. 1.3), it is possible to solve the degeneracy between the mass and the inclination, and get the exact mass of the planet. Assuming a radius for the star (for instance, from the spectroscopic information and the values tabulated in Cox, 2000), and using Eq. 1.8, the radius of the planet can be measured. Combining these two physical quantities, it is possible to measure the mean density of the planet.

1.2.2 The false positives

Not everything that looks like a transit is caused by a Hot Jupiter. There are a number of stellar systems that can mimic transit shapes, specially when dealing with data whose signal is close to the noise level. For wide-field searches, the expected most common cases are (Brown, 2003):

- **Stellar binaries.** Two large stars, when eclipsing at an inclined angle, can produce shallow transit-like dips in the lightcurve. These cases produce, on average, rather deep signals in the lightcurve and are the easiest to discriminate. Several hints are usually present in the lightcurve itself, such as a V-shaped transit curve, ellipsoidal modulations due to tidal effects, or a mismatch between the transit duration and the transit depth assuming a planet-sized transiting body. Nevertheless, at low signal-to-noise such systems can also be mistaken for planetary transits. They are easy to resolve with spectroscopic observations, thanks to the presence of the two sets of stellar lines in the spectra with large velocity variations. An eclipsing binary can be confused with a transit signal in two cases:

1. The stars have a similar $R_{\star 1}/R_{\star 2}$ as a main sequence star and a planet (typically, the star radius is 10 times bigger than the planet radius to produce 1% eclipses): this can be the case if one of the stars has an age as to have burned all the hydrogen in its nucleus and have started the postmain sequence stage, increasing its radius. Also, several combinations of main-sequence binary stars can have similar ratios of radii (Cox, 2000). A recent observational proof of the similar sizes for the lowest mass stars and the Hot Jupiters is the detection by Pont et al. (2005) of a $1.17^{+0.2}_{-0.13}$ R_J object with a mass of $96 \pm 9M_J$ and a period of 7.3 days. This was one of the transiting planet candidates identified by the OGLE survey (Udry, Mayor & Santos, 2003), and it constitutes the lowest mass star for which the radius has been measured. It is, thus, the densest (measured) main sequence star.

2. The stars can also be similar in size, but only produce grazing eclipses. These will be usually triangular in shape, but with signals close to the noise level, they can be confused with a transit. Planetary transits can also be grazing, and produce triangular-shaped transits if there are no 2nd and 3rd contacts. For this to be possible, the inclination must be between the values:

$$\arccos\left(\frac{R_\star + R_p}{a}\right) \leq i \leq \arccos\left(\frac{R_\star - R_p}{a}\right) \tag{1.12}$$

– **M-dwarf transiting companions.** A small M-dwarf transiting a larger star can produce a photometric signal closely similar to a planetary transit. If the companion is not larger than a hot Jupiter, and the orbital distance is too large for tidal and reflection effects to be detectable in the lightcurve, then the photometric signal is strictly identical to that of a planetary transit. In both cases, an opaque, Jupiter-size object transits the target star. These cases can only be resolved by Doppler observations, the amplitude of the reflex motion of the star revealing the mass of the transiting companion.

– **Triple (or multiple) stars systems.** An eclipsing binary can produce shallow transit-like signals if the eclipse is diluted by the light of a third star. There are many possible configurations for such systems, and as a result they can be very difficult to disentangle, even with Doppler information. In most cases, multiple systems are readily discriminated with high-resolution spectroscopy from the presence of several systems of lines in the spectra (Figure 1.7, lower left panel). However, in some cases, the parameters can conspire not only to mimic the lightcurve of a planetary transit, but also to induce planet-like variations of the inferred radial velocity, produced by the blending of several sets of lines in the spectra.

– **Generic false positives** Stellar variability and systematic trends in the photometry can produce fluctuations in the lightcurve interpreted as a possible transit signal, especially as one tries to detect shallower signals near the detection threshold. Further photometric observations at the epoch of the detected signal are needed in these cases to distinguish *bona fide* transits from false positives.

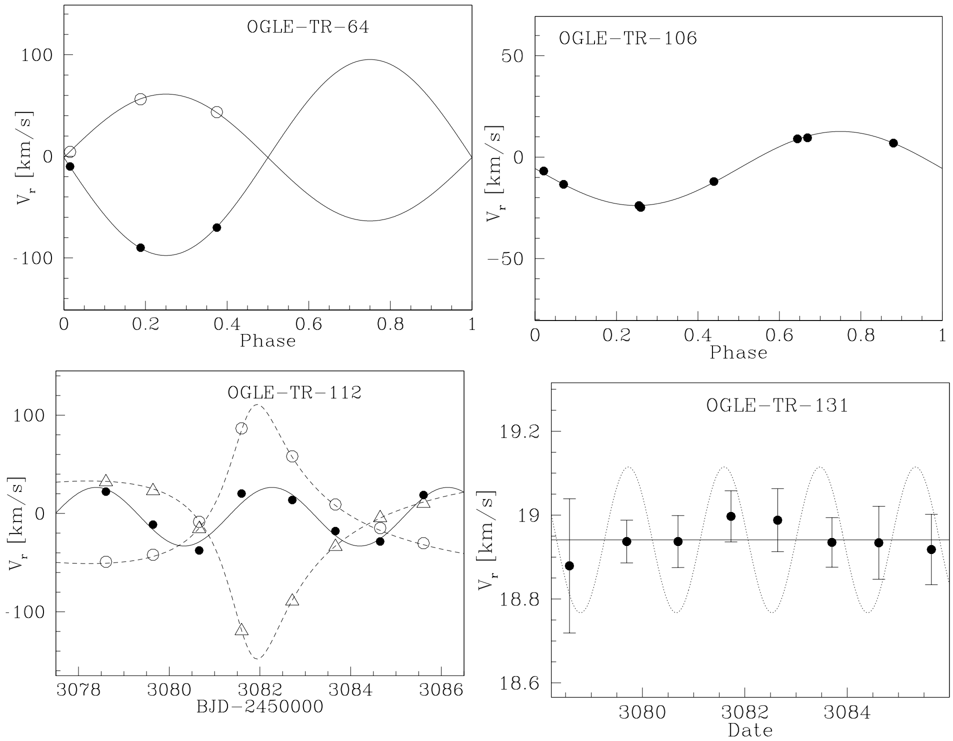

Figure 1.7: Example of radial velocity data for the four types of planetary transit false positives: grazing binary (*top left*), low-mass companion (*top right*), multiple system (*bottom left*) and false positive (*bottom right*, the dotted line indicates a Jupiter-mass orbit) (from Pont et al., 2005).

It has been noticed that the results up to now, however, have been meager in comparison with initial expectations. Most surveys have failed to confirm any transiting exoplanet candidate. The reason reside in the fact that deep transit surveys using large telescopes will produce candidates that are to faint to be confirmed spectroscopically with present-day telescopes ($V > 17$), and therefore will not lead to any confirmed transiting planet detection. This is in contrast to the very good detection rates "on paper" promised by the transits programs and represents a large drawback for them.

1.2.3 White and red noise

In theory, estimating the detection threshold and expected yield of a given transit survey is rather straightforward. The transit detection procedure is akin to finding a periodic square-shaped decrease in the flux from the target. The signal-to-noise ratio of the detection is the significance of the difference between the signal during the putative transit and the signal outside the transit. If most data points are outside the transit, the uncertainty on the continuum level is negligible, and the detection signal-to-noise is simply the transit depth divided by its uncertainty:

$$SNR = \frac{\text{transitdepth}}{\sigma/\sqrt{N}} \tag{1.13}$$

where σ is the photometric uncertainty on individual points and N is the number of data points during the transit.

To compute the expected yield of a given survey, one can simulate the population of target stars, assume a frequency of planet, then compute the expected number of detections given two conditions:

1. that at least two or three transits are observed (to establish the periodicity of the signal);

2. that the detection SNR is above some threshold, SNR_{min}. The SNR_{min} threshold is usually assumed between 7 and 10 according to the number of false detections deemed acceptable.

However, there is an important hidden assumption in equation 1.13 above: it is based on the assumption of white, independent noise. If the noise is not independent and has some covariance structure, then the equivalent formula is:

$$SNR = \frac{\mathrm{transitdepth}}{\sqrt{\sigma^2/N + 1/N^2 \sum_{i \neq j} cov[i;j]}} \tag{1.14}$$

where the $cov[i;j]$ are the elements of the covariance matrix. Therefore, the estimated yields based on the assumption of white noise are correct only if $\sigma^2/N >> 1/N^2 \sum_{i \neq j} cov[i;j]$. However, in real ground-based data in the relevant regime for hot Jupiters, the opposite is true. Plugging representative numbers shows that generally $1/N^2 \sum_{i \neq j} cov[i;j] > \sigma^2/N$.

In the jargon of signal analysis, the noise in photometric data has a *white* component (mainly photon noise) and a *red* component. The noise on ground-based millimagnitude photometry is *"pink"*. The red component comes from the systematics caused by the variations in atmospheric conditions, telescope tracking and detector characteristics. Figure 1.8 (left panel) displays an example of these three kinds of noise, white, red and pink. Ground-based photometric data at the millimagnitude level look like the bottom curve, with some white noise superimposed on some systematics trends on longer timescale.

It is clear that the systematic trends will limit the detectability of transit signals, especially the trends operating on hour timescale − the timescale of transits. What equation 1.14 expresses is that the detection threshold of transit surveys will depend on the average of the photon noise over a transit-length duration and the average of the covariance over this duration. The right panel of figure 1.8 shows the average of the curves in the left panel over a transit duration. It shows graphically what was found algebraically from Eq. 1.14: for transit detections, the effect of the red components dominates over that of the white component (because the white component averages out to very small values over the duration of transits, whereas the red component does not).

The implications of the presence of red noise in the photometric data on the expected yields of transit surveys are fundamental. In fact, in many cases a good approximation is to ignore the white noise entirely, and to base the detection threshold on the red noise only. As shown in Pont et al. (2005), this profoundly modifies the predictions for the sensitivity of ground-based transit surveys. Not only the resulting detection threshold is higher than with the white noise assumption, it also has a different dependence on period and magnitude. For instance, the presence of red noise favours the detection of very short-period transiting planets (Very Hot Jupiters) compared to longer periods.

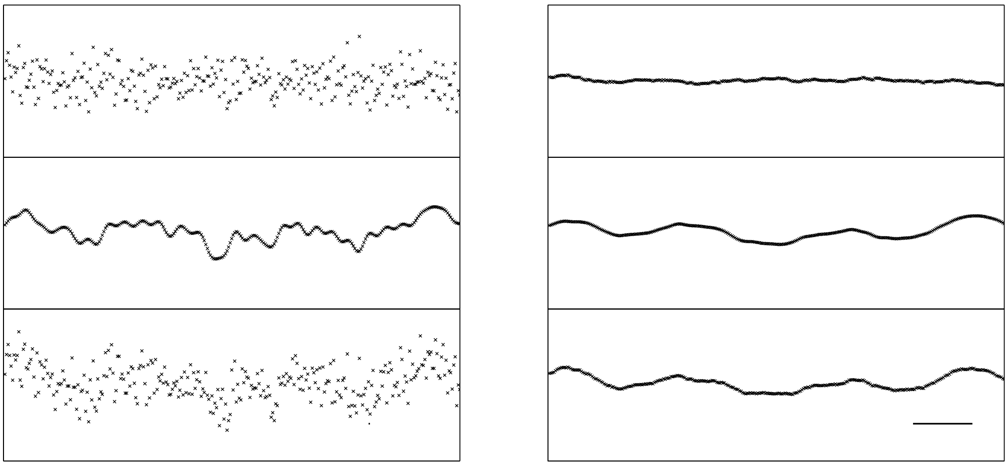

Figure 1.8: *Left:* A photometric time series with white, red or pink noise. The global dispersion is the same for the three curves. *Right:* the same series averaged over a transit duration (the transit duration is shown by the bar at the bottom right) (from Pont et al., 2005).

Pont et al. (2005) has shown that white noise calculations predict the detectability of transit signals around the brightest stars in the survey down to very small transit depths − thanks to the averaging of the independent noise. But taking into account the red noise leads to a much higher effective threshold, and to a floor value that is higher than the typical depth of hot Jupiter transits.

Pont et al. (2005) concluded that some authors have predicted that with large telescope, transiting planets of much smaller size than hot Jupiters ("*hot Neptunes*") will become detectable from the ground (Gillon et al., 2005; Hartmann et al., 2005). However, the reasoning used to reach these conclusions are based on the same white-noise assumptions as those leading to the predictions of very high rates of hot Jupiter detections by the on-going surveys. When the red component of the noise is taken into account, we find that hot Neptunes are not likely to be detected in significant numbers from the ground, and that space missions like Corot and Kepler will be needed to avoid the type of hour-timescale red noise that the Earth's atmosphere is causing in lightcurves.

1.2.4 *Analysis of the lightcurves*

A first inspection of the transit shape and the parts of the lightcurve without transits can quickly identify a false positive. This is the cheapest way, in time and cost, to identify false positives, so no further telescope time is needed.

1.2.4.1 Inspection of the lightcurves parts without transits

A known effect of several binary stars is the *ellipsoidal variability* (Shobbrook et al., 1969, and references therein): the tidal forces are responsible for making the primary star elongated towards the companion. The changes in the angular size of the star, and the gravity darkening produce a sinusoidal modulation of the lightcurve with half the period of the system. The maximum light will be provided in the quadratures of the binary, and the minima will happen in the primary and secondary eclipse. This effect will be more evident when the companion is closer to the star and more massive. The ellipsoidal variability induced by a planetary companion would produce a signal that is not detectable from ground (Pont et al., 2005, estimate an ellipsoidal variability of 0.06 millimags for OGLE-TR-122, which is a 96 M_J star; in the case of planets, this would be of the order of a few mags, assuming a theoretical dependence of the variability of M_s/P^2). Using this results, Drake (2003) and Sirko & Paczynski (2003) fitted the data of the OGLE candidates (Udalski et al., 2002a,b,c), and identified ellipsoidal variability in several of the candidates, with different statistical significance. Sirko & Paczynski (2003) claim that 50% of the OGLE candidates they analyzed might have stellar companions, based only on the study of the photometric data.

Another known effect is the *reflection effect*, caused by the emission of the heated hemisphere of the secondary, that is commonly tidally locked. This event appears in the lightcurve as a sinusoidal shape, with maximum at the secondary eclipse, and with the same period as the system. In some cases (when the secondary eclipse is not detected), it is difficult to distinguish among this two effects mentioned above, such as some cases of OGLE candidates studied by Sirko & Paczynski (2003).

1.2.4.2 Inspection of the lightcurves transits part

Seager & Mallen-Ornelas (2003) provide a simple test to identify the more valuable candidates. It consists of estimating the stellar density from the transit shape (with known P, t_F , t_T , and F, see equations 1.9 and 1.11), and then comparing this stellar density with the one expected for a main sequence star. If the stellar density obtained from the transit shape is typical of a giant star ($\log(\rho/\rho_\odot) < -1.5$, see Cox, 2000, for stellar densities as a function of the spectral type, in main sequence and giant stars), then the depth of the transit cannot be due to a planetary-sized object.

If the stellar density closely resembles the density of the star obtained by a different approach (estimation of the spectral type by photometry or spectroscopy, and a value of the density for that spectral type taken from Cox, 2000), then the candidate should be further observed. The input parameters t_T and t_F are of crucial importance in this test, and can be obtained by a Levenberg-Marquardt fit of the time series to a function:

$$y = \begin{cases} 0 & x < t_c - t_T/2 \\ (t_c - x - t_T/2)\frac{\delta}{t_{ie}} & t_c - t_T/2 < x < t_c - t_F/2 \\ -\delta & t_c - t_F/2 < x < t_c + t_F/2 \\ (x - t_c - t_F/2)\frac{\delta}{t_{ie}} - \delta & t_c + t_F/2 < x < t_c + t_T/2 \\ 0 & x > t_c + t_T/2 \end{cases} \tag{1.15}$$

where the four fitted parameters are the center of the transit t_c; the total duration t_T; the depth in magnitude units δ, and the ingress-egress time t_{ie}; the duration of the transit between second and third contacts t_F. The relationship between the depth expressed in magnitudes (δ) and the $\sqrt{\Delta F}$ is $\sqrt{\Delta F} = 1 - 10^{-0.4\delta}$.

1.3 HD 209458b

Currently, the best-known and best-studied exoplanet is orbiting around the G0V star HD 209458.

In this section we describe several studies carried out on this planet, which constitute a benchmark in this field. The planet was discovered (Mazeh et al., 2000) with the RV technique. The spectra were taken using both the HIRES (Vogt et al., 1994) and ELODIE (Baranne et al., 1996) spectrographs, and completed with spectra from CORALIE (Queloz et al., 2000). In September 1999, the STARE telescope was used to monitor the first transits of an exoplanet around its star (Charbonneau et al., 2000, and Figure 1.7). An independent ingress was observed by Henry et al. (2000).

There was some skepticism from diverse authors, like the observations by Gray (1997) apparently showing distortions in the spectral line bisectors; if confirmed, these would argue against the planetary origin of the radial velocities observed in these stars. These observations could not be reproduced (Gray, 1998; Brown et al., 1998), and a definite demonstration of the existence of these exoplanets to the more skeptical community came with the detection of transits in HD 209458. These allowed a determination of the planetary radius.

Combining the data with the radial velocity observations, which give $M_p \sin i$, the mass was measured, and thus the mean planetary density equal to 0.38 g/cm^3 in the work of Charbonneau et al. (2000), refined to 0.35g/cm^3 in Brown et al. (2001). This measurement confirmed the suspected gaseous nature of these objects. Several ground-based multi-color observations were conducted to improve the stellar and planetary parameters, and to measure the limb darkening coefficients, for the first time in a star other than the Sun (Jha et al., 2000; Deeg, Garrido & Claret, 2001).

The best quality lightcurve was obtained using the spectrograph STIS on board the HST telescope (Brown et al., 2001, and Figure 1.10). Attaining an unprecedented precision of $1.1 \cdot 10^{-4}$ per sample point, enough to identify a transit of an Earth-sized object, they improved the parameters of HD 209458b: $R_p = 1.347 \pm 0.060 R_J$, an orbital inclination of $i = 86^\circ.6 \pm 0^\circ.14$, and a stellar radius of $R_\star = 1.146 \pm 0.050 R_\odot$. The residuals of the fit were used to search for satellites and rings around the planet. Upper limits on the mass and sizes of potential satellites were established in $3M_\oplus$ and $1.2R_\oplus$, respectively. The presence of large opaque rings was also constrained, to a lesser degree, establishing a maximum size for this structures (if present) of 1.8 radii of the planet.

The spectral information contained in these data set was used by Charbonneau et al. (2000) to detect for the first time an exoplanet's atmosphere. The technique used was transit spectroscopy, whose basic idea consists of measuring the wavelength dependence of the radius of the exoplanet. This dependence is caused by different opacities of the atmosphere components. In a region close to the Na D lines at $589.3nm$, they compared the ratio of the star's spectrum outside of transit to the spectra when the planet is crossing the stellar disk. Thus, in relative flux, the transit was 0.000230 ± 0.00006 deeper in the region where the sodium absorption was expected. The strength of the sodium absorption was ~ 3 times weaker than that predicted by a fiducial model, which assumed solar sodium abundance for the star. The authors interpret this discrepancy in the measured sodium absorption as a consequence of a high cloud deck, a low atomic sodium abundance, or a combination of both effects. Also, the effect of the strong UV bombardment on the planet might play an important role, with possible formation of photochemical hazes.

Later on, Vidal-Madjar et al. (2003) used STIS on board HST to observe the Lyman-α

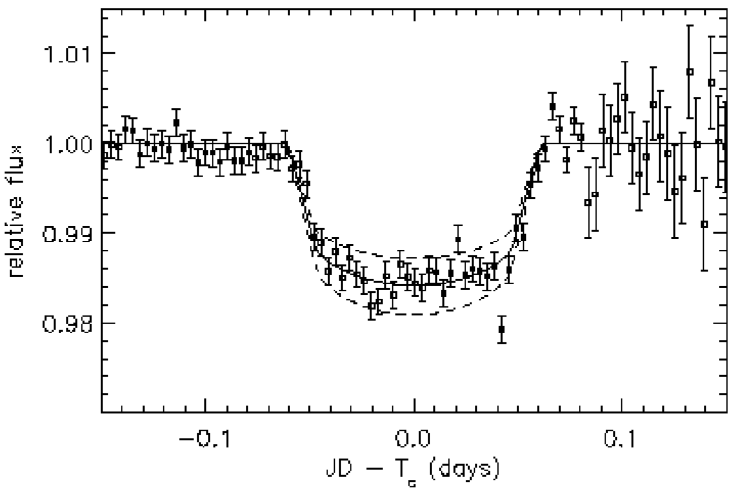

Figure 1.9: Transit of HD 209458*b* observed with the STARE telescope, in September 1999. The curvature at the bottom of the transit is a consequence of the star's limb darkening. Points are 5 min bins, and the error bars are the standard deviations of the mean in each bin. (from Charbonneau et al., 2000).

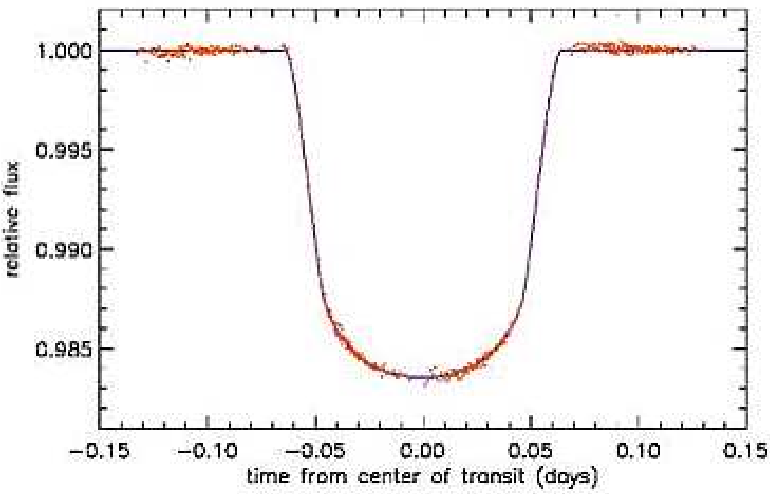

Figure 1.10: HST observations of transits of HD 209458*b*. The precision per sample point achieved is 1.1×10^{-4} (from Brown et al., 2001).

emission line of the star. When the planet was transiting, the emission was reduced by a $15 \pm 4\%$ (1σ), which according to these authors is a proof for an extended upper atmosphere on HD 209458*b*. The implied radius of the planet at these wavelengths is $4.3 R_J$. This radius suggests that the upper atmosphere material fills and overflows the *Roche lobe* (which has a radius of $3.6 R_J$. Thus, the atmosphere of this planet is in process of *evaporation* due to the heavy UV-irradiation of the star at such close distance. They estimate the evaporation rate as 10^{10} g/s. In a later work (Vidal-Madjar et al., 2004), they used a lower resolution (and wider spectral range) band to search for different species in the planetary upper atmosphere. In this second search, they claim the detection of absorption also in the OI ($13 \pm 4.5\%$) and CII ($7.5 \pm 3.5\%$) lines. Surprisingly, these results would imply that these components are higher in the atmosphere than the less-massive HI, which seems unlikely, and can not be explained if the molecular diffusion dominates at high altitudes, nor if an extreme eddy diffusion transport is able to transport the oxygen and carbon up to the Roche level. To explain the observation, the authors need a mechanism that is able to transport oxygen and carbon up to about the Roche lobe while maintaining their velocity dispersion of at least ~ 10 km/s. They propose that the HI is escaping at a high rate, and the hydrodynamical flow of this process drags up the other species, preserving their abundances. This mechanism has been called *blow-off* (Watson, Donahue & Walker, 1981), and it is supposed to keep velocity dispersions for the oxygen and carbon similar or greater than the sound speed ($\sim$ 10 km/s at 10000 K, which is the estimated upper atmosphere temperature). With these velocity dispersions, the conditions at the upper atmosphere would be such that the whole stellar line would be absorbed by the planetary carbon and oxygen, thus allowing a 10% absorption if they flow up to the Roche lobe.

Richardson et al. (2006) have measured the infrared transit of HD209458 b using the *Spitzer Space Telescope*. They observed two primary eclipse events (one partial and one complete transit) using the 24 μm array of the Multiband Imaging Photometer for Spitzer (MIPS). At this long wavelength, the transit curve has a simple box-like shape, allowing robust solutions for the stellar and planetary radii independent of stellar limb darkening, which is negligible at 24 μm. They derive a stellar radius of $R_\star = 1.06 \pm 0.07 R_\odot$, a planetary radius of $R_p = 1.26 \pm 0.08 R_J$, and a stellar mass of $1.17 M_\odot$. Within the errors, Richardson et al. (2006) results agree with the measurements at visible wavelengths. The 24 μm radius of the planet therefore does not differ significantly compared to the visible result.

1.4 On the radii of the transiting planets

One important physical parameter that can be obtained with the transit method is the radius of the planet. Soon after the discovery of 51 Peg *b* (Mayor & Queloz, 1995), models for strongly irradiated planets appeared in the literature (Guillot et al., 1996). These models predicted that these short period planets, with effective temperatures above 1000 K, should have their radii significantly larger than Jupiter. The first measurement of an exoplanet's radius came with the discovery of HD 209458*b*'s transits (Charbonneau et al., 2000; Henry et al., 2000). The most precise numbers for its radius are given in the work by Brown et al. (2001), where the high-quality HST photometry allowed to fit independently $R_\star$ and R_p. The measured radius in that work was $R_p = 1.347 \pm 0.060 R_J$. A subsequent analysis of the same HST data by Cody & Sasselov (2002), state a value of $R_p = 1.42 \pm 0.10 R_J$. In any case, the published value proved that the planet was a gas giant planet, composed basically of hydrogen. A theoretical study of the radius of HD 209458*b* by Guillot & Showman (2002), required unrealistically hot temperature of the deep atmosphere of the planet in order to reproduce the observed radius. Under more realistic temperature conditions, an extra source of energy seemed to be lacking, to make the radius match the observations. These authors proposed one mechanism to account for this extra energy: if a fraction ($\leq 1\%$) of the incident stellar flux is transformed into kinetic energy at the planet atmosphere, then it could be converted into thermal energy at deeper levels (tens of bars) of the atmosphere, by dynamical processes.

Other studies proposed different extra sources of energy in the planet. Bodenheimer, Lin & Mardling (2001) also find a difference of $\sim 0.3R_J$ between the observed and predicted radius (without an extra source of energy). They suggest (Bodenheimer, Laughlin & Lin, 2003) that the energy arising from ongoing tidal circularization of the planet's orbit could account for such an increased radius. This would require the presence of a yet unseen companion to HD 209458 b, which can still be consistent with their residuals of the radial velocity measurements. In fact, they obtain a good fit to the spectroscopic measurements with an eccentricity of $e \sim 0.03$. This low, but nonzero eccentricity, could explain the increased radius of HD 209458b, if a model without a core for the planet is assumed. For models with a solid core, the eccentricity needed would be of the order of $e \sim 0.1$, which seems inconsistent with the current velocity measurements. A two-body fit of the radial velocity data seems to indicate a possible second companion (companion "c") with a period of $\sim$ 80 days, and mass of $\sim 0.12M_J$. Recently, Charbonneau et al. (2005) showed that infrared photometric time series from Spitzer Space Telescope confirmed a zero value of eccentricity, ruling out the second planetary companion scenario.

In the study carried by Chabrier et al. (2004), a simple model of one dimensional irradiation, with incoming flux deposited uniformly over the dayside and non-dynamical redistribution of the incident flux because of day-night temperature differences, is found to adequately reproduce the radius of OGLETR-56b. But, in order to reproduce the radius of HD 209458b, a significant fraction (0.5%) of the incident flux must be transported downward and converted into thermal energy at the radiative-convective boundary. This confirms the results by Showman & Guillot (2002). But it is still necessary to invoke an unknown mechanism able to transport kinetic energy from the top of the atmosphere downwards to the adiabat level, which lies at $P \sim 500$ bar for HD 209458b and $P \sim 4000$ bar for OGLE-TR-56b. The calculated radii and the measured values are plotted in Figure 1.11. It seems, from these plots, that this mechanism might be taking place in HD 209458b, while for OGLE-TR-56b it is not necessary to invoke any extra source of energy.

Finally, Burrows, Sudarsky & Hubbard (2003) argue that the radius measured in a transit is systematically larger than the radius that result from the planet evolution codes. This is a consequence of the stellar photons passing obliquely to the limb of the planet. The measured radius of a transit implies an effective optical depth of ~ 1. But the effective optical depth is for a chord that is parallel to the line between the centers of the planet and the star. This can be quite different from the optical depth measured radially from the center of the planet. In fact, there is a significant difference between the pressure level at which the transit beam becomes opaque (1 mbar, according to Fortney et al., 2003), and the one that is calculated for opacity equal to 1 with the models ($\sim$ 0.1 bar, Figure 5 in Baraffe et al., 2003). Burrows, Sudarsky & Hubbard (2003) estimated that this effect might add $\sim 0.1R_J$ to the estimated radii, and, in the case that the real measurement of the radius of HD 209458b lies in the bottom part of the observational error bar, then no extra source of heating might be necessary to account for the observed radius.

To summarize, there have been three different proposed explanations for the radius of HD 209458b:

- The radius is anomalously large; the transport of a small fraction of the incident flux by kinetic energy (winds) to deep levels of the planet's atmosphere, at this level can account for this increased radius. This effect might take place in all the Hot Jupiters, and consequently, all the transiting planets might show strongly inflated radii. and the subsequent conversion

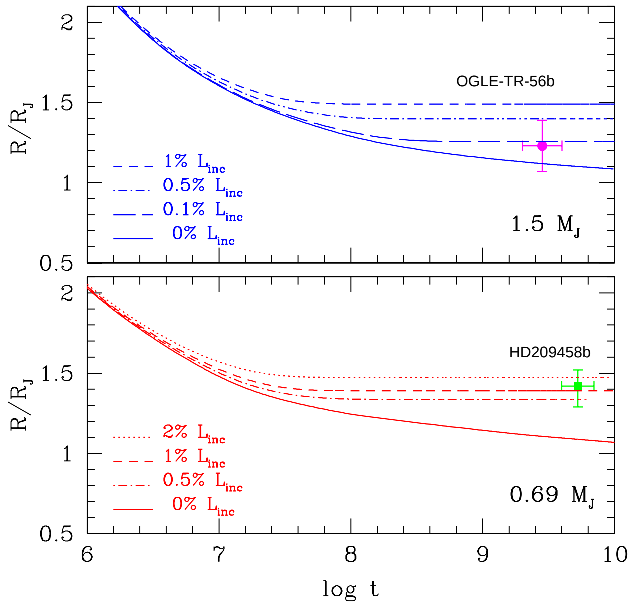

Figure 1.11: Evolution of the planetary radii of OGLE-TR-56*b* (*top*) and HD 209458*b* (*bottom*), for models without invoking an extra source of energy (solid lines), and assuming conversion of several fractions of the incident luminosity into thermal energy deposited at the adiabatic level (from Chabrier et al., 2004).

of this energy into thermal energy

- The radius is anomalously large; this is due to ongoing tidal circularization, which needs the presence of a yet unidentified third body in the system. If this were the case, HD 209458*b* might be the anomalous case, and the next found transit planets should all show smaller radii.

- The radius is within theoretical expectations, taking into account the factors discussed by Burrows, Sudarsky & Hubbard (2003). The new found transiting planets, according to this approach, should all show bigger radii than estimated.

1.5 Formation models of giant planets

Observational evidence that the mass function of young objects in star-forming regions extends down to below the deuterium burning limit (Zapatero Osorio et al., 2000) and the absence of good theoretical reasons against it, point towards the same formation mechanism for stars, brown dwarfs and isolated high mass planetary objects (fragmentation during collapse of a molecular cloud). On the other hand, the existence of a *brown dwarf desert* (no objects with masses in the brown dwarf regime orbiting close to a star) in all the radial velocity surveys, and the increasing number of planetary mass objects with smaller masses (Halbwachs et al., 2003) point to a different formation mechanism for orbiting exoplanets than for stars and isolated objects. The fragmentation model is not valid to explain the formation of these objects (Bodenheimer, Hubickyj & Lissauer, 2000). Out of the different formation models that have been proposed (Wuchterl, Guillot & Lissauer, 2000, and references therein), the two hypotheses receiving most attention are the core *instability model* (or *nucleated instability*) and the *disk instability* (or *gravitational instability*) model.

- ▷ According to the core instability model (Bodenheimer & Pollack, 1986), the planet is formed in a similar way as a terrestrial planet is, until it reaches a mass that allows to accumulate significant amounts of the surrounding gas in the disk. The *gas accretion rate* becomes comparable to the planetesimal bombardment when the core reaches a mass of $\sim 10 M_{\oplus}$. At this point, the gas accretion happens very fast, in a phase called *runaway accretion*. The primary question regarding this scenario is whether planets with small cores can accrete very massive gaseous envelopes within the lifetimes of gaseous protoplanetary disks ($10^6 - 10^7$ y, Strom, Edwards & Skrutskie, 1993; Alencar & Batalha, 2002).

- ▷ In the disk instability model (Cameron, 1978; Boss, 1997), the giant planet forms directly from the contraction of a clump formed by gravitational instability in the protoplanetary disk. It seems that this model has never been demonstrated for realistic disk conditions (Lissauer, 2004). Besides, it has difficulties explaining the super-solar abundances of heavy elements in Jupiter and Saturn, and it does not explain the origin of planets like Uranus and Neptune. But the timescales for this process are smaller than those derived from the core instability model (few hundred years).

There is some theoretical controversy associated with the possibility that the planets experience *orbital migration*, as a consequence of the gravitational torque between the disk and the planet. This torque may allow planets to clear gaps around themselves (Goldreich & Tremaine, 1980; Ward, 1986; Bate et al., 2003; Thommes & Lissauer, 2005). Planetary orbits can migrate towards (or, in some circumstances, away from) their parent stars, as a consequence of angular momentum exchange between the planet and the disk. It is thus possible that planets may form at several AU away from their parent star and then migrate inwards to the locations where they are currently observed. This raises several problems, such as the necessity for a stopping mechanism to avoid the planet falling onto the star (for more detailed information, Thommes & Lissauer, 2005, and references therein.).

1.6 Motivation for the following study

As has been explored in this Introduction, exoplanets that transit their host stars can provide us with valuable physical information, such as a mass measurement (without the degeneracy imposed by the inclination of the orbit in the non-transiting planets), and a radius estimation that is inaccessible by other means. With the occurrence of transits, a new set of follow-up studies becomes possible, as was discussed in §1.3. The discovery of transits in the HD 209458 system allowed the development of a series of techniques and studies that served to increase the knowledge on these objects. At the time of beginning this thesis, HD 209458*b* is not still the only planet to produce transits: infact up to now, more than 30 are known (Figure 1.12). Three of them were discovered by radial velocity planet searches, and six by ground-based photometric transit surveys. In the Table 1.1 there is a list of planets candidates detected by transit, updated to 6th November 2007 (`http://www.extrasolar.eu/catalog-transit.php`).

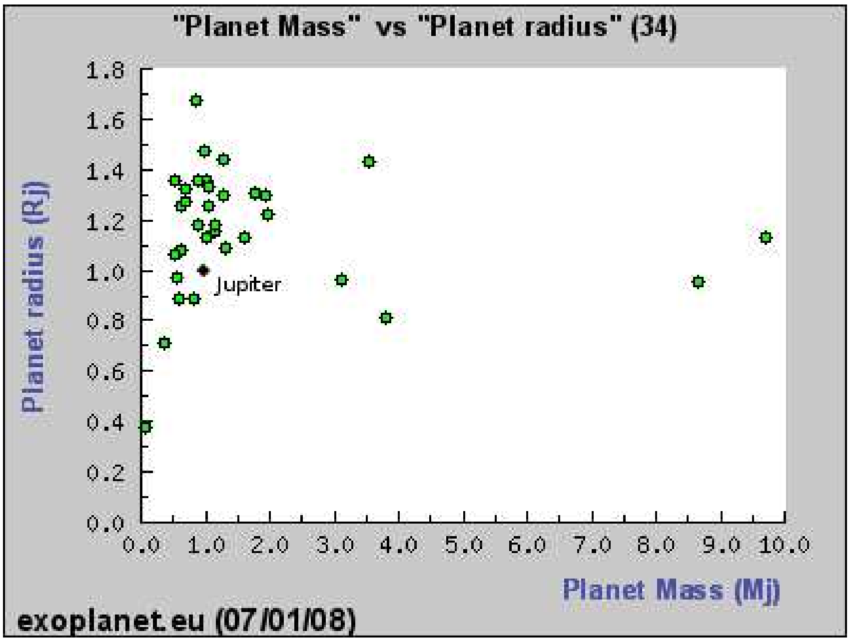

Figure 1.12: Mass-radius relation for the known extrasolar transiting planets. Jupiter is shown for comparison and marked with filled diamond (from Extrasolar Planets Encyclopaedia, maintained by J. Schneider ©2008).

This thesis work was intended principally to search for more transiting planets, in order to establish what is common and what is peculiar in for searching this kind of objects. Though it seems obvious, we point out that this field of investigation is strongly governed by observations; this will be demonstrated in the following chapters. As we saw in the previous sections, there are different proposed theories to explain the apparently "too big" size of the planet HD 209458*b*. Some of them would implicitly require that the newly found transiting planets should also exhibit an increased radius. This subject remained an open question until the new transiting planets were detected.

Planet name	M_p (M_J)	P (days)	e_p	$M_\star$ ($M_\odot$)	$[Fe/H]_\star$	Transit discovery reference
CoRoT-Exo-1b	1.3	1.5	NA	NA	NA	*CoRoT web page*
GJ 436b	0.072	2.64385	0.15	0.452	-0.32	Butler et al. (2004)
HAT-P-1b	0.53	4.46529	0.09	1.12	0.13	Pont & ISSI Working Group (2006)
HAT-P-2b	8.64	5.63341	0.517	1.298	0.12	Winn (2007)
HAT-P-3b	0.599	2.899703	0	0.936	0.27	Torres et al. (2007b)
HAT-P-4b	0.68	3.056536	0	1.26	0.24	Kovacs et al. (2007)
HAT-P-5b	1.06	2.788491	0	1.16	0.24	Bakos et al. (2007)
HAT-P-6b	1.057	3.852985	0	1.29	-0.13	Noyes et al. (2007)
HD 149026b	0.36	2.8766	0	1.3	0.36	Sato et al. (2005)
HD 17156b	3.08	21.2	0.67	1.2	0.24	Fisher et al. (2007)
HD 189733b	1.15	2.2185733	0	0.8	-0.03	Bouchy et al. (2005)
HD 209458b	0.69	3.52474859	0.07	1.01	0.04	Charbonneau et al. (2000)
OGLE-TR-10b	0.63	3.10129	0	1.18	0.12	Udalski et al. (2002a)
OGLE-TR-111b	0.53	4.0144479	0	0.82	0.12	Udalski et al. (2002b)
OGLE-TR-113b	1.32	1.4324757	0	0.78	0.14	Udalski et al. (2002b)
OGLE-TR-132b	1.14	1.689868	0	1.26	0.37	Udalski (2003)
OGLE-TR-182b	1.01	3.9791	0	1.14	0.37	Udalski (2003)
OGLE-TR-56b	1.29	1.211909	0	1.17	NA	Udalski et al. (2002a)
SWEEPS-04	3.8	4.2	NA	1.24	NA	Shu et al. (2007)
SWEEPS-11	9.7	1.796	NA	1.1	NA	Shu et al. (2007)
TrES-1	0.61	3.0300737	0.135	0.87	0.001	Alonso et al. (2004)
TrES-2	1.98	2.47063	0	0.98	-0.15	Alonso et al. (2004)
TrES-3	1.92	1.30619	NA	0.9	NA	Alonso et al. (2004)
TrES-4	0.84	3.553945	NA	1.22	NA	Alonso et al. (2004)
WASP-1b	0.89	2.51997	NA	1.24	NA	Collier et al. (2006)
WASP-2b	0.88	2.152226	NA	0.84	NA	Collier et al. (2006)
WASP-3b	1.76	1.846834	NA	1.24	0	Pollaco et al. (2007)
WASP-4b	1.27	1.34	NA	NA	NA	*WASP web page*
WASP-5b	1.6	1.63	NA	NA	NA	*WASP web page*
XO-1b	0.9	3.941534	NA	1	NA	McCullogh et al. (2006)
XO-2b	0.57	2.615838	NA	0.98	0.45	Burke et al. (2007)
XO-3b	12	3.19	0.2	NA	-0.25	Johns-Krull et al. (2007)

Table 1.1: Data for the known planets candidates detected by transit as listed in the web page of the Extrasolar Planets Encyclopaedia, updated to 6th November 2007, in alphabetic order.

Chapter 2

The RATS project

In this chapter RATS (*RAdial velocities and Transit Search*) project and the instruments involved are fully described. We explain in detail how stellar fields has been selected and the peculiar observation strategy applied. Moreover, we describe the hardware and software environment in which this project works.

2.1 The RATS project

RATS is an Italian collaboration between several INAF Observatories (Padova, Catania, Napoli, Palermo), the Astronomy Department and Physics Department of the University of Padova and ESA. The project is devoted to search for extrasolar planets using the transit photometric technique together with a spectroscopic follow up strategy for reconnaissance of false alarms.

The main aim of the RATS project is twofold. The detection of extra solar planets that transit the disk of their parent star is the scientific drive of the whole project. We planned to observe simultaneously thousands of stars (magnitude range between 9th to 14th) in selected star fields for five years since the beginning of 2006. In this manner we are confident to find 10 (goal: 20) new transiting planets. The second aim of the project is to use its observing strategy and the scientific data management as a bench work for future planetary transits search mission.

In order to achieve the RATS project goals we use two different telescope for both the photometry search and the spectroscopic follow up. The photometric transit search will be conducted with the C.ma Ekar 92/67 Schmidt telescope equipped with one of the frame transfer CCD forecast for the ESA Eddington space mission. The CCD is positioned onto the folded focal plane of the Telescope. The spectroscopic follow up will be conducted with the "Copernico" Telescope (182 cm Cassegrain Ritchey Chretien) equipped with the Echelle spectrograph.

Candidate identification requires a preparatory work starting from stellar field selection with higher probability to find a transit event.

An automatic photometric pipeline with a real time images reduction, will directly provide light curves of object in the field. The light curves themselves will be analyzed in order to catch light dimming due to a transit. Once a transit alarm is found, it is observed with the spectroscopic telescope to rule out astrophysical false alarm like e.g. eclipse binary blended with giant stars.

Figure 2.1: The 92/67 cm schmidt telescope.

RATS will contribute to disentangle the planetary formation mechanism, to identify the environmental condition where these objects form or not and to have more hints about their physics. The transit, infact, allows an estimate of the projected area of the planet hence of its radius. Thus, if the planetary mass is known, e.g. by radial velocity observations ($edge - on$ orbits allow reduction of the planetary mass uncertainty), it is possible to determine the density of the planet, its surface gravity and have hints about the atmospheric gas composition (escape velocity) and lay down limits on structural model of extra solar planets. The case of the more than 30 up to day detected transiting planets has shown that this is possible in practice.

2.2 The RATS instruments

2.2.1 The Schmidt telescope and the CCD cameras

2.2.1.1 The telescope

The 92/67 cm Schmidt telescope (Fig. 2.1), built in 1966, is located at Cima Ekar Observing Station (see Table 2.1) close to the 182 cm telescope. It was moved from the original position at the Observatory site near Asiago in July 1991 to take advantage of the higher altitude and lower light pollution of Cima Ekar.

The aperture of the telescope is 67 cm, with a spheric mirror of 95.9 cm of diameter. The focal length is 215 cm, giving a scale of 95.9 arcsec/mm and a and a focal ratio $f/3.2$.

The building is not a traditional dome: the rotating part is of octagonal shape for easier mechanical assembling and was designed in part to test the proposed solution for the Galileo National Telescope *Telescopio Nazionale Galileo* (*TNG*).

Until 1998 the telescope was used with a photographic plate of 20 x 20 cm. The corresponding field of view was 5.1 x 5.1 degrees. Since 1999 the telescope mounts different CCD detectors, as illustrated in the next paragraph.

The telescope also now equipped with two prisms:

	Longitude	Latitude
Astronomical Coordinates	$0^h46^m17^s.48$ E	+45°50′40".18
Geodetic Coordinates	$0^h46^m16^s.52$ E	+45°50′58".00
Elevation: 1410.2 m		
Elevation above sea level: 1370 m		

Table 2.1: Coordinates of the central pillar of schmidt telescope at Cima Ekar.

	ITANET	SITe	Eddington
Chip	KODAK KAF-4202	SITe-424A	e2v 42-C0
Format	2032 x 2044	2048 x 2048	2048 x 6144
Pixel size	9.0 μm	24.0 μm	13.5 μm
Full well	90000 e^-	200000 e^-	150000 e^-
Read-out speed	50 kpx/s	50 kpx/s	450 kpx/s
Read-out noise	8.4 e^- (50 kHz)	8.4 e^- (50 kHz)	8.4 e^- (50 kHz)
Read-out mode	Full frame	Full frame	Full transfer
Temperature	-40°C (Peltier)	-100°C (LN2)	-100°C (LN2)
Dark current	2.5 e^-/pix/h	$\leq$ 1 e^-/pix/h	2 e^-/pix/h
Dynamics	10000:1	20000:1	30000:1
Scale	0.9"/pix	2.3"/pix	1.3"/pix
Field of view (FoV)	0.51°	1.31°	0.7 x 1.1°
Optical filters	BVRI Johnson	None	None

Table 2.2: Characteristics of the RATS CCD cameras (from Scuderi et al., 2006).

1. a 67 cm, 4.5 degrees angle UV-transparent objective prism with a reciprocal dispersion at H_γ of 650 Å/mm;

2. a 67 cm, one UV-transparent objective prism with a reciprocal dispersion at H_γ of 1010 Å/mm.

Both the two prisms can be used in direct or reversed combination.

2.2.1.2 The CCD cameras

As one of the goal of the project is to test the observational strategy of the Eddington mission, wide field imaging will be performed using one of the CCDs manufactured by e2v for the mission. This CCD will be loaned by ESA to the project consortium in late summer 2005. In the meanwhile we have started the project using two other CCDs. The first CCD camera is called ITANET camera and the second one SITe camera. Table 2.2 summarize the main characteristics of the CCD cameras which have been used during the project.

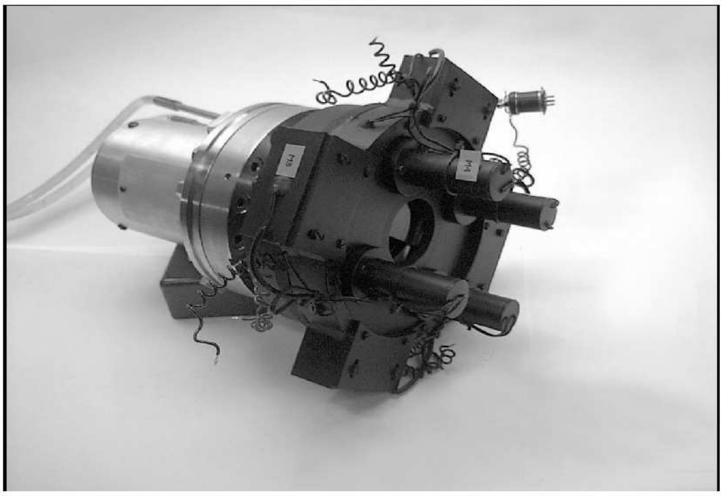

Figure 2.2: A sketch of the ITANET camera showing the filter system and CCD dewar.

2.2.1.3 The ITANET camera

The ITANET project (Gandolfi et al., 2005) is an Italian national project whose aim is the study of Near Earth Objects. The CCD camera, that has been completely designed and realized at the Catania Astrophysical Observatory (Fig. 2.2), is used by the RATS project too (Scuderi et al., 2006). Due to its small field of view and to its low quantum efficiency, the CCD is a bare front illuminated device, the camera will not be used for the survey itself. Instead as it will be the only one equipped with a set of BVRI Johnson filter will be very useful for the characterization of the fields selected for the RATS search. An example of this kind of analysis (Scuderi et al., 2006) is shown in Figure 2.3 showing a preliminary color–magnitude diagram for one of the RATS field obtained during one the nights of testing at the Schmidt telescope.

2.2.1.4 The SITe camera

The SITe camera is based on the SITe-424A back-illuminated 2048 x 2048 device. The CCD has been characterized at the Catania Astrophysical Observatory and its quantum efficiency is shown in Figure 2.4. The CCD has been mounted inside a LN2 dewar. Cold finger, wire cabling and mechanics (Fig. 2.5) have been realized at the Padua Astronomical Observatory. The window that seals the dewar is a field flattener lens with a 1500 mm focal length. Presently the camera is mounted on the Cima Ekar Schmidt telescope.

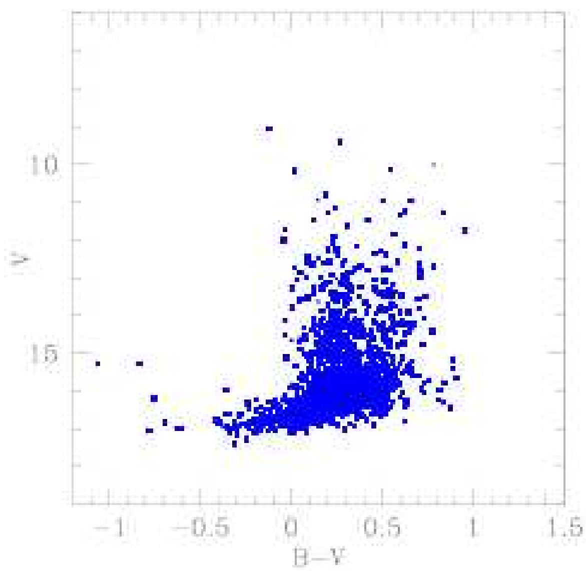

Figure 2.3: The color–magnitude diagram in the B and V Johnson filters for one of the RATS fields. Exposure times for the B and V images were 15 seconds (from Scuderi et al., 2006).

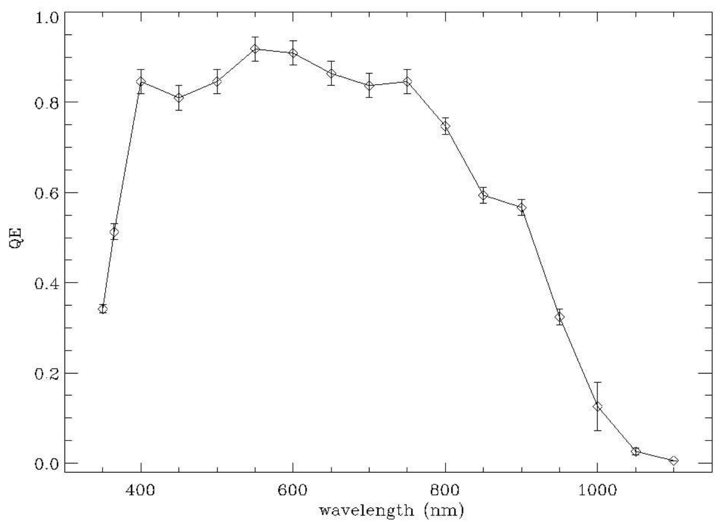

Figure 2.4: The quantum efficiency curve of the SITe CCD obtained at the Catania Astrophysical Observatory (from Scuderi et al., 2006).

2.2.1.5 The Eddington camera

The final CCD camera will use one of the CCD chips developed by e2v for the focal plane of Eddington (Fig. 2.6). The CCD is a back illuminated frame transfer device. All the mechanical

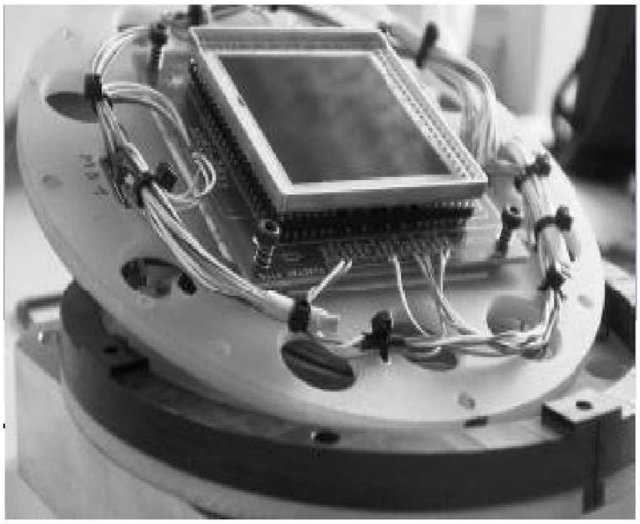

Figure 2.5: The SITe CCD mounted on its cold finger before being placed inside the dewar.

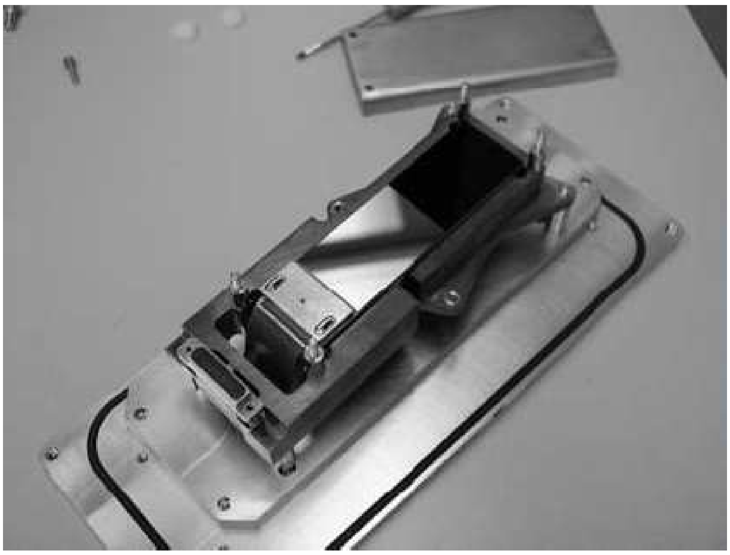

Figure 2.6: The e2v 42-C0 Eddington CCD.

interfaces, necessary to integrate the CCD inside the dewar presently hosting the SITe CCD, are being realized in Asiago and Catania.

2.2.1.6 The CCD controllers

To run the CCD cameras the RATS project will make use of the CCD controllers developed for the "Telescopio Nazionale Galileo" (TNG). At the moment we are using the old version of the

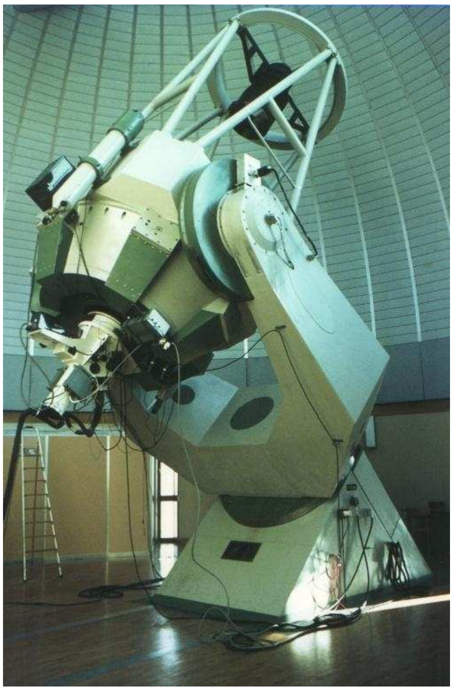

Figure 2.7: The "Copernico" telescope at Cima Ekar.

controller based on a technology whose main limitation is the read-out speed that cannot be greater than 50 kpix/s. The "new generation" of controllers (Bonanno et al., 2004) that we plan to use for the Eddington CCD, will overcome this limitation allowing a rate up to 450 kpix/s.

2.2.2 The Copernico telescope and Echelle spectrograph

The 182 cm telescope is located at Cima Ekar (Asiago) and is the largest astronomical telescope in Italy. It is dedicated to Nicolas Copernicus and has been in operation since 1973 but on 1997 November the observatory at Cima Ekar has been dedicated to Professor Leonida Rosino (Treviso 1915 – Padova 1997).

The telescope is used for optical imaging and low-medium resolution spectroscopy using two main instruments: AFOSC (an imager/spectrograph) and an high dispersion Echelle spectrograph. The telescope and its instruments are operated by the Astronomical Observatory of Padova that is part of the Istituto Nazionale di Astrofisica (INAF).

2.2.2.1 The telescope

The telescope (Fig. 2.7) is a classic Cassegrain reflector with a primary mirror of 182 cm.

Optical design of the telescope is a classic Cassegrain with equivalent focal number $f/9$. The primary mirror M_1 (made of Zerodur/ Schott Duran 50) has a diameter of 182cm. An active system for the movements of the secondary mirror (Fig. 2.8) was implemented in 1990. This unit, in addition to the standard focusing, allows one to control both (x, y) positions of M_2 and tilt angle (α, δ). The whole system is controlled by a dedicated PC. The main characteristics of

Figure 2.8: The secondary mirror at the "Copernico" telescope.

	M_1	M_2
Total mass (Kg)	1500	67.4
Diameter (mm)	1820	580.0
Thickness (external ring) (mm)	300	110.3
Diameter of central hole (mm)	383	-
Radius of curvature (mm)	10840	4592
Focal length (mm)	5393	3855
F/number	$f/3$	-

Table 2.3: The main characteristics of the Copernico's mirrors.

the mirrors are given in Table 2.3

The telescope has a fork mounting that allows rotation around the right ascension (α) axis for 450° in each direction. The limit of pointing for the declination (δ) axis is dependent on the altitude of the target. The minimum altitude is fixed at 15° by an hardware limit switch. The pointing accuracy is approximately 2 arcmin and is dependent of the position on the sky. Coordinates are read by two encoders with a resolution of approximately 4 arcsec.

The Cassegrain focus ($f/9$, scale 12.6 arcsec/mm at about 20 cm from the rear main flange, see Fig. 2.9) is the main focus of the telescope. Focusing is performed by moving the secondary mirror along the z axis; this movement is controlled by a dedicated PC.

A 450° third mirror can be inserted to deviate the beam to the Nasmyth focus in the east side of the fork, where a photographic camera is available.

The dome of the telescope is on the third floor of the telescope building and has a diameter of 30 m. Aperture and rotation of the dome are controlled by a PC. Pointing of the telescope is performed manually using a console. This employs three different speed of telescope movement (large, medium and micro) to set the telescope position and for guiding. The finest setting

Figure 2.9: The "Copernico" Cassegrain focus.

(micro) is reserved for guiding. An auto-guiding system is implemented through a guide probe and a TV camera that allows an usable field of view of approximately 30 arcmin. For targets with appreciable proper motion ($<$ 200 arcsec/hr) in the sky a differential guiding can be applied using the guide-probe movements. During observations the dome is automatically rotated such that the dome window is always aligned with the telescope pointing.

2.2.2.2 The Echelle spectrograph

The Echelle spectrograph basically consists of a collimator, an Echelle grating, a set of cross disperser gratings mounted on an orientable support, a calibration arm and a slit viewer intensified camera (Fig. 2.10). The mechanical stability is well suited for the measurement of accurate radial velocity, with flexure in the spectrograph focal plane and in the wavelength dispersion direction not exceeding 7μm (about 2.7 km/s at H_α) for $\pm$2 hours telescope slewing in hour angle from the meridian at any declination.

The *Reosc* Echelle spectrograph (Fig. 2.11) provides high dispersion spectra (from 5 Å/mm in the far blue to 10 Å/mm at 6000 Å), with cross-dispersion provided by a grating. The spectrograph can also be used in normal dispersion mode by replacing the Echelle grating with a flat mirror and interchanging the slit and comparison lamp slots.

The slit (Fig. 2.12), placed at the focal plane of the telescope, is 30 mm long (380 arcsec) and its aperture ranges between 50 μm and 2.5 mm (0.65 $-$ 31.5 arcsec) with 50 μm steps set by a micrometer. The slit length can be selected using a decker. A Proxitronix tv intensified camera displays the telescope field of view superimposed on the slit. The measured limiting magnitude is approximately 16.2. The camera parameters (gain, offset and electronic shutter exposure time) can be adjusted using the instrument software.

A calibration arm enables wavelength calibration exposure to be made. A thorium lamp

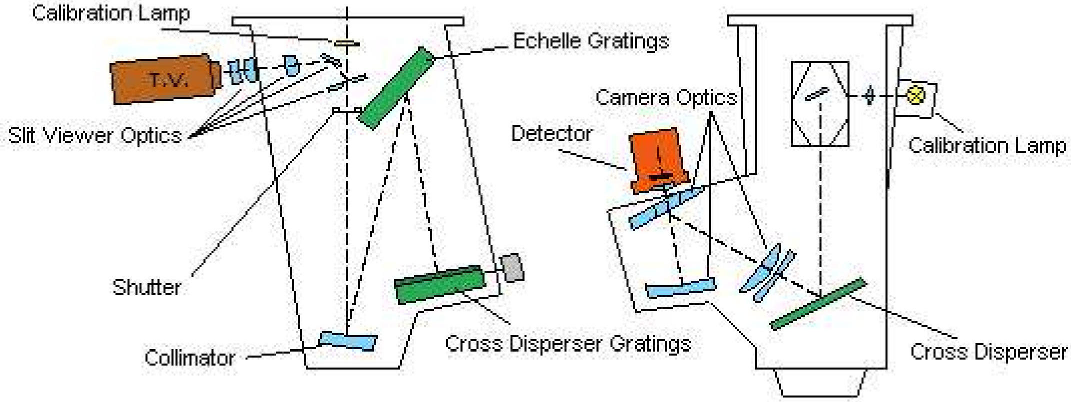

Figure 2.10: Echelle overview scheme at the "Copernico" telescope.

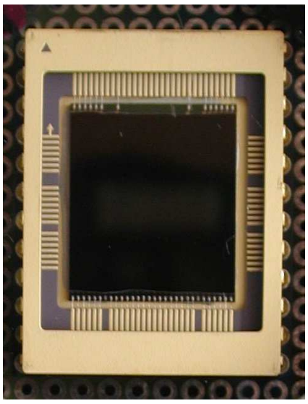

Figure 2.11: The *Reosc* Echelle spectrograph.

provides a good calibration exposure for the total spectral range.

2.2.2.3 The optical fiber feeding project

An optical fiber (or *fibre*) is a single, hair-fine filament drawn from molten silica glass. It works as a cylindrical dielectric that transmits light along its axis by the process of total internal reflection. This causes the fiber to act as a waveguide.
Fibers which support many propagation paths or transverse modes are called *multi-mode* fibers; fibers which support only a single mode are called *single-mode* fibers. The former generally have a large-diameter core and are used for short-distance communication links or for applications where high power must be transmitted. The latter are used for most communication links longer than 200 meters, as for RATS project case.

The fiber consists of a *core* surrounded by a *cladding layer* (Fig. 2.13). To confine the optical signal in the core, the refractive index of the core must be greater than that of the cladding. The boundary between the core and cladding may either be abrupt, in the so-called step-index fiber, or gradual, as in the graded-index fiber. The cladding is usually coated with a tough resin

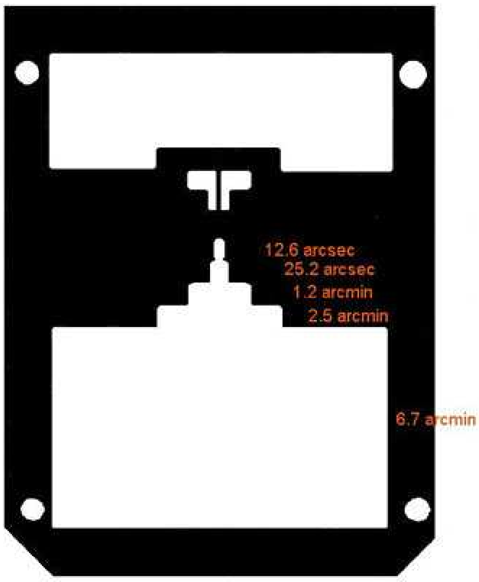

Figure 2.12: Decker which allows the choice of the slit length for the Echelle spectrograph. The projected dimensions of the slit are reported in red.

buffer layer, which may be further surrounded by a jacket layer, usually plastic (Fig. 2.14). These layers add strength to the fiber but do not contribute to its optical waveguide properties.

In particular, we can distinguish two kind of optical fiber:

1. Fiber with low content of SiO_2: these fiber assure a good transmission in the IR band;

2. Fiber with high content of SiO_2: these fiber assure a good transmission in the UV band;

The astronomical spectroscopy favours optical fibers of the second type. An optical fiber connection between the telescope and a spectrograph assures their mechanical decoupling. Moreover, in this configuration, the spectroscope can be thermally checked in order to reduce the structural dilation which cause high errors in the radial velocity measurements.
Important examples spectrographs coupled with optical fibers are: ELODIE and HARPS, mounted from 2003 on the telescopes of Observatoire de Haute Provence (France) and of La Silla Observatory (Chile), respectively.

In order to use the Echelle spectrograph in the RATS project future without precision loss –as we are looking for small variation in the radial velocities curve– Campagnari (2005, *graduation thesis*) has studied the possible configuration for the fiber coupling with the Echelle spectrograph. The resulting configuration foresees an optical fiber which connect the focal plane of the Copernico Telescope with the slit of the spectrograph while a second fiber could catch light from the Thorium lamp.

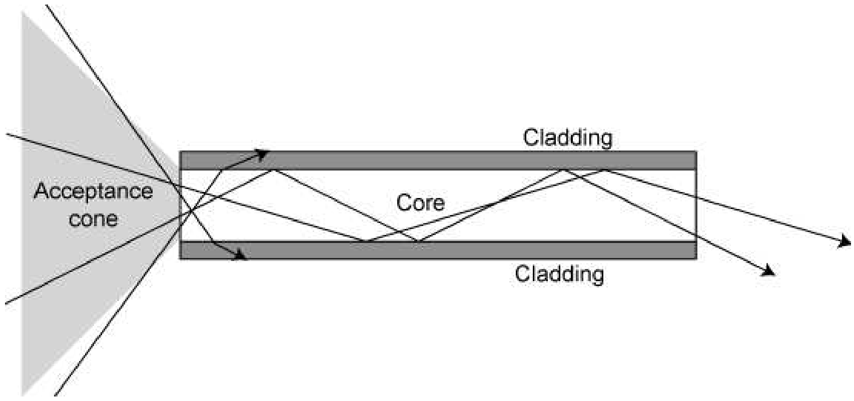

Figure 2.13: The propagation of light through a multi-mode optical fiber.

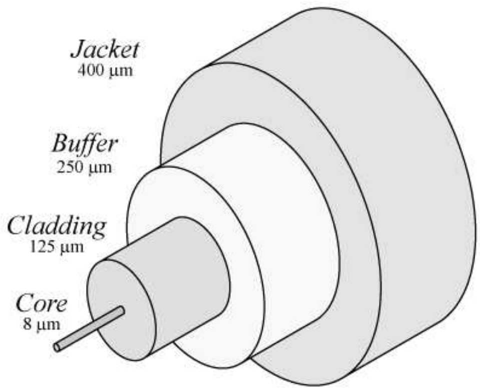

Figure 2.14: A typical single-mode optical fiber, showing typical diameters of the component layers.

2.3 RATS stellar fields selection

RATS observing strategy imposes the survey magnitude range. The faintest magnitude is defined by the efficiency of the spectrograph and its radial velocity precision.

The brighter magnitude will be a compromise between star counts and the possibility to observe the bright star without saturate the detector. For this reason we defocalize the Schmidt telescope so that we can observe, with the necessary photometric precision, stars as bright as 9^{th} without CCD saturation and stars as faint as $13^{th}(14^{th})$ with an already useful signal to noise ratio.

The major obstacle in the transit search is the large number of astrophysical false alarms (Brown, 2003) that can affect the survey. This situation is made worse by the RATS observing strategy that impose to have a $10 \div 11$ arcsec telescope defocusing. For this reason we paid attention to the crowding issue in stellar field selection, estimating the number of unpolluted stars. We define *unpolluted* those stars that have not any catalogue objects within 15 arcsecs from their center.

In addition, to maximize the star counts without telescope PSF blend, the next basic criteria has also been followed in the selection of RATS stellar fields (Claudi et al., 2005):

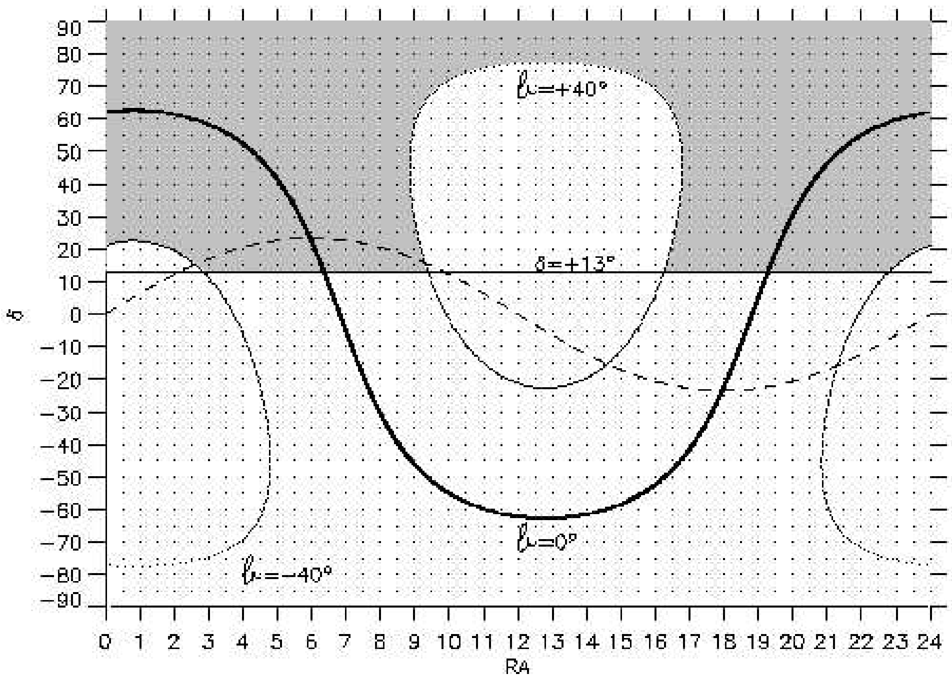

Figure 2.15: The sky fraction limited by "geographical" field selection requisites is shown in gray color (from Claudi et al., 2005).

1. in order to have more than eight hour of visibility from the Schmidt location ($00^h46^m17.3^s$ East Longitude and $+45°50'36.2$" North Latitude) the field declination is $\delta \geq 13°$);
2. to maximize the number of stars per square degree we will observe close to the galactic plane, that is $-40° \leq b \leq +40°$;
3. as FGK dwarf are the best stellar candidates as hosting planets, Claudi et al. (2005) maximized their number in the field.

Once the sky zone that satisfy to the geometrical requisites (Fig. 2.15) was limited, Claudi et al. (2005) developed an algorithm able to explore one or more catalogue searching for the stellar field that maximize the number of suitable stars. At first, in order to minimize the CPU time, Claudi et al. (2005) explored the Tycho Catalogue for one square degree fields. Several fields, almost one for units of right ascension (Fig. 2.16) where selected among those that maximize the merit function:

$$QF = f\frac{N}{N_{\max}} \cdot \frac{Nb_{\max} - Nb}{Nb_{\max}} \quad (2.1)$$

where N is the number of the stars in the field; $N_{\max}$ is the largest number of stars found among all explored fields, Nb is the number of stars brighter than 9^{th} magnitude, $Nb_{\max}$ is the number

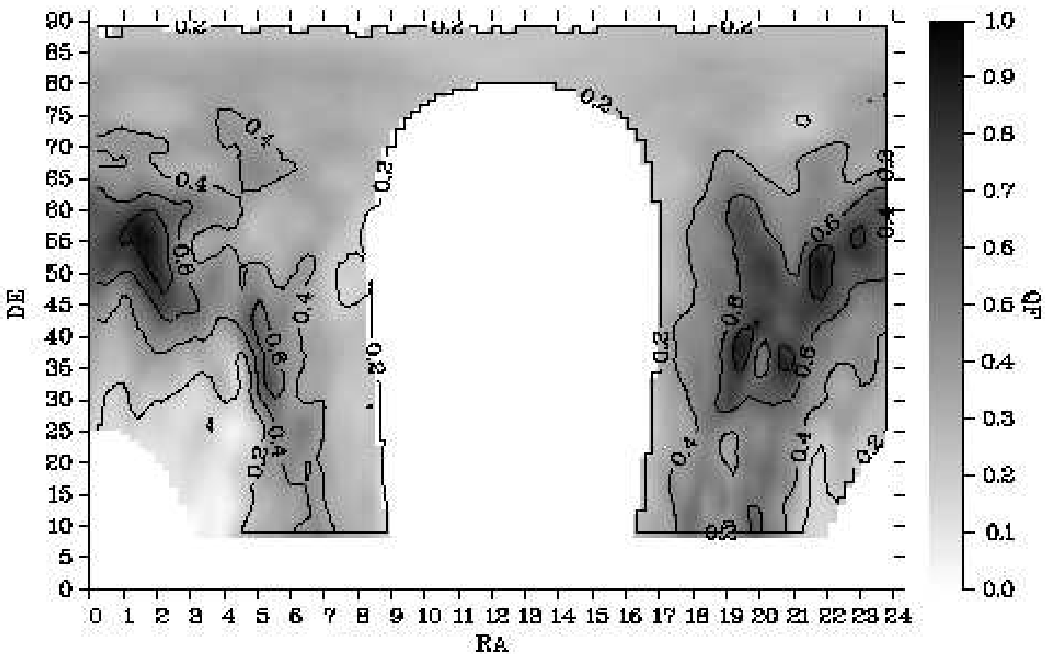

Figure 2.16: The fields distribution in equatorial coordinates, related to the quality factor QF. The grey levels represent different QF values, as shown in the scale on the right, wrapped by the corresponding curve normalized to 1. Curves with $QF > 0.6$ are not shown here in order to avoid to jeopardize the Figure comprehension (from Claudi et al., 2005).

of stars brighter than 9^{th} magnitude permitted in the field without CCD saturation problems and contamination on stars in their neighborhoods and f is a normalization factor.

Successively the selected fields were confirmed by a re-analysis on more complete catalogues. At present time there are three whole sky stellar catalogues which might be appropriate for the confirmation of fields: *2MASS*, *GSC2* and *USNO B1*. The last two catalogues are created from photographic plate digitalization. For this reason they contain a significant number of spurious objects, and the number of objects in the field is a strong function of the original plate sensitivity. In the Eddington Planet Finding Field selection Barbieri et al. (2004) have checked that the limit magnitude of *USNO B1* catalogue seems to be a strong function of the original plate sensitivity.

GSC2 is less affected by these limitations and in particular it contains some status flags that allow to classify the objects in the field (stellar or not stellar objects, dimension etc.). On the other hand, GSC2 is not useful for the spectral classification and giant/dwarf classification. So in order to confirm the selection of RATS fields Claudi et al. (2005) used both 2MASS and GSC2. Moreover, as an ulterior check, we plan to characterize the selected stellar field with photometric and spectroscopic observing campaign.

From this analysis, whose results are shown in Figure 2.16, we selected some fields. The coordinates of their centers are shown in Table 2.4.

RATS fields	Coordinates	
	α	δ
RATS-1	$00^{h}\ 59^{m}\ 19^{s}$	$56^{\circ}\ 08'\ 32''$
RATS-2	$01^{h}\ 46^{m}\ 17^{s}$	$57^{\circ}\ 27'\ 56''$
RATS-3	$02^{h}\ 04^{m}\ 06^{s}$	$56^{\circ}\ 04'\ 09''$
RATS-4	$19^{h}\ 39^{m}\ 32^{s}$	$39^{\circ}\ 10'\ 54''$
RATS-5	$20^{h}\ 24^{m}\ 54^{s}$	$51^{\circ}\ 30'\ 09''$
RATS-6	$21^{h}\ 55^{m}\ 50^{s}$	$52^{\circ}\ 12'\ 06''$
RATS-7	$22^{h}\ 53^{m}\ 36^{s}$	$55^{\circ}\ 27'\ 47''$

Table 2.4: Central coordinates for the seven best selected RATS stellar fields.

2.4 Magnitude interval selection

To detect a planetary transit, we need high photometric accuracy and we need a spectroscopic follow up to confirm that the photometric variation is indeed due to a planet transit.

This last requirement limits the range of magnitudes that we can sample during the survey. In fact, the limiting magnitude to reach a precision in the radial velocity measurements of 10 m/s using the Echelle spectrograph at the Copernico Telescope in one hour exposure is about 14. On the other side the minimum magnitude is set by the observational strategy (see §2.5). A 15 seconds exposure (as foreseen for the Eddington mission) at the Schmidt of Cima Ekar taken in integrated light easily saturates a star with visual magnitude of 13.

The solution adopted to avoid CCD saturation is to *defocus* the telescope. However, one has to guarantee high S/N ratio for the weakest magnitude and also an adequate number of stars per square degree with brightest magnitude. We found that $m_V = 9$ is a good compromise between the number of target stars and the necessary defocus.

The $FWHM$ of a stellar image can be considered as the convolution of seeing, diffraction (airy's figure) and, in our case, defocusing, so that:

$$FWHM^2 = \text{seeing}^2 + \text{airy}^2 + \text{defocus}^2 \tag{2.2}$$

Figure 2.17 shows an example of calculation of defocusing for a star with $m_V = 9$. To avoid troubles with CCD saturation we put a limit to the signal that can be collected at a given exposure time in a CCD pixel, in particular:

$$S_{\text{pix}} \leq 0.75 \times FullWell - S_{\text{sky}} \times t_{\text{exp}} \tag{2.3}$$

where S_{pix} is the limit mentioned above, $FullWell$ is, S_{sky} is sky background per pixel per second and t_{exp} is the considered exposure time. Dividing the star total flux by S_{sky} one obtains the number of pixels over which to spread the signal. Multiplying this quantity for the pixel sky projection one obtains the area A which is related to the $FWHM$ of the stellar image (assumed to be a Gaussian) by the following expression $A = \pi FWHM^2$. Using then equation (2.2) one can calculate the amount of defocusing. Infact, once the exposure time has been set, the defocusing depends on the seeing, on the sky background and on the characteristics of the CCD.

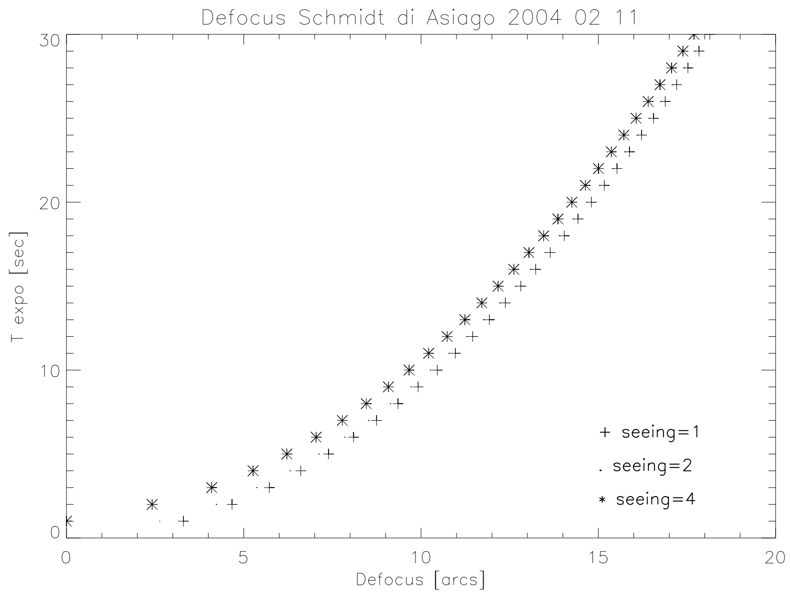

Figure 2.17: The relation between defocus for a star of $m_V = 9$ and the exposure time at the Asiago Schmidt telescope, depending on different seeing values (from Claudi et al., 2005).

2.5 RATS observing strategy

From stellar counts one finds that the number of stars per square degree with $9 \leq m_V \leq 14$ and spectral types F,G,K is about 200 (Claudi et al., 2005). With three fields selected and a CCD field of view of about 0.8° the total field of view covered by the survey would be 2.4°. This means that the total number of possible candidates is about 480 stars. The probability of having a hot Jupiter is about 1% while the probability of observing an Hot Jupiter transit is 10% so the total probability to observe a transit is 0.1%. This number has to be reduced by a factor that take into account the observing conditions (temporal coverage, duration of transit, period of transit etc). In particular, the probability of observing a transit during a night is $P_t = \Delta T/T_{\mathrm{orb}}$ where ΔT is the total observing time and T_{orb} is the orbital period ($\Delta T < T_{\mathrm{orb}}$).

The total probability of detecting a transit observing the same field for n nights is then:

$$P = 1 - (1 - P_t)^n \tag{2.4}$$

Using typical numbers for observing conditions at Cima Ekar, $\Delta T = 4.2$ hours, $n = 40$ days and $T_{\mathrm{orb}} = 4$ days, one obtains $P = 0.83$ which gives us a total probability of detecting a transit of 0.083%. This yields 0.4 transit per year and a total number of detected transits during the survey of 2.

This number can be increased only increasing the sky coverage of the survey. The idea is to have for each of the fields selected a number of different but adjacent pointings. This solution has a drawback. In fact, for each true transit detection, the number of expected false alarms varies between 6 and 60 (Brown, 2003). This has an impact on the spectroscopic follow up in terms of pressure on the Echelle spectrograph. In Figure 2.18 we have plotted the pressure on

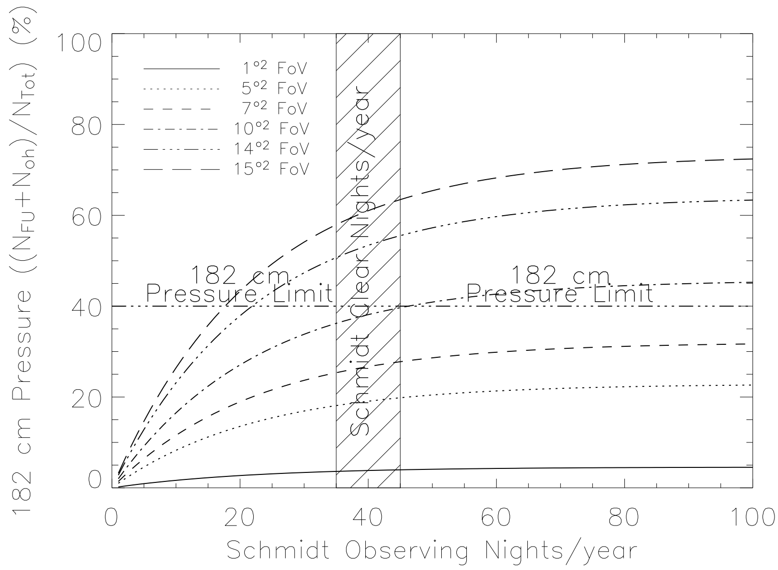

Figure 2.18: The percentage of necessary spectroscopic follow up time as a function of the number of observing nights per year at Cima Ekar for different numbers of pointings (from Claudi et al., 2005).

the Copernico telescope as a function of the observing nights for different numbers of pointings. Assuming that the maximum acceptable value of night sharing on the Copernico telescope is 40% of the total nights the number of pointings compatible with this limit is about 7. An increase in the sky coverage by a factor of 7 will increase the number of detected transits per year to 2.8 and the total number to 14. Having several adjacent pointings will have an impact on the observational duty cycle too, because an observer cannot observe continuously the same field but one has to move among adjacent subfields. For 7 subfields, assuming a 4×15 seconds exposure time for each pointing, 5 seconds to go from one pointing to the next and 30 seconds to go back to the first pointing yields a total duty cycle interval of about 10 minutes, that should give a fair sampling of the transit curve. We did not include the CCD readout time in the overheads because the CCD is frame transfer so the readout is done during the exposure.

2.6 RATS hardware and software environment

2.6.1 Hardware dataflow

The hardware layer includes the Schmidt telescope, the server and workstation PCs, the storage devices such as external hard disk and DVD/CD burner. It includes all access to the actual telescope configuration. All data capture information are provided to the rest of the program from this component and actual communication with the telescope and or images (or any other resource external to the software) takes place through this component.

In Figure 2.19, we present the scheme of the operational environment and the interfaces between the different external components for the RATS project. A personal computer with a `WinNT` operative system, called `cold60` and installed at Cime Ekar, is plugged in a local network with the Schmidt telescope and devoted to the data capture.

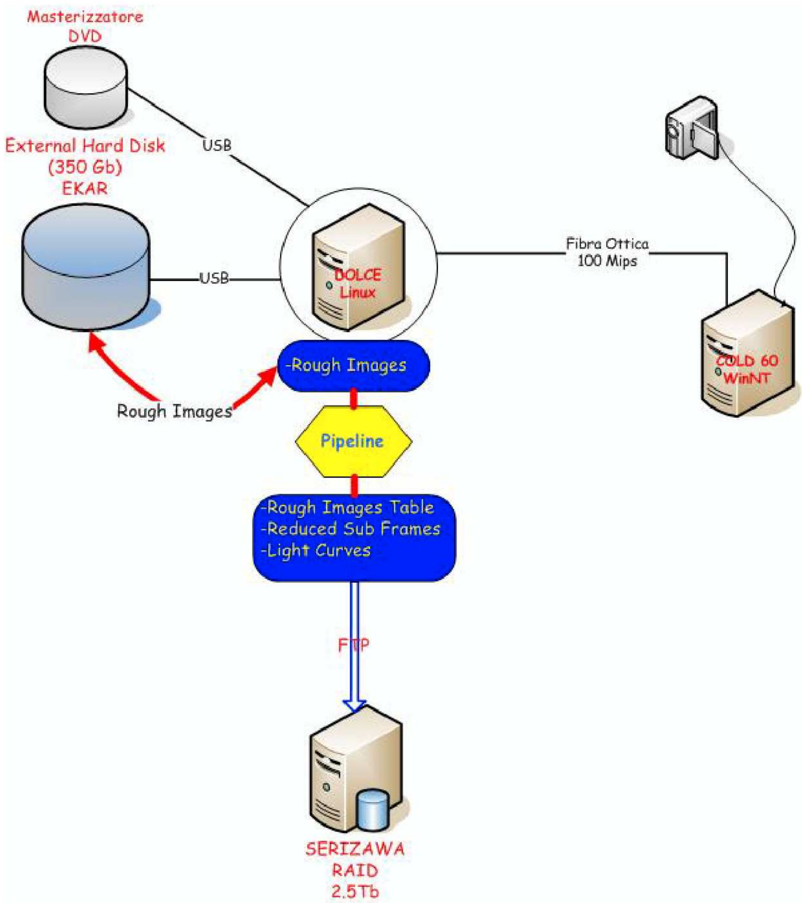

Figure 2.19: Hardware interfaces and software relationship with external environment.

The morning after the observations, the rough images are moved to another PC, `dolce` with a `Linux` operative system, setted near the Copernico telescope. It is connected at `cold60` with a optical fiber backbone. The nominal transfer rate for this network is about 100 Mibs. External hard disk and a DVD burner are connected to `dolce` and used as back up devices. The RATS reduction pipeline is installed on this last work station. After images reduction, data files are sent to the server **`serizawa`**, via FTP protocol, located at Padova Observatory server room. The RATS database will be installed on this `Linux` machine.

As RATS–*ARP* (see chapters 4 and 5) –the automatic reduction software– shall run at the end of the observations, any performance requirements are requested from external systems. The reduction of a single image of the selected night shall be 180″ or less. This quantitative performance is referred to specified conditions listed below:

- **Interface requirements:** defines those elements with which the pipeline must interface and communicate.
  - ▷ *Software interface requirements:* RATS–*ARP*P shall be executed under `Linux` and, specifically, the Fedora 6.0 operating system or higher.

- ▷ *Hardware interface requirements:* the software shall run on Pentium IV workstation of 1 GHz and 256 MB RAM.
- ▷ *Communications interface requirements:* RATS–*ARP*P shall use the standard communications protocols as intrinsic to and offered by the above specified operating system.

- **Operational requirements:** describes the requirements on the operation mode, the man/machine interface and the RATS–*ARP* operator skill profile
  - ▷ *Operation mode:* the operation mode of RATS–*ARP* shall be automatic.
  - ▷ *Man/machine interface:* the man-machine interface shall be a display screen, a pointing device (typically a mouse or a pen) and a keyboard. The RATS–*ARP* screen interface shall be a user-friendly windows. The User needs to perform plain editing of text and/or program source code. Thus, all necessary RATS–*ARP* commanding and interactions with the User (data entry, computations, display) shall be performed via window-based interface.
  - ▷ *Operator skill profile:* RATS–*ARP* shall be operable by multi-users both with basic and specialist knowledge of the transit observational technique. Special hardware, software and programming knowledge shall not be required by Users.

- **Resource requirements:** describes the physical-technical resource requirements such as processing power, RAM memory, disk space, disc access time and screen resolution.
  - ▷ *Processing power:* Pentium IV workstations (1 GHz clock rate) is required as minimum. Faster machine are not required but it shall be clear that they lead to an significant improvement in the performances in case of intensive computations.
  - ▷ *RAM memory:* 256 MB RAM is required, even if more RAM is recommended. 512 MB or 1 GB RAM shall allow performance improvements.
  - ▷ *Disk space:* 50 GB free disk space is required. More disk space is highly recommended in expectations of future RATS observations. Free disk space of 500 GB or more provides suitable room for a multiple of nights' reductions.
  - ▷ *Disk access time:* even if a disk access time of 10 msec is enough, any faster access improves the RATS–*ARP* performance and is recommended.
  - ▷ *Screen resolution:* a screen resolution of at least 1152 x 900 pixels is required, a resolution of 1280 x 1024 pixels or higher is recommended for improved on-screen plotting.

- **Portability requirements:** the software shall be portable to platforms other than Pentium-based `Linux` workstations with limited efforts (*e.g.* `SUN`-based workstation machines).

Detailed hardware requirements are available in appendices B and C, both compiled according to ESA Software Engineering Standards (1991) format.

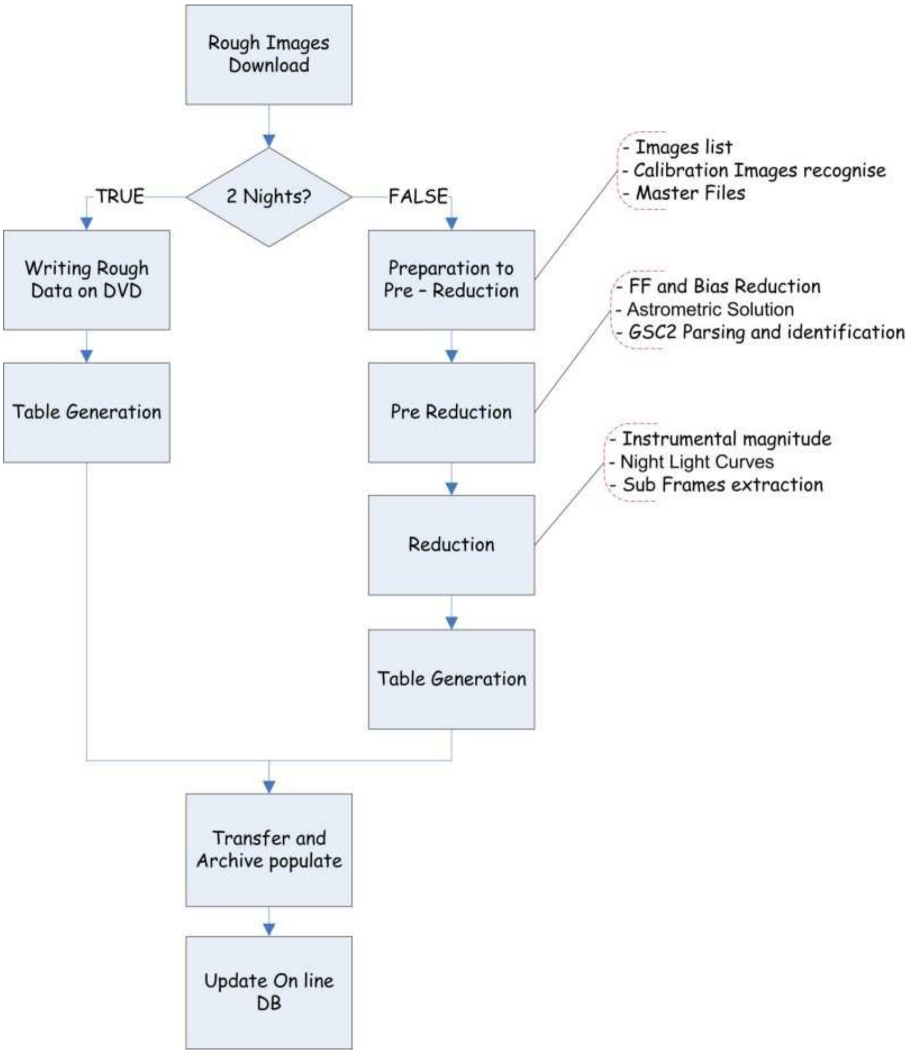

Figure 2.20: Scheme for the software dataflow for the RATS project.

2.6.2 Software dataflow

After the images download is completed on `dolce` (see Fig. 2.19 and §2.6.1 for details), in order both to archive and work on RATS photometric data, we operate at two distinct levels at the same time, as outlined in Figure 2.20. On one hand, row data are burned on a DVD device as a backup archive. On the other hand, the pipeline is triggered and starts the pre-reduction and reduction process (see chapters 4 and 5 for details).
At the end of both of these two parallel paths, both raw and reduced images have sent to RATS database (see chapter 7 for details) in order to populate and update the on-line archive.

The time spent by the Schmidt telescope to have the seven adjacent pointings is more or less 3 minutes. Considering this datum, for the SITe-424A CCD camera we have calculated the space amount occupied by all the raw images acquired during all the RATS project life (5 years), assuming that not even one night is loss. The results, summarized in Table 2.5, show that 2Gb of raw data are acquired during each night.

Month	h/night (h)	Useful day (d)	h/month (h)	# Exp/month	Dataflow raw images (Gb)
August	6.00	15.00	90.00	2.40E+03	3.02E+01
September	8.07	15.00	121.05	3.23E+03	4.06E+01
October	9.77	15.00	146.55	3.91E+03	4.92E+01
November	11.00	14.00	154.00	4.11E+03	5.17E+01
December	11.59	14.00	162.26	4.33E+03	5.44E+01
January	11.25	14.00	157.50	4.20E+03	5.28E+01
February	10.22	14.00	143.08	3.82E+03	4.80E+01
March	8.66	15.00	129.90	3.46E+03	4.36E+01
Total/year			1.10E+03	2.94E+04	3.71E+02
Total			5.52E+03	1.47E+05	1.85E+03

Table 2.5: Counting of occupied space by RATS images during 5 years of observations. In the first column, there a list of suitable months for observations; in the second one, a list of the hours fraction per night suitable for the observation is presented; the third column lists the number of observable nights; in the second one, a list of the hours fraction per month suitable for the observation is presented; the fifth column shows the number of exposures per month and the last column gives the space amount allocated for all the images of the month. Corresponding total amount of space are listed in the last two lines.

2.7 RATS Users

The pipeline's Users will be scientists and technicians with different levels of knowledge of the observation methods –with particular regard to the transit search mechanism– and a minimum level of expertise in scientific programming. In particular, a background in astronomical reduction technique and observational strategy technique are necessary requirements for RATS pipeline Users who, thereby, will be scientists with basic or specialist knowledge and engineers with a basic knowledge, of the transit observation technique who wish to have a software for supporting mission planning and performance evaluation of the entire system with particular interest in technical effects. Details are fully illustrated in section §B.2.5.

Chapter 3

RATS headerfits

In the late 1970s, the Westerbork Synthesis Radio Telescope (WSRT) in Westerbork, Holland and the Very Large Array (VLA) in New Mexico began producing high quality images of the radio sky. Since the two groups were observing at different frequencies, they wished to collaborate in constructing spectral index maps by combining data obtained from the two instruments. These two different institutions would normally structure their data in different ways because machines at the two different installations might have different architecture. Lacking a standard format for transporting images, an astronomer taking data from an observatory to a home institution would have to create special software to convert the data to the format used at the home institution.
An obvious substitute for all these cumbersome processes was the creation of a single standard interchange format for transporting digital images among cooperating institutions. The *Flexible Image Transport System* (hereafter, *FITS*) was created to provide such a transfer format. From its initial applications, the use of `FITS` has expanded to include the entire spectrum of astronomical data, becoming the standard format.

In this chapter, we describe the typical `FITS` format for the header of a RATS image: each keyword has been chosen *ad hoc* as input parameters for the reduction software described in chapters 4 and 5.

3.1 What is `FITS`?

The fundamental unit of `FITS` is the *.fits* file, which is composed of a sequence of Header Data Units (HDUs), optionally followed by a set of special records. (The rather prosaic name HDU was the result of over a year's community discussion and failure to find anything better.) The first part of each HDU is the header, composed of ASCII card images containing keyword=value statements that describe the size, format, and structure of the data that follow. It may contain any information about the data set that its creator regards as important, such as information about the history of the data or the file, about the physical entity the data describe, or about the instrument used to gather the data. The data follow, structured as the header specifies. The size of logical records in both header and data is 23040 bits, equivalent to 2880 8-bit bytes or 36 header cardinboth images. The HDUs may be followed by special records; the only restrictions on these special records are that they have the standard 23040-bit logical record size and that they not begin with the string XTENSION. A FITS file is terminated by a logical end of file, whose precise physical nature will depend on the medium.

In its original form, a FITS file consisted solely of a single HDU, consisting of the header and a data array that was regarded as containing a digital image. This simple, one-HDU structure is known as Basic FITS. The header card images would describe the data array–the number and length of the axes and the data type of the values: unsigned one-byte, signed two-byte or four-byte integers. The original use of FITS to transport digital images is reflected in the "Image" in its name. However, even the data matrix of Basic FITS could be used to transmit any kind of multidimensional array, not simply an image. The first HDU of a FITS file, called the primary HDU, must still follow the Basic FITS format, although it need not contain any data.

FITS is no longer restricted to integer arrays. The array data may be Institute of Electrical and Electronics Engineers (IEEE) 32-bit or 64-bit floating point. The Basic FITS primary HDU may be followed other HDUs, called extensions, containing different data structures. Standard data formats include two kinds of tables: tables with ASCII entries and tables with binary entries, as well a multidimensional array extension format that allows extensions to contain the same type of data that is in the primary HDU. It is also possible to create non-standard formats, for use locally or as prototype designs for new standard formats.

Although its name implies "image" transport, FITS is not a graphics format designed simply for the transfer of pictures; it does not incorporate "FITS viewers", packages for decoding the data into an image. Users must develop or obtain separate software to read and display the data from the FITS file. Because of its wide use, FITS is supported by all the major astronomical imaging packages, and a number of other packages of FITS utilities and software are publicly available. The data structure is an essential part of the format and is available to the users. This property distinguishes FITS from many other data standards–those that are primarily labeling systems, and those for which the user accesses a hidden data structure through a set of standard tools.

3.2 The FITS's philosophy

FITS incorporates a philosophy along with the data format. The underlying goal is to provide a standardized, simple, and extensible means to transport data between computers or image processing systems. Any FITS reader should be able to cope with any FITS formatted file, skipping over portions (extensions) and ignoring keywords that the reader does not and need not understand.

Simplicity requires that reading and writing FITS should be implemented in a fairly straightforward way on any computer used for astronomical reduction and analysis. Simplicity also implies that the structure of the file should be self-defining and, to a large degree, self-documenting.

The first word in FITS is "flexible". The format needs to be flexible to facilitate extensibility for different applications. Hence, the number of strict rules is not large. Because the files are self-defining, FITS can fulfill a large range of data transport needs. FITS can be used not only for unambiguous transportation of n-dimensional, regularly-spaced data arrays, but also for additional information associated with such a matrix. FITS can also transport arbitrary amounts of text within standard data files. The history of manipulations of the data can thus easily be recorded in self-documenting data files. FITS is sufficiently general for a wide variety of applications. The introduction of new keywords permits addition of new information as needed, and the use of extensions allows almost unlimited flexibility in the type of information to be stored. Thus, FITS can grow with the needs of the astronomical community.

The great flexibility of FITS is a potential weakness as well as a strength. While there is a great temptation to proliferate keywords and new extension types, caution should be exercised in this process. Because FITS is a worldwide medium of data exchange, extension formats need to be coordinated under the International Astronomical Union FITS Working Group (IAUFWG) to prevent duplication and inconsistencies in usage, and agreements should be reached governing keyword conventions in particular fields. The structure under the IAUFWG provides an overall authority for the FITS standard, but additions to FITS are not created by the IAUFWG but are designed by FITS users and then acted upon by the international structure. Although the number of strict rules is not large, there is an extensive set of recommended practices. Creators of FITS files should adhere to these recommendations if at all possible; in particular, the rules of FITS should not be exploited to create files that try to mimic the local format, and, although in technical compliance with the rules, depart from the recommendations to such an extent that they don't look like FITS files. General adherence to recommended practice will simplify the task of the FITS software developers; if a FITS file contains too many unconventional but permitted constructs, many FITS readers may not be able to handle it. Not everything that is permitted is wise.

Users who develop extensive libraries of FITS files need assurance that they will not have to periodically revise these files because of changes in the standard. This requirement gives rise to one of the fundamental principles of FITS: no change in the rules should render old FITS files unreadable or out of conformance–the principle of "once FITS, always FITS". This philosophy is reflected in data reduction and analysis packages in which all obsolete implementations are trapped and processed in the most accurate manner possible. While adherence to this principle has perpetuated some constructs that have proven with time to be awkward, it is better than the alternative of requiring revision of existing FITS files.

Changes in the FITS rules may add new structures that old software cannot handle. Revised software will be required for new standard extensions, but revising a software package is a far smaller effort than updating a full data library would be. As far as is possible, however, FITS should be expanded in such a way that the old software will still be able to process those parts of the file which it is capable of handling. In such a case, software should not fail or give incorrect results when confronted with the new extension or conventions; it should simply ignore them and continue to process those parts of the file that it can understand.

FITS is defined as a logical structure, not tied to the properties of any particular medium, thus allowing its continued use as the technology changes. Conventions for its adaptation to any medium are independent of the logical structure of FITS. Because its original development was for 1/2 inch magnetic tape, its structure is well adapted to that medium and the conventions are long established. More recently, more generalized conventions have been adopted for the expression of FITS on magnetic tape and on magnetic and optical disk. Conventions can be defined for new media as they develop.

3.3 The ASCII Tables

The concept of a standard flexible format for the transfer of astronomical data was so appealing that astronomical software designers sought to apply the format to data and information structures other than simple arrays. For example, astronomers make extensive use of catalogs.

Such information would most naturally be stored as a table. The wide variety of tabular information led to the development of the ASCII table extension. The following three main classes of potential applications were envisioned

1. Standard catalogs such as star or source catalogs.

2. Observing information such as observing logs, calibration tables, and intermediate tables related to the observing. The results of the observations might appear as the Basic FITS matrix, and the auxiliary information would follow in a table.

3. Tabular results extracted from observational data by data analysis software. As an example, many programs automatically detect sources in digitized images and write parameters such as position, flux, size, spectral index, and polarization into output files. Astronomers need to transmit these output tabular files; recipients can then use software designed to manipulate, merge, and intercompare these tables.

The ASCII table FITS extension (Harten et al., 1988, hereafter FITS Paper IV) conforms to the standard FITS rules and to the generalized rules for FITS extensions. The column headings are provided in an extension header that describes the contents of the table. The table data are stored as a large character array. Each row of the table consists of a sequence of fields. Each field is described by a series of keywords specifying the field format using FORTRAN 77 notation, the location in the row where it begins, and possibly a column heading or other information about the field.

3.4 Basic FITS

The fundamental unit of a FITS data set is the file, which begins with the ASCII string SIMPLE = T, where the first 6 bytes of the file contain SIMPLE, the "=" is in byte 9, the T is in byte 30, and the intervening bytes contain ASCII blanks. This 30-character string is the signature of FITS, the way in which generalized software can identify the file as FITS. The string is not to be used if the file deviates from the rules for FITS in any way. A FITS file ends with an end-of-file mark appropriate to the medium on which it is written. A FITS file is composed of 23040-bit (2880 8-bit byte) logical records, organized into a sequence of header data units (HDUs). This logical record length was chosen because it was an integral multiple of the byte and word lengths of all computers that had been sold in the commercial market in or before 1979, the time of the original FITS agreement. Each HDU consists of one or more logical records containing an ASCII header followed by zero or more records of binary data. The first HDU is called the primary HDU; those following are called extensions. The last extension may be followed by 23040-bit special records, which need not be organized as HDUs.

Each FITS header record consists of 36 80-byte "*card images*" written in 7-bit printable ASCII code (ANSI 1977) with the sign bit set to zero. The header may contain as many records as are needed for the card images. The END card image is the last. The remainder of the last record of the header is filled with ASCII blanks to its full 23040-bit length. These header records should contain all the information necessary to read and label the associated data.

The first or primary HDU is governed by special rules. Its data records, if present, contain a matrix of data values, in one of several binary formats, called the primary data array. The array may have no more than 999 axes.

3.4.1 Primary header

Each card image in the header is in the following form:

`keyword = value /comment`

Keywords can be no more than eight characters long. The only characters permitted for keywords are upper case (capital) Latin alphabetic, numbers, hyphen, and underscore. Leading and embedded blanks are forbidden. There are two special classes of keywords: *required keywords* and *reserved keywords*. If a keyword is required, then a card image with that keyword must appear in the header. Reserved keywords do not have to appear in any header, but they may be used only with the reserved meaning if they do. Users may define their own additional keywords for any FITS file.

The contents of the keyword field determine the structure of the value field. Keywords that have values associated must contain "= " in columns 9 and 10; otherwise, columns 9 – 80 are regarded as comment. Except for the special cases of the `HISTORY` and `COMMENT` keywords and a blank keyword field, if a keyword does not have a value, column 9 must not contain "=". The name of the keyword governs whether a value is present. Keyword values have one of four types: *logical*, *character string*, *integer*, or *floating point*.

The following notation will be used to show what type of value must be associated with each keyword:

`keyword (value type)`

The discussion that follows the keyword name will describe the meaning of the value.

The following content is required for the first ten columns of a header card image:

- Keyword name beginning in column 1, ending in or before column 8. The remainder of columns 1 – 8 is blank filled.
- If the keyword has a value associated with it, "=" in column 9, followed by a blank in column 10.
- If the keyword has no value and is not the reserved `HISTORY`, `COMMENT`, or blank field, any content other than "= " in columns 9 and 10 must be present.
- For the reserved `HISTORY`, `COMMENT`, and blank field keywords, the contents of columns 9 and 10 are not restricted.

The following fixed format is mandatory for values of the required keywords and its use is strongly recommended for other keywords. The structure of a fixed format value field depends upon its type:

- (*Logical*) `T` or `F` in column 30.
- (*Character string*) A beginning single quote (`'`) in column 11 and an ending single quote (`'`) in or after column 20 but no later than column 80, with the string in between.
- Real part (*integer* or *floating*) right justified, ending in column 30, 20 columns maximum.

- Imaginary part (*integer* or *floating*) right justified, ending in column 50, 20 columns maximum, i.e., starting in column 31 or after.

When the fixed format is not used, the value field must be written in a notation consistent with the list-directed read operations in FORTRAN 77. Such a notation has the following requirements for the different formats:

- (*Logical*) The first non-blank character in columns 11 – 80 is T or F.
- (*Character string*) Begins with a single quote (') in column 11 or later, and ends with a single quote (') no later than column 80, with the string in between. Starting in column 11, only blanks are permitted in the value field before the opening quote.
- (*Integer*) May occupy any of columns 11 – 80.
- (*Floating*) May occupy any of columns 11 – 80. The decimal point must always appear explicitly, whether or not exponential notation is used. When exponential notation is used, all letters, (*i.e.*, E, indicating an exponential) must be in capitals.
- (*Complex*) Consists of real and imaginary components (integer or floating point), anywhere in columns 11 – 80, separated by at least one column.

Many keywords, called *indexed keywords*, consist of an alphabetic root and a number (*i.e.*, CTYPE*n*). If there is only one index, the number does not have leading zeroes.

Any information in a character string value that the reading software needs to retrieve the data from the FITS file should be in the first eight characters, for the benefit of primitive systems.

Comments may be incorporated in a header card image whether or not a value is present. If a value is present, place a slash (hexadecimal 2F) between the value and comment field, with at least one blank between the end of the value and the slash. For the fixed format, the slash and space are not required, but using them when writing a FITS file will simplify the task of the reader. If the fixed format is not used, a slash serving as a delimiter, a requirement derived from FORTRAN list-directed read, is required before the comment. If the keyword has no associated value (which is immediately apparent when column 9 does not contain "="), then the entire content of columns 9 – 80 is a comment. In such a case, it is best to leave column 9 blank.

3.4.1.1 Required keywords

The following keywords are required for all basic FITS headers and must appear in the order given below. The value field must appear in the fixed format described above.

1. SIMPLE (*logical*) – A value of "T" signifies that the file conforms to FITS standards. A value of "F" is used for files that resemble FITS files but depart from the standards in some significant way. Such files might be convenient for internal use by a particular organization or for exchange between Users who wish the files to have an overall FITS-like structure. Communication with outside Users is much more difficult in this case. Files with SIMPLE = F should not be described as FITS files.
2. BITPIX (*integer*) describes how an array value is represented:

8 ASCII characters or 8-bit unsigned integers;
16 16-bit, twos complement signed integers;
32 32-bit, twos complement signed integers;
-32 IEEE 32-bit floating point values;
-64 IEEE 64-bit floating point values.

No other values for are valid. With the use of negative values of BITPIX to signify floating point array values, the number of bits per data array member is the absolute value of BITPIX.

3. NAXIS (*integer*) is the number of axes in the data following the associated primary data array. A value of zero is acceptable and indicates that no data are associated with the current header. The maximum possible value is 999. Negative values are not allowed.

4. NAXIS$n, n = 1, \ldots N$ (*integer*) is the number of elements along axis n of the array, in order of most rapidly index variations. A value of zero for any of the NAXISn signifies that no data array is associated with the header. None of the NAXISn may be negative.

5. END (*no value*) – The last keyword must be END. This card image has no "=" in column 9 or value field but is filled with ASCII blanks.

Other keywords may appear only between the last NAXISn and END keywords. The remainder of the last header record should be filled with ASCII blanks.

3.4.1.2 Reserved keywords

Many of the following reserved keywords were originally suggested by Wells, Greisen & Harten (1981). If a reserved keyword is used, the meaning and structure must be as described here. Keywords other than the reserved keywords should not be used in their place to express the same concepts. Reserved keywords may appear in any order between the required keywords and the END keyword.

Some of the following keywords describe the **data array**:

- BUNIT (*character*) represents the physical units of the quantity stored in the array, *i.e.*, magnitudes/pixel. The name stands for "*brightness units*".

- BSCALE (*floating*) is a scale factor used in converting array elements stored on the FITS data set to physical values, as:

$$\text{physical\_value} = \texttt{FITS\_value} \times \texttt{BSCALE} + \texttt{BZERO} \tag{3.1}$$

  If this keyword is not present, the scale factor is assumed to be 1.

- BZERO (*floating*) is the offset, the physical value corresponding to a stored array value of zero, in Eq. (3.1). If this keyword is not present, the offset is assumed to be zero.

- BLANK (*integer*) should be regarded as a code, not a number. If the text "BLANK " appears in columns $1-8$, then the value will be stored in those elements of an integer array that have an undefined physical value. The BLANK keyword does not have the same meaning as filling columns $1-8$ with ASCII blanks.

The reserved keywords permit complete specification of a linear **coordinate system** for any axis:

- CTYPEn (*character*) is the name of the physical coordinate for axis n (*i.e.*, right ascension and declination). The convention of using the first four characters of the value field of this keywords to identify the standard system has been adopted, as shown in Table 3.1. The

'RA--',	'DEC-':	equatorial coordinates (α, δ)
'GLON',	'GLAT':	galactic coordinates (l, b)
'ELON',	'ELAT':	ecliptic coordinates (λ, β)
'SLON',	'SLAT':	supergalactic coordinates
'HLON',	'HLAT':	helioecliptic coordinates

Table 3.1: Identification of sky coordinate systems.

  values of the CTYPEn provide both the world coordinate system and the projection used. For example, if the data matrix contained a sky map in right ascension and declination projected on the plane using the tangent projection, as for RATS images, the CTYPEn values would be:

```
CTYPE1 = 'RA---TAN'
CTYPE2 = 'DEC--TAN'
```

  Obviously, the coordinates must be logically consistent.

- CRPIXn (*floating*) is a location along axis n called the *reference pixel*, or *reference point*, used in defining the range of values for the physical coordinate of axis n. It is given in units of the counting index that runs from 1 to the value of NAXISn, incrementing by one for each pixel or array position. The value of CRPIXn may be a fractional index number and/or be outside the limits of the array.

- CRVALn (*floating*) is the value of the physical coordinate identified by CTYPEn at the reference point on axis n.

- CDELTn (*floating*) is the rate of change of the physical coordinate along axis n per unit change in the counting index, evaluated at the reference point.

- CROTAn (*floating*) is the rotation angle, in degrees, of actual axis n of the array from the coordinate type given by CTYPEn. As there is no prescribed rule for describing such rotations, its nature should be explained in detail using comments.

Default values have not been defined for any of these keywords.
These reserved keywords, allow the definition of simple rectangular coordinate systems, but they do not prescribe the relation between the plane rectangular coordinate system of the FITS array and the spherical coordinate region of the sky that it represents.

- DATAMAX (*floating*) is the maximum data value in the array, after any scaling transformation has been applied to the stored array value.

- ✘ DATAMIN (*floating*) is the minimum data value in the array, after any scaling transformation has been applied to the stored array value.

Note that DATAMAX and DATAMIN apply to the physical values represented, not to the numbers in the FITS file.

Some keywords provide **information on the observations** represented or the production of the data set.

- ✔ DATE (*character*) is the date the file was written (dd/mm/yy order). UT is recommended. The value may refer to the creation date of the original file rather than that of the current copy so that the value of the DATE keyword does not change in coping the files. Note that with this format, the century is unfortunately ambiguous.

- ✔ DATE-OBS (*character*) is the date of data acquisition (UT recommended) and it tells when the observations were made (dd/mm/yy order). Whether this value refers to the start, midpoint, or end of the relevant time interval should be specified in comments.

- ✔ TELESCOP (*character*) is the data acquisition telescope.

- ✔ INSTRUME (*character*) is the data acquisition instrument.

- ✔ OBSERVER (*character*) is the observer name or other identification.

- ✔ OBJECT (*character*) is the object observed.

- ✔ EQUINOX (*floating*) is the equinox of the coordinate system (in years). In early FITS data sets, the keyword EPOCH was used with this meaning.

- ✔ COMMENT (none) means columns $9 - 80$ are a comment.

- ✔ HISTORY (none) means columns $9 - 80$ are a comment. This keyword discusses the history of how the data were processed.

These keywords are the only ones without values that can have "=" in column 9. Users may define other keywords to contain comments as well. For these keywords, column 9 may not contain "=".

3.5 World Coordinate Systems (WCS)

While every point in the FITS data array can be located in the cooordinate system determined by the array axes, scientific interpretation requires knowledge of the physical or world coordinates corresponding to the index points. The original FITS papers reserved several keywords (CTYPEn, CRPIXn, CRVALn, CDELTn, and CROTAn) for use in specifying this relation. While the original paper (Wells, Greisen & Harten, 1981) defined these keywords only for linear transformations, they can be also be adapted for non linear transformations using the definitions in section §3.4.1.2. However, for a non linear transformation, some keywords in addition to those reserved will be required to provide a full description.

To create FITS arrays representing the images of objects in the sky requires projection of the celestial sphere onto the array plane. The original FITS papers did not specify how this process was to be carried out. The first approach to this problem, implemented in the Astronomical Image Processing System (AIPS) and described in AIPS Memo 27 (Greisen, 1983), has been widely used, but no conventions have been formally endorsed by the IAU `FITS` Working Group. (Greisen & Calabretta, 1996, , hereafter GC) have expanded the AIPS approach into a comprehensive proposal for conventions to be used in projecting spherical coordinates onto a two-dimensional plane.

Following these conventions in creating a data set will make it easier for many others to read and understand the data. Because these conventions have not been formally approved as part of standard `FITS`, data sets that use other conventions are not out of conformance. However, these conventions are widely used and have the best software support.

3.5.1 Coordinate Keywords

There are a number of standard equatorial coordinate systems. Hanisch & Wells (1988) proposed the following keywords to supplement the reserved keywords discussed in section §3.4.1.1.

- `RADECSYS` (*character*) standing for RA/DEC system specifies the reference frame for the equatorial coordinate system. It should be used when the `CTYPE`n values are an `RA--xxxx/DEC-xxxx` pair. Table 3.2 shows the four values defined. The default value is FK4. Under the FK4, the date of equinox (value of the `EQUINOX` keyword) is interpreted as a Besselian epoch and under FK5 as a Julian epoch. If there is no `EQUINOX` keyword (or `EPOCH` for old `FITS` files), the equinox is assumed to be 1950.0 for FK4 and 2000.0 for FK5 by default.

- `MJD-OBS` (*floating*) specifies the time of observation in the form of a Modified Julian Date (JD - 2400000.5), in the International Atomic Time time scale. Whether this point refers to the starting, midpoint, or ending time is not defined: comments should be used to make it clear. Use of this keyword permits greater precision than `DATE-OBS` (see §3.4.1). Because the FK4 reference frame is not inertial (there is a small but significant rotation relative to distant objects) epoch or time of observation is required to specify when the mean place was correct.

`'FK4     ':`	mean place old (before the 1976 IAU) system
`'FK4-NO-E':`	mean place old system but without e-terms
`'FK5     ':`	mean place new (after the 1976 IAU) system
`'GAPPT   ':`	geocentric, apparent place, after the 1976 IAU system

Table 3.2: Reference frames for equatorial coordinate systems.

3.6 RATS headerfits: an example

In Table 3.3 we present the characteristic headerfits selected *ad hoc* for RATS images. The first 5 keywords and the last one are the required keywords explained in section §3.4.1 ("Required keywords" paragraph).

Table 3.3: Example of RATS header FITS image.

```
SIMPLE  =                    T /
BITPIX  =                   16 /
NAXIS   =                    2 /
NAXIS1  =                 2200 /
NAXIS2  =                 2200 /
EXTEND  =                    F / File may contain extensions
DATE-OBS= '2005-10-28T23:45:19'/
EXPTIME =                   12 /
TERROR  =                      /
RELEASE =  CIA Solare-COLD-1.0 /
PIX_HI  =                65535 /
PIX_LO  =                    0 /
IMATYPE =             'OBJECT' /
BINNX   =                    1 /
BINNY   =                    1 /
STARTXY =              '0 * 0' /
OBSERVER=            'Granata' /
AREACCD =        '2200 * 2200' /
DETECTOR=            'SITE_2k' /
TCAMERA =                 6.87 / CAM Temp.
TCCD    =               -38.73 / CCD Temp.
COMMENT ='40rats10
BIAS1   =               11.991 / VRD
BIAS2   =               14.587 / VDD
BIAS3   =                9.469 / NU
BIAS4   =               20.331 / NU
BIAS5   =                0.995 / NU
BIAS6   =                3.849 / VOG
BIAS7   =               10.100 / Guard
BIAS8   =                2.018 / VSS
OBJECT  =           '39rats10' / Name of the object observed
SLTWDTH =                      /
GRAT_TYP=                   ?? /
EQUINOX =             2005.827 /
SEEING  =                   '' /
TELESCOP=      'Schmidt Asiago' /
INSTRUME=     'Photometer BVRI' / Instrument name
CDELTM1 =                0.024 / scale axis1 (mm/pxls)
CDELTM2 =                0.024 / scale axis2 (mm/pxls)
CDELT1  =            0.0006396 / image scale axis1 (deg/pxls)
CDELT2  =            0.0006396 / image scale axis2 (deg/pxls)
```

(To be continued ...)

(. . . Continued)

```
CRPIX1  =                 1023 / XCoo in pixels
CRPIX2  =                 1023 / YCoo in pixels
OBS-TYPE=                   '' / Tipo di osservazione
CTYPE1  =           'RA---TAN' / nome asse X
CTYPE2  =           'DEL--TAN' / nome asse Y
CRVAL1  =               .00000 / RA (Deg)
CRVAL2  =               .00000 / DEC
CMP_TYPE=                      / Tipo di campagna
IMAGE   ='OPD_O_20051028_234517.fits' / Nome Immagine
RON     =             17.42513 /Box X:950 Y:500 DX:20 DY:100
MJD     =       53671.98980324 / Modified Julian Day
EMAIL   =                      /
FIELVIEW=                      / Campo di vista del detector
JDMIDDLE=     2453672.48987269 / JD medio della posa
PHISPARA=                "ADU" / Parametro Fisico dei dati
JDAY    =     2453672.48980324 / Julian Date
GAIN    =                 1.65 / CCD Gain
UT      =           '23:33:19' /
SID-TIME=          ' 02:49:09' /
AIRMASS =                1.728 /
RA      =          ' 21:38:24' /
DEC     =          '+50:08:49' /
OBJMAGNI=                    - /
OBJSIZE =                  '-' /
UTMIDDLE=             23:45:24 /
FILTER  =                  'V' /
END     = (SiteRATS PBr150305) / End of Header.
```

Let's see the meaning of all the keywords different from the required and that are not explicitly explained in comments (the numbering corresponds to the line number of the keyword):

7. `DATE-OBS`: date of observation, referred to the starting time (see §3.4.1);
8. `EXPTIME`: exposure time;
9. `TERROR`: time error, counting shutter dead time;
10. `RELEASE`: release of CCD guide;
11. `PIX_HI`: the uppermost pixel value;
12. `PIX_LO`: the lowest pixel value;
13. `IMATYPE`: image type ('object', 'sky flat', 'dome flat','bias');
14. `BINNX` : binning of pixels on x axis;

15. `BINNY` : binning of pixels on y axis;
16. `STARTXY` : coordinate of initial pixel;
17. `OBSERVER`: Observer surname;
18. `AREACCD` : CCD pixels dimensions;
19. `DETECTOR`: detector type;
32. `SLTWDTH` : width of the slit (if used);
33. `GRAT_TYP`: type of the grating. The '`??`' here mean that no grating were mounted on the telescope during this observation.
34. `EQUINOX` : epoch. It has the same meaning of `EQUINOX` (see §3.4.1).
35. `SEEING` : seeing value, referred to the starting time of observation;
36. `TELESCOP`: telescope used for the observation;
53. `EMAIL` : email address of the Observer;
59. `UT` : Universal Time, referred to the starting time of observation;
60. `SID-TIME`: Sidereal Time;
61. `AIRMASS` : air mass;
62. `RA` : right ascension of the field;
63. `DEC` : declination of the field;
64. `OBJMAGNI`: magnitude of the object;
65. `OBJSIZE` : size of the object;
66. `UTMIDDLE`: Universal Time, referred to the midpoint time of observation;
67. `FILTER` : filter mounted on the telescope during the exposure.

All these RATS keywords are automatically created by an appropriate software written by Pietro Bruno (Astronomical Observatory of Catania) for the RATS project, selected accordingly to the RATS team members.

Chapter 4

RATS–ARP: Automatic Reduction Pipeline for RATS

THE theory of photometric transit searches has been postulated and discussed by a number of authors (Rosenblatt, 1971; Borucki & Summers, 1984; Schneider & Chevreton, 1990; Howell & Merline, 1995; Giampapa et al., 1995; Howell et al., 1996), who presented numerous details of the theory and methods of extra-solar planet search techniques. The photometric transit search method is not only sensitive to planetary systems such as those observed by spectroscopic methods (Jupiter-sized planets in orbit around F-G dwarfs), but is also the only current method which can detect terrestrial-sized planets. Transits by planets orbiting F-M dwarfs can be detected, with K-M dwarfs allowing earth-sized bodies to be possibly detected even with medium sized ground-based telescopes. Photometric transit searches are between the first scientific objectives for the COROT and Kepler satellites missions and other smaller endeavors.

The aim of the RATS–ARP is the detection of ESPs that transit the disk of their parent star and the production of lightcurve's files for candidates transit. In order to reach its target, the software processes photometric data provided by the CCD mounted on the C.ma Ekar 67/92 Schmidt telescope. Moreover, the pipeline provides detection of unknown Variable Stars by means of automatically generated lightcurves. In addition, the software performs false alarms reconnaissance which allow to determine the real nature of transiting objects. The pipeline can work also as support for the simulation and definition of Top Level requirement for the FCU camera of WSO mission. Thanks to the results obtained by the pipeline, the whole scientific community can improve the knowledge of planets formation mechanism.

To detect a planetary transit it is necessary an high photometric accuracy and a spectroscopic follow up to confirm the event. This latter requirement limits the fainter magnitude of the survey: the RATS project reaches about $10-20$ m/s radial velocity precision with the refurbished echelle spectrograph at Cima Ekar in 1h exposure for a G star of about $V = 13-14$. On the other side, the brighter magnitude is set by the observational strategy. But a 15 seconds exposure at the Schmidt of Cima Ekar easily saturates a star with $V = 13$. The solution adopted is to defocus the telescope. Up to now, no reduction tools similar to the one described in this thesis has been developed. The proposed automatic pipeline is intended to be such a tool which performs all relevant analysis and management of observational data.

Therefore, due to its innovative observational strategy, RATS–*ARP* is totally a new project among the current transits surveys. Here we outline the detailed structure of the whole pipeline: as we said before, the software is completely automated. For this reason the pipeline can be used also in space missions where human actions are impossible.

4.1 Photometric reduction background and introduction to the software development

The process of reducing the data is no more than a means to recover science data from images that, in their raw form, contain extraneous data related to imperfections in the optics of the telescope, flaws and sensitivity variations in the CCD, non uniformities in filter transmissivity, debris in the optical train, vignetting of the optical beam, electronic signature, and more. All of these effects add up to what is called an *instrumental signature* that is contained within the image, along with the science data. A series of preliminary tests were conducted to discover how to get the greatest sensitivity in our measurements.

4.1.1 Shell script programming

The shell is a so called *command interpreter*. More than just the insulating layer between the operating system kernel and the user, it's also a fairly powerful programming language. A shell program, called a script, is an easy-to-use tool for building applications by "gluing" together system calls, tools, utilities, and compiled binaries. Virtually the entire repertoire of UNIX commands, utilities, and tools is available for invocation by a shell script. Moreover, internal shell commands, such as testing and loop constructs, give additional power and flexibility to scripts. Shell scripts lend themselves exceptionally well to administrative system tasks and other routine repetitive jobs not requiring the bells and whistles of a full-blown tightly structured programming language.

Normally shells are interactive. It means that shell accepts command from an user (via keyboard) and execute them. For example, if an user uses command one by one (a sequence of N number of commands), then he can store this sequence of command to text file and tell the shell to execute this text file instead of entering the commands. This is known as shell script.

A shell script is a "quick and dirty" method of prototyping a complex application. Getting even a limited subset of the functionality to work in a shell script is often a useful first stage in project development. Shell scripting hearkens back to the classic UNIX philosophy of breaking complex projects into simpler subtasks, of chaining together components and utilities. Many consider this a better, or at least more esthetically pleasing approach to problem solving than using one of the new generation of high powered all-in-one languages, such as `Perl`, which attempt to be all things to all people, but at the cost of forcing you to alter your thinking processes to fit the tool.

The cases when to use shell scripts are:

– shell script can take input from user, file and output them on screen;

– useful to create our own commands;

- saving lots of time;

- automation of some task.

The last point shares the same philosophy of a pipeline programming approach.

There are three categories of commands which can be used in shell scripts:

- **Unix commands:** a shell script can make use of any Unix commands generally described as commands for file and text manipulation.

- **Concepts: pipes, redirection and backtick**. They are not really commands but they are very important concepts.

  ➢ *pipes* (|) send the output of one command to the input of another command. In this way, one can concatenate as many commands as one likes (within reasonable limits);

  ➢ *redirection* writes the output of a command to a file (>) or appends data to a file (>>);

  ➢ *backtick* (`) is the output of a command that can be used as command line arguments (not as above, command line arguments are any strings that you specify behind the command such as file names and options) for another command. One can as well use it to assign the output of a command to a variable.

- **Control structures**, among which there are:

  ➢ "*if*" statement tests if the condition is true (exit status is 0, success);

  ➢ "*&&*" can be used as a short if-statement. The right side gets executed if the left is true. It can be read as AND;

  ➢ "*case*" statement can be used to match (using shell wildcards such as "∗" and "?") a given string against a number of possibilities.

  ➢ "*select*" statement is a bash specific extension and is very good for interactive use. The user can select a choice from a list of different values;

  ➢ "*loop*" statements:

    ◦ the *while-loop* will run while the expression that we test for is true;

    ◦ the *for-loop* takes a list of strings and assigns them to a variable;

  ➢ "*quoting*" before passing any arguments to a program the shell tries to expand wildcards and variables. To expand means that the wildcard (e.g. ∗) is replaced by the appropriate file names or that a variable is replaced by its value. To change this behavior you can use quotes. Single quotes are most strict, they prevent even variable expansion. Double quotes prevent wildcard expansion but allow variable expansion;

  ➢ "*functions*" as soon as one has a more complex program he will find that he use the same code in several places and also find it helpful to give it some structure. One needs to "declare" functions at the beginning of the script before using them.

4.1.1.1 Debugging

The most simple debugging help is of course the command `echo`. One can use it to print specific variables around the place where he suspect the mistake. This is probably what most shell programmers use 80% of the time to track down a mistake. The advantage of a shell script is that it does not require any re-compilation and inserting an "echo" statement is done very quickly.

The shell has a real debug mode as well. If there is a mistake in a script "strange script" then it can be debugged in this way:

```
sh -x My-script
```

This will execute the script and show all the statements that get executed with the variables and wildcards already expanded. The shell also has a mode to check for syntax errors without actually executing the program. To use this run:

```
sh -n My-script
```

If this returns nothing then the program is free of syntax errors.

4.1.2 DAOPHOT

DAOPHOT is a stellar photometry package designed by Peter Stetson at Dominion Astrophysical Observatory (DAO) to deal with crowded fields. The package performs various tasks including finding objects, aperture photometry, obtaining the point spread function, and profile fitting photometry. Profile fitting in crowded regions is performed iteratively, which improves the accuracy of the photometry.

This section deals with `DAOPHOT II: The Next Generation.` It replaces the previous version which is known as `DAOPHOT Classic`. The main changes concern the choice of the point spread fitting function and the handling of under-sampled data.

A document written by Peter Stetson (Stetson, 1987) gives the background to the algorithms used by DAOPHOT. A user's manual is also available at `http://www.star.bris.ac.uk/~mbt/daophot/`.

DAOPHOT does not directly use an image display, which is one of the reasons why the package has been successfully ported round the world. Three additional routines have therefore been supplied which allow results obtained with DAOPHOT to be displayed on an image device.

The routine DAOGREY will display a grey scale image of the data on a suitable device. DAOPLOT will indicate the positions of objects found with DAOPHOT on top of the grey image. DAOCURS will put up a cursor on the display to allow positions to be measured from the screen.

DAOPHOT is copyright of Peter Stetson at the DAO. The algorithms should not be changed without his permission.

DAOPHOT II is a computer program for obtaining precise photometric indices and astrometric positions for stellar objects in two-dimensional digital images. It is intended to run as non-interactively as possible and, furthermore, the possibility that DAOPHOT II would be used at other places than the DAO was kept in mind as it was approaching its present form. Therefore DAOPHOT II performs no operations related to the display or manipulation of the digital image on an image-display system, even though at some stages in the data reduction it is useful to be able to examine the picture visually. Picture-display operations and some other steps in the pre-reduction procedure, such as editing intermediate data or combining results from different frames to obtain instrumental colors, may be done outside of `DAOPHOT II`, for example using `IRAF`.

It is assumed that:

1. before running `DAOPHOT II`, the user will have performed all necessary preparation of the images, such as flat fielding, bias-level subtraction, and trimming worthless rows and columns from around the perimeter of the picture;

2. the brightness data in the image are linearly related to true intensities.

The user is also assumed to have a priori knowledge of the following pieces of information:

– the approximate size (full-width at half-maximum) of unresolved stellar objects in the frame;

– the number of photons corresponding to one analog-to-digital conversion unit;

– the readout noise per pixel;

– the maximum brightness level (in analog-to-digital units ADU) at which the detector still operates linearly.

These conditions being satisfied, `DAOPHOT II` will perform the following primary tasks:

1. find star-like objects above a certain detection threshold, rejecting with a certain degree of reliability bad pixels, rows, and columns, and avoiding multiple hits on individual bright objects;

2. derive concentric aperture photometry for these objects, estimating a local sky brightness for each star from a surrounding annulus of pixels;

3. obtain a point spread function for the frame from one star or from the average of several stars, in an iterative procedure intended to fit and subtract faint neighbor stars which contaminate the profile;

4. compute precise positions and magnitudes for the program stars by fitting the point spread function to each star;

5. erase stars from the picture by subtracting appropriately scaled point spread functions corresponding to the positions and magnitudes derived for the stars during the photometric reductions.

In addition to the aforementioned tasks, `DAOPHOT II` contains routines to perform some bookkeeping operations more easily than may be the case with standard facilities: *i.e.*, estimating an average sky brightness for a frame, sorting the stars' output data according to their positions in the frame or their apparent magnitudes, and dividing the stars in the frame into natural groupings.

A few other global considerations of which the user should be aware.

- Although `DAOPHOT II` is designed to be non-interactive, in fact many of the operations run quickly enough that they are conveniently executed directly from the terminal or workstation. Only the multiple-star profile fits take long enough that they are more conveniently performed in batch mode: they may require anywhere from a few CPU minutes to a few CPU hours per frame, depending upon the number of stars to be reduced, the degree of crowding, and –of course– the speed of the machine.

- The derivation of the point spread function can also be performed non-interactively with a reasonable degree of success.

- The shape of the point spread function is assumed to be spatially constant or to vary smoothly with position within the frame; it is assumed not to depend at all on apparent magnitude. If these conditions are not met, systematic errors may result.

- Although the star-finding algorithm is by itself not sophisticated enough to separate badly blended images (two stars whose centers are separated by significantly less than one FWHM), by iteratively subtracting the known stars and searching for fainter companions, it is still possible to identify the separate stars in such a case with a good degree of reliability:

    1. one runs the star-finding algorithm, derives aperture magnitudes and local sky values for the objects just found, and obtains a point spread function;

    2. one performs a profile fitting reduction run for these objects, and they are subtracted from the data frame. This new picture, with the known stars subtracted out, is then subjected to the star-finding procedure; stars which were previously concealed in the profiles of brighter stars stand out in this frame, and are picked up quite effectively by the star-finding algorithm. Sky values and aperture magnitudes for these new stars are obtained from the original data frame, and the output from this reduction is appended to the most recent photometry file for the original star list. This augmented set of stars is then run through the profile fitting code, and the entire list of fitted stars can be subtracted from the original frame. The process through this point can be set up in a command procedure and carried out in batch mode.

- A principal source of photometric error for the faint stars is the difficulty of defining what is meant by the term *sky brightness* in crowded fields. For aperture photometry the term "sky brightness" encompasses not only emission from the terrestrial night sky, from diffuse interplanetary and interstellar material, and from faint, unresolved stars and galaxies. It also includes the possibility of a contribution of light from some bright star or galaxy. The specific value is well predicted by the modal value of the brightnesses in the sample of sky pixels. This is why `DAOPHOT II` uses the mode of the intensities within the sky annulus to define the value that should be subtracted from the intensities inside the star aperture; not because it is a robust estimator of the local diffuse sky brightness, but because it is a sort of maximum-likelihood estimator – it yields the most probable value of the brightness of a randomly chosen pixel in this region of the picture.

4.2 Data analysis

The state of art concept to perform photometry on crowded CCD images is the *differential imaging analysis* (Alard & Lupton, 1998; Alard, 2000). Basically, it consists of choosing one high quality image of the field, taken at the best possible conditions of seeing and atmospheric transparency. We will refer to this image as the reference image. Every science image is shifted, interpolated to the same grid as the reference frame and convoluted with a kernel image, in order to correct for possible seeing and focus variations, and then subtracted from the reference image. The photometry is later done on the resultant image, which should only have significant signal in the objects whose flux has changed from the reference image. These include variable stars, asteroids, artificial satellites and trailing stars, among others. In this section, we describe in more detail all the process, from the calibrated images and the standard star list to the final light curves.

4.2.1 Images calibrations

All the science images are corrected for the usual effects needed to perform CCD photometry, namely:

- **Bias subtraction.** 20 zero-second exposure time images. They are taken every observing night, and averaged (and sigma-clipped) to produce one master bias image for that night. This image is zero-scaled with the overscan region of every science image taken on that night, and subtracted from it.

- **Flat field correction.** The differences in the response of the different CCD pixels, and the effect of the vignetting affecting the telescope are corrected with a division of every science image by an image of an uniformly illuminated field. These images are taken following two approaches: images taken at twilight, and images taken pointing to a wall of the dome, which is illuminated by a lamp. The twilight images provide a measurement of the large-scale structures, but it is difficult to accumulate enough photons to measure the small-scale gain structure accurately. This is achieved with the dome images, in which more photons can be accumulated, but it is hard to achieve a constant illumination throughout the field of view. Thus, a combined flat field (called *master flat field*) is constructed using the sky twilight images as a measurement of the large scale structures, while the small scale structures are measured with the dome flats. Typically, one master flat field, constructed using a combination of all the available flat images in the observing period of one specific campaign, is used to correct all the images of the campaign.

- **Dark current correction.** The non-zero temperature operation of the CCD causes several ADUs to arise from thermal action. The signal depends on the temperature of the CCD and on the pixel impurities. This signal can be measured taking long exposures with the telescope covered (the electrons due to dark current accumulate at a constant rate for each pixel). All the signal appearing in these images is the bias plus the effect of the temperature. Typically, 20 images of $600s$ exposure time are taken in cloudy nights, and averaged to get a *master dark image* that is scaled to the science images exposure time before being subtracted.

All these aspects are detailed explained in §5.1 for RATS–*ARP*.

4.2.2 Building a stars list

All images with focused stars taken on the same fields and the same observational loop are chosen to construct a star list of all the objects whose light curves are desired. These images are inspected for unusual signals, such as satellite or plane trails, meteors, diffuse light, etc. and only those do not have significant spurious signals are taken into account to built a list of photometrical reference stars, called hereafter *masterlist*.

In order to achieve this list, we have exploited ISIS (`http://www2.iap.fr/users/alard/package.html`) a prepackaged free software which is based on the image subtraction method (Alard & Lupton, 1998; Alard, 2000).

Following the ISIS 2.2 dataflow, we can identify the two first essential steps to make the list of focused and photometric variables objects:

1. **Image registration and interpolation**
   Firstly we need to get rid of the shift and possibly of the small rotation between the images caused by the observational loop peculiar for RATS. To do that, we need to chose one reference frame for this astrometric procedure. This reference can be specified in the configuration file `process_config`, the relevant keyword is `REFERENCE`. The User must also choose a degree for the 2 dimensional polynomial of the astrometric re-mapping to the reference, the relevant keyword is `DEGREE`. To run the registration and interpolation script the User has to just type: `./interp.csh`. In the log file `log_interp2`, the User could take notice of the residual relevant to the astrometric transformation along the (x, y) image direction and the effective number of stars used to compute the astrometric transformation.

2. **Building a composite reference frame**
   To build the reference frame the User needs to stack a number of the best images. To identify them, some aspects should be considered such as: the sky background, the saturation level of the bright stars, the exposure time and so on. Usually, these best frames are the images with best seeing. Once chosen the set of frames, the User can write this list of files in a `ref_list` input file and call the procedure `./simple_ref.csh`. The resulting built up image is called `ref.fits`, our raw masterlist.
   Of course, the drawback of this procedure is that if there defects in the individual image (*i.e.*, cosmic rays), they will accumulate in the stacking process, leading to an unuseful reference image. Thus before comparing the images some adjustment has to be made. For instance, one must implement some method to remedy at the fact that images have different backgrounds and seeing. One way to do that is to use the image subtraction method in order to transform each frame to the same seeing and same background level as a given image. This given image can be the best image, achieved running: `./ref.csh`. Comparing the new `ref.fits` image to the previous one, this has a better resolution and becomes our final masterlist.

3. **Photometry on masterlist**
   In order to be able to compare the masterlist file with those obtained from the reduction pipeline, we should calculate the flux of the stars listed on the masterlist. To do that, we run in order:

   - `./daophot` on `ref.fits`, obtaining the aperture file for the masterlist;

- `./allstar` on `ref.fits`, obtaining the file `masterlist.als` which is used in the reduction procedure.

On the contrary to the automatic RATS–*ARP* procedure, all the above mentioned steps should be run in an interactive mode: each passage is tricky and the User could be compelled to re-run some of the steps if the resulting masterlist is unsatisfactory to his purpose. Thus by its very nature, the masterlist creation should be a preparatory activity after the observations and before starting the RATS–*ARP*.

4.3 Analysis and pipeline requirements definition

4.3.1 The pipeline model

The RATS pipeline was constructed using the tasks and scripting language contained in the `IRAF` package and `DAOPHOT II`. This is complemented by Linux shell scripts, invoked directly from within the Linux environment.
For more complicated and peculiar tasks, some FORTRAN code can be linked to the shell script environment.
We have chosen this form of pipeline implementation rather than coding directly from because of the obvious gains in development speed and flexibility. Although not the most computationally efficient solution, computational speed is not a bottleneck for our purposes.

The reduction process is split mainly into two parts:

1. **pre-reduction** `IRAF` script algorithm (§5.1): it performs bias subtraction, flat fielding, bad pixel correction and cosmic ray correction. In Fig. 4.1 the dataflow of this process is shown.

2. **reduction** algorithm (§5.2): it performs stellar centering, aperture photometry, matching frame, transformation of coordinates, light curves calculation. In Fig. 4.2 the dataflow of this process is shown.

RATS–*ARP* will support the future missions dedicated to transit search, in particular the software will be use in WSO-UV mission reduction phase. Therefore, the pipeline will provide sufficient functionality and extensibility.

The main constraints for the pipeline are shortly summarize as follows:

a. the S/W will be able to use a batch mode algorithm;

b. the `Fortran` modules will be compiled with GNU `FORTRAN 77` (`g77`) free source compiler;

c. the S/W will be able to manage data affected by astronomical distortions;

d. the S/W will be able to improve the results in centering and reducing of images;

e. the S/W will be able to read and write file in `IRAF` format;

f. the S/W will be able to read and write file in `DAOPHOT` format;

g. the S/W will be able to keep stored the lightcurves and plots;

h. the S/W will run on the `LINUX` platform;

i. the S/W will be extendable and adaptable.

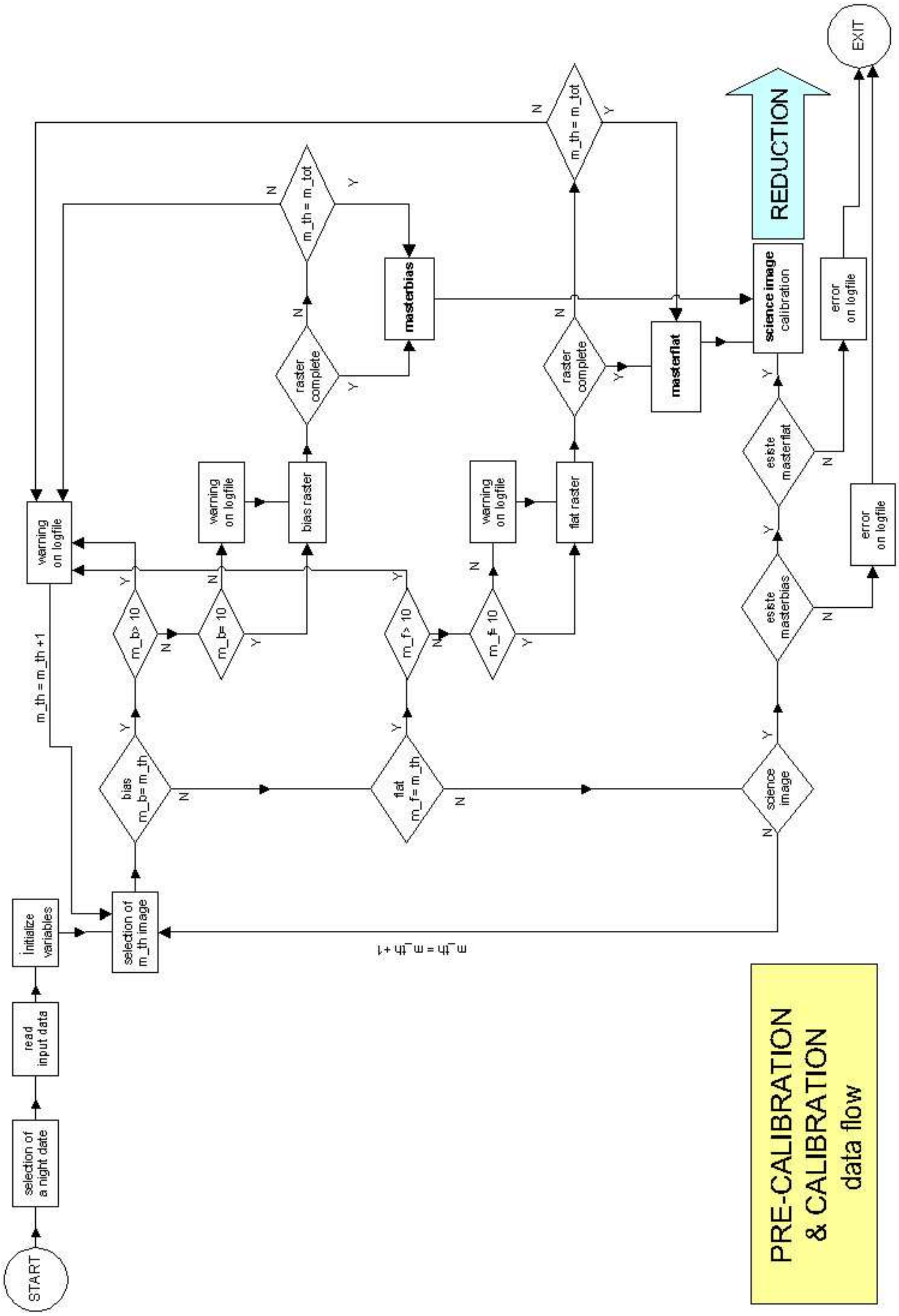

Figure 4.1: Dataflow pre-reduction diagram.

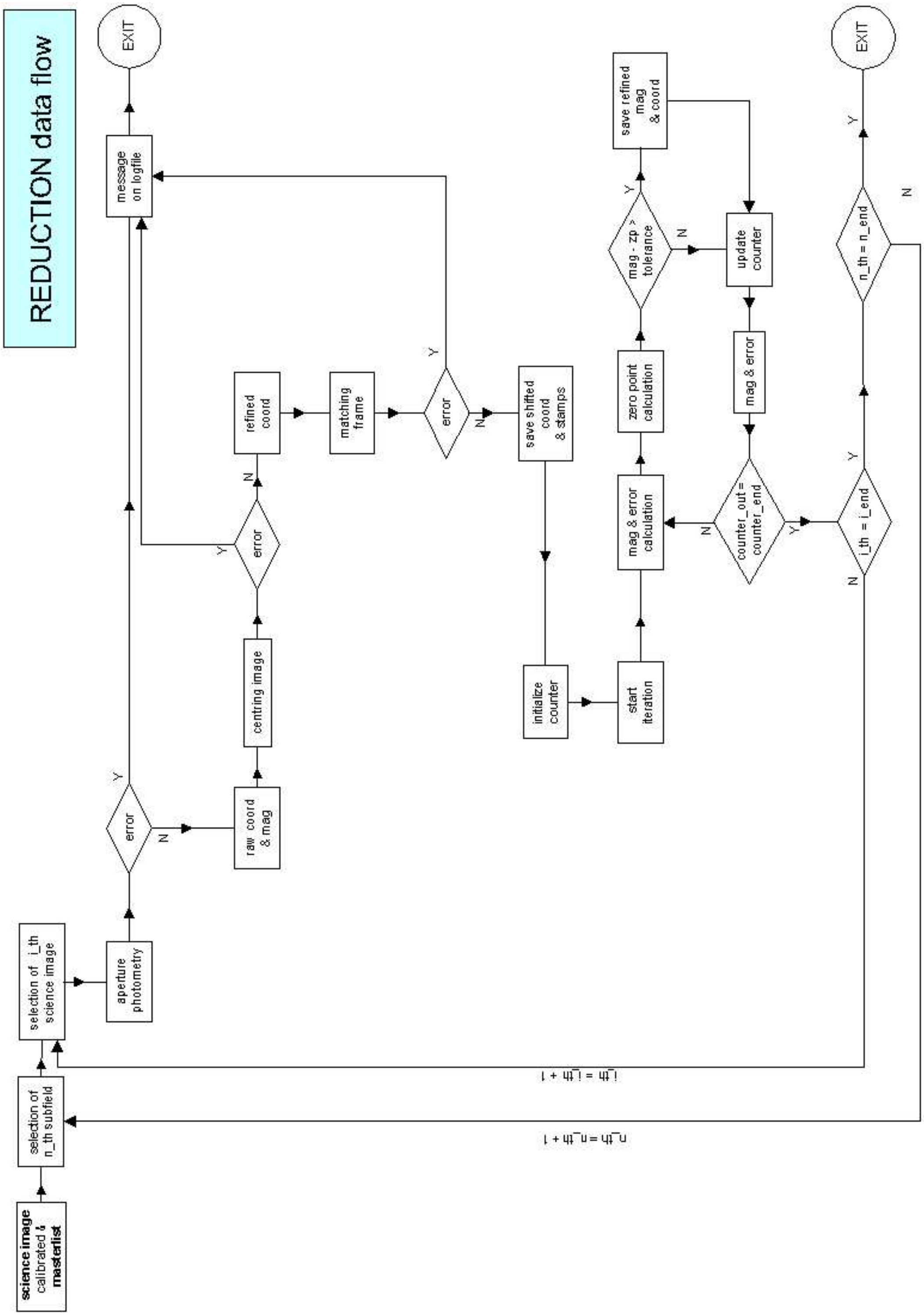

Figure 4.2: Dataflow reduction diagram.

4.3.2 Software environment

The pipeline's Users will be scientists and technicians with different levels of:

- ☑ knowledge of the transit search mechanism;
- ☑ knowledge of the theory above which the software is founded on;
- ☑ reasons of usage of the software;
- ☑ expectations to the functionality of the software.

All these aspects are assumed to be appropriate guidelines to define the way in which the Users will interact with the software and the level of performance and reliance required. These guidelines trace the necessary background in astronomical reduction technique, in planetary transit technique, in observational strategy technique required for the S/W usage.
Thereby, the Users of the software will be:

- ✗ Scientists with specialist knowledge of the transit observation technique who want a software which automatically generate the light curves of the survey's targets from the raw images;
- ✗ Scientists with basic knowledge of the transit observation technique who will exploit the RATS lightcurves DB (TBD) as final User;
- ✗ Engineers with a basic knowledge, generally, of the transit observation technique who wish to have a software for supporting mission planning and performance evaluation of the entire system with particular interest in technical effects.

RATS–*ARP* will run on an `Intel Pentium IV` based IBM-compatible PC running `Fedora 6.0`. The Fortran compiler will be GNU Fortran (`g77`) free source compiler.

4.3.3 System design and architecture

The design method used in order to develop the software is the *object-oriented* design. In particular, we use the *Object Modeling Technique (OMT)* (Rumbaugh et al., 1991). Following a top-down approach, the software to be developed into components for the purpose of modularization of the design, described in the form of an OMT-style object diagram in which the classes have been partitioned into 4 main layers. This partition has been chosen to bundle classes with a certain goal together and keep the interfaces between the different components as simple as possible.

The identified partitioning layers are:

- ➢ **H/W LAYER** (Fig. 4.3): the H/W layer includes the Schmidt telescope, the server and workstation PCs, the storage devices such as external hard disk and DVD/CD. It includes all access to the actual telescope configuration. All data capture information are provided to the rest of the program from this component and actual communication with the telescope and or images (or any other resource external to the software) takes place through this component.

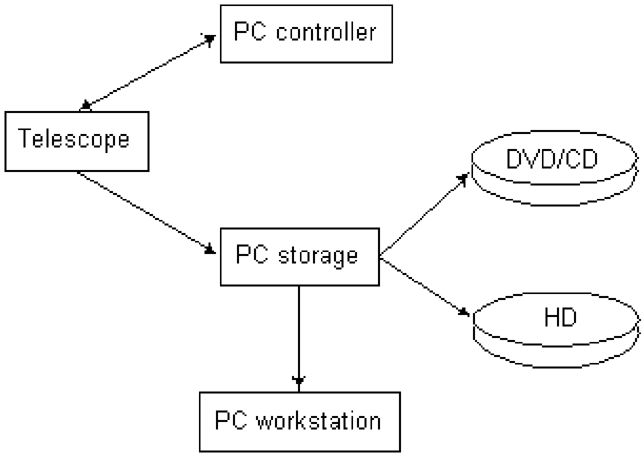

Figure 4.3: Hardware layer scheme for the software architecture.

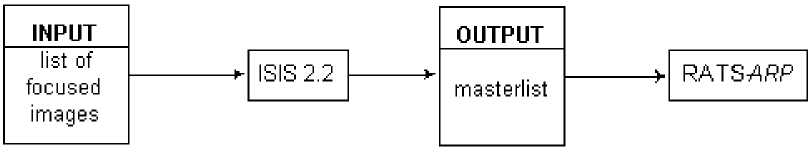

Figure 4.4: "*Off-line analysis*" scheme with ISIS 2.2 package.

➢ **OFF-line ANALYSIS LAYER** (Fig. 4.4): this layer includes all the ISIS procedure for data preparation in order to obtained from focused images the input masterlist for the RATS–*ARP*. This set of tools performs an interactive analysis.

➢ **APPLICATION LAYER** (Fig. 4.5): this is the core of RATS system. It contains the code necessary to compute the reduction to be executed. It is split up in an automatic **calibration pipeline** and a automatic **reduction pipeline**, whose breakdowns are both presented in the figure mentioned. Section §5.3 will specify the components in sufficient details.

➢ **USER INTERFACE LAYER** (Fig. 4.6): this component is responsible for all the interfaces to the RATS–*ARP* Users as well as the interpreter used to execute files. It takes care of monitoring and updating the reduction processes on screen, writing to a logfile and/or for the final User interfacing the access to a RATS database.

Following the Fig. 4.5, the schematic list of subsystem decomposition and dependencies is:

- `calibration.csh`: calibration pipeline
  - ➢ `calibra.cl`: `IRAF` script which perform calibration of raw science images.

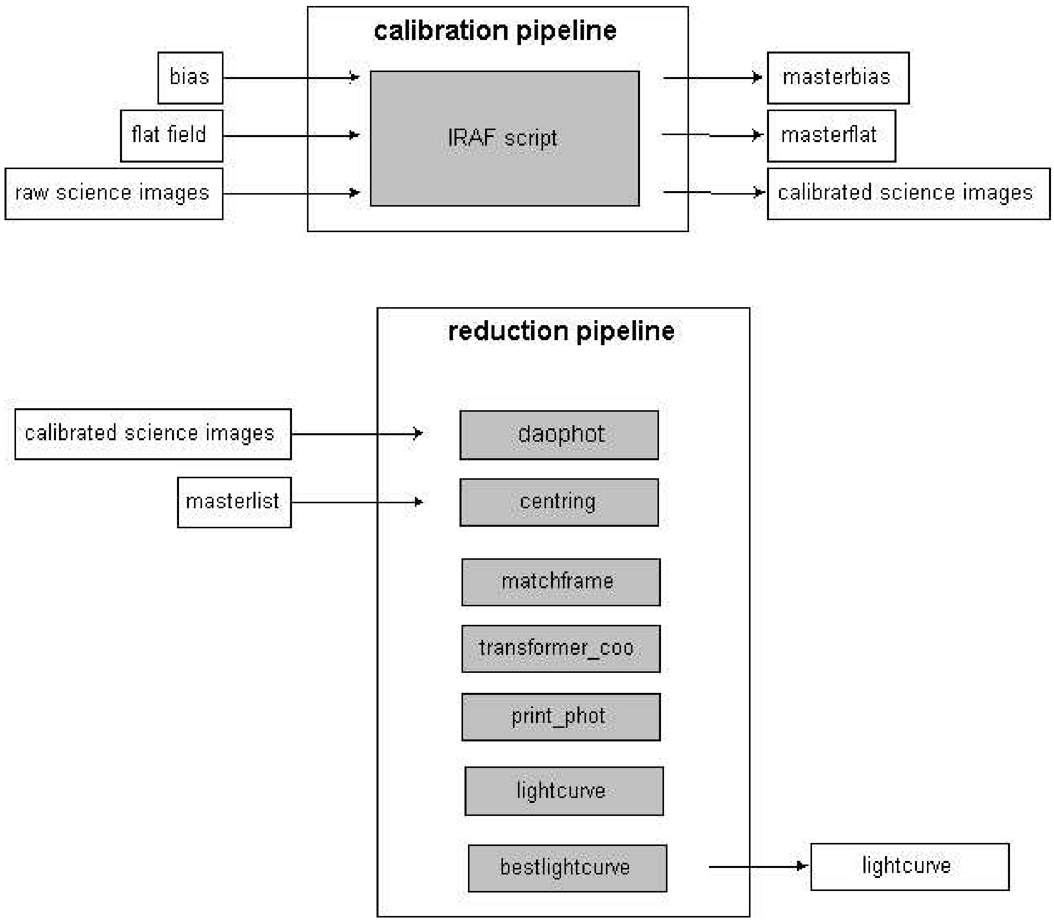

Figure 4.5: "*Application layer*" scheme: the calibration pipeline (*panel above*) and the reduction pipeline (*panel below*).

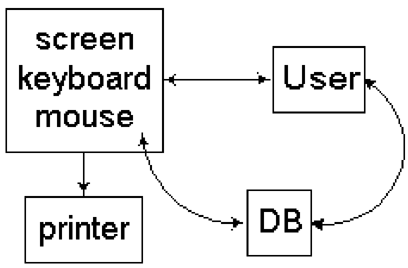

Figure 4.6: User interface relationship scheme.

- `procedura.csh`: reduction pipeline
  - ➢ `daophot`: photometry module

- ➢ `centring`: centring images module
- ➢ `matchingframe`: frames match module
  - – `daomatch`
  - – `masterframe`
    - >> `daomaster`
- ➢ `transformer_coo`: transformation of coordinates module
- ➢ `lightcurve_creation`: lightcurves extractions module

A detailed description of each of the component above can be found in section §5.3.

4.3.4 Functional requirements for the pipeline

In the following, we present a list of specific functional requirements RATS–*ARP* satisfies according to the context the software places itself:

- **Requirement 1.** The input parameters will be supplied by input files.
- **Requirement 2.** The data capture system has to acquire images in the following order: biases, flat fields and scientific images.
- **Requirement 3.** The input parameters will be:
  - ➢ lists of biases: the data capture system has to acquire 10 biases images;
  - ➢ lists of flat fields: the data capture system has to acquire 10 flat fields images;
  - ➢ lists of scientific images;
  - ➢ aperture parameters, required for the `DAOPHOT` aperture file:
    - – 12 different value for the aperture radius;
    - – estimated inner and outer sky radii of the annulus around a star.
  - ➢ photometry parameters:
    - – Read noise of the CCD;
    - – Gain factor of the CCD;
    - – FWHM in pixels of the object;
    - – Fitting radius of the centroid of the object;
    - – PSF radius of the circle within which the PSF is to be defined;
    - – Analytic model PSF for the first approximation to the PSF;
    - – Variable PSF, the degree of complexity with which the PSF is to be modeled;
    - – High good datum, the level above which a pixel value is defective;
    - – A threshold value to consider a positive brightness enhancement as real.
  - ➢ a kernel size;
  - ➢ a "stamp" size around the selected star and a counter of them.
- **Requirement 4.** The S/W will reduce all the images acquired in a selected night of observation.

- **Requirement 5.** All selected stellar fields will be divided in 6 sub-fields of one square degree each.
- **Requirement 6.** All the images acquired will be in fits format.
- **Requirement 7.** The fits files naming convention is *YYMMDDhhmmssX0nm.fits*, where:
  - ➢ YY is the last two digit of the year;
  - ➢ *MM* is the month;
  - ➢ *DD* is the day;
  - ➢ *hh* are the hours;
  - ➢ *mm* are the minutes;
  - ➢ *ss* are the seconds;
  - ➢ X identify the object: it can be B = Bias, F = Flat, O = Object;
  - ➢ n is the RATS field;
  - ➢ m is the subfields.

  If $X = B$ or $X = F$, $n = m = 0$.
- **Requirement 8.** Only the one image (the first in time order) will be the reference frame.
- **Requirement 9.** The creation of the masterlist will be manage by some selected ISIS's packages (re-mapping).
- **Requirement 10.** The aperture photometry will be obtained by `DAOPHOT`.
- **Requirement 11.** The `DAOPHOT` version will be slightly modified in order to fine-tune some values.
- **Requirement 12.** The matching frame will be obtained by `DAOMATCH` and `DAOMASTER`.
- **Requirement 13.** The calibration masterbias and masterflat will be obtained by `IRAF`.
- **Requirement 14.** The S/W will focus only on the most bright and isolated stars.
- **Requirement 15.** The S/W will indicate missing or erroneous input data as a warning in a log file.
- **Requirement 16.** The S/W will provide files containing:
  - ➢ magnitude of stars and errors;
  - ➢ (X, Y) coordinates of the images respect to the reference frame;
  - ➢ (x, y) coordinates of the candidate transit stars on a single frame;
  - ➢ Exposure time;
  - ➢ Julian Day (JD);
  - ➢ Universal Time (UT);
  - ➢ air mass;
  - ➢ filters;
  - ➢ CCD type.

Chapter 5

The RATS–ARP implementation

ONCE the Observer has taken all of RATS field images and has transferred them to a computer, the pipeline have to reduce them in order to get rid of background noise due to bias, dark, and flats and to obtain the lightcurves desired. To do that, the night Observer has to run RATS–*ARP*.

5.1 Pre-reduction algorithm of astrophysical images

The data reduction process is initialized by a Linux shell script which starts first `IRAF` and then the master `IRAF` script. At startup of `IRAF`, the `loginuser.cl` task is executed. It loads the required `IRAF` packages and defines the individual `IRAF` tasks of the pipeline and various `IRAF` environment variables necessary to the pipeline.

The master script creates the input and output file lists and starts the individual subtasks one after another. The subtasks access a parameter file where all relevant `IRAF` parameters are stored.
If a particular parameter is not found in the parameter file (or the parameter file itself is not present or accessible), standard parameters, which are stored in the subtasks, are used.

The basic steps in CCD image reduction are *bias-level subtraction*, *dark current subtraction*, *flat field division*, and cleaning images of *cosmic rays* and *bad pixels*. As we have data in more than one filter, the bias subtraction and dark-level subtraction can be done on all the images in single step but flat fielding required that the images be previously processed in individual filter groups.

5.1.1 Bias

Bias-level refers to the number of counts present in each pixel with zero exposure time and zero photons counted. It is attributable to electrons that accumulate in the pixels due to the voltage maintained across the chip. This base-level charge accumulation in the pixels is sometimes called a 'pedestal', since it represents a foundation of charge on top of which the science and other charge accumulates.

We are able to create a *Superbias* frame from our 20 bias frames, listed in "zero.list" file.

The `IRAF` task **zerocombine** will perform the addition of individual bias frames. The task parameters are set as shown in table 5.1.

cl>	epar zerocombine	
	input = "@zero.list"	List of zero level images to combine
	(output = "Superbias")	Output zero level name
	(combine = "average")	Type of combine operation
	(reject = "minmax")	Type of rejection
	(ccdtype = "zero")	CCD image type to combine
	(process = no)	Process images before combining?
	(delete = no)	Delete input images after combining?
	(clobber = no)	Clobber existing output image?
	(scale = "none")	Image scaling
	(statsec = "")	Image section for computing statistics
	(nlow = 0)	minmax: Number of low pixels to reject
	(nhigh = 1)	minmax: Number of high pixels to reject
	(nkeep = 1)	Minimum to keep (pos) or maximum to reject (neg)
	(mclip = yes)	Use median in sigma clipping algorithms?
	(lsigma = 3.)	Lower sigma clipping factor
	(hsigma = 3.)	Upper sigma clipping factor
	(rdnoise = "7.3")	ccdclip: CCD readout noise (electrons)
	(gain = "5.1")	ccdclip: CCD gain (electrons/DN)
	(snoise = "0.")	ccdclip: Sensitivity noise (fraction)
	(pclip = -0.5)	pclip: Percentile clipping parameter
	(blank = 0.)	Value if there are no pixels
	(mode = "ql")	

Table 5.1: Parameters file for `zerocombine` `IRAF` task, setted for RATS images

In this case the parameter `combine` is set to '*average*', but it could also be set to '*median*'. The appropriate choice depends on the data being combined and the looked for result. In this case, we want to combine images whose count levels are very nearly constant at very nearly the same values, and we want an estimate of the average bias-level of these frames, so 'average' is appropriate. The minmax rejection algorithm will reject nlow and nhigh low and high pixels as deviant. With this settings, a given Superbias' pixel will be the average of that pixel from all the zeros except the zero with the highest count. This should keep radiation events from the combined frame.

In the pre-reduction algorithm, for bias-level subtraction this task is run as:

```
cl> zerocombine @zero.list
```

The next step is to subtract the zero-level bias structure from all RATS data frames. Many bias frames are averaged together to make the Superbias so that stochastic bias variations unrelated to chip structure will be smoothed out, and so that errors associated with the bias-level correction can be minimized with respect to read out noise.

To subtract the zero-level bias structure from the rest of your data, the pre-reduction algorithm runs

```
cl> imarith @inbiaslist - Superbias @outbiaslist
```

where `@inbiaslist` lists the filenames of bias files and `@outbiaslist` lists the filenames of bias files fully bias-subtracted.

5.1.2 Dark current

The so-called *dark current* is no more than the contribution to pixel count levels of thermal electrons from the chip silicon itself. The chip is cooled down to some empirically determined temperature that optimizes efficiency and minimizes thermal noise.

The dark current value for RATS fields is very less than noise level, so that we don't consider this kind of subtraction.

5.1.3 Flat Fielding

The *flat field* is, by definition, the response of the detector to a uniform source of illumination. Uniform illumination is usually accomplished by exposing the chip to the twilight sky, or by exposing on a dome screen illuminated by a tungsten lamp projector. If the sensitivity of each pixel were identical, and there were no other effects, the flat field would have a constant value (every pixel would record the same value).
This is not the case though: different pixels have different quantum efficiencies due to small structural variations in the CCD, structure that might be present due to chip manufacturing processes, and filters or other elements in the instrument optical train (including debris). The flat field measures the resultant pixel to pixel intensity variations in sensitivity. Unlike the previous corrections, which were additive, the flat field correction is *multiplicative*: one pixel may have only 30% the quantum efficiency of the median, so to correct one has to adjust the counts in that pixel by a factor of ~ 3. Therefore the images must be *divided* by the normalized flat field.

A series of flat field exposures has been taken through each filter and each RATS fields to during observations, taking care to keep the total chip illumination level as uniform as possible from exposure to exposure.
The flat field frames will be combined by filter type into a master *flat field* for each filter, using the task **imcombine**. Its parameters, for a list of flats with blue filter (`bflat.list`), are setted as shown in table 5.2.

Note that the hidden parameter combine is set to '*median*', rather than the '*average*' value seen in the zerocombine task, and the rejection algorithm is different. This is because the images to be combined now are fundamentally different and the desired results are not the same.
With the zeros we expected minor statistical variations from image to image but all with very nearly the same mean and standard deviation, and sought only an average bias level. The flat fields are finite time exposures of a variable illumination source, more vulnerable to radiation events, and serve a different purpose: we want to combine the flats on an 'equal footing' in order to obtain a statistically 'smoothed' template to use for correction of the system flat field response.

In order to combine images with rejection of pixels based on deviations from some average or median they must be scaled to a common level. The `scale = "mode"` phrase causes each

```
cl>  epar imcombine
     input = "@bflat.list"        List of images to combine
     output = bflat               List of output images
     (plfile = "")                List of output pixel list files (optional)
     (sigma = "")                 List of sigma images (optional)
     (logfile = "STDOUT")         Log file
     (combine = "median")         Type of combine operation
     (reject = "avsigclip")       Type of rejection
     (project = no)               Project highest dimension of input images?
     (outtype = "real")           Output image pixel datatype
     (offsets = "none")           Input image offsets
     (masktype = "none")          Mask type
     (maskvalue = 0.)             Mask value
     (blank = 0.)                 Value if there are no pixels
     (scale = "mode")             Image scaling
     (zero = "none")              Image zero point offset
     (weight = "none")            Image weights
     (statsec = "[x1:x2,y1:y2]")  Image section for computing statistics
     (expname = "")               Image header exposure time keyword
     (lthreshold = INDEF)         Lower threshold
     (hthreshold = INDEF)         Upper threshold
     (nlow = 1)                   minmax: Number of low pixels to reject
     (nhigh = 1)                  minmax: Number of high pixels to reject
     (nkeep = 1)                  Minimum to keep (pos) or maximum to reject (neg)
     (mclip = yes)                Use median in sigma clipping algorithms?
     (lsigma = 3.)                Lower sigma clipping factor
     (hsigma = 3.)                Upper sigma clipping factor
     (rdnoise = "7.3")            ccdclip: CCD readout noise (electrons)
     (gain = "5.1")               ccdclip: CCD gain (electrons/DN)
     (snoise = "0.")              ccdclip: Sensitivity noise (fraction)
     (sigscale = 0.1)             Tolerance for sigma clipping scaling correction
     (pclip = -0.5)               pclip: Percentile clipping parameter
     (grow = 0)                   Radius (pixels) for 1D neighbor rejection
     (mode = "ql")
```

Table 5.2: Parameters file for `imcombine` `IRAF` task, setted for RATS images

image to be scaled by it's mode before combining. The flats are then combined into a master flat whose pixels represent the median of the individual flat field image pixels.

The rejection algorithm is also different than the zerocombine choice, primarily because the flats have been processed a bit and there are fewer of them. Possible choices are `pclip`, `ccdclip`, `crreject`, `sigclip`, and `avsigclip`. `ccdclip` and `crreject` are based on mathematical noise models and require known readout noise and gain, while `sigclip` and `avsigclip` rely on image statistics. `crreject` and `avsigclip` are appropriate choices when there are few images to combine. Different circumstances will dictate the choice of one or the other of these algorithms. We chose **avsigclip** for RATS pre-reduction.

The pre-reduction algorithm proceeds as follows.

1. It creates a list for each filter containing the names of the individual flat fields for a filter and uses imcombine to combine the filter images together, obtaining a master flat file for each filter:

   ```
   cl> imcombine @bflat.list bflat comb=median sc=mode statsec=[x1:x2,y1:y2]
   cl> imcombine @vflat.list vflat comb=median sc=mode statsec=[x1:x2,y1:y2]
   cl> imcombine @rflat.list rflat comb=median sc=mode statsec=[x1:x2,y1:y2]
   cl> imcombine @iflat.list iflat comb=median sc=mode statsec=[x1:x2,y1:y2]
   ```

   where **statsec** is the region of the chip we want to use to get median and mode statistics. When the algorithm has done we have images "bflat", "vflat", "rflat", and "iflat" that are the master flat field frames for your B images, V images, R images, I images.

2. It gets the statistics on the master frames for each filter:

   ```
   cl> imstat bflat[x1:x2,y1:y2]
   cl> imstat vflat[x1:x2,y1:y2]
   cl> imstat rflat[x1:x2,y1:y2]
   cl> imstat iflat[x1:x2,y1:y2]
   ```

   The **imstat** task prints to the screen the *mean*, *standard deviation* etc. of the image and makes a note of them in an apposite file.

3. It normalizes the master flat and names the normalized flat *normbflat* (*normvflat*, *normrflat*, *normiflat*) with the command:

   ```
   cl> imarith bflat / mean normbflat
   cl> imarith vflat / mean normvflat
   cl> imarith rflat / mean normrflat
   cl> imarith iflat / mean normiflat
   ```

   The *normbflat* (*normvflat*, *normrflat*, *normiflat*) are divided into our object images to give flat field corrected images. The pre-reduction algorithm pays attention to divide only the object images taken through the B filter by the bflat (and so on). These images are listed, sorted by filter, with the `IRAF` command:

   ```
   hselect bimages* $I,FILTER,IMAGETYP yes | grep B | grep -v flat > bobject.list
   hselect rimages* $I,FILTER,IMAGETYP yes | grep R | grep -v flat > robject.list
   hselect vimages* $I,FILTER,IMAGETYP yes | grep V | grep -v flat > vobject.list
   hselect iimages* $I,FILTER,IMAGETYP yes | grep I | grep -v flat > iobject.list
   ```

   Now, the algorithm executes:

   ```
   imarith @bobject.list / normbflat f//@bobject.list
   imarith @robject.list / normrflat f//@robject.list
   ```

```
imarith @vobject.list / normvflat f//@vobject.list
imarith @iobject.list / normiflat f//@iobject.list
```

Bias-subtracted and flat fielded B V, R, I RATS images are now renamed with the starting letter 'f'.

5.1.4 Bad pixels and cosmic rays

5.1.4.1 Bad pixels

CCD chips can have a variety of defects, ranging from isolated bad pixels or bad columns, to whole areas of the chip that are not reliable. Cleaning an image of these defects is not necessarily a trivial task.

The **fixpix** routine manages bad pixels, overwriting on the original images. The task needs the list of images to be cleaned and a bad pixel table. The table should have entries of the form "xbegin xend ybegin yend". Before running the pre-reduction algorithm, the User must check the coordinates in a file "badpix" put automatically by the telescope staff, and the images to be processed in a list "pixlist", then run `IRAF` epar `fixpix` as shown in table 5.3.

`cl>`	`epar fixpix`	
	`images = @pixlist`	`List of images to be processed`
	`masks = badpix`	`List of bad pixel masks`
	`(linterp = "INDEF")`	`Mask values for line interpolation`
	`(cinterp = "INDEF")`	`Mask values for column interpolation`
	`(verbose = no)`	`Verbose output?`
	`(pixels = no)`	`List pixels?`
	`(mode = "ql")`	

Table 5.3: Parameters file for `fixpix` `IRAF` task, setted for RATS images

The pre-reduction algorithm automatically executes:

```
fixpix @pixlist badpix
```

5.1.4.2 Cosmic rays

Cosmic rays can strike the CCD during an exposure leaving a characteristic signature: one or a few very high count pixels. They are normally quite unlike images of astronomical sources which distribute light over a larger area of the chip due to diffraction by the telescope optics and atmospheric turbulence. Cosmic ray removal may not be needed if one dithered while observing: when one combine the dithered images the cosmic rays may be removed by the rejection algorithm chosen in `imcombine`. Otherwise, one can use `fixpix` to remove cosmic rays, but he will need a bad pixel file for every image. This is too time-consuming and ... corresponding to the pipeline philosophy.

One defines the parameters `threshold` and `fluxratio` in the parameter file of the the task **cosmicrays** to set the criteria the task uses to identify and replace cosmic ray hits, as shown in table 5.4.

cl>	epar cosmicrays	
	input = @rayfile	List of images in which to detect cosmic rays
	output = @goodfile	List of cosmic ray replaced output images (optional)
	answer =	Review parameters for a particular image?
	(badpix = "")	List of bad pixel files (optional)
	(ccdtype = "")	CCD image type to select (optional)
	(threshold = 25.)	Detection threshold above mean
	(fluxratio = 2.)	Flux ratio threshold (in percent)
	(npasses = 5)	Number of detection passes
	(window = "5")	Size of detection window
	(interactive = yes)	Examine parameters interactively?
	(train = no)	Use training objects?
	(objects = "")	Cursor list of training objects
	(savefile = "")	File to save train objects
	(mode = "ql")	

Table 5.4: Parameters file for `cosmicrays` `IRAF` task, setted for RATS images

The value of `threshold` determines the minimum count reading needed for a pixel to be considered a cosmic ray hit, based on some multiple of the background standard deviation (at least 5 for background areas).
The `fluxratio` parameter is the ratio of the flux of neighboring pixels to that of the target pixel. It's used to choose which pixels to replace. We keep it between 2 and 6 to avoid removing good pixels.

As we are processing a batch of images with sources at very different count levels, we may lose faint sources if we set parameters on higher count level source images so that we have run `cosmicrays` task preliminary on some selected images to set the value of parameters mentioned above.

The `IRAF` command line that automatically executed by the pre-reduction algorithm is:

```
cl> cosmicrays inputfile outputfile fluxratio=a threshold=b interactive+
```

or in the parameter file.

5.1.5 *Implementation of the pre-reduction algorithm*

On the basis of `FITS` header keywords, raw frames are automatically grouped and processed. The pipeline is header-driven.

Existing keywords `OBJECT & IMAGETYP` determine whether each frame is a bias, dark frame, flat field, lamp spectrum, or scientific target. For the latter, all frames of a given target are grouped together.

The pipeline's own scripts perform the automatic processing of the calibration products first: bias co-addition and checking, imaging flat fields production. (the CCD dark current is so low that we have no dark frames to calibrate as yet). Individual flat field frames are automatically scaled and weighted by their median/mode values before co-addition, and automatically normalized or response-corrected afterwards.

Further scripts apply these calibration products to the science frames, according to the correct night/readout-speed/filter etc.

5.2 Reduction algorithm of astrophysical images

The pre-reduced images are then passed to the second part of the master shell script, made up of various secondary shell scripts and FORTRAN modules in succession, which perform some operation on images.

As we obtain seven different and subsequent snapshot for each single RATS field, at first the reduction algorithm has to match the frame on another. Infact they are shifted each other because of the Earth rotation and telescope guiding pursuit (not guide star is foreseen in the RATS observing strategy).

To do that, an around of the center of photometrically good stars is detected with `DAOPHOT II` package.

An `IRAF` script involving the `convolve` and FORTRAN programs choose the center of defocused good stars using an peculiar mask. The script operates the convolution of the stellar images with an appropriate built kernel.

A shell script matches the seven images of a single observation run in respect to the first one and the stellar center coordinates are related to that of the first.

`DAOPHOT` package is then re-run to find the aperture photometry of well detected good stars.

All these operation are performed on the whole mount of images of a single night.

At the end, a FORTRAN program write ASCII files containing the magnitude trend of each good star during the night.

After completion, each program module is written to disk; this allows for recovery of information in the event of failure and simplifies debugging. The modules also contain detailed methods for producing markup of the data products (images and catalogs) for archiving purposes.

5.2.1 Implementation of the reduction algorithm

Precise transit photometry can reveal the signature of planets moving across the disk of their star.

As the pre-existing photometry software for the automatic search of transit events is inadequate for the wide FOV of the RATS cameras, a custom-built data pipeline has been developed.

With an exposure of $10s$, each of which is $\sim$ 9 Mb in size, we expected to obtain at least 5 Gb every clear night. To handle such a large dataset, the reduction of the data happens via an automated pipeline as soon as the data is obtained, in order to avoid the build-up of an insurmountable back-log. This reduction will provide a catalog of photometric, positional and quality control data on every object detected in every time. In this way, we are also able to detect and monitor transient events in great detail. We aim to make this catalog publically available, via the web interface of the RATS project, `www.rats.it`, as the data will provide an invaluable resource for a large number of different projects.

The developed algorithm do not use any catalog as photometric input file, as we have described in our observational strategy. Joint with the fact that we defocus our frames, these create some disadvantage we take into account for the data retrieval and analysis: infact, the photometric measurements are associated with unknown objects and the aperture for every object is not centered (because of the defocusing) at a precisely determined and consistent position on the CCD. The matching between the transients object and a catalog is finally obtained.

The software creates a list for each sub-fields (pointings) of the RATS field observed in order to match the right frames, shifted because of the rotation of Earth during the pointings. Aperture photometry is then performed in circular aperture of radius 5 pixels (these apertures were selected by inspection of images of known blended and unblended objects, at this spatial resolution) using a modified `DAOPHOT`, version 2004 provided by P. Stetson to a member of the RATS team, which we called `DAOPHOT1`.

The sky background is computed in an annulus of inner radius 10 pixels and outer radius 15 pixels, so that the sky annulus has ten times the area of the 5 pixel aperture. Pixels flagged in the area as being occupied by stellar images or cosmic rays are excluded from the sky background calculation.

Since the aperture is not centered on the star position, we convolve the images in order to reconstruct a synthetic Gaussian form of the stellar profile. In this way we have obtained the actual position of the star on the single frame.

The next step is the matching between each frame of every RATS sub-fields. We always arbitrarily select the first temporal image of each sub-fields as the reference coordinates image so that all the following frames are referred to the first. Using Stetson's `DAOMATCH` and `DAOMASTER`, we calculate the shift the images of the same star in every frame. We apply this shift to the refined convolved coordinates and we match all the object above an *a priori* established limit.

We then re-performed the aperture photometry with the same circular aperture used at the beginning. Once the instrumental magnitudes have been corrected to a standard airmass near the middle of the observed range, a linear equation for the zero-point is used to select the promising target. From a typical RATS field, 4000 stars are rejected as they have a below threshold number of data points (either because they are too faint or that they saturate the detector). The corrected stellar magnitude and the zero-points are written on an ASCII file for every good star.

5.2.2 DAOPHOT modified

We modified the Stetson's packet in order to have some other information about the sky value and the comparison with photometric system. In order to achieve these information, we wrote on file the value of sigma and mode of the sky, and made some control with $< FK >$ catalog. As DAOPHOT packet is a Stetson copyright and the changes brought about are not so remarkable to make difference with the original version, we cannot published the modified algorithm.

5.3 Fortran, `IRAF` and shell script programs: the components description

In this section we include a complete descriptions of each component of the pipeline, as listed in §4.3.3. For each module, in the following sections we illustrate all the specs as required by ESA Software Engineering Standards (1991). Each component has been given an unique identifier of the form ADDCn, with n a number in the range $[1; 9]$.

5.3.1 [ADDC1]: calibration.csh

- ✔ Type: Shell script pipeline.
- ✔ Purpose: See subordinate components.
- ✔ Function: Perform images calibration in order to obtain refined science images.
- ✔ Subordinates: `calibra.cl` (ADDC2, §5.3.2).
- ✔ Dependencies: None.
- ✔ Interfaces: It starts interactively, by a command line, when the Operator begins the reduction process of a night of observation.
- ✔ Resources: See subcomponents and their descendants.
- ✔ References: None.
- ✔ Processing: See subordinate components at following sections.
- ✔ Data: See subordinate components at following sections.

5.3.2 [ADDC2]: calibra.cl

- ✔ Type: IRAF script.
- ✔ Purpose: It reduces all the images acquired in a selected night of observation.
- ✔ Function: Calibration of raw science images.
- ✔ Subordinates: None.
- ✔ Dependencies: None.
- ✔ Interfaces: Called up by the parent.
- ✔ Resources: No special or different requirements from (Granata, 2007).
- ✔ References: Granata (2007).
- ✔ Processing:
  - ➢ A masterbias is created from bias frames;
  - ➢ a masterbias is subtracted from flat fields images;
  - ➢ a masterflat is created from flat fields frames;
  - ➢ raw science images are bias subtracted and divided by masterflat.
- ✔ Data:
  - ➢ Masterbias
  - ➢ masterflat
  - ➢ calibrated science images

5.3.3 [ADDC3]:

- ✔ Type: Shell script pipeline.
- ✔ Purpose: See subordinate components.
- ✔ Function: Performs automatic reduction in order to create lightcurve files.
- ✔ Subordinates:
  - ➢ `Daophot` (ADDC4, §5.3.4)
  - ➢ `centring` (ADDC5, §5.3.4)
  - ➢ `matchframe.csh` (ADDC6, §5.3.4)
  - ➢ `transformer-coo` (ADDC7, §5.3.4)
  - ➢ `print-phot` (ADDC8, §5.3.4)
  - ➢ `lightcurve` (ADDC9, §5.3.4)
  - ➢ `bestlightcurves` (ADDC10, §5.3.4)
- ✔ Dependencies: ADDC1 (§5.3.1) and ADDC2 (§5.3.2)
- ✔ Interfaces: It starts automatically when ADDC1 stops.
- ✔ Resources: See subcomponents and their descendants.
- ✔ References: None.
- ✔ Processing: See subordinate components.
- ✔ Data: See subordinate components.

5.3.4 [ADDC4]:

- ✔ Type: *Fortran77* executable.
- ✔ Purpose:
  - ➢ It computes concentric aperture photometry.
  - ➢ A separate sky value is determined for each source using specified inner and outer sky radii.
  - ➢ Find positive brightness perturbations (*i.e.* stars) in a 2 dimensional image and compute centroids and shape parameters
- ✔ Function: For each science frame, this component performs the aperture photometry.
- ✔ Subordinates: None.
- ✔ Dependencies: A collection of images must exist.
- ✔ Interfaces: Called up by parent component.

- ✔ Resources: No special or different requirements from (Granata, 2007).
- ✔ References: Granata (2007).
- ✔ Processing:
  - ➢ Find the raw coordinates of the stellar centroids;
  - ➢ calculate an aperture magnitude of the defocused stars.
- ✔ Data:
  - ➢ `File.coo`
  - ➢ `file.ap`

5.3.5 [ADDC5]: centring.f

- ✔ Type: `Fortran77` executable.
- ✔ Purpose: It computes centroid coordinates of a stellar object.
- ✔ Function: For each science frame, this component refines the calculation of coordinates.
- ✔ Subordinates: None.
- ✔ Dependencies: A collection of files with stellar coordinates must exist.
- ✔ Interfaces: Called up by parent component.
- ✔ Resources: No special or different requirements from (Granata, 2007).
- ✔ References: Granata (2007).
- ✔ Processing: Find the refined coordinates of the stellar centroids.
- ✔ Data: `File.coo`

5.3.6 [ADDC6]: matchframe.csh

- ✔ Type: Shell script pipeline.
- ✔ Purpose: See subordinate components.
- ✔ Function: For each science frame, this component find a match among the science frames that are shifted because of the different observing time.
- ✔ Subordinates:
  - ➢ `Daomatch`
  - ➢ `masterframe.csh`
- ✔ Dependencies: A reference frame among all the science frames must exist.

- ✔ Interfaces: Called up by parent component.
- ✔ Resources: No special or different requirements from (Granata, 2007).
- ✔ References: Granata (2007).
- ✔ Processing: See subordinate components.
- ✔ Data: See subordinate components.

5.3.7 [ADDC7]: daomatch.f

- ✔ Type: `Fortran77` executable.
- ✔ Purpose: It derives the shifts between the frames.
- ✔ Function: This component combines the photometry from multiple science frames, finding the translation, rotation, and scaling solution between your different photometry files.
- ✔ Subordinates: None.
- ✔ Dependencies: A collection of aperture photometry related to each image must exist.
- ✔ Interfaces: Called up by parent component.
- ✔ Resources: No special or different requirements from (Granata, 2007).
- ✔ References: Granata (2007).
- ✔ Processing: Find the transformation (rotation and shifting) of coordinates of every stellar centroids compare to the reference frame.
- ✔ Data: `File.mch`

5.3.8 [ADDC8]: masterframe.csh

- ✔ Type: Shell script pipeline.
- ✔ Purpose: See subordinate components.
- ✔ Function: See subordinate components.
- ✔ Subordinates: `Daomaster`.
- ✔ Dependencies: See subordinate components.
- ✔ Interfaces: Called up by parent component.
- ✔ Resources: No special or different requirements from (Granata, 2007).
- ✔ References: Granata (2007).
- ✔ Processing: See subordinate components.
- ✔ Data: See subordinate components.

5.3.9 [ADDC9]: daomaster.f

- ✔ Type: `Fortran77` executable.
- ✔ Purpose: It improves the offsets calculated by daomatch.
- ✔ Function: It performs the actual file merging.
- ✔ Subordinates: None.
- ✔ Dependencies: A `file.mch` must exist in order to execute the merging.
- ✔ Interfaces: Called up by parent component.
- ✔ Resources: No special or different requirements from (Granata, 2007).
- ✔ References: Granata (2007).
- ✔ Processing: This component iteratively solves for zero-point shifts in the magnitude scales from image to image by essentially using all of the stable stars as ”comparison” stars.
- ✔ Data: A refined `new_file.mch`.

5.3.10 [ADDC10]: transformer_coo.f

- ✔ Type: `Fortran77` executable.
- ✔ Purpose: It applies the improved offsets and recompute the unshifted coordinates.
- ✔ Function: It performs an interpolation of coordinates values according to the transformation file.
- ✔ Subordinates: None.
- ✔ Dependencies:
- ✔ Interfaces: Called up by parent component.
- ✔ Resources: No special or different requirements from (Granata, 2007).
- ✔ References: Granata (2007).
- ✔ Processing: Find the stellar transformed coordinates.
- ✔ Data: File with stellar transformed coordinates.

5.3.11 [ADDC9]: lightcurve_creation

- ✔ Type: `Fortran77` executable.
- ✔ Purpose: For each star, it produces the file with the magnitude versus Julian Day.
- ✔ Function: For a selected star, this component prints in a file the magnitude it has in each frame, calculate a zero point and iteratively refined the stellar magnitude.
- ✔ Subordinates: None.
- ✔ Dependencies: A masterlist must exist.
- ✔ Interfaces: Called up by parent component.
- ✔ Resources: No special or different requirements from (Granata, 2007).
- ✔ References: Granata (2007).
- ✔ Processing: Create the stellar lightcurve files.
- ✔ Data: File `lightcurve.dat`.

Obviously, the software aims to be self-explanatory as much as possible: in order to obtain this purpose, each pipeline's file contains an header description of the name of the file, the purpose of the code, the author, the date of last revision and remarks on changing. Moreover, each pipeline's procedure is preceded by comments defining its functionality, input parameters unless it is clear, and output results. On one hand, all variables and constants are commented unless their name is self-explanatory and, on the other hand, non obvious statements in the code is commented immediately before the statements it refers to.

The following documents about RATS–*ARP* are produced and submitted to revision:

1. User Requirements Document (URD) (see appendix B)
2. Software Requirements Document (SRD) (see appendix C)
3. Architectural and Design Document (ADD) (see appendix D)
4. Software User Manual (SUM) (see appendix E)
5. Code Documentation (see appendix F)

The SUM will be simplified compare to ESA Software Engineering Standards (1991) but it describes RATS–*ARP* at a level of detail suitable also for non-specialist Users. The format and size of this documentation will be standard A4 format. If necessary, drawings and diagrams may vary from this format.

Chapter 6

Software testing and results

In this chapter, we present the lightcurve obtained analyzing the images taken at Schmidt telescope of Asiago within the RATS project through RATS-*ARP* software.

It important to remark that the observations has come to a standstill during the 2006 because the CCD mounted on the telescope we were using has surprisingly called back from the Catania Observatory which was the owner of the device. Only after great efforts and expenditure of both time and money, the P.I. of the RATS project has been able to find a new CCD which was mounted on the Schmidt telescope at the very end of 2007.

In the following, we present some of the results obtained both for the focused (§6.1) and defocused images (§6.2) acquired on 18^{th} February 2005 and from 22^{nd} – 27^{th} April 2006, respectively.

6.1 Focused images

6.1.1 The introductive data

In this section we present the lightcurves of RATS_10 field. The coordinates of the center of the 7° field are shown in Table 6.1. All these images were taken with ITANET camera 2.2.1.3, based on the KODAK KAF-4202 2100 x 2100 device. A portion of RATS_10 field is given in Figure 6.1: in the `SAOImage DS9` screen-shot are clearly visible the stellar point sources.

In Table A.1 we give an account of the observation journal for on 18^{th} February 2005 during the overture of the RATS project. In the first column a list of the file fits name is presented: this nomenclature is different from the final rule adopted for naming RATS images because any agreement has been achieved in that initial phase. The second column list the modified Julian Day (MJD) taken from the header fits of each image and the last column list the UT middle of the observations.

These images were processed with RATS–*ARP*. Time processing is about $90''$ per image.

6.1.2 The master images for calibration

In order to obtain a good photometric reduction of the science images according to what explained in section §4.2.1, we have produced the *masterbias* and *masterflat* frames starting from

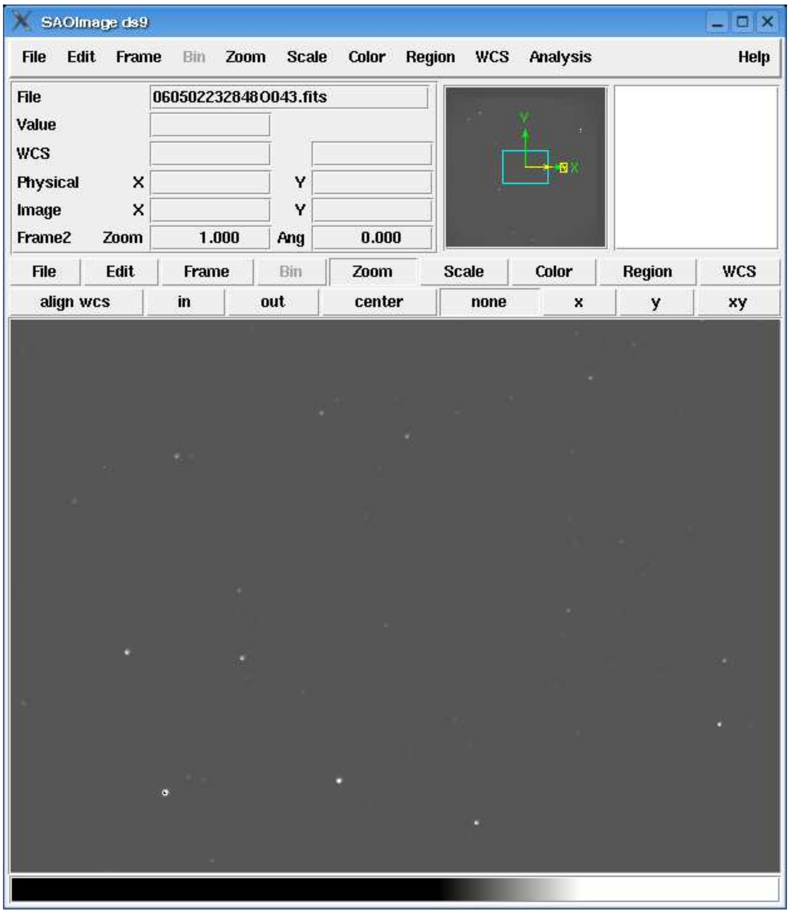

Figure 6.1: `SAOImage DS9` screen-shot of a portion of RATS_10 field in focus: all stars are point sources.

α	δ	epoch	QF
$21^{\rm h}\ 38^{\rm m}\ 24^{\rm s}$	$+50^\circ\ 08'\ 49''$	2005.827	714.54003906

Table 6.1: RATS_10 stellar field parameters: in the first two columns there are the coordinates α and δ of the center of the field at referred to the epoch 2005.827 (3^{th} column). In the last column we recall the quality factor (or merit function) QF calculated according to Eq. (2.1).

all the bias and flat fields frames acquired during the night. These images are all in focus. In Figure 6.2 the screen-shots of `SAOImage DS9`[1] displaying both of them are presented.

6.1.2.1 Masterbias

None of the 10 bias frames acquired has shown noteworthy presence of cosmic rays, spots, hotter regions, or the so called "salt-and-pepper" noise which could suggest a coupling of pixels with an

[1]SAOImage DS9 is an astronomical imaging and data visualization application supporting `FITS` images. DS9 is a stand-alone application. It requires no installation or support files.

high and low noise. All the 10 images are given in input to the calibration pipeline (see §5.3.2) according to the procedure illustrated in section §5.1.1. The resulting masterframe is shown in Figure 6.2 (*top panel*).

6.1.2.2 Masterflat

We have acquired dome flat images in a *ad hoc* selected empty field with coordinates as much as possible similar to those of RATS_10 in order to have a similar airmass amount. This latter set of images resulted corrupted and not suitable to obtain a good calibration, so we have ruled-out them. The former set, instead, became our input file for the calibration pipeline (see §5.3.2) as it is explained in section §5.1.1. As it can be seen in Figure 6.2 (*bottom panel*) some of the stars in the empty field start to appear in the images. Producing the masterflat image can smooth their contribution to the light count.

6.1.3 The lightcurves

As an example of the very first observations and data reduction carried out by the Schmidt telescopes, in this section we present two particular lightcurves performed on the night of 18^{th} February 2005 without the use of any filter. The raw images were taken using KODAK KAF-4202 CCD camera. None defocus was applied. Calibration of the images involved flat fielding, subtracting the bias level, using the `IRAF`'s script routine (§5.3.2). All the images were aligned and aperture photometry was performed in the more than 200 reference stars. The aperture to perform the photometry was varied in order to looking for the best result and the chosen one in equal to 5 pixel radius as the images are in focus.

According with this procedure, we find some first results: a V-shaped lightcurve (Fig. 6.3, on the left) and a lightcurve proper of a pulsating variable star (Fig. 6.3, on the right). The former object could be:

a) a Mira-like variable star: its shape is shows the same trend of χCyg giant star Mira variable;

b) the primary star of an eclipse binary.

We are not yet able to unveil its real nature as we should need more observations of ingress and egress phases, in particular.
The latter object, instead, resembles a contact variable shape, W UMa system-like: its lightcurve, infact, shows a second, deeper minimum typical of these objects.

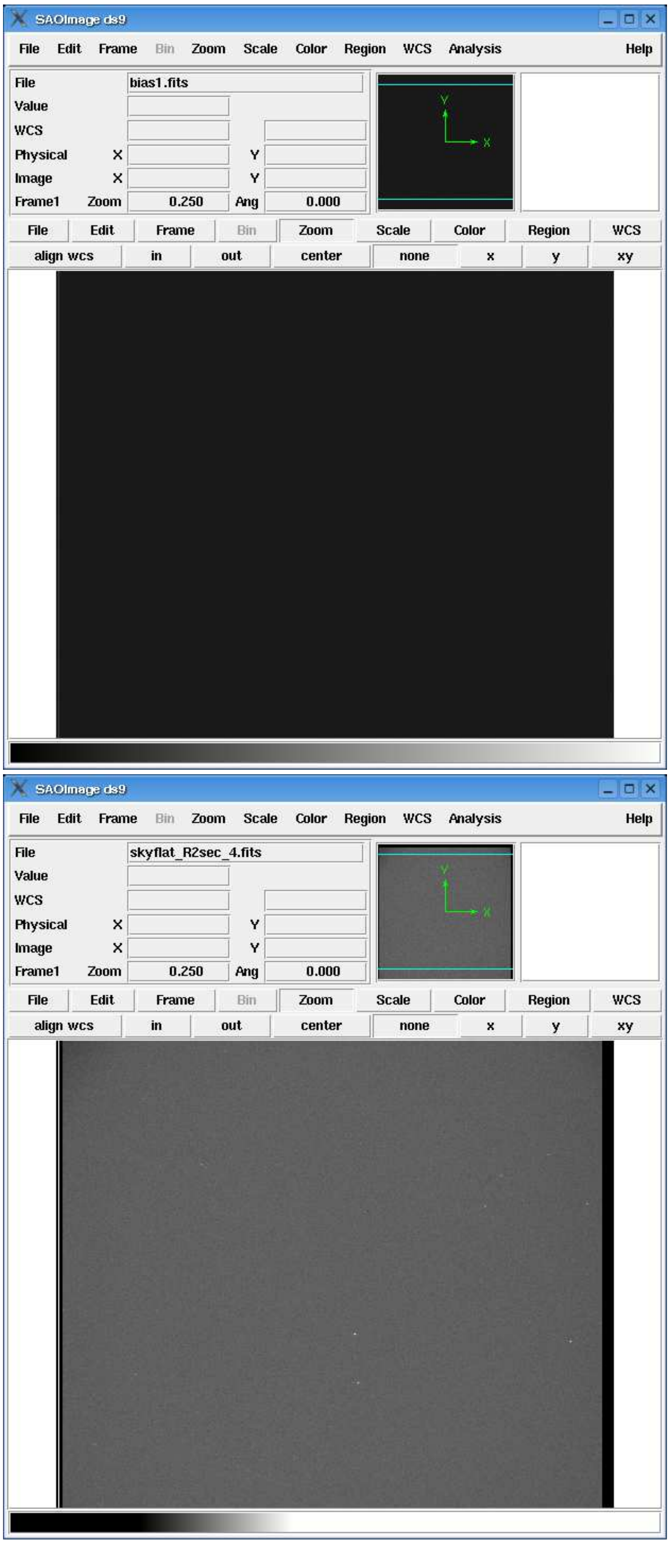

Figure 6.2: Screen-shots of `SAOImage DS9` displaying the masterbias (*top panel*) and masterflat (*bottom panel*) image obtained with the RATS-*ARP* calibration procedure for the images listed in the first column of Tab. A.1 and relative to RATS_10.

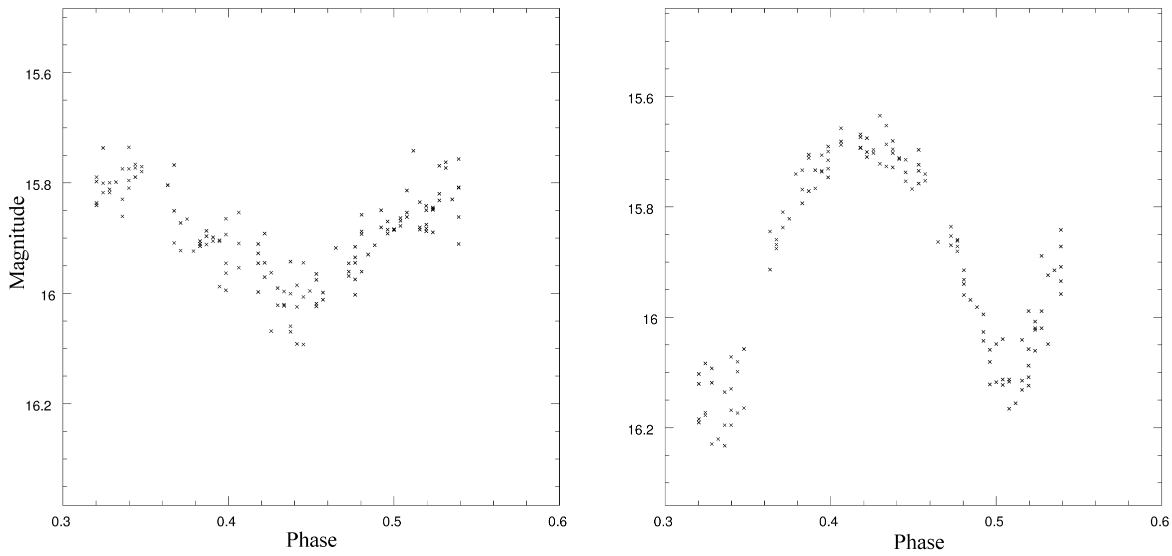

(a) $RATS\_V_1$

(b) $RATS\_V_2$

Figure 6.3: *On the left*: V-shaped lightcurve of an object called $RATS\_V_1$. According to the theory, this object could have a stellar companion which transit in front of the stellar disk or it could be a variable Mira-like star. *On the right*: Typical lightcurve of a contact variable star, like the primary star of W UMa system. This object is called $RATS\_V_2$.

6.2 Defocused images

6.2.1 The introductive data

In this section we present the lightcurves of RATS_4 field. The coordinates of the center of the 7° field are shown in Table 6.2. All these images were taken with SITe camera (see §2.2.1.4), based on the SITe-424A back-illuminated 2048 x 2048 device. A portion of RATS_4 field is given in Figure 6.4: in the `SAOImage DS9` screen-shot are clearly visible the little holes in the stellar center caused by defocusing.

In Table A.2 we give an account of the observation journal for on $22^{\rm nd}$ – $27^{\rm th}$ April 2006 during the second year of the RATS project. In the first column a list of the file fits name is presented: this nomenclature is different from the final rule adopted for naming RATS images because any agreement has been achieved in that initial phase. The second column list the modified Julian Day (MJD) taken from the header fits of each image and the last column list the UT middle of the observations.

These images were processed with RATS–*ARP*. Time processing is about 180″ per image.

6.2.2 The master images for calibration

As previous explained, also for these observations we have produced the *masterbias* and *masterflat* frames starting from all the bias and flat field frames acquired during the night. These

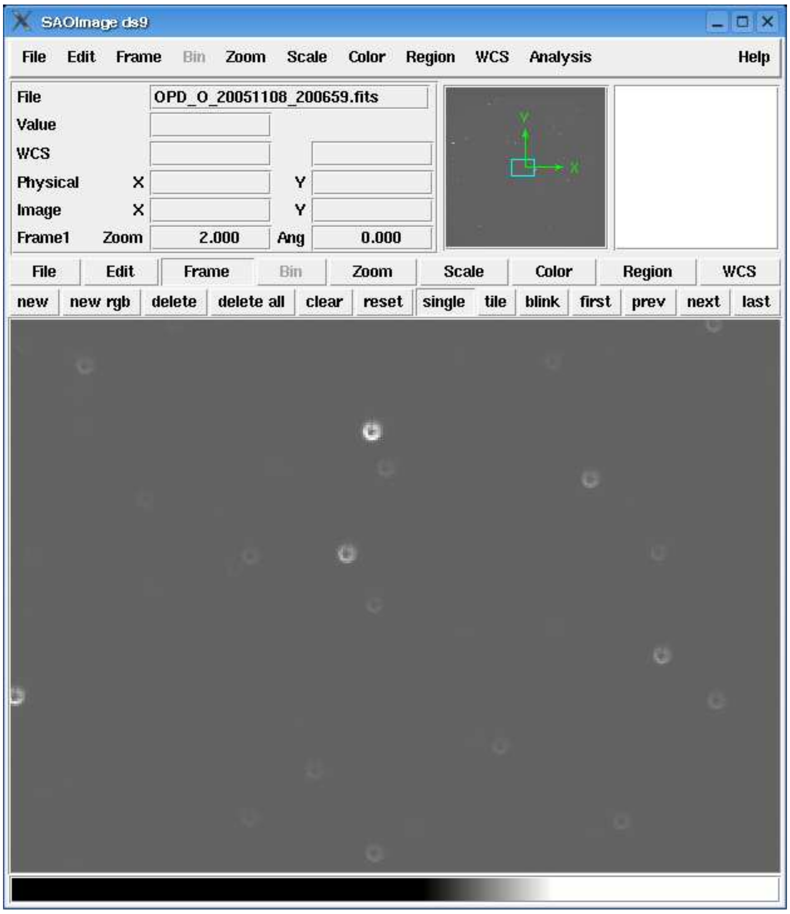

Figure 6.4: `SAOImage DS9` screen-shot of a portion of RATS_4 defocused field: the little holes in the stellar center caused by defocusing are clearly visible.

α	δ	epoch	QF
$16^{\mathrm{h}}\ 59^{\mathrm{m}}\ 43^{\mathrm{s}}$	$+13^{\circ}\ 05'\ 25''$	2006.318	397.05096436

Table 6.2: RATS_4 stellar field parameters: in the first two columns there are the coordinates α and δ of the center of the field at referred to the epoch 2006.318 (3^{th} column). In the last column we recall the quality factor (or merit function) QF calculated according to Eq. (2.1).

images are all defocused. As an error was initially written in the images header, the `IRAF` script failed to produce the masterframes. In order to fulfill the automatic procedure requirements, it was necessary to change manually the keywords value thanks to the `IRAF keyhead` utility:

```
keyhead -r @list_wrong
```

where the `-r` allowed the name of the wrong keyword to be changed into the right one. Prefacing the name of the file containing the list with a symbol allows to made changes at one time. So that:

`CTYPE2 = 'DEC--TAN'` has been changed in `CTYPE2 = 'DEL--TAN'`

In Figure 6.5 the screen-shots of `SAOImage DS9` of both of them are presented.

6.2.2.1 Masterbias

The bias images listed in Table A.2 showed the presence of cosmic rays and weak "salt-and-pepper" noise. Nevertheless all biases are given in input to the calibration pipeline (see §5.3.2) in order to best compensate the scientific images. The resulting masterframe is shown in Figure 6.5 (*top panel*): the "salt-and-pepper" noise is now scarcely visible.

6.2.2.2 Masterflat

We have acquired dome flat images because none *ad hoc* empty field with coordinates similar to those of RATS_4 are available. This set became our input file for the calibration pipeline (see §5.3.2) as it is explained in section §5.1.1. As it can be seen in Figure 6.5 (*bottom panel*), the spots that are present onto the sheet are not smoothed after the median evaluation of counts; anyway, these imperfections did not become a problem for the calibration step.

6.2.3 The lightcurves

As an example of the observations and data reduction carried out by the Schmidt telescopes, in this section we present the lightcurves performed on the nights of $22^{\text{nd}} - 27^{\text{th}}$ April 2006. The raw images were taken using SITe-424A CCD camera. A slight defocus of the image was applied and equal to 5 pixels. Calibration of the images involved flat fielding, subtracting the bias level, using the `IRAF`'s script routine (§5.3.2). All the images were aligned and aperture photometry was performed for more than 120 reference stars. The aperture to perform the photometry was varied in order to looking for the best result and the chosen one in equal to 10 pixel radius as the images are defocused.

According with this procedure, we find some lightcurves presented in Figure 6.6. As it can be seen, the central part of each plots is empty of data because in the halfway observations interval full moon arisen and observations were hampered. The dots refer only to those images marked with a ✪ symbol in Table A.2. Moreover, the point are spread because of the presence of veils during the nights.

We are not yet able to re-observe the two objects mentioned in section §6.1.3 in defocusing mode because in the period when RATS_10 is arisen, any CCD were mounted on the telescope.

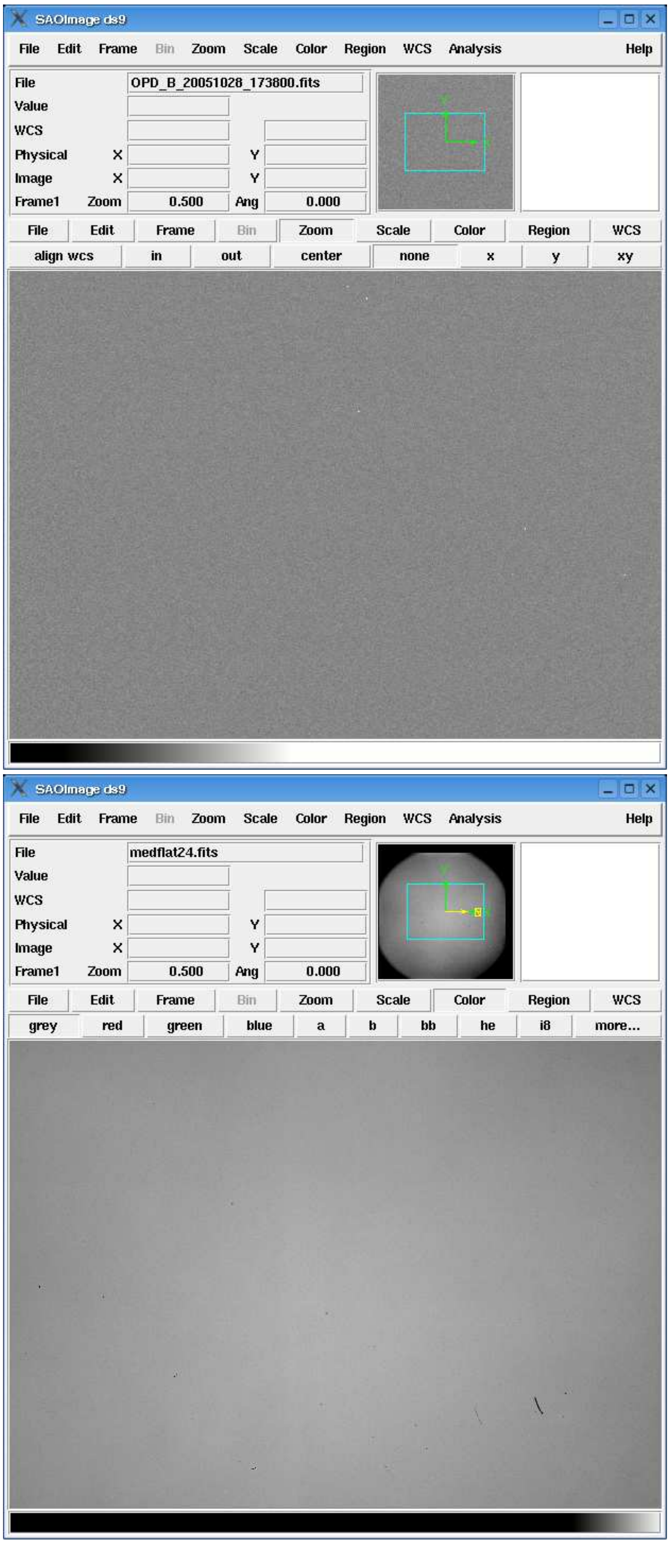

Figure 6.5: Screen-shots of `SAOImage DS9` displaying the masterbias (*top panel*) and masterflat (*bottom panel*) image obtained with the RATS-*ARP* calibration procedure for, respectively, the biases and flats frames listed in Tab. A.2 and relative to RATS_4.

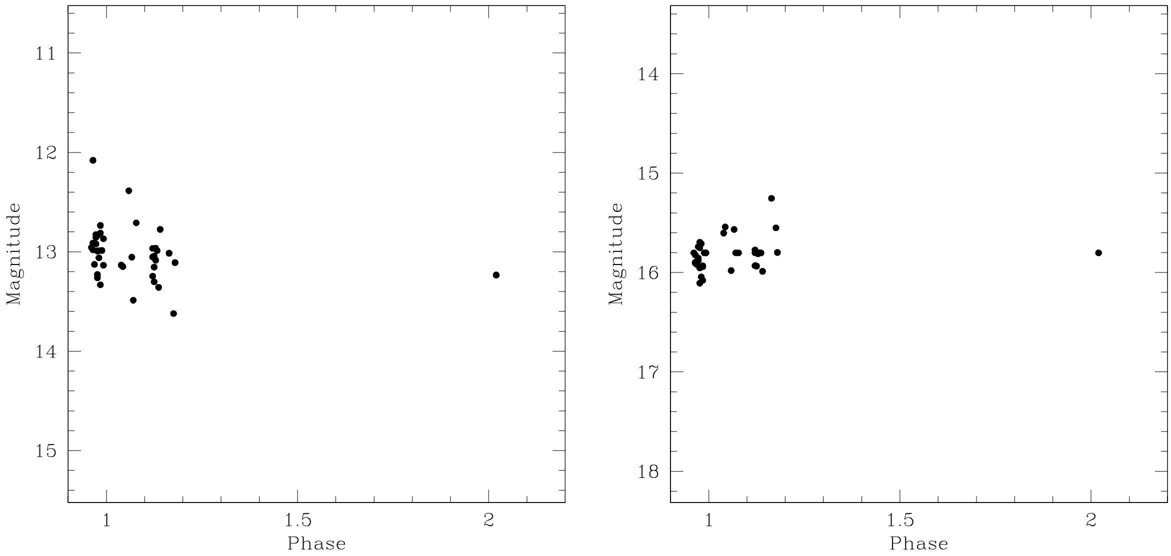

Figure 6.6: Partial lightcurves obtained from the automatic reduction performed with RATS–*ARP*. Missing observations because of full moon are responsible for lack of points in the central part of the plots.

Chapter 7

The RATS database: analysis

SCHEDULING observations with RATS requires a careful selection of the fields and targets that satisfies the exoplanet search transit programme. In order to maximize the scientific return, this selection relies critically on information that have been accumulated over the years –either from dedicated ground based observations or from existing catalogs– on the objects of interest in the sky regions accessible to RATS. For this purpose, all the relevant data which are of any use for the target and field selection have been gathered in a dedicated database, the RATS–DB database, that will be accessible through the internet directly from a WEB interface.

7.1 The database key concepts

The term *database* originated within the computing discipline and although its meaning has been broadened by popular use, even to include non-electronic databases, we refer only about computer databases.

The central concept of a database is that of a collection of records, or pieces of information. Many professionals consider a collection of data to constitute a database only if it has certain properties: for example, if the data is managed to ensure its integrity and quality, if it allows shared access by a community of Users, if it has a schema, or if it supports a query language. However, there is no definition of these properties that is universally agreed upon.

Typically, for a given database, there is a structural description of the type of facts held in that database: this description is known as a *schema*. The schema describes the objects that are represented in the database, and the relationships among them. There are a number of different ways of organizing a schema, that is, of modeling the database structure: these are known as *database models* (or *data models*). The model in most common use today is the relational model, which represents all information in the form of multiple related tables each consisting of rows and columns (the formal definition uses mathematical terminology). This model represents relationships by the use of values common to more than one table. Other models such as the hierarchical model and the network model use a more explicit representation of relationships. *Database Management System (DBMS)*, the software which allows the query on the collection of records, are usually categorized according to the data model that they support: relational, object-relational, network, and so on. The data model will tend to determine the query languages that are available to access the database. A great deal of the internal engineering of a DBMS, however, is independent of the data model, and is concerned with managing factors such as performance, concurrency, integrity, and recovery from hardware failures.

7.1.1 Database models

Various techniques are used to model data structure. Most database systems are built around one particular data model, although it is increasingly common for products to offer support for more than one model. For any one logical model various physical implementations may be possible, and most products will offer the User some level of control in tuning the physical implementation, since the choices that are made have a significant effect on performance. An example is the relational model, the one RATS–DB will be based on: all serious implementations of the relational model allow the creation of indexes which provide fast access to rows in a table if the values of certain columns are known.

In the following section, a brief description of the *hierarchical model* and *network model* will be given while a grater space is reserved to the *relational model*, as it is the most widespread model data structure.

7.1.1.1 Hierarchical model

In a hierarchical data model, data are organized into a tree-like structure. The structure allows repeating information using parent/child relationships: each parent can have many children but each child only has one parent. All attributes of a specific record are listed under an entity type. In a database, an entity type is the equivalent of a table; each individual record is represented as a row and an attribute as a column. Entity types are related to each other using $1 : N$ mapping, also known as "one-to-many relationships". Hierarchical structures were widely used in the first mainframe database management systems. Hierarchical relationships between different types of data can make it very easy to answer some questions, but very difficult to answer others. If a one-to-many relationship is violated, then the hierarchy becomes a network. The most common form of hierarchical model used currently is the `LDAP` [1] model. Other than that, the hierarchical model is rare in modern databases. It is, however, common in many other means of storing information, ranging from file systems to the `Windows` registry to `XML` documents.

7.1.1.2 Network model

The network model is a database model conceived as a flexible way of representing objects and their relationships. Where the hierarchical model structures data as a tree of records, with each record having one parent record and many children, the network model allows each record to have multiple parent and child records, forming a lattice structure. The chief argument in favour of the network model, in comparison to the hierarchic model, was that it allowed a more natural modeling of relationships between entities. Although the model was widely implemented and used, it failed to become dominant for two main reasons. Firstly, IBM chose to stick to the hierarchical model with semi-network extensions in their products. Secondly, it was eventually displaced by the relational model, which offered a higher-level, more declarative interface. Un-

[1] The Lightweight Directory Access Protocol, or LDAP, is an application protocol for querying and modifying directory services running over TCP/IP.

til the early 1980s the performance benefits of the low-level navigational interfaces offered by hierarchical and network databases were persuasive for many large-scale applications, but as hardware became faster, the extra productivity and flexibility of the relational model replaced the network model in corporate enterprise usage.

7.1.1.3 Relational model

Three key terms are used extensively in relational database models: relations, attributes, and domains. A relation is a table with columns and rows. The named columns of the relation are called attributes, and the domain is the set of values the attributes are allowed to take. The basic data structure of the relational model is the table, where information about a particular entity (*i.e.*, a student) is represented in columns and rows (also called *tuples*). Thus, the term "relation" in this model name refers to the various tables in the database. A relation is a set of tuples. The columns enumerate the various attributes of the entity (the student's name, the register number, etc., for example), and a row is an actual instance of the entity (a specific student) that is represented by the relation. As a result, each tuple of the employee table represents various attributes of a single student.

All relations and tables in a relational database have to adhere to some basic rules to qualify as relations. First, the ordering of columns is immaterial in a table. Second, there can't be identical tuples or rows in a table. Finally, each tuple will contain a single value for each of its attributes.

A relational database contains multiple tables, each similar to the one in the "flat" database model. One of the strengths of the relational model is that, in principle, any value occurring in two different records (belonging to the same table or to different tables), implies a relationship among those two records. Yet, in order to enforce explicit integrity constraints, relationships between records in tables can also be defined explicitly, by identifying or non-identifying parent-child relationships. Tables can also have a designated single attribute or a set of attributes that can act as a "*key*", which can be used to uniquely identify each tuple in the table. A key that can be used to uniquely identify a row in a table is called a *primary key.* Keys are commonly used to join or combine data from two or more tables. For example, a *STUDENT* table may contain a column named "classroom" which contains a value that matches the key of a *CLASSROOM* table. Keys are also critical in the creation of indices, which facilitate fast retrieval of data from large tables. Any column can be a key, or multiple columns can be grouped together into a compound key. It is not necessary to define all the keys in advance: a column can be used as a key even if it was not originally intended to be one.

Users (or programs) request data from a relational database by sending it a query that is written in a special language that will probably be `Oracle` in the case of RATS–DB. Although was originally intended for end-Users which use both `Windows` and `Unix` platform, it is much more common for `Oracle` queries to be embedded into software that provides an easier User interface. Many web sites perform `Oracle` queries when generating pages. In response to a query, the database returns a result set, which is just a list of rows containing the answers. The simplest query is just to return all the rows from a table, but more often, the rows are filtered in some way to return just the answer wanted. Often, data from multiple tables are combined into one, by doing a *join*, a "temporary table" that is the result of combination records from two initial tables in a relational database. There are a number of relational operations other than join.

7.1.2 Storage and physical database design

Database tables/indexes are typically stored in memory or on hard disk in one of many forms, ordered/unordered flat files, ISAM, heaps, hash buckets or B+ trees. These have various advantages and disadvantages, but the most commonly used are B+ trees and ISAM. Let's summarize each of them:

- **Flat files**: a flat file is a file that contains records, and in which each record is specified in a single line. Fields from each record may simply have a fixed width with padding, or maybe delimited by whitespace, tabs, commas or other characters. Extra formatting may be needed to avoid delimiter collision. There are no structural relationships. The data are "flat" as in a sheet of paper, in contrast to more complex models such as a relational database.
- **ISAM**: In an ISAM (*Indexed Sequential Access Method*) system, data is organized into records which are composed of fixed length fields. Records are stored sequentially, originally to speed access on a tape system. A secondary set of hash tables known as indexes contain "pointers" into the tables, allowing individual records to be retrieved without having to search the entire data set. Thus, as the indexes are small and can be searched quickly, then the database accesses only the records it needs. Additionally modifications to the data do not require changes to other data, only the table and indexes in question. MySQL implements and extends ISAM.
- **heaps**: is a specialized tree-based data structure that satisfies the heap property: if B is a child node of A, then $\text{key}(A) \geq \text{key}(B)$. This implies that the element with the greatest key is always in the root node, and so such a heap is sometimes called a *max heap*. This is why heaps are used to implement priority queues.
- **hash buckets**: (or a **hash map**) is a data structure that associates keys with values: given a key, find the corresponding value. It works by transforming the key into a number that is used as an index in an array to locate the desired location where the values should be. Hash tables may be used as in-memory data structures.
- **B+ trees**: is a type of tree, which represents sorted data in a way that allows for efficient insertion, retrieval and removal of records, each of which is identified by a key. It is a dynamic, multilevel index, with maximum and minimum bounds on the number of keys in each index segment (usually called a *block* or *node*). In a B+tree, in contrast to a B-tree, all records are stored at the lowest level of the tree; only keys are stored in interior blocks. The `NTFS` filesystem for `Microsoft Windows` and `ReiserFS` filesystem for `Unix` and `Linux` all use this type of tree for block indexing.

All of these databases can take advantage of indexing to increase their speed, and this technology has advanced tremendously since its early uses in the 1960s and 1970s. The most common kind of index is a sorted list of the contents of some particular table column, with pointers to the row associated with the value. An index allows a set of table rows matching some criterion to be located quickly. Typically, indexes are also stored in the various forms of data-structure mentioned above. Usually, a specific technique is chosen by the database designer to increase efficiency in the particular case of the type of index required.

The database chooses between many different strategies based obviously on which one it estimates will run the fastest and indexes are transparent to the application or end-User querying the particular database.

7.2 Database management system (DBMS)

A database management system is computer software designed for the purpose of managing databases. Typical examples of DBMSs are: `Oracle`, `Microsoft Access`, `Microsoft SQL Server`, `MySQL`, just to mention a few and the main ones. DBMSs are typically used by database administrators in the creation of database systems.

7.2.1 DBMS description

A DBMS is a complex set of software programs that controls the organization, storage, management, and retrieval of data in a database. Typically, a DBMS includes:

1. A modeling language to define the logical schema of each database hosted in the DBMS, according to the DBMS data model.
    - The four most common types of organizations are the hierarchical, network, relational and object models (see §7.1.1). A given database management system may provide one or more of the four models. The optimal structure depends on the natural organization of the application's data, and on the application's requirements, which include transaction speed rate, reliability, maintainability, scalability, and cost.
    - The dominant model in use today is the ad hoc one embedded in SQL, despite the objections of purists who believe this model is a corruption of the relational model, since it violates several of its fundamental principles for the sake of practicality and performance.
2. Data structures (fields, records, files and objects) optimized to deal with very large amounts of data stored on a permanent data storage device (CD, DVD, hard disks), which implies relatively slow access compared to volatile main memory.
3. A database query language and report writer to allow Users to interactively interrogate the database, analyze its data and update it according to the Users privileges on data.
    - It also controls the security of the database.
    - Data security prevents unauthorized Users from viewing or updating the database. Using passwords, Users are allowed access to the entire database or subsets of it, called *subschemas*. For example, RATS database can contain all the data about an individual observing night, but one group of Users may be authorized to view only lightcurves graphs, while others are allowed access to the entire data, from row to reduced images.
4. A transaction mechanism, that ideally would guarantee the ACID (Atomicity, Consistency, Isolation, Durability) properties[2], in order to ensure data integrity, despite concurrent User

[2]ACID is a set of properties that guarantee that database transactions are processed reliably. In the context of databases, a single logical operation on the data is called a transaction.

accesses (concurrency control), and faults (fault tolerance).

- It also maintains the integrity of the data in the database.
- The DBMS can maintain the integrity of the database by not allowing more than one User to update the same record at the same time. The DBMS can help prevent duplicate records via unique index constraints; for example, no two customers with the same customer numbers (key fields) can be entered into the database (redundancy avoidance).

The DBMS accepts requests for data from the application program and instructs the operating system to transfer the appropriate data.

When a DBMS is used, information systems can be changed much more easily as the organization's information requirements change. New categories of data can be added to the database without disruption to the existing system. Organizations may use one kind of DBMS for daily transaction processing and then move the detail onto another computer that uses another DBMS better suited for random inquiries and analysis. Overall systems design decisions are performed by data administrators and systems analysts. Detailed database design is performed by database administrators.

DBMS and related software run on database servers, specially designed computers that are usually multiprocessor computers, with RAID disk arrays used for stable storage.

7.2.2 Features and abilities of DBMS

One can characterize a DBMS as an "attribute management system" where attributes are small chunks of information that describe something. Lately databases have been modified to accept large or unstructured (pre-digested or pre-categorized) information as well, such as images (as for RATS–DB) and text documents. However, the main focus is still on descriptive attributes.

DBMS run together frequently-needed services or features of attribute management. Such features include:

- ☑ **Query ability.** Querying is the process of requesting attribute information from various perspectives and combinations of factors. A database query language and report writer to allow Users to interactively interrogate the database, analyze its data and update it according to the Users privileges on data. It also controls the security of the database in order to prevents unauthorized Users from viewing or updating the database. Using passwords, Users are allowed access to the entire database or its subschemas. If the DBMS provides a way to interactively enter and update the database, as well as interrogate it, this capability allows for managing personal databases. However, it may not leave an audit trail of actions or provide the kinds of controls necessary in a multi-User organization. These controls are only available when a set of application programs are customized for each data entry and updating function.
- ☑ **Backup and replication.** Copies of attributes need to be made regularly in case the primary disks or other equipment fails. A periodic copy of attributes may also be created for a distant organization that cannot readily access the original. DBMS usually provide utilities to facilitate the process of extracting and disseminating attribute sets. When data is replicated between database servers, so that the information remains consistent

throughout the database system and Users cannot tell or even know which server in the DBMS they are using, the system is said to exhibit replication transparency.

- ☑ **Rule enforcement.** Often one wants to apply rules to attributes so that the attributes are clean and reliable. For example, we may have a rule that says each RATS image can have only one name associated with it (identified by a precise name structure). If somebody tries to associate a second name with a given image, we want the DBMS to deny such a request and display an error message. However, with changes in the model specification such as, in this example, name structure, rules may need to change. Ideally such rules should be able to be added and removed as needed without significant data layout redesign.

- ☑ **Security.** Often it is desirable to limit who can see or change which attributes or groups of attributes. This may be managed directly by individual, or by the assignment of individuals and privileges to groups, or (in the most elaborate models) through the assignment of individuals and groups to roles which are then granted entitlements.

- ☑ **Computation.** There are common computations requested on attributes such as counting, summing, averaging, sorting, grouping, cross-referencing and so on. Rather than have each computer application implement these from scratch, they can rely on the DBMS to supply such calculations.

- ☑ **Change and access logging.** Often a database administrator wants to know who accessed what attributes, what was changed, and when it was changed. Logging services should allow this by keeping a record of access occurrences and changes.

- ☑ **Automated optimization.** If there are frequently occurring usage patterns or requests, some DBMS can adjust themselves to improve the speed of those interactions.

- ☑ **Meta-data repository.** Meta-data is data describing data. For example, a listing that describes what attributes are allowed to be in data sets is called ”meta-information”. For RATS–DB, meta-data would be headers as they include many important informations about images, such that coordinates, image type, and all the details of the observation settings.

- ☑ **Navigational DBMS.** Navigational databases are characterized by the fact that objects in the database are found primarily by following references from other objects. Navigational access is traditionally associated with the hierarchical and network models (see §7.1.1) of database interfaces and these techniques use ”pointers” and ”paths” to navigate among data records (also known as ”nodes”). This is in contrast to the relational model (see §7.1.1) –implemented in relational databases–, which strives to use logic programming techniques in which you ask the system for what you want instead of how to navigate to it.

- ☑ **Relational DBMS.** This is a new database concept developed for storing and working with large databases. Instead of records being stored in some sort of linked list of free-form records as in navigational DBMS, the idea is to use a *table* of fixed-length records. A linked-list system would be very inefficient when storing ”sparse” databases where some of the data for any one record would be left empty. The relational model solved this by splitting the data into a series of normalized tables, with optional elements being moved out of the main table to where they would take up room only if needed. For instance, a common use of RATS database system will be to track information about images, their name, coordinates and observing time. In the navigational approach all of these data would be placed in a single record, and unused items would simply not be placed in the database. In the relational approach, instead, the data would be normalized into a "image table", a "name table", a "coordinates table", and so on. Records would be created in these optional tables only if the name or coordinates were actually provided. Linking the information back together is the key to this system. In the relational model, some bit of information was used as a "key", uniquely defining a particular record. When information will being collected about an image, information stored in the optional (or related) tables will be found by searching for this key. For instance, if the name of a RATS image is unique, coordinates and observing time for that image will be recorded with the image name as its key. This "re-linking" of related data back into a single collection is something that traditional computer languages are not designed for. Just as the navigational approach would require programs to loop in order to collect records, the relational approach would require loops to collect information about any one record. For this reason, we strongly suggest a relational DBMS for RATS database.

7.3 RATS–DB

The development of a well designed and properly implemented data archive and access system is considered as a fundamental objective by the RATS project for the full exploitation of the vast observational data sets, such as analysis and observational technique, instrumentations involved and reduction procedures.

The huge observational effort necessary in the preparatory phase of the project, and the needs planned for the best exploitation of the RATS detections will led to implement both a data archive and an access system, which aims at becoming a reference point among exoplanet databases including lightcurves plots. The content of the data base will increase in the near future with the data from the survey's observations and the results derived from their scientific analysis. It will make possible to conduct global archive searches to investigate the properties of the new planetary systems will be detected with RATS observing strategy. Investigations of stellar astronomy to be carried out on the exoplanet lightcurves will take benefit of this well documented stellar population. Not only transiting planets, but any kind of relations among these data-sets may be found, with the potential to lead to important new insights on planets.

Thinking at this database in this analysis, our aim was going well beyond the simple archiving of the observational material. By gathering information on a very large sample of stars used as targets for planet search, we intend to build a complete stellar data base, necessary to conduct the foreseen statistical and data analysis of the properties of the planetary systems to be discovered.

Based on a relational database structure (see §7.1.1), the information available in RATS–DB should easily be cross-correlated with already published data. In this context, RATS–DB will be used to:

- offer an update lightcurves database oh thousands of stellar which show peculiar features in their flux. Thus, a new catalogue of stars hosting planets or a stellar companion and variables stars would be generated.

- produce an archive of row images available to both scientists and technicians who will want to make photometric reductions by themselves.
- produce an archive of reduced images available to both scientists and technicians who will want to analyse prospective stellar flux variations.
- prepare an optimal future selection of targets for future missions devoted to exoplanets search. This would be made on the ground from the estimate of lightcurves performed for RATS survey, allowing the selection of the most suitable stars for planetary search via transit method.
- secure the transit detection process: for stars with transit-like lightcurves, the available information will help to discriminate stellar signatures against planetary transits. Linking the stars' properties to the lightcurve analysis will provide reliable clues to identify and rule out confusing transit cases.
- optimize the spectroscopic follow-up chain and minimize the time necessary for observations on dedicated high resolution spectrographs for Doppler measurements, previously known the precise spectral type and the stellar $v \sin i$.

RATS–DB will be composed of three main tables, linked between them through defined external keys:

1. **Raw Images:** this table will contain the frames obtained during the five years RATS survey, including the calibration images (flat fields, biases).
2. **Reduced Images:** this table will contain the frames obtained from the calibration process, including the de-biased flat fields.
3. **Lightcurves:** this table will contain the lightcurves ASCII files and plots obtained with RATS–*ARP* algorithm.

A fourth support table, containing the keys list necessary for linking the first two previous tables and inaccessible to the Users, is also available.

7.3.1 Technical specifications

RATS–DB will primarily contain the information derived from photometric observations of more than thousands objects during the nominal five years of RATS survey. It will also include at least one or two catalogues (USNO-A2, 2-MASS), all cross-correlated against our groundbased photometric observations. The database will be continuously maintained up-to-date with the insertion of new data.

RATS–DB will be an `Oracle`–based relational database system with an User interfaces developed using a set of independent, portable tools, based on open source license, which can be used to build a data access system via web services. These interfaces should be based on a `JAVA` built common architecture and will be compliant with the latest JRE version available at the moment of develop. With this kind of system new plug-ins additions will be easily allowed with minimal effort in order to maintain RATS–DB always moved with the times.

Moreover, the general architecture environment will be accessible by one or more client applications. To set up and then run this system, the manager will have to perform several phases: installation, parameterization, configuration, administration. The system might run locally on a single machine, or be distributed over several machines or even several laboratories and it will have to be flexible enough to handle different type of data and tools.

Some basic services which can be "plugged in" in this framework should be:

- ✔ On-line catalog: provides access to meta-data (see §7.2.2) and data accessible on-line:
  - ✥ a catalog contains one or more data sets;
  - ✥ a data set is characterized by a common structure (a single table), referenced in the catalog.

  This solution has to be preferred to an "element/attribute" model, which is more dynamic but not as easy to maintain.

- ✔ Off-line catalog: identical to the previous with batch access to data:
  - ✥ the Off-line catalog is implemented in the same way as the on-line one.
  - ✥ since the data is not on line, the catalog supplies the data items in batch mode when requested by the command processing service.

- ✔ Repository: links all accessible services to form a global system:
  - ✥ catalog management and synonym association (providing the link between meta-data with the same meaning, but not the same syntax for different data sets);
  - ✥ data set grouping management (*i.e.*, for a given subject);
  - ✥ management of added-value services, access, dynamic parameters;
  - ✥ management of user rights;
  - ✥ based on a configuration using `XML` files, in order to be loaded into an `XML`-capable browser, such as `Firefox` or `Internet Explorer`.

- ✔ Command processing: end-to-end management of user commands.
  - ✥ it handles the data command process;
  - ✥ Reception of data and list of result files.

- ✔ Users space: manages the command and processing result space, where the Users will find command results.

This framework should be designed for two kind of Users: the end-User, the scientist who consults the final system set up to look for and download useful data; the manager, the entity (scientific laboratory, organization, etc.) which will set up and run the system to provide access to its data.

7.3.2 RATS–DB language: `Oracle`

`Oracle` database is a relational database management system (RDBMS) software product released by `Oracle Corporation`® that has become a major feature of database computing. Up to now, many widespread computing platforms have come to use the `Oracle` database software extensively because of its versatility to be hosted both on `windows`, `Linux/Unix`, `Sun Solaris` and `Apple Mac OS` platforms.

Thus, thanks to its compatibility with other database language such as `Access`, RATS–DB will be developed in `Oracle`.

7.3.2.1 Physical and logical structuring

An `Oracle` database system comprises at least one *instance* of the application, along with data storage. An instance comprises a set of operating-system processes and memory-structures that interact with the storage. In addition to storage, the database consists of on-line redo logs (an history that records all changes made in datafiles). Processes can in turn archive the on-line redo logs into archive logs (off-line redo logs), which provide the basis for data recovery and data replication.

The `Oracle` RDBMS stores data logically in the form of tablespaces and physically in the form of data files. Tablespaces can contain various types of memory *segments*, such as *Data Segments*, *Index Segments*, etc. Segments, in turn, comprise one or more *extents*. Extents comprise groups of contiguous *data blocks*. Data blocks form the basic units of data storage. At the physical level, data-files comprise one or more data blocks, where the block size can vary between data-files. `Oracle` database management keeps track of its computer data storage with the help of information stored in the `SYSTEM` tablespace, which contains the data dictionary[3] and often, by default, indexes and clusters.

The `Oracle` DBMS can store and execute stored procedures and functions within itself and object-oriented language Java can invoke such code objects and/or provide the programming structures for writing them.

7.3.2.2 Memory and process architecture

Each `Oracle` instance uses a shared-memory area to store its data and control information and allocates itself a memory when it starts and de-allocates it at shut-down time. The information in the shared-memory area consists of the following elements, each of which has a fixed size, established at instance startup:

- **database buffer cache**: it stores the most recently-used data blocks. These blocks can contain modified data not yet written to disk, unmodified blocks, or blocks written to disk since modification. Because the buffer cache keeps blocks based on a most-recently-used algorithm, the most active buffers stay in memory to improve performance.

- **redo log buffer**: it stores redo entries, a log of changes made to the database. The instance writes redo log buffers to the redo log as quickly and efficiently as possible. The redo log aids in instance recovery in the event of a system failure.

[3] A data dictionary consists of a special collection of tables that contains information about all user-objects in the database.

➢ **shared pool**: it stores shared-memory structures such as library cache and internal information in the data dictionary. An insufficient amount of memory allocated to the shared pool can cause performance degradation.

`Oracle` RDBMS typically relies on a group of processes running simultaneously in the background and interacting to further and monitor database operations. Such processes can include:

- archiver processes;
- database writer processes;
- job-queue processes;
- log-writer process;
- recoverer process;
- client-requests server processes.

7.3.3 Analysis of the storage of RATS data

An `Oracle` database is made up of physical and logical structures. Physical structures are those that can be seen and operated on from the operating system, such as the physical files that store data on a disk. Logical structures are created and recognized by `Oracle` database and are not known to the operating system. The primary logical structure in a database, a tablespace, contains physical files. The RATS–DB Developer or/and User would be aware of the logical structure, but he will be not usually aware of this physical structure. The database administrator will have to understand the relationship between the physical and logical structures of a database. Figure 7.1 shows the relationships between logical and physical structures: on similar structures will be based RATS–DB. This figure also shows recovery-related structures that are optionally kept in the flash recovery area.

7.3.3.1 Storage performance requirements

As Oracle database can automate much of the management of its structure, we stress the RATS–DB manager to exploit this facility during the database development. Let's consider in detail the requirements RATS–DB has to fulfil for a satisfactory storage performance.
Each requirement presented has the form:

ST-XX-nn
Text

where:	**XX**	is an identifier denoting the specific functionality of the requirement;
	nn	is an ascending number giving the logical order of the requirement;
	Text	is the textual description of the requirement.

Control File
CF-PR-01
A control file tracks the physical components of the database, being the root file that the

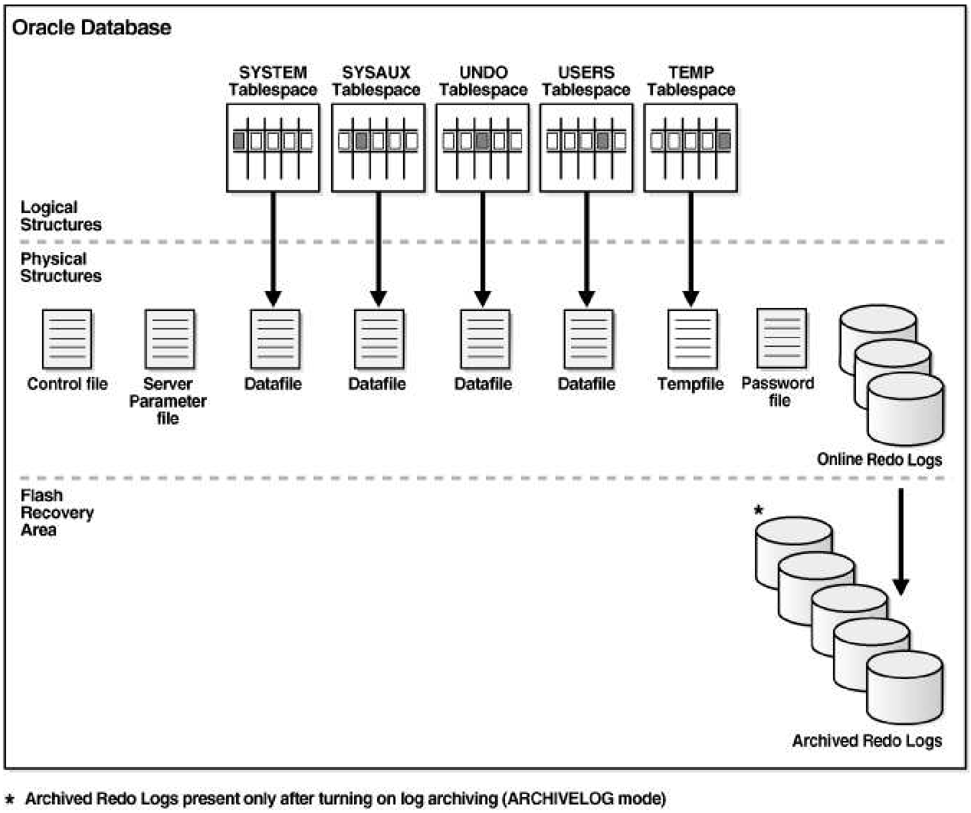

Figure 7.1: This diagram shows the logical, physical, and recovery-related structures of the `Oracle` database, and the relationships between them. Dotted horizontal lines divide the image into three sections. The top section shows logical structures, the middle section shows physical structures, and the bottom section shows recovery-related structures in the Flash Recovery Area. The logical structures are all tablespaces. Each tablespace points to a datafile or tempfile, which are physical structures. Other physical structures include a control file, the on-line redo log files, a server parameter file, and a password file. The flash recovery area contains the archived redo log files, which are copies of redo log files after they are filled.

database uses to find all the other files used. Because of the importance of the control file, it will be multiplexed: the control file should have multiple identical copies, automatically created and kept synchronized one each other.

CF-PR-02
If any control file fails, then the database becomes unavailable. As long as RATS–DB will have a control file copy, however, the administrator would shut down it and re-create the failed control file from the copy, then restart the database.

CF-PR-03
Deletion the failed control file from the `CONTROL_FILES` initialization parameter and restart the database using the remaining control files.

On-line Redo log files

OR-PR-01

Each group the redo log for RATS–DB consists of will be defined by a number.

OR-PR-02

If a failure will require a datafile to be restored from backup, then the recent data changes that are missing from the restored datafile would be obtained from the redo log.

OR-PR-03

The redo log will be used to recover a database after hardware, software, or media failure.

OR-PR-04

To protect against a failure involving the redo log itself, RATS–DB would multiplex the redo log so that two or more identical copies of the on-line redo log would be maintained on different disks.

OR-PR-05

The database log writer process will write redo records from the memory buffer to a redo log group until the log files in that group will reach their storage size limit, or until the administrator will request a log switch operation.

OR-PR-06

RATS–DB will have an archive of redo log files. An optional archive to multiple locations, including a standby database would be take into account.

OR-PR-07

Archived redo log files will require to recover a backup of the database from the time of the backup to the current time.

Tablespaces

TS-PR-01

A datafile location for a certain tablespace will be specified as a designated host directory.

TS-PR-02

Any schema objects assigned to a particular tablespace then will get located in the specified storage location.

TS-PR-03

Tablespaces will provide a unit of backup and recovery.

TS-PR-04

New tablespaces to support Users and application data requirements would be created. Each of them would be a:

- Permanent tablespace: to store permanent data, such as system data.
- Undo tablespace: to create and manage undo data in order to help with database recovery.

➢ Temporary tablespace: to store temporary data.

TS-PR-05
Each user will be assigned a default permanent tablespace.

TS-PR-06
If an extremely large database is needed, then additional temporary tablespaces might be configured.

TS-PR-07
Depending on the type of Users, the status RATS–DB tablespaces would be:

➢ Read & Write: Users can read and write to the tablespace after it is created.

➢ Read Only: the tablespace cannot be written to till its status will be unchanged.

TS-PR-08
Each tablespace will be set to automatically extend itself by a specified amount when it reaches its size limit.

Initialization Parameter file
IP-PR-01
Initialization parameters should be set and used at startup to determine the run-time properties and resources for the database.

Password file
PW-PR-01
All the password for authentication of Users with connection privileges should be put in a password file.

Backup Files
BU-PR-01
Copies of the database should be available.

BU-PR-02
Backup files would be used to recover the database if a failure causes loss of data.

7.3.4 Analysis of the management of RATS data: access and tools

The database will be accessible to the whole scientific community. Nonetheless, a username and password will however be requested for security, to keep the login under control and to avoid the bad use of the server CPU time RATS-DB will run on. The login and password will be probably obtained by simply sending an e-mail to the database administrator.

The web interface will be available through the official RATS web site `www.rats.it` and the database will be accessed by clicking on some appropriate button.

Three tools will be available in the main menu of the database interface that cannot be renounced:

1. Search This tool would be used in three different ways:

   i. It will be possible to search certain raw images in order to calibrate them with a process different from RATS–*ARP* calibration pipeline.

   ii. It will be possible to search certain reduced images in order to analyse them with a reduction process different from RATS–*ARP* reduction pipeline obtaining various lightcurves depending on distinct initial parameters.

   iii. It will be possible to search certain lightcurves plots in order to compare them with others or to used for a targets selection for future surveys and missions. Anyway, the results of each request can be displayed graphically.

2. Help This tool will explain how to use the RATS–DB with some instructions and examples of requests. There will be also some explanations on how to treat the results.

3. Administration This tool will be reserved to internal administrator in order to manage the database.

RATS–DB will be develop in the next years and it will collect all the results obtained from RATS survey and, thus, it will be continuously maintained up-to-date. Moreover, in order to respect the open source philosophy RATS–*ARP* is based on, all the services will be developed with open source tools exclusively.

7.3.5 Analysis of the testing of RATS–DB

Database validation and verification involves checking the database file to ensure that the various data structures retain their integrity and internal consistency. This section is intended as a plan and record for the minimal technical reviews and tests that RATS–DB Developer will have to carry out. It shall be used to assess that the database is of sufficient quality, contains sufficient internal documentation, responds correctly to commands provided by the User, performs the query to the required speed and completeness, and meets the performance requirements.

Test plan #1

Feature to be tested:	Query for raw images.
Test pass/fail criteria:	If the visualization outputs represent the expected raw image, the test is considered to be passed.

Test plan #2

Feature to be tested:	Query for reduced images.
Test pass/fail criteria:	If the visualization outputs represent the expected reduced image, the test is considered to be passed.

Test plan #3

Feature to be tested:	Query for lightcurve plots.
Test pass/fail criteria:	If the visualization outputs represent the expected lightcurve plot, the test is considered to be passed.

Test plan #4

Feature to be tested:	Query for lightcurve ASCII files.
Test pass/fail criteria:	If the visualization outputs represent the expected lightcurve ASCII file, the test is considered to be passed.

Test plan #5

Feature to be tested:	Output format of images: *.gif* or *.ps*
Test pass/fail criteria:	If the format output comes out to be the expected .gif or .ps, the test is considered to be passed.

Test plan #6

Feature to be tested:	Contemporaneous accesses to the web interface.
Test pass/fail criteria:	If contemporary accesses are supported and managed by the User interface, the test is considered to be passed.

7.3.5.1 Acceptance test procedures

The acceptance tests shall comprise the previous test plans results performed on a computer identified by the RATS–DB administrator.
The database will be considered to have passed the acceptance tests if will passe all the tests.

7.3.6 DB filling

Filling a database means that the administrator should insert data in it. In a relational database, this consist of creating the rows of the tables of the database. Normally, the storage of a single information corresponds to the insertion of one or more rows in one or more tables.

Assuming that we have to insert new data in RATS–DB, we will populate the following fields for each row accessible to all the Users in the following order:

- **1st field**: image name;
- **2nd field**: right ascension (α), read from keyword `RA` of RATS headerfits (see §3.6);
- **3rd field**: declination (δ), read from keyword `DEC` of RATS headerfits (see §3.6);
- **4th field**: date of observation starting (UT), read from keyword `UT` of RATS headerfits (see §3.6);
- **5th field**: hour of observation starting (*hhmmss*), read from keyword `DATE-OBS` of RATS headerfits (see §3.6);
- **6th field**: image type ('object', 'flat', 'bias'), read from keyword `IMATYPE` of RATS headerfits (see §3.6);
- **8th field**: RATS field;
- **9th field**: RATS subfield.

The order of the previous fields is not casual as the image name works as the external key for each row. If this order will be violate, the DBMS will forbid the operation of database population.

The `SQL` –the language `Oracle` is based on– instruction which performs the insertion of a new row in a table is `INSERT` and the syntax will be:

```
INSERT INTO table_name [(fields_list)]
VALUES (values_list)
```

where `table_name` is the name of table the new row will be insert in and for RATS–DB its values can be '*raw*' or '*calibrated*'.
The `fields_list` is the list containing the names of all the fields that a value has to be assigned to, parted from a comma one each other. All the fields that are not included in the list will be assigned the default or Null value. Inserting in the list a field that cannot assume a default or `Null` value will be considered an error by the DBMS. If `fields_list` will be not specified, all the values of each field will be itemize.
The `values_list` is the list containing the values for each field of the table, returned with the same order and number specified in `fields_list` or according to table definition if any list of fields is provided. The possible values could be a proper scalar expression or the keyword `Default` or `Null` if these values are allowed for the fields.

For RATS–DB, the `SQL` instructions that allow the insertion of the previous fields are:

```
INSERT INTO Raw_Image (Name, α, δ, Date, Time, Type, Field, Subfield)
VALUES ('OPD_O_20051028_234517.fits', 21:38:24, +50:08:49, 28102005, 23:45:24,
'O', 1, 7)
```

Another plausible syntax for RATS–DB could be:

```
INSERT INTO table_name [(fields_list)]
SELECT (instruction)
```

where the `SELECT` instruction returns a list of data that could be organized in a new relation. With this syntax, we are allowed to insert in the specified fields of a table data coming from different tables. This is the case of RATS–DB as we will have two different tables: `Raw_Image` containing the pre-processed frames, and `Cal_Image` containing the calibrated frames. Obviously, in order to fulfill the instruction, all data coming from `SELECT` instruction will have to be compatible with all the bonds and domains of each field where data have to be insert in.

7.3.7 RATS–DB User interface

The RATS–DB Query Form interface will consist of *action buttons* which initiate an action when clicked, *query fields* which are used to constrain searches, *additional parameters* which can be added to the query output, and *output controls* which control how query output is formatted and how many data rows are retrieved by a query.

7.3.7.1 Action buttons

Four action buttons, which are displayed at the top and the bottom of the query form page, should be present:

1. **search**: start searching the archive with the constrains specified in the query fields;
2. **reset**: empties the query form;
3. **help**: retrieve an help page on the query form;
4. **home**: go to the Padova Astronomical Observatory Home Page.

7.3.7.2 Query fields

Query fields are used to select entries in the archive that satisfy some User's specified criteria. Within query fields search operands (Table 7.1) can be used wherever a search string is required (that is wherever the User must supply a string in order to constrain searches) to further qualify searches.

Operand	Meaning
`<`	Less than
`>`	Greater than
`<=`	Less than or equal to
`>=`	Greater than or equal to
`!=`	Not equal to
`=`	Equal to
`~`	As = but ignoring case
`==`	Exact match
`*`	$A * B$ will match AB, $A \times B$, $\ldots$ (in strings)
`..`	A range of values
`OR`	Will match any of the specified expressions

Table 7.1: List of operands that can be used wherever a search string is required.

The query page will be divided into two section: "*Target Information*" and "*Observation Parameters*". In the former, there will be the following query fields:

- **Object Name**: the User will enter a string that will be used as a substring to be searched (case insensitively) for in the object name field manually inserted by the Observer at acquisition time. The User will change search behavior by adding one or more of the search operands (Table 7.1).
- **Ra**: right ascension, specified in the following format: `hh:mm:ss` or a range.
- **Dec**: declination, specified in the following format: `dd:pp:ss` or a range.

In the latter, there will be the following query fields:

- **Observer**: the string that you enter will be used for a case insensitive substring search.
- **Observation date**: dates are specified in the format day/month/year, where day will be enter always as a two digits number, month will be entered as a three digits number, year can be entered as a four digits number.

- **Exposure time**: specifying a floating point number will select observations with exactly that duration in seconds.
- **Observation type**: choose among: 'object', 'bias, 'flat fields'.
- **Filter**: the entered string will be used for a case insensitive substring search on the filter automatically inserted by the data capture at acquisition time.
- **Field**: RATS field.
- **Subfield**: RATS subfields.
- **Comments**: the entered string will be used for a case insensitive substring search on this field containing comments inserted by the Observer at acquisition time.

7.3.7.3 Additional (non query-able) parameters

Besides query fields parameters, the following parameters will be selected for inclusion in tabular output and always appear in full screen output.

- **Code**: sequential number automatically assigned to each observation.
- **File**: file name.
- **Exp. Start Time**: exposure start time (UT).
- **Sidereal Time**: sidereal time when exposure started.
- **Airmass**: airmass when exposure started.
- **Telescope**: telescope identification string.
- **Detector Name**: detector identification string.
- **Dimensions**: dimensions of CCD readout area.

7.3.7.4 Output control

If the User will submit a query that returns more than one row of data, output will appear on screen in a tabular form. The User will control which columns are to be displayed in the output by clicking the toggle button placed at the left of the query field in the query form.
For example, the output of a query where the selected fields are *Name*, *RA*, *Dec*, *Date*, *Type* and *Field* will be:

More	Name	RA	Dec	Date	Type	Field
MORE	OPD_B_20051028_223717.fits	22:37:20	+41:56:20	28/10/2005	bias	1
MORE	OPD_F_20051028_224417.fits	22:44:07	+41:56:20	28/10/2005	flat	1
MORE	OPD_O_20051028_234517.fits	21:38:24	+50:08:49	28/10/2005	object	1

Values at the leftmost column ("`More`") in the tabular output are hyperlinks that lead to a full screen display of the parameters stored in the database for the corresponding observation. This columns will always appear regardless of the kind of fields the User will submit in the query. At the end of the query form there will be two additional output controls that can be changed to control the output of a query: full–screen output format can be forced by clicking on the proper toggle button; also the maximum number of rows to return as result of a query can be adjusted.

Part II

Dynamical simulations

Chapter 8

Planets in binaries: transitional members of multiple star systems

PRIOR to the discoveries of the extrasolar planetary systems, theoretical models of star and planet formation were developed but they only explained systems like our own. Recent surveys have shown that over half of star systems contains more than one stellar components. The probability of a star formation without a stellar companion and later becoming a member of a binary via encounters with other stars is very low in most environments (except dense globular clusters).

If a significant fraction of binary star systems spent some time as inclined triple systems, either during their formation process or as the outcome of several close dynamical encounters in a crowded stellar environment, then the number of planets in binaries would be significantly lower than around single stars.

We perform numerical simulations of the dynamical evolution of hierarchical triple star systems with planets hosted around the primary star of the inner binary. Different values of mutual inclination, binary separation and singleton initial semimajor axis are explored in a statistical way. We find that a significant mutual inclination between the singleton and the binary is a key factor for instability of the planetary system. The combination of eccentricity and inclination oscillations of the binary companion induced by the secular perturbations of the singleton and the sequence of close encounters preceding the ejection of one star fully destabilize a planetary system extending beyond 1 AU from the star. The frequency of planets in binaries with low separation may be strongly reduced by the residence of the pair in the past in a temporary inclined hierarchical triple.

My contribution to this study was focused on the development of some accessories modules applied into the main integration algorithm.

8.1 Introduction

Over 65% of the main sequence stars in the solar neighborhood are members of binary or multiple star systems (Duquennoy & Mayor, 1991). As a consequence, answering the question of whether planets can form and resist near one of the stars in a binary has far-reaching implications for the overall frequency of planetary systems. Studies on the long term stability of planets in binaries have shown that a planet cannot be located too far away from the host star or its orbit will be destabilized by the gravitational perturbations of the companion star. Holman & Wiegert (1999) found that the stable/unstable boundary depends on the mass ratio and eccentricity of the binary, but for a wide range of parameters stable orbits may extend well beyond one tenth of the binary semimajor axis. However, in terms of the probability of finding a planet in binary systems the dynamical stability analysis is not exhaustive since it does not take into account the profound influence that stellar dynamic interactions may have had on the early evolution of a planetary system in a binary.

It is generally accepted that the vast majority of stars that will become binaries have already established their binarity by the time that planets begin to form. Observational support for this assumption comes from observations of young binary stars and protostars that have circumstellar and circumbinary disks of the type in which planets are thought to form around single stars.

8.2 Binary stars

It is perhaps because our own solar system has only one stellar component that much focus has been placed on understanding star formation as a process that causes just one star to be formed, models of which produce an unresolved mystery concerning how angular momentum is dissipated from the new star. This problem of angular momentum dissipation is easily mitigated when stars form as multiples: the excess in angular momentum is transferred to orbital motion.

It has been suggested that most binaries originate from the decay of multiple systems (Reipurth, 2000; Larson, 2001; Kroupa, 1995). The wide range of orbital parameters observed among binaries might be a consequence of the chaotic dynamics of the primordial multiple systems. Dynamical interactions among the members of the system cause an exchange of energy and angular momentum often resulting in the ejection of a star from the system. This may occur in the early stages of the system evolution or it may take some time for instability to build up.

The most common configuration among multiple systems is the hierarchical triple, where a singleton orbits around the baricenter of a binary system. A hierarchical triple can become unstable after some time, depending on its initial orbital parameters, leading to the disintegration of the triple (Eggleton & Kiseleva, 1995; Kiseleva et al., 1996). This disintegration occurs via a phase of chaotic evolution whose outcome is the ejection of one of the three stars (typically the least massive body) on an unbound trajectory. The other two stars, members of the original binary, are left in a more tightly bound binary. In Marzari & Barbieri (2007) it is showed that the orbital changes of the binary and the strong gravitational perturbations during the chaotic phase, occurred prior to the singleton ejection, can influence the final configuration of a planetary system hosted by the primary star of the pair. However, in the context of near–coplanarity between the binary and the singleton, planets can survive the triple decay in most cases and adapt to the new orbital parameters of the binary. The major effect would be a significant change in the orbital configuration of the system after the triple instability with respect to the original configuration, as an outcome of the planet formation process.

8.3 Planets in binaries

Current theory is that planets form in and from material of dusty disks observed around young stars. Most scientists think that planet formation is difficult or inhibited in binary or multiple stars because these disks might be more short–lived. However, more than twenty of the current sample of over two hundred extrasolar planets are in binary or multiple systems. This means that the entire issue of planets in binary and multiple stars cannot be ignored.

Numerical simulations of the collapse of molecular cloud cores to form binary stars suggest that disks form within binary star systems (Bodenheimer, Hubickyj & Lissauer, 2000). The presence of disk material has been indirectly observed around one or both components of some young binary star systems (Mathieu et al., 2000). Terrestrial planets and the cores of giant planets are thought to form by an accretion process within a disk of dust and gas (Safronov, 1969; Lissauer, 1993), and therefore may be common in binary star systems. A lower limit of 30 M_J extrasolar planets have been detected in so–called *S–type* orbits, which encircle one member of a binary star system. Most of these extrasolar planets orbit stars whose stellar companion is quite far away, but three (γ Cep, GL 86A and HD 41004B) are in systems with stellar semimajor axes of only 20 AU. The effect of the stellar companion on the formation of these planets remains uncertain. Extrasolar planets have yet to be detected in *P–type* orbits (which encircle both components) of a main-sequence binary star system, but close binaries are not included in precise Doppler radial velocity search programs because of their complex and varying spectra. The radial velocity detections of planets in binary systems are quite surprising results since binary stars are often avoided by these surveys . Since, despite this bias, planets are detected in stellar binaries, there is a well justified and important question of the occurrence and properties of planets in such systems. It has been recognized by Zucher & Mazeh (2002) who has noted that there may be a deficiency of high mass planetary companions with short period orbits around single stars whereas the opposite may be true for planets in binary systems. Indeed, the recent discoveries mentioned above of γ Cep, GL 86A and HD 41004B lend credence to this idea.

In this chapter we consider the dynamic effects of the decay of *i*nclined hierarchical triples on planetary systems. In particular, we will focus on planet survival during the unstable triple configuration. At present, determinations of the mutual inclinations of the two orbits in hierarchical triple stellar systems are available only for a very limited number of cases and are often ambiguous. Fekel (1981) determined that at least 1/3 of a sample of 20 triple star systems have an inclination exceeding 15° and are not co-planar. Sterzik & Tokovinin (2002) analyzed a different set of 22 visual triples finding an average mutual inclination of 79°. However, in both the studies the mutual inclination was derived from incomplete observational data. To compute unambiguous mutual inclinations for triples, both radial velocities and visual orbits are required for the inner and outer system. So far, only six nearby systems have been observed with both methods and have direct and precise measured orbits (Muterspaugh et al., 2006). The values of mutual inclination for these systems range from 24° to 132° but the sample is too small to give hints on the real distribution of inclinations among triples. The mutual inclination of triples may either be primordial and related to the formation process of the triple by fragmentation of a molecular cloud or it may form at later times because of dynamical interactions, like encounters, between single stars and binaries in a dense cluster–like environment. In the latter case, the inclination is due to the encounter geometry between the binary and the single star and should be randomly distributed. Any deviation from randomly oriented orbits may be an important indication of the relative importance of the two formation mechanisms. Assuming that planets can form in the binary before the bound hierarchical triple becomes unstable, the dynamical interactions between the stars during the chaotic phase can strongly affect the stability of the planetary system.

8.3.1 Circumstellar and circumbinary disks

The first examples of the circumstellar disks in a binary system is the case of L1551-IRS-5. Rodriguez et al (1998) have shown that it is a binary pre-main sequence star (hereafter, PMS) with separation of 45 AU in which each component is surrounded by a disk. The radii of the disks are 10 AU and the estimated masses are 0.06 and $0.03 M_{\odot}$, enough to produce planets. Recently, McCabe, Duchene & Ghez (2003) have spatially resolved mid-infrared scattered light from the protoplanetary disk around the secondary of the PMS binary HK Tau AB. The inferred sizes of the dust grains are in the range $1.5 - 3\mu m$ which suggests that the first step in the planet formation, the dust grain growth, has occurred in this disk.

Altogether, there is ample evidence for the presence of disks in binary systems. Observational indicators such as excess emission at near-infrared to millimeter wavelengths, spectral veiling, Balmer and forbidden emission lines and polarization suggest that disks can be found around each of the components (circumprimary and circumsecondary disks) as well as around the entire systems (circumbinary disks, for a review see Mathieu et al., 2000). Specifically, millimeter and submillimeter measurements of dust continuum emission enable measurement of the total disk mass. These observations show that circumbinary disks may be reduced in size and mass but still are present even in close systems. The presence of circumbinary disks is observed at millimeter wavelengths around many PMS spectroscopic binaries. Such massive disks are however rare around wide binaries with separations $1 - 100$ AU. This is reflected in theoretical calculations that predict circumstellar and circumbinary disks truncated by the companions (Lubow & Artymowicz, 2000). The circumstellar disks have outer radii $0.2 - 0.5$ times the binary separation while the circumbinary disks have the inner radii two or three times the semi-major axis of the binary. Finally, the measurements of the infrared excess emission show no difference in frequency of the excess among binaries and single stars. It indicates that the circumstellar material in binary systems may be similar in temperature and surface density to that in disks surrounding single stars (Mathieu et al., 2000). Hence it seems that, with the current data available, planet formation in close binary systems is possible.

8.3.2 Planet formation in binaries

We can envision two different scenarios for planet formation and subsequent destabilization within an inclined hierarchical triple:

1. a primordial binary star system forms in a star cluster and planets accumulate from a circumstellar disk around the main star either by core–accretion (Pollack et al, 1996) or by disk instability (Boss, 1997). The existence of a few gas giant planets in binary systems with separation of a few tens of AU (γ Cephei and GL 86) suggests that the perturbations of the companion star are not strong enough to prevent the formation of planets in binaries (Thébault et al., 2006; Boss, 2006). Successively, a temporary hierarchical triple builds up because of dynamical interactions between the primordial binary, with planets, and a passing by singleton or binary (Ford et al., 2000). In a dense stellar environment with a large abundance of binaries this is a frequent event (McMillan et al., 1991). In the presence of a significant inclination between the singleton and the binary orbit, the planetary system

in the binary is strongly destabilized during the transitional triple state by both the secular perturbations of the singleton and the frequent stellar encounters during the chaotic phase preceding the break up of the triple into a binary and singleton. The destruction of the triple may occur either because it is unstable and after a short timescale the singleton escapes or because of an encounter with other objects, single stars or binaries. After the ejection of the singleton in a hyperbolic orbit, the primordial binary has different orbital parameters but it is also depleted, in most cases, of its original planetary system;

2. a primordial inclined hierarchical triple forms by fragmentation of a single, rotating, dense molecular cloud (Boss, 1988). Planets can grow on S–type orbits around the primary star of the binary, possibly by disk instability (Boss, 1997). Self-gravitating density clumps can contract into planets in only a few hundred years. It is unrealistic to expect that planets can form by core–accretion in this scenario because of the strong secular perturbations that the singleton would apply on a long timescale on the secondary star and then, indirectly, to a putative planetesimal disk around the binary (assuming that planetesimals could form in such a highly perturbed circumstellar disk). Even in this case, the combined destabilizing effects of secular perturbations and stellar encounters in the chaotic phase preceding the ejection of the singleton in a hyperbolic orbit destabilize the planetary system around the primary.

The theories of planet formation in binary stellar systems are still at early stages. The two mechanisms proposed here above for giant planet formation in circumstellar disks –core accretion and fragmentation via gravitational instabilities– make conflicting predictions about the formation rate of planets in binaries. This is primarily due to the differences in formation timescales: core-accretion requires $1 - 10$ million years as compared to thousand year timescales for gravitational collapse. Mayer et al. (2004) indicate that gravitational fragmentation models of planet formation predict different efficiencies for giant planet formation in binaries than in single stars, whereas core-accretion models do not. It is argued that a stellar companion will disrupt protoplanetary disks on timescales shorter than required for core-accretion. Whitmire et al. (1998) studied planet growth in the circumprimary habitable zones in binary systems. They considered a 4-body system of 2 stars and 2 planetesimals for which, by varying binary semi-major axis, eccentricity, and mass ratio, they were able to determine a critical semi-major axis of the binary below which the secondary does not allow a growth of planetesimals (planetesimals are accelerated by the secondary, the relative velocity of planetesimals is larger than critical and their collisions become destructive). Based on this criterion, they concluded that about 60% of nearby solar-type binaries cannot be excluded from having a habitable planet.

Marzari & Scholl (2000) analyzed α Cen (semi-major axis of 23 AU, eccentricity of 0.52, mass ratio of 1.1/0.92), a prototype close binary system, and demonstrated that planetesimals can accrete into planetary embryos. Barbieri et al. (2002) continued the study and showed that planetary embryos can grow into terrestrial planets in about 50 Myr.

Fragmentation models by Boss (1998) claimed that giant planet formation is enhanced by the presence of stellar companions: when no binary is present, the disk is more stable and less likely to fragment into planets. However, Nelson (2000) argued that gas heating causes both mechanisms to fail to produce planets in binaries of moderate separation (50 AU).

Clearly, there is a lack of consensus and the planet formation theories would certainly benefit from observational constraints.

8.3.3 Binary planet stability

Theoretical work of planet formation in close binary systems is at a rudimentary stage. Yet, as demonstrated by numerical studies (Holman & Wiegert, 1999), planets (if formed) in binary systems can enjoy a wide range of stable orbits. There is a clear need to supply observational constraints on the occurrence and orbital properties of extrasolar planets in binary systems to provide the key information for the theories of their formation. Unfortunately, it is well known that current RV surveys are biased against binary stars (*e.g.*, see Patience et al., 2002). The radial velocity surveys exclude binaries with separations of less than 2 arcsecond to avoid the problem posed by the contamination caused by the second star (Vogt et al., 2000). Imaging and in particular coronographic surveys are similarly biased (mainly because current coronographs can suppress light from only one object in the field).

The problem of stability of the planetary orbits in binaries has been recognized for a long time. Most often, it was approached with the aid of numerical studies of the elliptic restricted three-body problem. The orbital configurations considered include the so–called *P–type* (Planet–type, circumbinary orbits), *S–type* (Satellite–type, circumprimary or circumsecondary orbits) and *L–type* orbits (Librator–type, orbits around stable Lagrangian points L4 or L5 for the mass ratio $\mu < 0 : 04$). There are many papers concerning the stability of S–type motions (Benest, 1988, 1989, 1993, 1996, 2003; Pilat-Lohinger & Dvorak, 2002; Rabl & Dvorak, 1988). These studies concentrated on developing empirical stability criteria in the framework of the circular three body problem (see *e.g.* Graziani & Black, 1981). The P–type motions have also been investigated (Holman & Wiegert, 1999; Pilat-Lohinger et al., 2003). Until now however, there is no observational evidence that they exist. The curious L-type orbits have also attracted the interest of researchers (see e.g. Laughlin & Chambers, 2002).

Most of these studies have been performed by means of direct numerical integrations, but they have many limitations: most of the analytical works are done for circular binaries, numerical studies have been restricted to special mass ratios and the integration have been limited to fairly short times. Also, they are almost exclusively restricted to the framework of the three body problem. These drawbacks have been addressed in the recent, remarkable work by Holman & Wiegert (1999) who studied a full range of mass ratios, eccentricities and long integration times (at least 10^4 periods of the binary). They demonstrated that planets in binaries can enjoy a wide range of stable orbits. The stability criteria are most sensitive to the ratio of planet-binary semimajor axis; one can derive the "observers' rules of thumb" from the collected theoretical work that P-type planets are stable if they have semimajor axis 3 times larger than that of the binary, and S–types are stable if they are in orbits closer than 1/7 the binary separation.

8.4 The "jumping stars model": the co-planar case

We have considered a scenario in which a triple star system is stable long enough to allow planet formation around the primary star of the binary pair. The subsequent destabilization of the triple, because of the onset of chaotic behavior, will end with the ejection of one star. The binary couple will have final orbital parameters that are different from those of the primordial binary in which planetary formation occurred. In some cases, during the stellar encounters, an exchange can also occur between the original companion star and the outer one leading to a new mass ratio of the binary system.

8.4.1 The numerical algorithm for the co-planar case

To analyse the dynamical evolution both of triple star systems and of planetary orbits around the primary star we have assembled a numerical model of the hierarchical three–body system. We have defined two initial osculating Keplerian orbits for the triple, an inner one for the binary pair m_1 and m_2 and an outer one, defined in the center of mass of the pair, for the single star m_3. Ten additional circular orbits for massless bodies starting at 1 AU from the primary star and extending by equal steps up to 10 AU are also computed. Their evolution allows us to evaluate to what extent the chaotic phase of stellar encounters affects a putative planetary system around the primary star. The evolution of the system is calculated with the numerical integrator `RADAU` (Everhart, 1985) which properly handles close encounters between massive bodies.

In our work we restricted ourself to a limited number of significant test cases showing how a detached binary system has its orbital elements changed when the triple is disintegrated and the single star escapes to infinity. A similar behavior occurs also in non–coplanar systems when the dynamics becomes chaotic, however we will perform a full exploration of the inclined case in the following chapter.

We started with the stars in a prograde and co-planar orbits with the semimajor axis of the binary a_b fixed to 35 AU. The semimajor axis of the single star a_s is instead regularly sampled starting within the empirical stability limit derived by Eggleton & Kiseleva (1995). We have considered different values both for the eccentricity of the binary e_b, and for e_s, the eccentricity of the singleton. Because of the chaotic dynamics, for each set of (a_b, a_s, e_b, e_s) we have performed 30 different simulations with random choices of the orbital angles. In this demonstrative set of simulations, the masses of the stars are 1, 0.4 and 0.4 $M_\odot$, respectively.

8.4.2 The onset of instability in the co-planar case

In Figure8.1 we plot the timescale t_{in} required for the onset of instability, and then close encounters between the single star and the binary, as a function of the semimajor axis of the singleton.

In the first case (red triangles) the initial orbital eccentricities e_b and e_s are both set to 0.2. There is a trend towards higher values of t_{in} for larger values of a_s that can be roughly described by an exponential law. Since we stop the simulations after 50 Myr because of too long integration times, the curve is biased at the end of the fit by vales that are all equal to 50 Myr. Despite this limitation of the fit, at a first sight the analytical dynamical stability threshold (Eggleton & Kiseleva, 1995; Kiseleva et al., 1996), located at about $a_s = 150AU$ for the singleton, appears to be in good agreement with our numerical results if one looks at the fast growing trend of the instability time when a_s is larger than 150 AU.

In the second case shown in Figure8.1 (blue triangles) we have increased both the initial eccentricities e_b and e_s to 0.4. The instability onset occurs, as expected, faster than the previous case and larger values of a_s are required to have long surviving systems. To find systems whose t_{in} is longer than 50 Myr we had to go beyond $a_s \sim 250$ AU. The stability limit set by the formula of (Eggleton & Kiseleva, 1995; Kiseleva et al., 1996) is at about 235 AU and it seems to be slightly less accurate at high eccentricities of the stars.

According to Boss (2006), a disk instability can form gas giant planets in a few hundred years. In this scenario, the time required by the gravitational perturbations among the stars to build up dynamical instability is not a crucial parameter. When a_s is beyond 70 AU, the

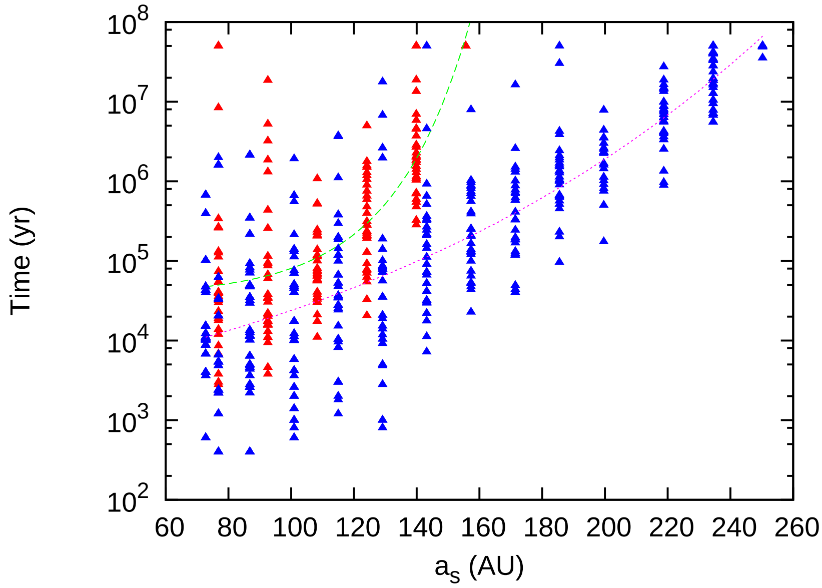

Figure 8.1: Time of the first close encounter between the binary and the singleton *vs.* a_s, the initial semimajor axis of the singleton. The red triangles mark the cases with binary eccentricity $e_b = 0.2$ and singleton eccentricity $e_s = 0.2$; the blue triangles are those with $e_b = 0.4$ and $e_s = 0.4$. The continuous lines are (green and magenta, respectively) least squares exponential fits to the data.

chaotic behavior onset occurs after a few thousand years giving enough time for planets to form. Eventually, if the planetary system is chaotic after its formation (Weidenschilling & Marzari, 1996; Marzari & Weidenschilling, 2002; Marzari et al., 2005; Rasio & Ford, 1996), it might have enough time to evolve into a stable state before the star system becomes in turn chaotic.

Instead, in the core accretion theory (Pollack et al, 1996), the formation of gas giant planets requires a few million years. By inspecting Figure8.1 we expect that only systems in the upper part of the plot are dynamically stable long enough to grant a quiet environment for planets to grow around the primary star. However, even in some cases where the singleton is close to the binary, the dynamics turns chaotic only after some million years.

In Figure8.2 we show the final orbital distribution in the (a_b, e_b) plane of the left–over binaries. While the initial values of e_b and e_s have a strong influence on the instability time t_{in}, they appear non influential for the final orbital distribution of the binaries. The two different distributions shown in Figure8.2 correspond to $e_b = 0.2$ and $e_s = 0.2$ (red dots) and to $e_b = e_s = 0.0$ (green dots). As we can see, there is no significant difference between the two distributions that overlap in the (a_b, e_b) plane. The final semimajor axis a_b is substantially smaller than the initial value ($a_{b0} = 35$ AU) as expected by orbital energy conservation since one of the stars escapes on a positive energy hyperbolic orbit. The spreading of a_b depends both on the different initial values of a_s and on the amount of energy taken away by the singleton. The final values of e_b are randomly distributed and are concentrated at high eccentricities, in most cases larger than 0.4.

In Figure8.3 we map the values of the semimajor axis a_p of the outer planetary orbit that remains stable after the chaotic phase *vs.* the final value of a_b in the case with $e_b = 0.2$ and

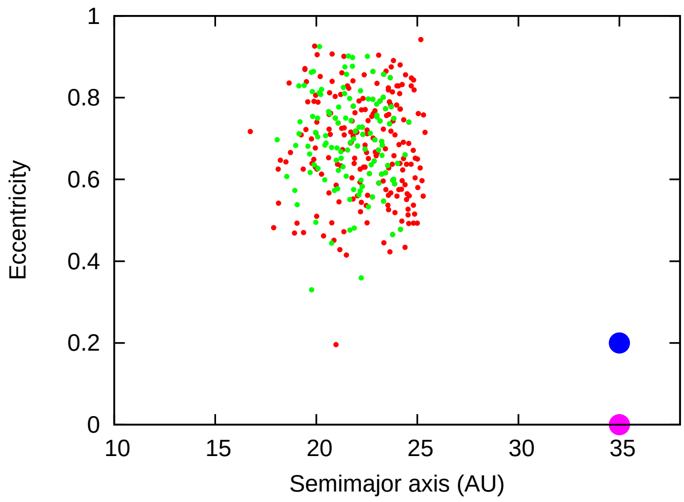

Figure 8.2: Distribution of the binary orbital elements after the third star of the system has escaped on a hyperbolic orbit. The red dots label binaries originated from triples with $e_b = 0.2$ and $e_s = 0.2$, the green dots those from triples with $e_b = e_s = 0$. The large dots in the plot represent the initial binary system, respectively.

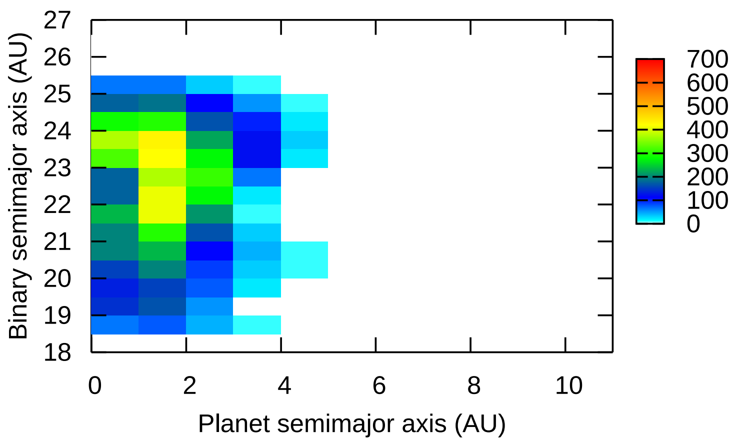

Figure 8.3: Histogram illustrating the number of systems in our simulations that, at the end of the chaotic phase, fall into bins in a_b, the binary separation, and a_p, the semimajor axis of the outer planetary orbit that survives the stellar chaotic phase.

$e_s = 0.2$. The color codes are linked to the number of cases that fall in each bin in a_p (x–axis) and a_b (y–axis). The repeated encounters between the stars set a limit of about $a_p = 4$ AU from the primary star within which planetary orbits can survive. Beyond that value of a_p, the gravitational disturbances produced during the chaotic evolution of the two outer stars destabilize any planetary body. It is remarkable that a significant number of binary systems with final values of a_b around 19 AU and high eccentricity, preserve the planetary system, or part of it, that formed when the binary was part of a triple system with $a_{b0} = 35$ AU. In 1% of our simulations, even the innermost planetary orbit we considered ($a_p = 1$ AU) is perturbed during the stellar chaotic phase and the planet is eventually ejected from the system. This implies that a fraction of planetary systems forming around binaries –part of a triple in the early stages of their evolution– may be totally destabilized during the stellar encounters. γ Cephei, Gl 86 and HD 41004A might well belong to this class of systems.

Even if our study is not exhaustive in terms of exploration of the parameter space, however it gives a clear idea of the dynamical evolution of the system. It also suggests caution when modelling planetary formation in an observed binary system by simply adopting its present orbital configuration. That configuration might indeed be the outcome of a complex and unpredictable chaotic evolution.

8.4.3 Statistical outcome for the co-planar case

Within stellar clusters, close stellar encounters may disrupt binaries or, more frequently, abruptly change their orbital elements (Kroupa, 1995). This mechanism is suspected to be one of the possible causes of the low frequency of binaries among low–mass field stars compared to that of young low–mass stars in star–forming associations (Duchene, 1999). In a scenario where a planet (or a full planetary system) has been formed around one of the stars of a binary, if a stellar encounter occurs, the dynamical configuration of the system may be significantly changed (Dalla Stella, 2005). We can see either of the following events:

- the binary system is destroyed and the surviving planets orbit a single star. In this case, the present dynamical configuration is not indicative of the formation process because of the large changes caused by the stellar encounter;

- the binary system survives the encounter but its orbital parameters and those of the planets are strongly altered.

In both cases, any attempt to model the formation of an observed planetary system would face the problem of discriminating which dynamical or physical features of the system are due to the formation process and which are related to the stellar encounter. In particular, we have investigated how the dynamical environment of a planet orbiting a star in a binary system is affected by a stellar encounter that does not disrupt the binary. We have adopted the same numerical model described in the previous section, but the singleton is now set on a hyperbolic orbit approaching the binary on a plane tilted by 45° with respect to the binary orbital plane. We have randomly sampled the impact parameter and eccentricity of the hyperbolic trajectory and we looked at the orbital configuration of the final system star–planet–star when the encounter is over.

In Figure8.4 we show the orbital distribution in the (a, e) and (a, i) planes of the binary systems after the stellar encounter. A significant number of systems has a post–encounter semimajor axis significantly smaller than the initial one ($a_{b0} = 35AU$) while during the decay of a triple system the final a_b cannot be lower than a value fixed by the conservation of the gravitational energy of the initially bounded system.

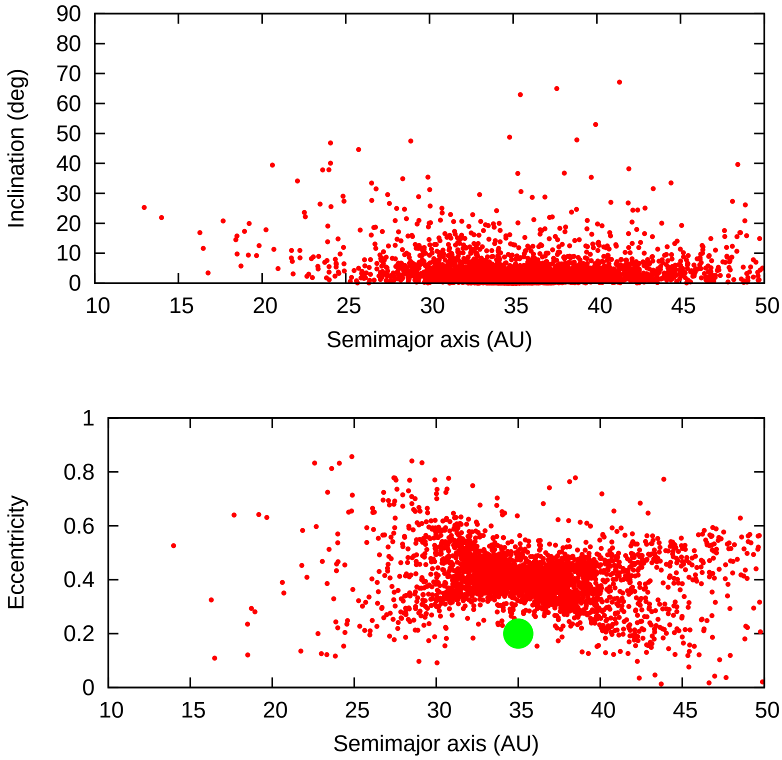

Figure 8.4: Distribution of the eccentricity and inclination of the binary system after the hyperbolic stellar encounter. All the systems shown in the plot allowed the survival of at least one planet around the primary star of the system. The large green dot represents the initial binary configuration.

The impact of a stellar encounter on planetary formation models is important: the planet(s) may have formed when the companion star was farther away and then less effective in perturbing the protoplanetary disk. For the core–accretion model (Pollack et al, 1996), this may be a crucial condition to allow planetesimal accumulation before the onset of strong binary perturbations when the companion stars is injected on a closer orbit (Thébault et al., 2004, 2006).

By inspecting the planetary orbits that are still bound to the primary star after the encounter shown in Figure8.5, we have observed a distribution very different from that of Figure8.3. We still have cases where planetary orbits up to 3 AU survive the encounter leaving the planets around a closer binary system than the initial one. When we look at γ Cephei, Gl 86 and HD 41004A we may be observing a system that survived a close stellar encounter. However, it appears that the single encounter with a star on a hyperbolic orbit has less dramatic consequences on the stability of a circum–primary planetary system than the frequent close encounters between bounded stars that lead to the decay of a triple. Most of the planetary systems show orbits that are still stable up to 10 AU when the stellar encounter is over. Of course, outer orbits far from the primary may become unstable because of the long term perturbations of the companion star (Holman & Wiegert, 1999).

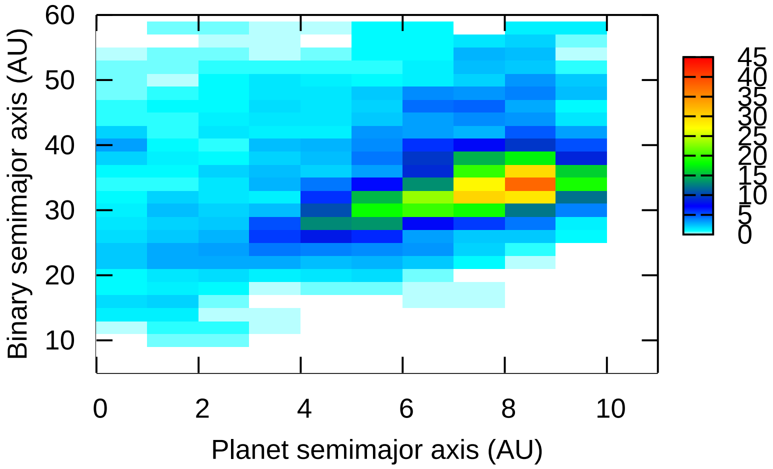

Figure 8.5: Plot showing the semimajor axis a_p of the outer planetary orbit that survives the stellar encounter *vs.* the post–encounter semimajor axis of the companion star a_b. To be compared with Fig.8.3.

While the onset of instability in a triple system always leads to tighter and more eccentric binary systems, by inspecting Figure8.4 we see systems where the orbit of the binary couple is broadened and, in a few cases, even circularized by the stellar encounter. In these cases we know that planetary formation was perturbed by the companion star in the initial stages, but the dynamical environment of the planetary system became significantly quieter after the stellar encounter. There are systems where the binary companion is moved beyond some hundreds of AU from the main star. If the stellar encounter occurred after the planets formed, we might observe a broad binary system with a small planetary system around the main star.

8.5 The "jumping stars model": the inclined case

There are two mechanisms that, acting in synergy, destabilize planets around the primary star:

I. a large initial mutual inclination between the outer stars excites consistent eccentricity–inclination oscillations of the binary companion with periods of the order of some thousand years and more. These oscillations, well described by a quadrupole–level secular theory (Mazeh & Shahan, 1979; Ford et al., 2000), strongly affect the orbits of the planets around the primary, forcing most of them to leave the system on hyperbolic orbits. In the phase of high eccentricity, the companion moves closer to the planetary system, reducing the region of stability (Holman & Wiegert, 1999) and perturbing the planetary orbits. After a few Kozai–cycles a large fraction of the planetary system is destroyed. For retrograde orbits the dynamics is more complex but the evolution is still characterized by wide oscillations of both eccentricity and inclination. This kind of Kozai mechanism in stellar triples is different to that described by Malmberg et al. (2007) where the secular interactions involved only the companion star of an isolated binary and the planets;

II. the second mechanism is the sequence of close encounters between the singleton and the companion star of the binary occurring during the chaotic phase preceding the disgregation of the triple. Close encounters between stars on mutually inclined orbits are much more effective in destabilizing the planets than in the low inclination case.

Both the eccentricity oscillations of the secondary star and the close encounters conspire against the survival of a planetary system around the main star of the binary. If indeed binary stars are born as triple or higher multiplicity stellar systems or they are temporarily involved in unstable triples, their planetary systems would be fully destabilized in most of the inclined cases. The fraction of planets in binaries observed at present would than be lower than that around single stars. The number of binaries depleted of planets would depend on the distribution of mutual inclination in the primordial triples. If co-planarity dominates, as might be the case if the majority of temporary triples originated directly from the fragmentation of an interstellar cloud (Boss, 1988), then the binaries stripped of their planets would be a minority. On the other hand, if most of the triples formed by gravitational interactions in a dense stellar environment, the large mutual inclinations would lead to a strong planet depletion among the surviving binaries. In this scenario, it is an important observational challenge to increase the statistics of known triple systems with unambiguous determination of the mutual inclination.

At present only about 15% of planets have been found in multiple stellar systems. This is probably an observational selection effect in favor of single target stars but it might also be a first indication that binary systems are depleted of planets by the past violent dynamical evolution of the stars.

We will not have explored in this work the full complexity of the hierarchical triple dynamics as performed in Ford et al. (2000). We were interested on the consequences of the large variations of the stellar orbital elements on the planets and for this reason we have performed statistical numerical simulations giving the fraction of planets surviving the chaotic phase of unstable triples. We also do not have investigated the planetary formation process in detail, but we have assumed that planets can form by either of the two mechanisms, core–accretion or gravitational instability.

8.5.1 The numerical algorithm for the inclined case

We have numerically modelled the orbital evolution of planets in S–type orbits in a binary member of an inclined unstable hierarchical triple. We consider different mutual inclinations between the binary and the singleton, while Marzari & Barbieri (2007) simulated only the planar case. We find that, contrary to the low inclined scenarios, only in a limited number of cases planetary systems extending beyond 1 AU survive after the chaotic phase of stellar encounters when the mutual inclination between singleton and companion is larger than $\sim 40^\circ$.

Our numerical model consists of 3 stars, two locked in a binary system and the third orbiting the baricenter of the pair. A set of 10 massless bodies started on circular orbits around the primary star simulate a planetary system that formed in the early phases of evolution of the binary. The semimajor axes of the test bodies are regularly spaced from 1 to 10 AU and the initial inclinations are all set to 0° with respect to the binary orbital plane. The trajectories of the stars and of the 'planets' are computed with the numerical integrator `RADAU` (Everhart, 1985). It handles in a very precise manner close encounters between massive bodies and it does not require a fixed hierarchical structure as other integrator such as `HJS` (Beust, 2003) or `SYMBA5`

(Duncan et al., 1998).

To model the outcome of the triple instability in all possible configurations is a difficult task since the parameter space to explore is wide. For this reason we have selected a limited number of parameters to be sampled while the others are left unchanged. To better compare our results with those presented in Marzari & Barbieri (2007), we adopt the same masses for the stars *i.e.* 1 and 0.4 solar masses for the binary, 0.4 solar mass for the singleton. An eccentricity of 0.2 is adopted for both the binary and the singleton, taking into account that the orbit of the singleton is defined with respect to the barycenter of the binary. The mutual inclination is sampled between 0° and 180° including in this way retrograde orbits of the singleton. For any value of the semimajor axis of the binary a_b, we have sampled different values of the semimajor axis of the singleton a_s and of the orbital angles other than those giving the mutual inclination. For any set of (a_b, a_s, i_m) we have performed 20 simulations with random initial orbital angles to increase the statistics on the star and planet dynamical behavior.

8.5.2 The onset of instability in the inclined case

In this section we discuss in detail the two mechanisms leading to destabilization of a putative planetary system extending beyond 1 AU around the primary star of a binary in an inclined temporary triple. In Figure 8.6 we show the evolution of a model with $a_b = 70$ AU, $a_s = 212$ AU and initial mutual inclination $i_m = 90°$. In this configuration, the critical semimajor axis for long–term stability of planetary orbits around the primary according to Holman & Wiegert (1999), is around 21 AU. Our initial planetary system, extending out to 10 AU, is well within the stability region. The perturbation of the singleton induces Kozai cycles on the binary companion that achieves an eccentricity of almost one over a timescale of 2.5×10^4 yrs. This behavior is well described by quadrupole and octupole–level secular equations described in Mazeh & Shahan (1979); Ford et al. (2000). All the planets beyond 2 AU are ejected from the system after the first cycle, while those orbiting at 2 AU are destabilized after the second cycle. Starting from 1×10^5 yrs the singleton and the companion star have mutual close encounters that quickly lead to the ejection of the last inner planet, that lived through the Kozai cycles of the companion. Finally, after about 5×10^5 yrs, the outer star is ejected on a hyperbolic orbit and the the binary system is left with a smaller separation and without planets.

This kind of behavior, typical of systems with high mutual inclination i_m, places in jeopardy not only the stability of planets around the primary but also the possibility that they can form. According to Boss (1997), several gaseous protoplanets can rapidly form by disk instability in a marginally gravitationally unstable protoplanetary disk. Within this scenario in a few hundreds years we might witness the formation of the unstable triple and of a planetary system made of gas giant planets around the primary before the Kozai cycle increases the eccentricity for the companion star.

On the other hand, core–accretion would not have enough time to accumulate a core by planetesimal accretion, and even planetesimals may have failed to form on such a short timescale. A protoplanetary disk around the primary star would be strongly perturbed and almost fully destroyed during the first Kozai cycle in eccentricity and inclination of the companion star. However, if the binary system was isolated during its formation and it became part of an unstable triple later on because of repeated stellar encounters in a dense star–forming region, then planets might have the time to grow even by core–accretion, before the onset of the strong perturbations

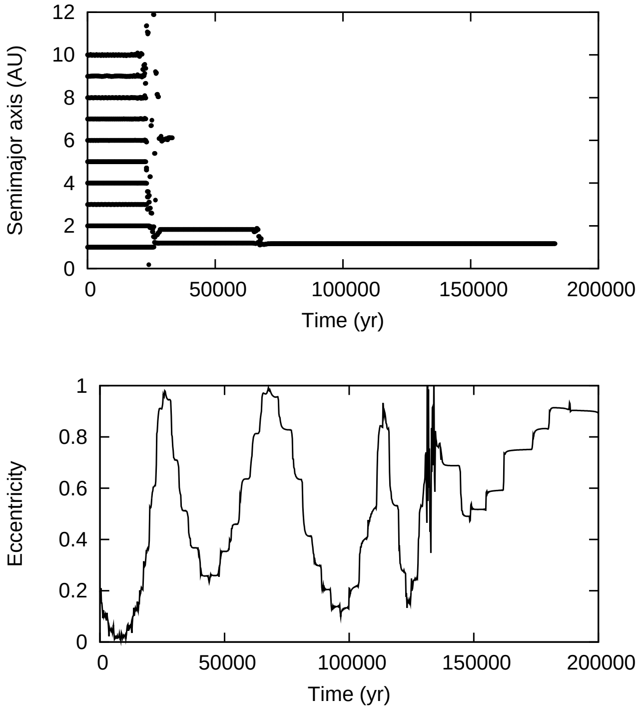

Figure 8.6: Semimajor axis evolution of the planets around the primary star of the binary under the perturbations of the companion star (*above*), in turn affected by the gravitational pull of the outer singleton star. Eccentricity oscillation of the secondary (*below*). The initial semimajor axis of the binary is 70 AU, the eccentricity is 0.2 both for the binary and the singleton, and the mutual inclination i_m is set to 90°.

related to the stellar interactions in the triple phase.

Only systems with large values of i_m are fully destabilized by the stellar perturbations of the triple. When the mutual inclination is lower than $\sim 40°$, close encounters between the stars, and the consequent impulsive changes of the orbital elements, are a source of instability for the planets but often not strong enough to destabilize the full planetary system.

In Figure 8.7 we illustrate the evolution of a model with $a_b = 70$ AU, $a_s = 212$ AU, as in the previous case, but with a lower initial mutual inclination $i_m = 30°$. The triple system quickly becomes unstable and the singleton has frequent close approaches with the binary companion marked by sudden steps in eccentricity and semimajor axis. The changes in the orbital elements of the companion leads to unstable planetary orbits as shown in Figure 8.7. However, contrary to the case shown in Figure 8.6, the planetary system is not fully destroyed and planets within 5 AU of the star survive the chaotic phase. Further perturbations by the binary companion after the triple disruption do not destabilize the planetary survivors since they are well within the critical semimajor axis for stable orbits (Holman & Wiegert, 1999).

If the companion and the singleton are on retrograde orbits, instability builds up in a similar way. For mutual inclinations lower than $\sim 140°$, large amplitude oscillations of the eccentricity begin to destabilize the planetary system which is finally destroyed by the stellar encounters in the chaotic phase. Contrary to the prograde case, the oscillations of eccentricity and inclination

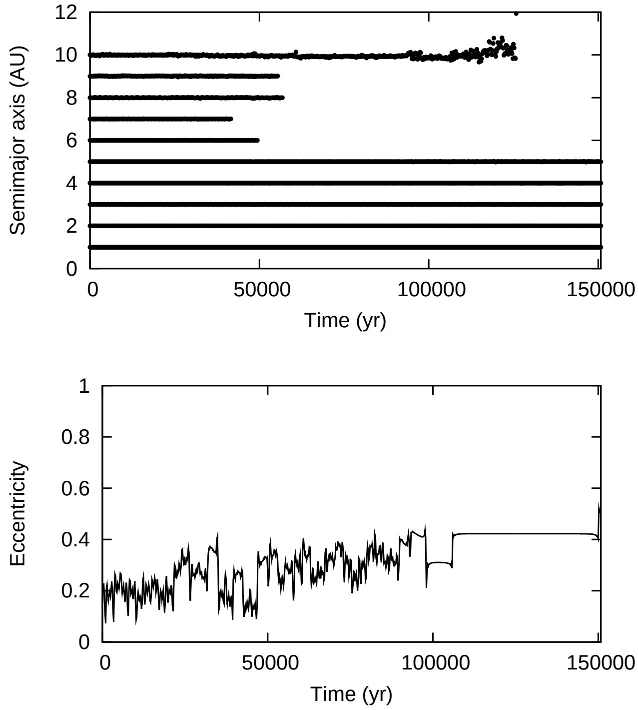

Figure 8.7: Same as in Fig.8.6 but for $i_m = 30°$.

are not in phase, as predicted by the quadrupole theory. Apparently, the two orbital parameters are no longer bound each other and they evolve with independent frequencies. For inclinations between $\sim 140°$ and $\sim 180°$, the oscillations in eccentricity are moderately low but some instability of planetary orbits is driven by the large inclination oscillations of the companion. In Figure 8.8 we show the evolution of the inclinations of the singleton and companion star when the mutual initial inclination is $\sim 150°$. The inclination of the companion becomes very high and becomes retrograde for a short while. The behavior is characterized also by the libration of the angle $\Delta\Omega_2 - \Delta\Omega_1$ (see Fig. 8.8, lower panel) with the same frequency as the inclination oscillations. Most of the planetary orbits are destabilized during these large inclination excursions of the stellar companion and after 1 Myr only the two inner planets survive. The onset of the chaotic phase of the stars ejects finally also these two survivors.

8.5.3 Statistical outcome for the inclined case

To test the chances of a planetary system in a binary to survive a period of stellar interactions typical of an unstable triple, we have run several models with the binary semimajor axis fixed to $a_b = 70$ AU. The initial orbital eccentricities of the stars are both set to 0.2. In Figure 8.9 we plot the percentage P_s of dynamical systems that, at the end of the period as a hierarchical triple, retain at least one of the initial 10 planets depending on i_m, the initial mutual inclination between the two outer stars. This percentage is very high for low inclinations, confirming the results presented in Marzari & Barbieri (2007) for low–inclination systems, while it declines very quickly when the inclination approaches 90°. This is a consequence of both the Kozai cycle that

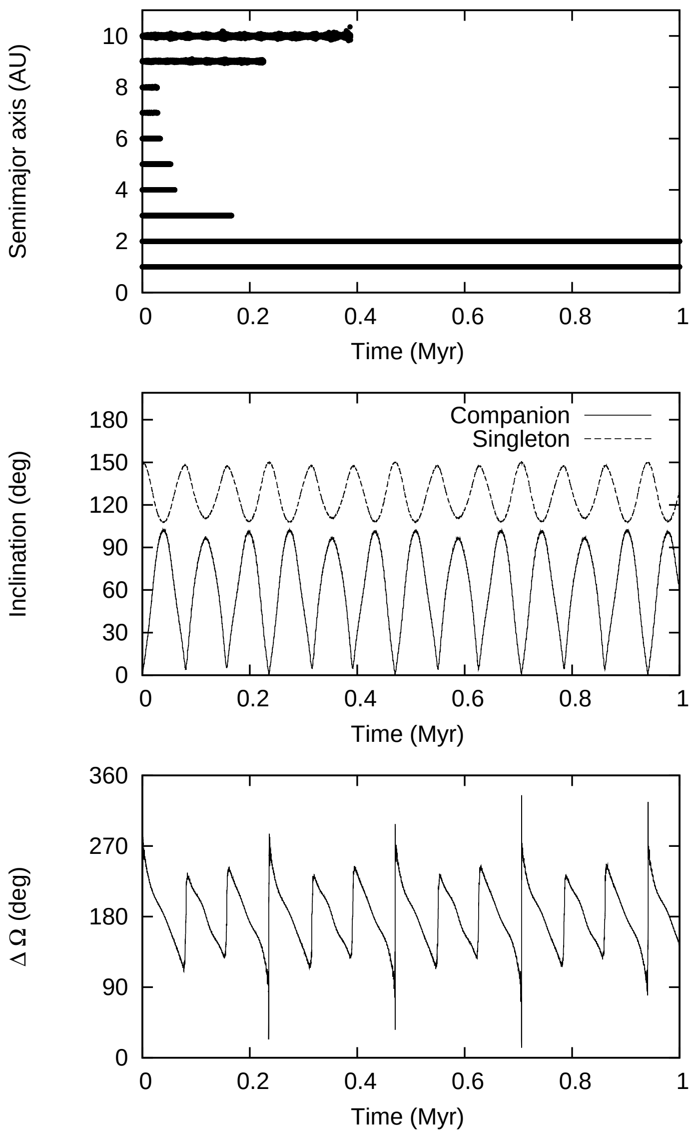

Figure 8.8: *Above*: Destabilization of planets around the primary when the singleton is on a retrograde orbit relative to the companion. *Middle*: The initial mutual inclination between the two outer stars is 150°. *Bottom*: The $\Delta\Omega$ angle librates around 180° while the inclinations of the two planets have wide oscillations. Only two planets, the closer ones, survive after 1 Myr of evolution.

pushes the binary companion closer to the planets, and of the more complex orbital behavior during close approaches between the stars when their orbits are inclined.

Retrograde orbits of the singleton also lead to fast instability of the planets when the mutual inclination is close to 90°. Wide oscillations of the eccentricity up to large values are observed, even if not related to the known Kozai type mechanism: there is no phasing between eccentricity and inclination. However, even in this case when the eccentricity is at its peak value, most of the planets are destabilized. Only when the mutual inclination has values beyond $\sim 140°$, the

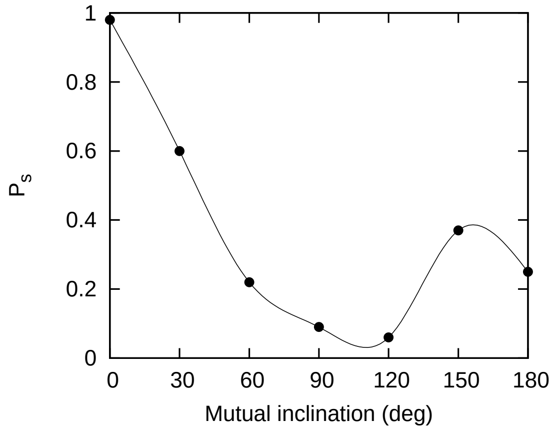

Figure 8.9: Fraction P_s of binaries that, at the end of the temporary triple phase, retain at least one of the planets in a stable orbit around the primary *vs.* i_m, the initial mutual inclination between the singleton and the binary companion.

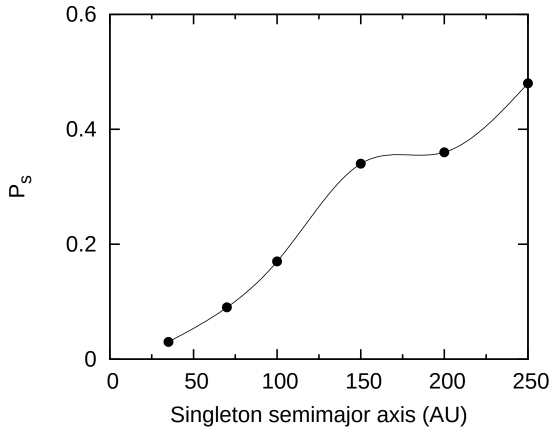

Figure 8.10: Fraction P_s of binaries that, at the end of the temporary triple phase, retain at least one of the planets in a stable orbit around the primary *vs.* a_b, the binary semimajor axis. The mutual inclination i_m is set to 90°, the worst case for planet stability.

planets around the primary are partly spared by the oscillations in eccentricity of the binary companion. However, as observed in the previous section, for mutual inclinations in the range $\sim 140° - 180°$ large inclination oscillations of the companion star destabilize planets even if to a lesser extent than the eccentricity oscillation.

As a result, the percentage of planets surviving the chaotic phase grows for inclinations larger than 90° but it does not return to 100%, halting at about 30%.

If we increase the semimajor axis of the binary a_b, the fraction of systems with surviving planets increases in an almost linear way. In Figure 8.10 we show the fraction of systems retaining planets *vs.* a_b for the worst case, *i.e.* with mutual inclination equal to 90°. The triple instability is a mechanism that easily destroys planetary systems of close binaries while it is less effective for wide binaries. For larger values of a_b, the planetary systems that survive are also more extended in semimajor axis. In most cases, for $a_b = 250$ AU, all the planets up to $a_p = 10$ AU survive the stellar chaotic phase.

Part III

Conclusions

Chapter 9

Conclusions and future works

The field of exoplanet research is evolving at astonishing velocities since the first discovery of an extrasolar planet around a solar-like star, 51 Peg (Mayor & Queloz, 1995). Among the different detection techniques, the transit method provides the strongest tool to date to measure physical parameters of these intriguing objects. Combined with the measurement of the radial velocity of the host star, it can yield the planetary density, which can provide clues about its formation history. The discovery of new transiting planets by ground and space projects in the next few years will certainly increase our knowledge of these exoplanets. We are beginning to be able to perform comparative planetology, and new insights on the real mass distribution of these objects will be provided in the near future. With more than 270 exoplanets discovered to date, we are approaching the status in which the statistical studies on these objects begin to be meaningful.

9.1 Conclusions

9.1.1 Part I: Photometric reduction and analysis software

This PhD Thesis has been developed in the scenario above mentioned.
The conclusions of this work are summarized in the following points:

- We have developed an automatic software which is able to calibrate and reduce the images acquired with the Schmidt telescope of Asiago, both in focus and defocused mode, developed within the RATS project. The resulting product of this pipeline, called RATS–*ARP*, is a collection of the lightcurves of hundreds of photometric stars in *a priori* selected stellar fields. Infact, candidate identification requires a preparatory work starting from stellar field selection with higher probability to find a transit event. The lightcurves themselves will be analyzed in order to catch light diming due to a potential transit. In this way, it is possible to detect:
  - a transit due to a *planetary companion*;
  - a transit due to a *stellar companion*;
  - a *variable star* (pulsating, contact type, etc.)

Although the CCD, lended by Catania Observatory –involved in RATS project–, was unexpectedly asked back during our second year, we were able to test our pipeline using both in focus and defocused images.
In particular, this algorithm rises to the occasion since it well treats all images taken in both modality:

➢ **In focus images**: we have found two interesting object in RATS_10 field, whose lightcurves present a diming:

  A. due to the possible presence of a transiting stellar companion, as the trend of the curve is typical V-shaped or its nature of variable;

  B. resembling a contact variable lightcurve shape, W UMa system-like, presenting the secondary, deeper, minimum peculiar for this class of objects.

➢ **Defocused images**:

  A. we have found many time series for RATS_4 field but, because of both the bad weather conditions and the full moon, data are missing and lightcurves are uncompleted;

  B. unfortunately, when RATS_10 was at its full visibility, any CCD were mounted on the Schmidt telescope so that any analysis could have been done for this field up to now: this will be a target for the future as to compare the results obtained from images acquired in defocused mode with those from images in focus.

- RATS-*ARP* was run on images taken with different CCD cameras. Therefore, the pipeline can manage different kind of images and it fulfills all its task. Thereby, we can say that RATS-*ARP* can be exported to projects different from RATS thanks to its pliability. In particular, thanks to its automatic development approach, it could be easily applicable to future space missions which intend to search exoplanets with the transit method with small adjustments.

- A detailed analysis for the future implementation of RATS database has been performed. Requirements and structure of this archive have been identified in order to help in developing a database that can be offered both to scientific community and to non-specialists.

9.1.2 Part II: Dynamical simulations

9.1.2.1 The co-planar case

Any attempt to model the formation and evolution of a planetary system around the component of a binary star system should account for the possibility that the binary orbit has changed with time. A dynamical event like the destabilization of an original triple system or a close stellar encounter can significantly alter the binary orbit after the formation of planets around the primary star. A system like γ Cephei, where a planet orbits the main star at about 2 AU and is perturbed by a secondary star presently moving at about 20 AU, might have had a different dynamical configuration when the planet formed. Trying to interpret the present configuration of the system using the observed orbital and physical parameters may lead to misleading deductions on the physical properties of the protoplanetary disk that generated the planets. Prior to the binary orbit change, the disk may have been more (or less) affected by the gravitational pull of the companion star that was on a different orbit. Planetesimal accretion, which is the first step of terrestrial planet formation and of the core–accretion model for giant planet growth, may occur differently depending on the binary orbit and companion star distance. Even gravitational instability might follow a different path if the companion star was farther away in the initial phase of the binary life.

In a few cases a stellar encounter may even cause the stripping of the companion star from the binary. The outcome would be a single star with a planetary system that formed when the star was part of a binary system and then perturbed by the gravity field of the companion star. In addition, stellar encounters may even push the orbit of the companion star out of its original plane leading to a significant mutual inclination between the planet and the companion. This is an efficient mechanism to produce planets in a Kozai resonance with the secondary star.

9.1.2.2 The inclined case

The fraction of binary systems hosting planets in S–type orbits can be lower than expected. If the binary is part of a crowded stellar environment, encounters with other stellar objects can lead to the formation of a transitional triple with large mutual inclination between the singleton and the binary. The subsequent dynamic evolution of the triple, in particular both the large oscillations in eccentricity of the companion star in the binary and the chaotic evolution during the triple destruction, destabilize planetary orbits around the main star. Even if the binary was born as part of an unstable inclined triple, the planetary system is fated to be disrupted.

Observing a binary system without planets in S–type orbits does not necessarily imply that the stars did not posses circumstellar disks in their early phases or that planet formation did not occur. The history of the binary and of its primordial environment must be taken into account since in most cases it may be the cause of the absence of planets.

Planet formation might be a very efficient process also in the presence of external perturbations, but the survival of planetary systems may be threatened by the binary dynamical history.

9.2 Future works

The RATS project will be working for at least three more years, surveying the night sky in search for new exoplanets. We wish to begin again the survey exploiting the new CCD mounted on the telescope at the beginning of December 2007.
Further work is needed to interpret the observations carried on this first years, especially to establish the real nature of the two objects candidate we have catalogued in this early stages as "variables" through more lasting observations. It will be worthwhile to observe RATS_10 filed in defocus mode in order to compare the results obtained with in focus images.

At the same time, we trust on a fast development of RATS database, in order to easily compare lightcurves with other extrasolar planets searching projects.

Finally, our aim is to apply this GNU license software to data coming from a space mission devoted to catching dimming light of observed stars. When a significant number of transiting planet candidates will be detected, it will be worthwhile to perform a detailed analysis of the rate of detections of false positives, and on the nature of each of those. This might serve to establish if the rate of occurrence of transiting planets is in good agreement with the rate of occurrence of planets detected so far by the radial velocity technique.

As regard our dynamical studies, for the future we will intend to extend our model considering close encounters with both more than one isolated star and in a stellar system more numerous than a triple one. A this kind of scenario better reflects real systems, in particular those present in stellar clusters.

Part IV

Appendix: Software documentation

Appendix A

RATS journal of observations

A.1 Journal of observations (February 2005)

Table A.1: Journal of observations for 18th February 2005: in the first column we list the image names according to a previous nomenclature, now abandoned in favour of a more detailed one; in the second column a list of modified Julian date is presented; in the last column the UT middle of the observations is listed.

File name	MJD	UT middle
001Rats10sec.fits	53420.31636574	19^h 35^m 38^s
002Rats10sec.fits	53420.31815972	19^h 38^m 14^s
003Rats10sec.fits	53420.32017361	19^h 41^m 08^s
004Rats10sec.fits	53420.32149306	19^h 43^m 02^s
005Rats10sec.fits	53420.32340278	19^h 45^m 47^s
006Rats10sec.fits	53420.32454861	19^h 47^m 26^s
007Rats10sec.fits	53420.32598380	19^h 49^m 29^s
008Rats10sec.fits	53420.32731482	19^h 51^m 25^s
009Rats10sec.fits	53420.32849537	19^h 53^m 06^s
010Rats10sec.fits	53420.32994213	19^h 55^m 12^s
011Rats10sec.fits	53420.33160880	19^h 57^m 36^s
012Rats10sec.fits	53420.33351852	20^h 00^m 21^s
013Rats10sec.fits	53420.33461806	20^h 01^m 56^s
014Rats10sec.fits	53420.33579861	20^h 03^m 38^s
015Rats10sec.fits	53420.33686343	20^h 05^m 10^s
016Rats10sec.fits	53420.33865741	20^h 07^m 45^s
017Rats10sec.fits	53420.33975694	20^h 09^m 19^s
018Rats10sec.fits	53420.34101852	20^h 11^m 09^s
019Rats10sec.fits	53420.34309028	20^h 14^m 08^s
020Rats10sec.fits	53420.34436343	20^h 15^m 58^s
021Rats10sec.fits	53420.34550926	20^h 17^m 37^s
022Rats10sec.fits	53420.34659722	20^h 19^m 10^s
023Rats10sec.fits	53420.34768519	20^h 20^m 45^s
024Rats10sec.fits	53420.36420139	20^h 44^m 32^s

(To be continued . . .)

(. . . Continued)

File name	MJD	UT middle
025Rats10sec.fits	53420.36533565	$20^h\ 46^m\ 10^s$
026Rats10sec.fits	53420.36652778	$20^h\ 47^m\ 53^s$
027Rats10sec.fits	53420.36789352	$20^h\ 49^m\ 51^s$
028Rats10sec.fits	53420.36905093	$20^h\ 51^m\ 31^s$
029Rats10sec.fits	53420.37015046	$20^h\ 53^m\ 06^s$
030Rats10sec.fits	53420.37130787	$20^h\ 54^m\ 45^s$
031Rats10sec.fits	53420.37454861	$20^h\ 59^m\ 26^s$
032Rats10sec.fits	53420.38197917	$21^h\ 10^m\ 08^s$
033Rats10sec.fits	53420.38312500	$21^h\ 11^m\ 47^s$
034Rats10sec.fits	53420.38476852	$21^h\ 14^m\ 09^s$
035Rats10sec.fits	53420.38593750	$21^h\ 15^m\ 50^s$
036Rats10sec.fits	53420.38709491	$21^h\ 17^m\ 30^s$
037Rats10sec.fits	53420.38831019	$21^h\ 19^m\ 14^s$
038Rats10sec.fits	53420.38944444	$21^h\ 20^m\ 52^s$
039Rats10sec.fits	53420.39060185	$21^h\ 22^m\ 33^s$
040Rats10sec.fits	53420.39172454	$21^h\ 24^m\ 10^s$
041Rats10sec.fits	53420.39290509	$21^h\ 25^m\ 52^s$
042Rats10sec.fits	53420.39401620	$21^h\ 27^m\ 28^s$
043Rats10sec.fits	53420.39510417	$21^h\ 29^m\ 01^s$
044Rats10sec.fits	53420.39623843	$21^h\ 30^m\ 40^s$
045Rats10sec.fits	53420.39732639	$21^h\ 32^m\ 14^s$
046Rats10sec.fits	53420.39872685	$21^h\ 34^m\ 14^s$
047Rats10sec.fits	53420.40042824	$21^h\ 36^m\ 42^s$
048Rats10sec.fits	53420.40157407	$21^h\ 38^m\ 21^s$
049Rats10sec.fits	53420.40666667	$21^h\ 45^m\ 41^s$
050Rats10sec.fits	53420.40785880	$21^h\ 47^m\ 24^s$
051Rats10sec.fits	53420.40938657	$21^h\ 49^m\ 36^s$
052Rats10sec.fits	53420.41648148	$21^h\ 59^m\ 49^s$
053Rats10sec.fits	53420.41953704	$22^h\ 04^m\ 13^s$
054Rats10sec.fits	53420.42077546	$22^h\ 06^m\ 00^s$
055Rats10sec.fits	53420.42186343	$22^h\ 07^m\ 34^s$
056Rats10sec.fits	53420.42310185	$22^h\ 09^m\ 21^s$
057Rats10sec.fits	53420.42434028	$22^h\ 11^m\ 08^s$
058Rats10sec.fits	53420.42559028	$22^h\ 12^m\ 56^s$
059Rats10sec.fits	53420.42670139	$22^h\ 14^m\ 32^s$
060Rats10sec.fits	53420.42787037	$22^h\ 16^m\ 13^s$
061Rats10sec.fits	53420.42905093	$22^h\ 17^m\ 55^s$
062Rats10sec.fits	53420.43019676	$22^h\ 19^m\ 33^s$
063Rats10sec.fits	53420.43129630	$22^h\ 21^m\ 09^s$
064Rats10sec.fits	53420.43243056	$22^h\ 22^m\ 47^s$
065Rats10sec.fits	53420.43359954	$22^h\ 24^m\ 27^s$
066Rats10sec.fits	53420.43471065	$22^h\ 26^m\ 04^s$
067Rats10sec.fits	53420.43616898	$22^h\ 28^m\ 10^s$
068Rats10sec.fits	53420.43730324	$22^h\ 29^m\ 48^s$
069Rats10sec.fits	53420.43849537	$22^h\ 31^m\ 30^s$
070Rats10sec.fits	53420.43980324	$22^h\ 33^m\ 24^s$
071Rats10sec.fits	53420.43980324	$22^h\ 33^m\ 24^s$
072Rats10sec.fits	53420.44232639	$22^h\ 37^m\ 02^s$
073Rats10sec.fits	53420.44232639	$22^h\ 37^m\ 02^s$
074Rats10sec.fits	53420.44479167	$22^h\ 40^m\ 35^s$
075Rats10sec.fits	53420.44594907	$22^h\ 42^m\ 14^s$
076Rats10sec.fits	53420.44744213	$22^h\ 44^m\ 24^s$

(To be continued . . .)

(. . . Continued)

File name	MJD	UT middle
077Rats10sec.fits	53420.44869213	22^h 46^m 11^s
078Rats10sec.fits	53420.44984954	22^h 47^m 52^s
079Rats10sec.fits	53420.45096065	22^h 49^m 28^s
080Rats10sec.fits	53420.45204861	22^h 51^m 01^s
081Rats10sec.fits	53420.45320602	22^h 52^m 42^s
082Rats10sec.fits	53420.45434028	22^h 54^m 19^s
083Rats10sec.fits	53420.45554398	22^h 56^m 04^s
084Rats10sec.fits	53420.45675926	22^h 57^m 48^s
085Rats10sec.fits	53420.45817130	22^h 59^m 51^s
086Rats10sec.fits	53420.46721065	23^h 12^m 52^s
087Rats10sec.fits	53420.46914352	23^h 15^m 39^s
088Rats10sec.fits	53420.47229167	23^h 20^m 10^s
089Rats10sec.fits	53420.47370370	23^h 22^m 13^s
090Rats10sec.fits	53420.47480324	23^h 23^m 48^s
091Rats10sec.fits	53420.47609954	23^h 25^m 40^s
092Rats10sec.fits	53420.47724537	23^h 27^m 18^s
093Rats10sec.fits	53420.47848380	23^h 29^m 06^s
094Rats10sec.fits	53420.47848380	23^h 29^m 06^s
095Rats10sec.fits	53420.48020833	23^h 31^m 34^s
096Rats10sec.fits	53420.48129630	23^h 33^m 09^s
097Rats10sec.fits	53420.48243056	23^h 34^m 47^s
098Rats10sec.fits	53420.48353009	23^h 36^m 22^s
099Rats10sec.fits	53420.48466435	23^h 38^m 00^s
100Rats10sec.fits	53420.48578704	23^h 39^m 37^s
101Rats10sec.fits	53420.48997685	23^h 45^m 39^s
102Rats10sec.fits	53420.49113426	23^h 47^m 19^s
103Rats10sec.fits	53420.49230324	23^h 49^m 00^s
104Rats10sec.fits	53420.49346065	23^h 50^m 40^s
105Rats10sec.fits	53420.49478009	23^h 52^m 34^s
106Rats10sec.fits	53420.49611111	23^h 54^m 29^s
107Rats10sec.fits	53420.49754630	23^h 56^m 33^s
108Rats10sec.fits	53420.49883102	23^h 58^m 23^s
109Rats10sec.fits	53420.50003472	00^h 00^m 08^s
110Rats10sec.fits	53420.50142361	00^h 02^m 08^s
111Rats10sec.fits	53420.50266204	00^h 03^m 54^s
112Rats10sec.fits	53420.50447917	00^h 06^m 32^s
113Rats10sec.fits	53420.50569444	00^h 08^m 16^s
114Rats10sec.fits	53420.50732639	00^h 10^m 37^s
115Rats10sec.fits	53420.50851852	00^h 12^m 20^s
116Rats10sec.fits	53420.50975694	00^h 14^m 07^s
117Rats10sec.fits	53420.51101852	00^h 15^m 56^s
118Rats10sec.fits	53420.51224537	00^h 17^m 42^s
119Rats10sec.fits	53420.51362269	00^h 19^m 41^s
120Rats10sec.fits	53420.51475694	00^h 21^m 19^s
121Rats10sec.fits	53420.51612269	00^h 23^m 18^s
122Rats10sec.fits	53420.51732639	00^h 25^m 01^s
123Rats10sec.fits	53420.51848380	00^h 26^m 41^s
124Rats10sec.fits	53420.51965278	00^h 28^m 23^s
125Rats10sec.fits	53420.52098380	00^h 30^m 18^s
126Rats10sec.fits	53420.52228009	00^h 32^m 09^s
127Rats10sec.fits	53420.52342593	00^h 33^m 49^s
128Rats10sec.fits	53420.52454861	00^h 35^m 26^s

(To be continued . . .)

(... Continued)

File name	MJD	UT middle
129Rats10sec.fits	53420.52577546	$00^h\ 37^m\ 11^s$
130Rats10sec.fits	53420.52693287	$00^h\ 38^m\ 52^s$
131Rats10sec.fits	53420.52809028	$00^h\ 40^m\ 31^s$
132Rats10sec.fits	53420.52931713	$00^h\ 42^m\ 18^s$
133Rats10sec.fits	53420.53057870	$00^h\ 44^m\ 06^s$
134Rats10sec.fits	53420.53180556	$00^h\ 45^m\ 52^s$
135Rats10sec.fits	53420.53440972	$00^h\ 49^m\ 37^s$
136Rats10sec.fits	53420.53618056	$00^h\ 52^m\ 11^s$
137Rats10sec.fits	53420.53738426	$00^h\ 53^m\ 54^s$
138Rats10sec.fits	53420.53856481	$00^h\ 55^m\ 36^s$
139Rats10sec.fits	53420.53974536	$00^h\ 57^m\ 14^s$
140Rats10sec.fits	53420.54109259	$00^h\ 59^m\ 08^s$

A.2 Journal of observations (April 2006)

Table A.2: Journal of observations for 22^{th}–26^{th} April 2006: in the first column we list the image names according to a previous nomenclature, now abandoned in favour of a more detailed one and different from the one used in Table A.1; in the second column the UT middle of the observations is listed. Those images signed with an encircled star are the only images used in the reduction process because they are not corrupted or photometrically bad.

File name	UT middle
Bias images	
060422210641B000.fits✪	$21^h\ 06^m\ 41^s$
060422210847B000.fits✪	$21^h\ 08^m\ 47^s$
060422211052B000.fits✪	$21^h\ 10^m\ 52^s$
060422211258B000.fits✪	$21^h\ 12^m\ 58^s$
060422211504B000.fits✪	$21^h\ 15^m\ 04^s$
060425213538B000.fits✪	$21^h\ 35^m\ 38^s$
060425213744B000.fits✪	$21^h\ 37^m\ 44^s$
060425213950B000.fits✪	$21^h\ 39^m\ 50^s$
060425214155B000.fits✪	$21^h\ 41^m\ 55^s$
060425214401B000.fits✪	$21^h\ 44^m\ 01^s$
060425214606B000.fits✪	$21^h\ 46^m\ 06^s$
060425214812B000.fits✪	$21^h\ 48^m\ 12^s$
060425215017B000.fits✪	$21^h\ 50^m\ 17^s$
060425215223B000.fits✪	$21^h\ 52^m\ 23^s$
060425215428B000.fits✪	$21^h\ 54^m\ 28^s$
060425215634B000.fits✪	$21^h\ 56^m\ 34^s$
060425215839B000.fits✪	$21^h\ 58^m\ 39^s$
060425220044B000.fits✪	$22^h\ 00^m\ 44^s$
060425220250B000.fits✪	$22^h\ 02^m\ 50^s$
060425220456B000.fits✪	$22^h\ 04^m\ 56^s$
060425220702B000.fits✪	$22^h\ 07^m\ 02^s$
060425220907B000.fits✪	$22^h\ 09^m\ 07^s$
060425221113B000.fits✪	$22^h\ 11^m\ 13^s$

(To be continued ...)

(. . . Continued)

File name	UT middle
060425221318B000.fits✪	$22^h\ 13^m\ 18^s$
060426221143B043.fits✪	$22^h\ 11^m\ 43^s$
060426221348B043.fits✪	$22^h\ 13^m\ 48^s$
060426221554B043.fits✪	$22^h\ 15^m\ 54^s$
060426221800B043.fits✪	$22^h\ 18^m\ 00^s$
060426222005B043.fits✪	$22^h\ 20^m\ 05^s$
060426222211B043.fits✪	$22^h\ 22^m\ 11^s$
060426222416B043.fits✪	$22^h\ 24^m\ 16^s$
060426222622B043.fits✪	$22^h\ 26^m\ 22^s$
060426222828B043.fits✪	$22^h\ 28^m\ 28^s$
060426223033B043.fits✪	$22^h\ 30^m\ 33^s$
060426223239B043.fits✪	$22^h\ 32^m\ 39^s$
060426223445B043.fits✪	$22^h\ 34^m\ 45^s$
060426223650B043.fits✪	$22^h\ 36^m\ 50^s$
060426223856B043.fits✪	$22^h\ 38^m\ 56^s$
060426224102B043.fits✪	$22^h\ 41^m\ 02^s$
060426224307B043.fits✪	$22^h\ 43^m\ 07^s$
060426224513B043.fits✪	$22^h\ 45^m\ 13^s$
060426224719B043.fits✪	$22^h\ 47^m\ 19^s$
060426224924B043.fits✪	$22^h\ 49^m\ 24^s$
060426225130B043.fits✪	$22^h\ 51^m\ 30^s$
Flat Fields images	
060424205901F000.fits✪	$20^h\ 59^m\ 01^s$
060424210152F000.fits	$21^h\ 01^m\ 52^s$
060424210413F000.fits	$21^h\ 04^m\ 13^s$
060424210704F000.fits	$21^h\ 07^m\ 04^s$
060424210958F000.fits	$21^h\ 09^m\ 58^s$
060424211241F000.fits	$21^h\ 12^m\ 41^s$
060425020230F000.fits	$02^h\ 02^m\ 30^s$
060425020437F000.fits	$02^h\ 04^m\ 37^s$
060425020643F000.fits	$02^h\ 06^m\ 43^s$
060425020849F000.fits	$02^h\ 08^m\ 49^s$
060425021055F000.fits	$02^h\ 10^m\ 55^s$
060425205151F000.fits	$20^h\ 51^m\ 51^s$
060425212153F000.fits	$21^h\ 21^m\ 53^s$
060425212359F000.fits	$21^h\ 23^m\ 59^s$
060425212605F000.fits	$21^h\ 26^m\ 05^s$
060425212812F000.fits	$21^h\ 28^m\ 12^s$
060425213018F000.fits	$21^h\ 30^m\ 18^s$
Object images	
060422204959O000.fits	$20^h\ 49^m\ 59^s$
060422205356O000.fits	$20^h\ 53^m\ 56^s$
060422205722O000.fits	$20^h\ 57^m\ 22^s$
060422210013O000.fits	$21^h\ 00^m\ 13^s$
060422210336O000.fits	$21^h\ 03^m\ 36^s$
060422225438O041.fits	$22^h\ 54^m\ 38^s$
060422225823O042.fits	$22^h\ 58^m\ 23^s$
060422230052O043.fits✪	$23^h\ 00^m\ 52^s$
060422230302O044.fits	$23^h\ 03^m\ 02^s$
060422230512O045.fits	$23^h\ 05^m\ 12^s$
060422232050O041.fits	$23^h\ 20^m\ 50^s$
060422232315O042.fits	$23^h\ 23^m\ 15^s$

(To be continued . . .)

(. . . Continued)

File name	UT middle
060422232526O043.fits	23^h 25^m 26^s
060422232736O044.fits	23^h 27^m 36^s
060422232950O045.fits	23^h 29^m 50^s
060422233205O041.fits	23^h 32^m 05^s
060422233422O042.fits	23^h 34^m 22^s
060422233641O043.fits	23^h 36^m 41^s
060422233900O044.fits	23^h 39^m 00^s
060422234116O045.fits	23^h 41^m 16^s
060422234759O041.fits	23^h 47^m 59^s
060422235011O042.fits	23^h 50^m 11^s
060422235221O043.fits	23^h 52^m 21^s
060422235433O044.fits	23^h 54^m 33^s
060422235646O045.fits	23^h 56^m 46^s
060422235856O041.fits	23^h 58^m 56^s
060423000115O042.fits	00^h 01^m 15^s
060423000325O043.fits	00^h 03^m 25^s
060423000535O044.fits	00^h 05^m 35^s
060423000745O045.fits	00^h 07^m 45^s
060423001017B045.fits	00^h 10^m 17^s
060423001222B045.fits	00^h 12^m 22^s
060423001428B045.fits	00^h 14^m 28^s
060423001633B045.fits	00^h 16^m 33^s
060423001839B045.fits	00^h 18^m 39^s
060423002044B045.fits	00^h 20^m 44^s
060423002250B045.fits	00^h 22^m 50^s
060423003149O041.fits	00^h 31^m 49^s
060423003401O042.fits	00^h 34^m 01^s
060423003618O043.fits	00^h 36^m 18^s
060423003833O044.fits	00^h 38^m 33^s
060423004049O045.fits	00^h 40^m 49^s
060423004419O042.fits	00^h 44^m 19^s
060423004633O043.fits	00^h 46^m 33^s
060423004844O044.fits	00^h 48^m 44^s
060423005056O045.fits	00^h 50^m 56^s
060423005306O041.fits	00^h 53^m 06^s
060423005518O042.fits	00^h 55^m 18^s
060423005734O043.fits	00^h 57^m 34^s
060423005958O044.fits	00^h 59^m 58^s
060423010256O045.fits	01^h 02^m 56^s
060423010512O041.fits	01^h 05^m 12^s
060423010726O042.fits	01^h 07^m 26^s
060423010936O043.fits	01^h 09^m 36^s
060423011200O044.fits	01^h 12^m 00^s
060423011528O045.fits	01^h 15^m 28^s
060424234128O041.fits	23^h 41^m 28^s
060424234344O042.fits	23^h 43^m 44^s
060424234613O043.fits	23^h 46^m 13^s
060424234831O044.fits	23^h 48^m 31^s
060424235041O045.fits	23^h 50^m 41^s
060425000639O041.fits	00^h 06^m 39^s
060425000916O042.fits	00^h 09^m 16^s
060425001346O042.fits	00^h 13^m 46^s

(To be continued . . .)

(. . . Continued)

File name	UT middle
060425001851O043.fits	$00^h\ 18^m\ 51^s$
060425002226O044.fits	$00^h\ 22^m\ 26^s$
060425002447O045.fits	$00^h\ 24^m\ 47^s$
060425002726O041.fits	$00^h\ 27^m\ 26^s$
060425002948O042.fits	$00^h\ 29^m\ 48^s$
060425003210O043.fits	$00^h\ 32^m\ 10^s$
060425003505O044.fits	$00^h\ 35^m\ 05^s$
060425003733O045.fits	$00^h\ 37^m\ 33^s$
060425004008O041.fits	$00^h\ 40^m\ 08^s$
060425004219O042.fits	$00^h\ 42^m\ 19^s$
060425004639O043.fits	$00^h\ 46^m\ 39^s$
060425004852O044.fits	$00^h\ 48^m\ 52^s$
060425005104O045.fits	$00^h\ 51^m\ 04^s$
060425005318O041.fits	$00^h\ 53^m\ 18^s$
060425005549O042.fits	$00^h\ 55^m\ 49^s$
060425005801O043.fits	$00^h\ 58^m\ 01^s$
060425010037O044.fits	$01^h\ 00^m\ 37^s$
060425010304O045.fits	$01^h\ 03^m\ 04^s$
060425010529O041.fits	$01^h\ 05^m\ 29^s$
060425010740O042.fits	$01^h\ 07^m\ 40^s$
060425010953O043.fits	$01^h\ 09^m\ 53^s$
060425011209O044.fits	$01^h\ 12^m\ 09^s$
060425011739O045.fits	$01^h\ 17^m\ 39^s$
060425012155O041.fits	$01^h\ 21^m\ 55^s$
060425014155O042.fits	$01^h\ 41^m\ 55^s$
060425014621O043.fits	$01^h\ 46^m\ 21^s$
060425014839O044.fits	$01^h\ 48^m\ 39^s$
060425015141O045.fits	$01^h\ 51^m\ 41^s$
060425222456O041.fits	$22^h\ 24^m\ 56^s$
060425223556O041.fits	$22^h\ 35^m\ 56^s$
060425224411O041.fits	$22^h\ 44^m\ 11^s$
060425225247O041.fits	$22^h\ 52^m\ 47^s$
060425225954O041.fits	$22^h\ 59^m\ 54^s$
060425231012O043.fits✪	$23^h\ 10^m\ 12^s$
060425231220O043.fits✪	$23^h\ 12^m\ 20^s$
060425231429O043.fits✪	$23^h\ 14^m\ 29^s$
060425231637O043.fits✪	$23^h\ 16^m\ 37^s$
060425231846O043.fits✪	$23^h\ 18^m\ 46^s$
060425232054O043.fits✪	$23^h\ 20^m\ 54^s$
060425232303O043.fits✪	$23^h\ 23^m\ 03^s$
060425232512O043.fits✪	$23^h\ 25^m\ 12^s$
060425232720O043.fits✪	$23^h\ 27^m\ 20^s$
060425232929O043.fits✪	$23^h\ 29^m\ 29^s$
060425233137O043.fits✪	$23^h\ 31^m\ 37^s$
060425233346O043.fits✪	$23^h\ 33^m\ 46^s$
060425233554O043.fits✪	$23^h\ 35^m\ 54^s$
060425233803O043.fits✪	$23^h\ 38^m\ 03^s$
060425234011O043.fits✪	$23^h\ 40^m\ 11^s$
060425234220O043.fits✪	$23^h\ 42^m\ 20^s$
060425234429O043.fits✪	$23^h\ 44^m\ 29^s$
060425234637O043.fits✪	$23^h\ 46^m\ 37^s$
060425234846O043.fits✪	$23^h\ 48^m\ 46^s$

(To be continued . . .)

(... Continued)

File name	UT middle
060425235055O043.fits✪	$23^h\ 50^m\ 55^s$
060426001606O043.fits	$00^h\ 16^m\ 06^s$
060426002931O043.fits	$00^h\ 29^m\ 31^s$
060426004446O043.fits	$00^h\ 44^m\ 46^s$
060426005722O043.fits✪	$00^h\ 57^m\ 22^s$
060426010128O043.fits✪	$01^h\ 01^m\ 28^s$
060426011006O043.fits	$01^h\ 10^m\ 06^s$
060426011530O043.fits	$01^h\ 15^m\ 30^s$
060426012432O043.fits✪	$01^h\ 24^m\ 32^s$
060426013746O043.fits✪	$01^h\ 37^m\ 46^s$
060426014104O043.fits✪	$01^h\ 41^m\ 04^s$
060426015009O043.fits✪	$01^h\ 50^m\ 09^s$
060426021622O043.fits	$02^h\ 16^m\ 22^s$
060426021943O043.fits	$02^h\ 19^m\ 43^s$
060426022151O043.fits	$02^h\ 21^m\ 51^s$
060426022400O043.fits	$02^h\ 24^m\ 00^s$
060426022608O043.fits	$02^h\ 26^m\ 08^s$
060426022817O043.fits	$02^h\ 28^m\ 17^s$
060426023026O043.fits	$02^h\ 30^m\ 26^s$
060426023234O043.fits	$02^h\ 32^m\ 34^s$
060426023443O043.fits	$02^h\ 34^m\ 43^s$
060426023652O043.fits	$02^h\ 36^m\ 52^s$
060426023900O043.fits	$02^h\ 39^m\ 00^s$
060426024431O043.fits	$02^h\ 44^m\ 31^s$
060426024646O043.fits	$02^h\ 46^m\ 46^s$
060426024902O043.fits✪	$02^h\ 49^m\ 02^s$
060426025117O043.fits✪	$02^h\ 51^m\ 17^s$
060426025333O043.fits✪	$02^h\ 53^m\ 33^s$
060426025548O043.fits✪	$02^h\ 55^m\ 48^s$
060426025804O043.fits✪	$02^h\ 58^m\ 04^s$
060426030020O043.fits✪	$03^h\ 00^m\ 20^s$
060426030237O043.fits✪	$03^h\ 02^m\ 37^s$
060426030454O043.fits✪	$03^h\ 04^m\ 54^s$
060426030927O043.fits✪	$03^h\ 09^m\ 27^s$
060426031135O043.fits✪	$03^h\ 11^m\ 35^s$
060426031344O043.fits	$03^h\ 13^m\ 44^s$
060426031553O043.fits✪	$03^h\ 15^m\ 53^s$
060426031802O043.fits	$03^h\ 18^m\ 02^s$
060426032010O043.fits	$03^h\ 20^m\ 10^s$
060426032219O043.fits	$03^h\ 22^m\ 19^s$
060426032428O043.fits	$03^h\ 24^m\ 28^s$
060426032636O043.fits	$03^h\ 26^m\ 36^s$
060426032845O043.fits	$03^h\ 28^m\ 45^s$
060426034259O000.fits	$03^h\ 42^m\ 59^s$
060426035337O043.fits✪	$03^h\ 53^m\ 37^s$
060426040650O043.fits	$04^h\ 06^m\ 50^s$
060426041105O043.fits✪	$04^h\ 11^m\ 05^s$
060426041419O043.fits✪	$04^h\ 14^m\ 19^s$
060426044748O043.fits	$04^h\ 47^m\ 48^s$
060427002107O041.fits	$00^h\ 21^m\ 07^s$
060427002333O042.fits	$00^h\ 23^m\ 33^s$
060427002553O043.fits✪	$00^h\ 25^m\ 53^s$

(To be continued ...)

(. . . Continued)

File name	UT middle
060427002824O044.fits	00^h 28^m 24^s
060427003204O045.fits	00^h 32^m 04^s
060427003609O041.fits	00^h 36^m 09^s
060427003837O042.fits	00^h 38^m 37^s
060427004128O043.fits	00^h 41^m 28^s
060427004348O044.fits	00^h 43^m 48^s
060427004642O045.fits	00^h 46^m 42^s
060427005408O041.fits	00^h 54^m 08^s
060427005735O042.fits	00^h 57^m 35^s
060427010001O043.fits	01^h 00^m 01^s
060427010216O044.fits	01^h 02^m 16^s
060427010433O045.fits	01^h 04^m 33^s
060427010810O041.fits	01^h 08^m 10^s
060427011044O042.fits	01^h 10^m 44^s
060427011309O043.fits	01^h 13^m 09^s
060427011556O044.fits	01^h 15^m 56^s
060427011814O045.fits	01^h 18^m 14^s
060427012053O041.fits	01^h 20^m 53^s
060427012350O042.fits	01^h 23^m 50^s
060427012847O043.fits	01^h 28^m 47^s
060427013203O044.fits	01^h 32^m 03^s
060427013450O045.fits	01^h 34^m 50^s

Appendix B

RATS Automatic Reduction Pipeline: User Requirement Document (URD)

Issue	Date	Section	Remarks
0.1	20/03/07	All	Creation of the document
0.2	27/03/07	All	First draft
0.4	10/04/07	All	Update after first draft revision
0.7	28/04/07	All	Update after second draft revision
0.9	08/05/07	All	Final draft revision
1.0	14/05/07	All	**Software review**

Table B.1: Change record for RATS–*ARP* URD document.

B.1 Introduction

The Italian project RATS (RAdial velocities and Transit Search) is a collaboration of different INAF Observatories (Padova, Catania, Napoli and Palermo), the Department of Astronomy and Physic of the University of Padova and ESA. This first chapter of the User Requirements Document (URD) summarizes the purpose of the software and the environment in which the software must run. There is a list of abbreviations, definitions and references and an overview of the rest of the document.

B.1.1 Purpose of the document

This document contains the User Requirements of *RATS Automatic Reduction Pipeline*.

B.1.2 Scope of the software

RATS Automatic Reduction Pipeline (RATS–*ARP*) shall provide the lightcurves of stars in selected fields during a 5 years-long survey for the searching of transit of extrasolar giant planets. The software shall be built to work with different scientific set up such as it is necessary for ground or space surveys of planetary transit. Moreover, the software provides tests for the adopted observing strategy and the management of scientific data.
The RATS–*ARP* shall support:

1. Detection of Extra Solar Planets (ESPs) that transit the disk of their parent star;
2. Detection of unknown Variable Stars (VSs);
3. Stellar flux measurements;
4. Automatic generation of stellar light curves;
5. False alarms (FA) reconnaissance;
6. Testing of spectroscopic follow up strategy (suspended);
7. Support for the simulation and definition of Top Level requirement for the FCU camera of WSO mission;
8. Improvement of planet formation mechanism knowledge (suspended);
9. Improvement of Solar System (SS) formation mechanism knowledge (suspended).

RATS–*ARP* software's benefits and goals are:

1. The software is extended to missions different from the RATS survey;
2. The strategy can be used for future mission planning;
3. Different data types can be used simultaneously;
4. The scientific data management can be used for future surveys planning;
5. Astrophysical parameters describing extrasolar transit planets will contribute to disentangle;
6. The planetary formation mechanism, to identify the environmental condition where these objects form or not and to have more hints about their physics.

B.1.3 Definitions, acronyms and abbreviations

Definitions, acronyms and abbreviations used in this document are listed below.

Applicable Document (AD)
Charge Coupled Device (CCD)
Central Processing Unit (CPU)
Database (DB)
European Space Agency (ESA)
Extrasolar Planet (ESP)
Extrasolar Planets (ESPs)
False Alarms (FA)
Field Camera Unit (FCU)
Flat Field (FF)
Field of view (FoV)
Full Width Half Maximum (FWHM)
Hardware (H/W)
Interface Description Language (IDL)
Julian Day (JD)
Not Available/Not Applicable (NA)
Operative System (OS)
Personal Computer (PC)
Point Spread Function (PSF)
Random Access Memory (RAM)
Radial Velocities and Transit Search (RATS)
RATS–Automatic Reduction Pipeline (RATS–ARP)

Reference Document (RD)

Software Requirements Document (SRD)

Solar System (SS)

Software (S/W)

To Be Defined (TBD)

To Be Written (TBW)

User Requirements Document (URD)

Universal Time (UT)

Variable Stars (VSs)

World Space Observatory UV (WSO-UV)

B.1.4 References

The following documents are relevant references for and applicable to the pipeline develop.

B.1.4.1 Referenced documents

[RD1] ESA Software Engineering Standards, ESA PSS-05-0 Issue 2 (BSSC), 1991

B.1.4.2 Applicable documents

[AD1] VLT-SPE-ESO 10000-0017:General safety requirements for scientific instrumentation

[AD2] R.U. Claudi, RATS-TRE-04, RATS dataflow, 2007

B.1.5 Overview of the document

The structure of the document is as follows:

Section 2 provides a general description of the S/W. In particular:

- subsection 2.1 describes the general capabilities of the S/W;
- subsection 2.2 describes the general constraints of the S/W;
- subsection 2.3 describes the characteristics of the Users;
- subsection 2.4 describes the operational environment.

Section 3 provides the specific requirements of the S/W. In particular:

- subsection 3.1 describes the notation adopted in the section;
- subsection 3.2 describes the capability requirements of the S/W;
- subsection 3.3 describes the constraints requirements of the S/W.

B.2 General description

This section gives the general description of the User requirements, following the guidelines given in the document [RD1]. In particular, the general descriptions of *Product Perspectives*, *User Characteristic*, *General Constraints*, *Assumptions and Dependencies* and the *Operational Environment* for RATS–*ARP* software follow.

B.2.1 Product perspectives

In the last 10 years, the discovery of more than 200 EPSs in our Galaxy constitutes one of the most advance in scientific knowledge of our Universe. ESA and NASA has started planetary surveys to investigate the existence of ESPs, in particular using the transit observation method. This technique holds important understanding of the planets formation mechanism and improving both the observational database and the theoretical models used by the scientists. It also provides predictions of the existence of other EPSs, in particular like-Earth objects.

In order to manage the enormous quantity of data obtained from such surveys, it is necessary to develop some software packages to analyse the light diming of a star due to a planetary transit. It is important to be able to access the full potential of the entire system. Therefore the software must be sufficient flexible to include updates as some parts of the entire set up becomes refined as new concept or a new observational strategy are introduced.

B.2.2 Relation to the current projects

To detect a planetary transit it is necessary an high photometric accuracy and a spectroscopic follow up to confirm the event. This latter requirement limits the fainter magnitude of the survey: the RATS project reaches about 10-20 m/s radial velocity precision with the echelle spectrograph at Cima Ekar in 1h exposure for a G star of about $V = 13 - 14$. On the other side, the brighter magnitude is set by the observational strategy. A 15 seconds exposure at the Schmidt of Cima Ekar easily saturates a star with $m = 13$. The solution adopted is to defocus the telescope.

Up to now, no reduction tools similar to the one described in this document has been developed. The proposed automatic pipeline is intended to be such a tool which performs all relevant analyzes and management of observational data.

B.2.3 General capabilities

The S/W shall be able to perform:

- Automatic setting up of the calibration images;
- Automatic calibration of the scientific images;
- Automatic setting up of the reference masterlist;
- Automatic matching between the shifted images;
- Automatic coordinate transformation;
- Automatic plotting of the lightcurves;
- Automatic evaluation of the stellar dimming.

B.2.4 General constraints

The theoretical basis for the pipeline will be founded on the outcome of the analyzes of the images taken from the Schmidt Telescope at the Asiago Observatory. In particular:

a) the S/W shall be based on a pipeline approach;

b) the Fortran modules shall be compiled with GNU Fortran 77 (g77) free source compiler;

c) the S/W shall be able to manage data affected by astronomical distortions;

d) the S/W shall be able to improve the results in centering and reducing of images;

e) the S/W shall be able to read and write file in IRAF format;

f) the S/W shall be able to read and write file in `DAOPHOT/DAOMATCH/DAOMASTER` format;

g) the S/W shall be able to keep stored the lightcurves and plots;

h) the S/W shall run on the LINUX platform;

i) the S/W shall be extendable and adaptable;

j) the language used in the S/W and all documents shall be English.

B.2.5 User characteristic

The pipeline's Users will be scientists and technicians with different levels of:

i. the S/W shall be based on a pipeline approach;

ii. the Fortran modules shall be compiled with GNU Fortran 77 ($g77$) free source compiler;

iii. the S/W shall be able to manage data affected by astronomical distortions;

iv. the S/W shall be able to improve the results in centering and reducing of images;

All these aspects are assumed to be appropriate guidelines to define the way in which the Users shall interact with the software and the level of performance and reliance required. These guidelines trace the necessary background in astronomical reduction technique, in planetary transit technique, in observational strategy technique required for the S/W usage.

Thereby, the Users of the software will be:

- *Scientists with specialist knowledge* of the transit observation technique who want a software which automatically generate the light curves of the survey's targets from the raw images;
- *Scientists with basic knowledge* of the transit observation technique who shall exploit the RATS lightcurves DB (TBD) as final User;
- *Engineers with a basic knowledge*, generally, of the transit observation technique who wish to have a software for supporting mission planning and performance evaluation of the entire system with particular interest in technical effects.

Taking into account these Users characteristics, their expectations, knowledge level and reasons for usage, the user requirements document as laid in the following sections have been derived.

B.2.6 Relation with the environment

The pipeline works as an automatic application tool, integrated in a workstation software environment allowing different applications by utilizing on-screen multi windowing. This software is embedded in such an environment and should perform downloading images files from database on local machine `DOLCE` and/or an external HD device initially acquired by local machine `COLD60`, keeping track both of the data stored, sending data files to local machine `SERIZAWA` obtained with the photometric reduction, sending printer lightcurve plots to the desired printing device.

The H/W platform of RATS–*ARP* is made up of computers employing a UNIX, running under Linux, and WINDOWS operating system. These provide via high-level User interfaces like X-Windows all functionality represented in the figure B.1 ([AD2]).

B.3 Specific requirements

This section contains the User requirements for the automatic pipeline.

At first, the requirement *Notation* is introduced. Then *Capability requirements*, which define the required functionality, and *Constraint requirements*, which define the rules that govern the software development process and other non-functional requirements, are listed.

B.3.1 Notation

Each requirement presented in this section has the form:

UR-XX-nn
Text

where:	**XX**	is an identifier denoting the specific functionality of the requirement;
	nn	is an ascending number giving the logical order of the requirement;
	Text	is the textual description of the requirement.

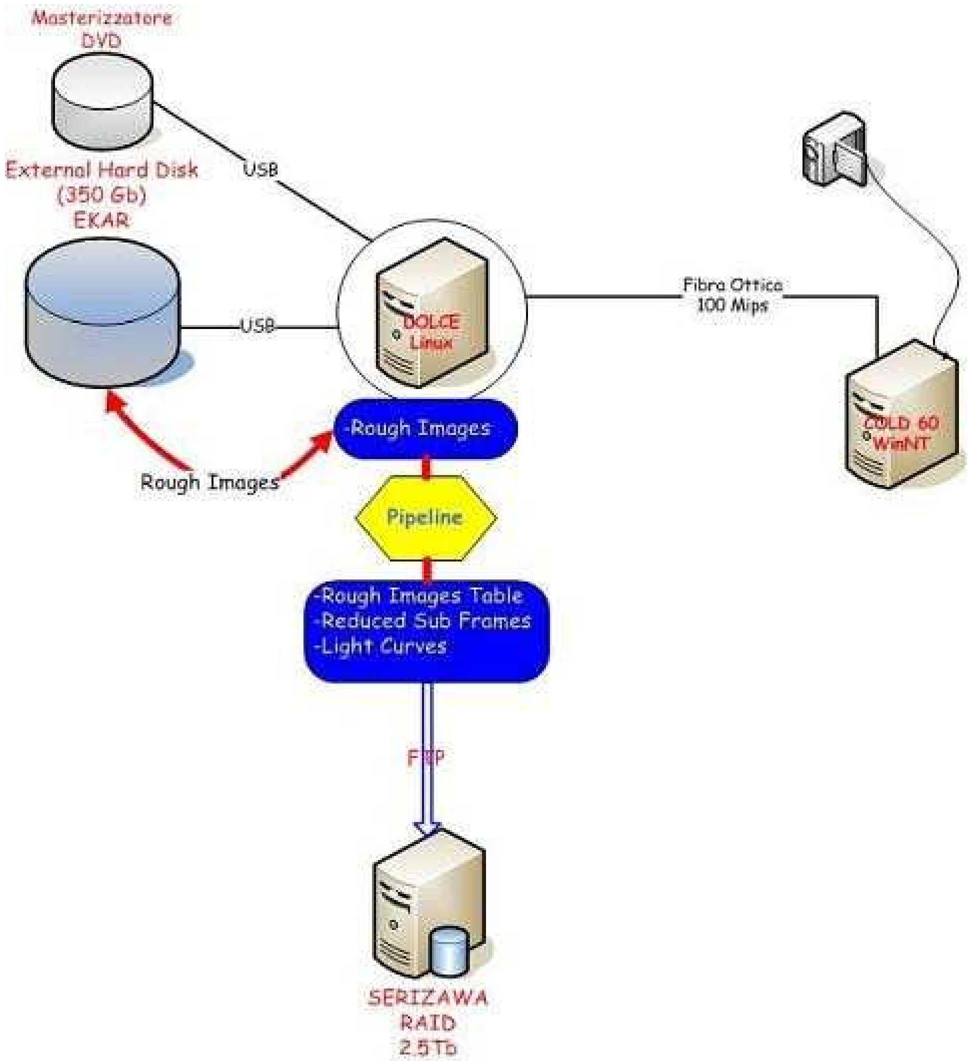

Figure B.1: S/W relationship with the external environment.

B.3.2 Capability requirements

In order to deal with the objectives and tasks proposed above, RATS–*ARP* has to fulfill the capability requirements detailed into:

- Functional requirements:
  - *Observational strategy:* requirements describing which observation technique must be decided by the User and supported by the software;
  - *Data pre-processing parameters:* requirements describing the input data of the pipeline to be given by the User;
  - *Data post-processing parameters:* requirements describing which output data shall be obtained from reduction and how they shall be processed in a form which is accessible by the User;
  - *User interface:* requirements describing the layout of the output data.
- Performance requirements;

- Accuracy requirements

B.3.2.1 Observational strategy

In this section there is the description of the requirements to be satisfied by RATS–*ARP* in order to properly carry out its foreseen tasks.

UR-OS-01
The RATS–*ARP* shall be able to manage with both focused images and defocused ones.

B.3.2.2 Data pre-processing parameters

In this section there is the description of the parameters the User shall be supply to the pipeline, as input files.

UR-PR-01
The User shall be able to select the date in order to start the reduction process.

UR-PR-02
For such given night, the User shall be able to supply the list of biases (10 images, at least), flat fields (10 images, at least) and scientific images, respectively.

UR-PR-03
For such given night, the User shall be able to supply the aperture parameters:

- ▷ 12 different value for the aperture radius;
- ▷ estimated inner Sky Radius of Annulus around a star;
- ▷ estimated outer Sky Radius of Annulus around a star.

All of them the parameters above are required for the `DAOPHOT` aperture file, `photo.opt`.

UR-PR-04
For such given night, the User shall be able to supply the photometry parameters:

- ▷ Read noise, in data numbers, of a single exposure made with the CCD;
- ▷ Gain factor of the CCD, in photon/electrons per data number;
- ▷ FWHM in pixels of the object, it determines the width of a Gaussian function;
- ▷ Fitting radius of the centroid of the object;
- ▷ PSF radius of the circle, in pixels, within which the PSF is to be defined;
- ▷ Analytic model PSF for the first approximation to the PSF;
- ▷ Variable PSF, the degree of complexity with which the PSF is to be modeled;
- ▷ High good datum, the level, in data numbers, above which a pixel value is to be considered defective;
- ▷ Threshold, the significance level, in standard deviations, that the User wants the program to use in deciding whether a given positive brightness enhancement is real.

UR-PR-05
For such given night, the User shall be able to select in the configuration file of ISIS package the:

- ▷ reference image;
- ▷ degree for the 2 dimensional polynomial of the astrometric re-mapping to the reference frame.

UR-PR-06
For such given night, the User shall be able to stack a number of the best images to build a reference frame.

UR-PR-07
For such given night, the User shall be able to supply the kernel (spatially variable in general) parameters:

- ▷ the kernel size;
- ▷ the ”stamp” size, the area considered around each stellar object;
- ▷ the number of these stamps (counter).

UR-PR-08
For such given night, the User shall be able to supply a threshold in order to eventually detect the VSs.

B.3.2.3 Data post-processing parameters

This section describes the outputs the pipeline shall produce to the User. All of them shall be stored in archive available to all the scientific community.

UR-PO-01
For a selected night, the RATS–*ARP* shall provide post-processing photometric parameters, such as:

- ▷ magnitude of stars;
- ▷ magnitude error.

UR-PO-02
For a selected night, the RATS–*ARP* shall provide post-processing spatial parameters, such as:

- ▷ (X, Y) coordinates of the images respect to the reference frame;
- ▷ (x, y) coordinates of the candidate transit stars on a single frame.

UR-PO-03
For a selected night, the RATS–*ARP* shall provide post-processing temporal parameters, such as:

- ▷ Exposure time;
- ▷ Julian Day (JD);
- ▷ Universal Time (UT).

UR-PO-04
For a selected night, the RATS–*ARP* shall provide post-processing observational parameters, such as:

- ▷ air mass;
- ▷ filters;
- ▷ CCD type.

UR-PO-05
For a selected night, the RATS–*ARP* shall provide a display output to PostScript file choice for printing.

B.3.2.4 User interface

This section describes the requirements to the User interface with particular attention to the display layout on the screen.

UR-UI-01
The RATS–*ARP* User interface shall be generally user-friendly as that User needs only to perform plain editing of text files or, eventually, program source code files for the most of RATS–*ARP* tasks. This implies that all necessary S/W commanding by the User (data entry and display) shall be possible via console.

UR-UI-02

The RATS–*ARP* shall allow, through its flexibility, the insertion of new models or parameters, and the implementation of access to them at console level, with limited effort for the User.

UR-UI-03
The RATS–*ARP* shall allow the User, via command line on the console, manual calls to `IDL` interface to:

- ▷ reading output data (lightcurves) files;
- ▷ an `IDL` display system with functionality fulfilling lightcurve' plots;
- ▷ performing simple statistics.

UR-UI-04
The RATS–*ARP* shall allow the User to submit jobs in batch mode. This functionality shall involve:

- ▷ possibility to accumulate multiple and independent batch jobs (i.e. During the weekend);
- ▷ independent integration of the tasks so that no problems occur if the User modifies other RATS–*ARP* tasks' code while batch operations work;
- ▷ automatic information for the User opening logfile about the current state of the batch jobs, one for each working job.

B.3.2.5 Performance

This section describes the criteria the software has to fulfill to answer the User's requirements.
In general, RATS–*ARP* shall work in an automatic manner (e.g. Processes as commands input, data entry work, reduction work, control work, plots work) for all potential task. Only display work shall be possible in an interactive manner.
A Pentium IV is used as a reference workstation, with a:

- CPU: 3.20 Ghz;
- RAM: 1 Gb;
- OS: Fedora 6.0 .

A (TBD) machine is used as telescope controller PC.

UR-PE-01
Command and data entry
On the reference workstation, the following performance is required of the command/data entry work: interactive without any significant system response time (commanding-to-completion time: order a few seconds or less).

UR-PE-02
Reduction
On the reference workstation, the following reduction performance is required of the single field of observation planning on a single night: automatic with acceptable system response time for the reduction time ranges up to half a day (commanding-to-completion time: order a few minutes or less).

UR-PE-03
Reduction
On the reference workstation, the following reduction performance is required of the multi-fields of observation planning on a single night: automatic with acceptable system response time for the reduction time ranges up to half a day (commanding-to-completion time: order a few minutes or less).

UR-PE-04
Reduction
On the reference workstation, the following reduction performance is required of the lightcurve production: automatic with acceptable system response time for the reduction of candidate transit profile of one occultation events (commanding-to-completion time: order a several minutes).

UR-PE-05
Control
On the reference workstation, the following performance is required of the control work: interactive with the short system response time for every display functionalities included (commanding-to-completion time: order a few tens of seconds or less).

UR-PE-06
Display
On the reference workstation, the following performance is required of the display work: interactive with the short system response time for every display functionality included (commanding-to-completion time: order a few tens of seconds or less).

B.3.2.6 Accuracy

This section describes the numerical accuracy requirements for the calculation performed by RATS–*ARP*.

UR-AC-01
All accuracy and critical computations shall be implemented based on the use of double precision data types in order to avoid any significant errors that could stem from computational inaccuracies.

B.3.2.7 Constraints requirements

This section describes the software development process requirements and the non-functional requirements for the pipeline.
Such requirement constraints are:

UR-CR-01
Existing `DAOPHOT` software shall be used.

UR-CR-02
Existing `DAOMATCH` software shall be used.

UR-CR-03
Existing `DAOMASTER` software shall be used.

UR-CR-04
Existing `IRAF` software shall be used.

UR-CR-05
In order to ensure the best use of the already existing software, to provide robustness and reliability, RATS–*ARP* shall be coded entirely by using as programming language:

- ▷ the FORTRAN-77 standard and/or compatible FORTRAN-90 standard for all computational routines;
- ▷ shell scripting language;
- ▷ IRAF scripting language;
- ▷ the `IDL` standard (`IDL` 6.1) for all other routines.

UR-CR-06
RATS–*ARP* shall run on Pentium IV workstation under Linux with X-windows and, specifically, the Fedora 6.0 operating system or higher.

UR-CR-07
RATS–*ARP* should be portable to OS other than Fedora with very limited effort.

UR-CR-08
The RATS–*ARP* software architecture shall allow to insert new routines with limited effort.

UR-CR-09
The final RATS–*ARP* software shall be made available via FTP from the Padova Astronomical Observatory web site.

UR-CR-10
The final RATS–*ARP* software shall be made available via another TBD high-storage-capacity device, as required.

Appendix C

RATS Automatic Reduction Pipeline: Software Requirement Document (SRD)

Issue	Date	Section	Remarks
0.1	20/03/07	All	Creation of the document
0.2	30/03/07	All	First draft
0.4	11/04/07	All	Update after first draft revision
0.7	30/04/07	All	Update after second draft revision
0.9	09/05/07	All	Final draft revision
1.0	14/05/07	All	**Software review**

Table C.1: Change record for RATS–*ARP* SRD document.

C.1 Introduction

The italian project RATS (RAdial velocities and Transit Search) is a collaboration of different INAF Observatories (Padova, Catania, Napoli and Palermo), the Department of Astronomy and Physic of the University of Padova and ESA. This first chapter of the User Requirements Document (URD) summarizes the purpose of the software and the environment in which the software must run. There is a list of abbreviations, definitions and references and an overview of the rest of the document.

C.1.1 Purpose of the document

This document contains the Software Requirements of *RATS Automatic Reduction Pipeline*.

C.1.2 Scope of the software

RATS Automatic Reduction Pipeline (RATS–*ARP*) shall provide the lightcurves of stars in selected fields during a 5 years-long survey for the searching of transit of extrasolar giant planets. The software shall be built to work

with different scientific set up such as it is necessary for ground or space surveys of planetary transit. Moreover, the software provides tests for the adopted observing strategy and the management of scientific data.
The RATS–*ARP* shall support:

1. Detection of Extra Solar Planets (ESPs) that transit the disk of their parent star;
2. Detection of unknown Variable Stars (VSs);
3. Stellar flux measurements;
4. Automatic generation of stellar light curves;
5. False alarms (FA) reconnaissance;
6. Testing of spectroscopic follow up strategy (suspended);
7. Support for the simulation and definition of Top Level requirement for the FCU camera of WSO mission;
8. Improvement of planet formation mechanism knowledge (suspended);
9. Improvement of Solar System (SS) formation mechanism knowledge (suspended).

RATS–*ARP* software's benefits and goals are:

1. The software is extended to missions different from the RATS survey;
2. The strategy can be used for future mission planning;
3. Different data types can be used simultaneously;
4. The scientific data management can be used for future surveys planning;
5. Astrophysical parameters describing extrasolar transit planets will contribute to disentangle;
6. The planetary formation mechanism, to identify the environmental condition where these objects form or not and to have more hints about their physics.

C.1.3 Definitions, acronyms and abbreviations

Definitions, acronyms and abbreviations used in this document are listed below.

Applicable Document (AD)
Charge Coupled Device (CCD)
Central Processing Unit (CPU)
Database (DB)
European Space Agency (ESA)
Extrasolar Planet (ESP)
Extrasolar Planets (ESPs)
False Alarms (FA)
Field Camera Unit (FCU)
Flat Field (FF)
Field of view (FoV)
Full Width Half Maximum (FWHM)
Hardware (H/W)
Interface Description Language (IDL)
Julian Day (JD)
Not Available/Not Applicable (NA)
Operative System (OS)
Personal Computer (PC)
Point Spread Function (PSF)

Random Access Memory (RAM)
Radial Velocities and Transit Search (RATS)
RATS–Automatic Reduction Pipeline (RATS–ARP)
Reference Document (RD)
Software Requirements Document (SRD)
Solar System (SS)
Software (S/W)
To Be Defined (TBD)
To Be Written (TBW)
User Requirements Document (URD)
Universal Time (UT)
Variable Stars (VSs)
World Space Observatory UV (WSO-UV)

C.1.4 References

The following documents are relevant references for and applicable to the pipeline develop.

C.1.4.1 Referenced documents

[RD1] ESA Software Engineering Standards, ESA PSS-05-0 Issue 2 (BSSC), 1991

C.1.4.2 Applicable documents

[AD1] VLT-SPE-ESO 10000-0017:General safety requirements for scientific instrumentation
[AD2] R.U. Claudi, RATS-TRE-04, RATS dataflow, 2007

C.1.5 Overview of the document

The structure of the document is as follows:

Section 2 provides a general description of the S/W. In particular:

- subsection 2.1 describes the S/W relation with current projects;
- subsection 2.2 describes the S/W relation with projects of past and future;
- subsection 2.3 describes the S/W main functions and products;
- subsection 2.4 describes where the S/W will be used and who will uses it;
- subsection 2.5 describes the related external systems and subsystems;
- subsection 2.6 describes the main constraints applied to the S/W;
- subsection 2.7 describes a conceptual description of the S/W.

Section 3 provides the specific requirements of the S/W. In particular:

- subsection 3.1 describes the notation adopted in the section;
- subsection 3.2 describes the function of each module;
- subsection 3.3 describes the S/W time and space performance;
- subsection 3.4 describes the S/W interface structures;
- subsection 3.5 describes the S/W functionality at the minimum level;

- subsection 3.6 describes the platform and operative system required;
- subsection 3.7 describes the plans for testing the system;
- subsection 3.8 describes the plans for satisfying the requirements;
- subsection 3.9 describes the suitable documentation;
- subsection 3.10 describes the requirement for the security;
- subsection 3.11 describes the S/W compatibility with other platforms;
- subsection 3.12 describes the requirement of S/W quality;
- subsection 3.13 describes the S/W reliant requirements;
- subsection 3.14 describes the S/W requirements to be maintained;
- subsection 3.15 describes the S/W level of safety.

Section 4 provides the tracing from User Requirements to Software Requirements in form of a requirement traceability matrix.

C.2 General description

The aim of the RATS–*ARP* is the detection of ESPs that transit the disk of their parent star and the production of lightcurve's files for candidates transit. In order to reach its target, the software processes photometric data provided by the CCD mounted on the C.ma Ekar 67/92 Schmidt telescope. Moreover, the pipeline provides detection of unknown Variable Stars by means of automatically generated lightcurves. In addition, the software performs false alarms reconnaissance which allow to determine the real nature of transiting objects. The pipeline can work also as support for the simulation and definition of Top Level requirement for the FCU camera of WSO mission. Thanks to the results obtained by the pipeline, the whole scientific community can improve the knowledge of planets formation mechanism.

C.2.1 Relation to the current projects

To detect a planetary transit it is necessary an high photometric accuracy and a spectroscopic follow up to confirm the event. This latter requirement limits the fainter magnitude of the survey: the RATS project reaches about 10-20 m/s radial velocity precision with the echelle spectrograph at Cima Ekar in 1h exposure for a G star of about $V = 13 - 14$. On the other side, the brighter magnitude is set by the observational strategy. A 15 seconds exposure at the Schmidt of Cima Ekar easily saturates a star with $m = 13$. The solution adopted is to defocus the telescope.

Up to now, no reduction tools similar to the one described in this document has been developed. The proposed automatic pipeline is intended to be such a tool which performs all relevant analysis and management of observational data.

C.2.2 Relation to predecessor and successor projects

Due to its innovative observational strategy, RATS–*ARP* is totally a new project among the current transits surveys.

C.2.3 Function and purpose

The purpose of RATS–*ARP* is to provide an automatic calibration and photometry reduction procedure for transit survey. It consists of functional blocks, responsible for bias and flat fielding calibration, aperture reduction and the production of lightcurves both for candidates transit and variables stars.
RATS–*ARP* shall support the future missions dedicated to transit search, in particular the software shall be use in WSO-UV mission reduction phase. Therefore, the pipeline shall provide sufficient functionality and extensibility.

C.2.4 User characteristic

The pipeline's Users will be scientists and technicians with different levels of:

1. knowledge of the transit search mechanism;
2. knowledge of the theory above which the software is founded on;
3. reasons of usage of the software;
4. expectations to the functionality of the software.

All these aspects are assumed to be appropriate guidelines to define the way in which the Users shall interact with the software and the level of performance and reliance required. These guidelines trace the necessary background in astronomical reduction technique, in planetary transit technique, in observational strategy technique required for the S/W usage.
Thereby, the Users of the software will be:

- *Scientists with specialist knowledge* of the transit observation technique who want a software which automatically generate the light curves of the survey's targets from the raw images;
- *Scientists with basic knowledge* of the transit observation technique who shall exploit the RATS lightcurves DB (TBD) as final User;
- *Engineers with a basic knowledge*, generally, of the transit observation technique who wish to have a software for supporting mission planning and performance evaluation of the entire system with particular interest in technical effects.

RATS–*ARP* shall run on an Intel Pentium IV based IBM-compatible PC running Fedora 6.0. The Fortran compiler shall be GNU Fortran (g77) free source compiler.

C.2.5 Relation with the environment

The pipeline works as an automatic application tool, integrated in a workstation software environment allowing different applications by utilizing on-screen multi windowing. This software is embedded in such an environment and should perform downloading images files from database on local machine `DOLCE` and/or an external HD device initially acquired by local machine `COLD60`, keeping track both of the data stored, sending data files to local machine `SERIZAWA` obtained with the photometric reduction, sending printer lightcurve plots to the desired printing device.
The H/W platform of RATS–*ARP* is made up of computers employing a UNIX, running under Linux, and WINDOWS operating system. These provide via high-level User interfaces like X-Windows all functionality represented in the figure C.1 ([AD2]).

C.2.6 General constraints

The theoretical basis for the pipeline will be founded on the outcome of the analysis of the images taken from the Schmidt Telescope at the Asiago Observatory. In particular:

a) the S/W shall be based on a pipeline approach;

b) the Fortran modules shall be compiled with GNU Fortran 77 (g77) free source compiler;

c) the S/W shall be able to manage data affected by astronomical distortions;

d) the S/W shall be able to improve the results in centering and reducing of images;

e) the S/W shall be able to read and write file in IRAF format;

f) the S/W shall be able to read and write file in `DAOPHOT/DAOMATCH/DAOMASTER` format;

g) the S/W shall be able to keep stored the lightcurves and plots;

h) the S/W shall run on the LINUX platform;

i) the S/W shall be extendable and adaptable;

j) the language used in the S/W and all documents shall be English.

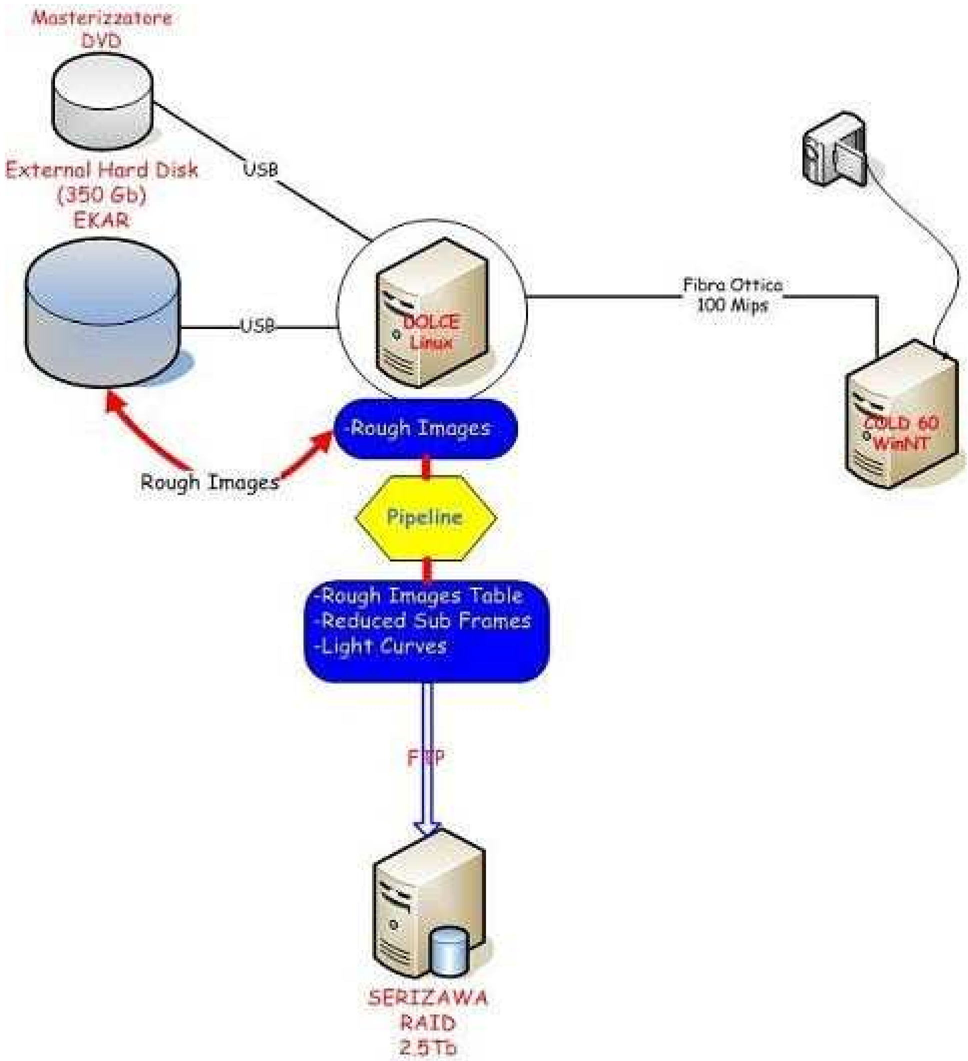

Figure C.1: S/W relationship with the external environment.

C.2.7 Model description

An overview of the software reduction concepts is shown in the figures C.2 and C.3, grouped in modules.

C.3 Specific requirements

This section describes the Software requirements for the pipeline, which implement the User requirements described in URD.

C.3.1 Notation

Each requirement listed in the following has the form:

SR-XX(X)-YY(Y)-ZZ(Z)-nn
Text

where:

XX(X)	is an identifier denoting the specific functionality of the requirement;
YY(Y)	is an identifier denoting the specific functionality of the sub-requirement;
ZZ(Z)	is an identifier denoting the specific functionality of the sub-sub-requirement;
nn	is an ascending number giving the logical order of the requirement;
Text	is the textual description of the requirement.

C.3.2 Functional requirements:

SR-FR-01
The input parameters shall be supply by input files.

SR-FR-02
The data capture system has to acquire images in the following order: biases, flat fields and scientific images.

SR-FR-03
The input parameters shall be:

- ▷ lists of biases: the data capture system has to acquire 10 biases images;
- ▷ lists of flat fields: the data capture system has to acquire 10 flat fields images;
- ▷ lists of scientific images;
- ▷ aperture parameters, required for the `DAOPHOT` aperture file:
  - 12 different value for the aperture radius;
  - estimated inner and outer Sky Radii of Annulus around a star.
- ▷ photometry parameters:
  - Read noise of the CCD;
  - Gain factor of the CCD;
  - FWHM in pixels of the object;
  - Fitting radius of the centroid of the object;
  - PSF radius of the circle within which the PSF is to be defined;
  - Analytic model PSF for the first approximation to the PSF;
  - Variable PSF, the degree of complexity with which the PSF is to be modeled;
  - High good datum, the level above which a pixel value is defective;
  - A threshold value to consider a positive brightness enhancement as real.
- ▷ a kernel size;
- ▷ a ”stamp” size and a counter of them;

SR-FR-04
The S/W shall reduce all the images acquired in a selected night of observation.

SR-FR-05
All selected stellar fields shall be divided in 6 sub-fields of one square degree each.

SR-FR-06
All the images acquired shall be in fits format.

SR-FR-07
The fits files naming convention is YYMMDDhhmmssX0nm.fits, where:

- ▷ YY is the last two digit of the year;
- ▷ MM is the month;
- ▷ DD is the day;
- ▷ hh are the hours;
- ▷ mm are the minutes;
- ▷ ss are the seconds;
- ▷ X identify the object: it can be B=bias, F=flat, O=object;
- ▷ n is the RATS field;
- ▷ m is the subfields.

If X=B or X=F, n=m=0.

SR-FR-08
Only the one image (the first in time order) shall be the reference frame.

SR-FR-09
The creation of the masterlist shall be manage by some selected ISIS's packages (re-mapping).

SR-FR-10
The aperture photometry shall be obtained by `DAOPHOT`.

SR-FR-11
The `DAOPHOT` version shall be slightly modified in order to fine-tune some values.

SR-FR-12
The matching frame shall be obtained by `DAOMATCH` and `DAOMASTER`.

SR-FR-13
The calibration masterbias and masterflat shall be obtained by IRAF.

SR-FR-14
An option to save the "stamps" around the most interesting stellar objects shall be provided (TBW).

SR-FR-15
The S/W shall focus only on the most bright and isolated stars.

SR-FR-16
The S/W shall indicate missing or erroneous input data as a warning in a log file.

SR-FR-17
The S/W shall provide files containing:

- ▷ magnitude of stars and errors;
- ▷ (X, Y) coordinates of the images respect to the reference frame;
- ▷ (x, y) coordinates of the candidate transit stars on a single frame;
- ▷ Exposure time;
- ▷ Julian Day (JD);
- ▷ Universal Time (UT);
- ▷ air mass;
- ▷ filters;
- ▷ CCD type.

C.3.3 Performance requirements

As RATS–*ARP* shall run at the end of the observations, any performance requirements are requested from external systems.
The reduction of a single image of the selected night shall be 180 sec or less. This quantitative performance requirement is referred to a Pentium IV workstation of 1 GHz and 256 MB RAM.

C.3.4 Interface requirements

This section describes software, hardware and communications interface requirements for RATS–*ARP* software. It defines those elements with which the pipeline must interface and communicate.

C.3.4.1 Software interface requirements

SR-IR-SI-01
RATS–*ARP*P shall be executed under LINUX and, specifically, the Fedora 6.0 operating system or higher.

C.3.4.2 Hardware interface requirements

SR-IR-HI-01
The software shall run on Pentium IV workstation.

C.3.4.3 Communications interface requirements

SR-IR-CI-01
RATS–*ARP*P shall use the standard communications protocols as intrinsic to and offered by the above specified operating system.

C.3.5 Operational requirements

This section describes the requirements on the operation mode, the man/machine interface and the RATS–*ARP* operator skill profile.

C.3.5.1 Operation mode

SR-OR-OP-01
The operation mode of RATS–*ARP* shall be automatic.

C.3.5.2 Man/machine interface

SR-OR-MM-01
The man-machine interface shall be a display screen, a pointing device (typically a mouse or a pen) and a keyboard.

SR-OR-MM-02
The RATS–*ARP* screen interface shall be a user-friendly windows. The User needs to perform plain editing of text and/or program source code. Thus, all necessary RATS–*ARP* commanding and interactions with the User (data entry, computations, display) shall be performed via window-based interface.

C.3.5.3 Operator skill profile

SR-OR-SP-01
RATS–*ARP* shall be operable by multi-users both with basic and specialist knowledge of the transit observational technique. Special hardware, software and programming knowledge shall not be required by Users.

C.4 Resource requirements

This section describes the physical-technical resource requirements such as processing power, RAM memory, disk space, disc access time and screen resolution.

C.4.0.4 Processing power

SR-RR-PP-01
Pentium IV workstations (1 GHz clock rate) is required as minimum. Faster machine are not required but it shall be clear that they lead to an significant improvement in the performances in case of intensive computations.

C.4.0.5 RAM memory

SR-RR-RM-01
256 MB RAM is required, even if more RAM is recommended. 512 MB or 1 GB RAM shall allow performance improvements.

C.4.0.6 Disk space

SR-RR-DS-01 50 GB free disk space is required. More disk space is highly recommended in expectations of future RATS observations. Free disk space of 500 GB or more provides suitable room for a multiple of nights' reductions.

C.4.0.7 Disk access time

SR-RR-DT-01
Even if a disk access time of 10 msec is enough, any faster access improves the RATS–*ARP* performance and is recommended.

C.4.0.8 Screen resolution

SR-RR-SS-01
A screen resolution of at least 1152 x 900 pixels is required, a resolution of 1280 x 1024 pixels or higher is recommended for improved on-screen plotting.

C.4.1 Verification and validation requirements

In this section, validation and verification requirements are presented. In particular, two types of validation/verification activities shall be performed: *unit tests*, *integration tests* and *acceptance/system tests*.

C.4.1.1 Unit Tests

SR-VV-UT-01
The unit tests shall be performed by the author of the Fortran modules in order to doubtless show the lack of errors in the code. Domain testing and special boundary cases where the S/W is most likely to fail shall be considered.

SR-VV-UT-02
The unit tests shall prove the correctness of each S/W modules before the delivery of reduction pipeline.

C.4.1.2 Integration Test

SR-VV-IT-01
The integration tests shall verify that input/output data formats of each S/W modules satisfy the formats decided

by the User.

SR-VV-IT-02
The integration tests shall prove the correctness of each S/W modules before the delivery of reduction pipeline.

C.4.2 Acceptance tests requirements

The RATS–*ARP* acceptance tests shall verify that all the S/W modules satisfy the UR, according to the [RD1] standard.

C.4.3 Documentation requirements

The following document will be produced:

- Architectural Design Document (ADD);
- Software User Manual (SUM).

The SUM shall be simplified compare to [RD1] but it will describe RATS–*ARP* at a level of detail suitable also for non-specialist Users.
The format and size of this documentation will be standard A4 format. If necessary, drawings and diagrams may vary from this format.

C.4.4 Security requirements

There are no security requirements.

C.4.5 Portability requirements

SR-POR-01
The software shall be portable to platforms other than Pentium-based LINUX workstations with limited efforts (e.g. SUN-based workstation machines).

C.4.6 Quality requirements

SR-QR-01
The software shall be self-explanatory as much as possible.

SR-QR-02
Each pipeline's file shall contain an header description of the name of the file, the purpose of the code, the author, the date of last revision and remarks on changing.

SR-QR-03
Each pipeline's procedure shall be preceded by comments defining its functionality, input parameters unless it is clear, and output results.

SR-QR-04
All variables and constants shall be commented unless their name is self-explanatory.

SR-QR-05
Non-obvious statements in the code shall be commented immediately before the statements it refers to.

C.4.7 Reliability requirements

There are no reliability requirements.

C.4.8 Maintainability requirements

SR-MR-01
The routines shall be written in Fortran77, shell scripts and IRAF scripts.

SR-MR-02
The S/W shall be modifiable by the User specialist in Fortran, shell and IRAF scripts with some limited effort.

SR-MR-03
The S/W shall be flexible in its implementation and it shall allow updates and additions (e.g. new data processing algorithms or models) with limited effort.

C.4.9 Safety requirement

There are no safety requirements.

C.5 UR vs. SR TRACEABILITY MATRIX

Table C.2: User Requirements *vs.* Software Requirements traceability matrix.

UR	SR
UR-OS-01	–
UR-PR-01	SR-FR-04
UR-PR-02	SR-FR-01, SR-FR-02, SR-FR-03
UR-PR-03	SR-FR-01, SR-FR-03
UR-PR-04	SR-FR-01, SR-FR-03
UR-PR-05	SR-FR-07
UR-PR-06	SR-FR-08
UR-PR-07	SR-FR-01, SR-FR-13
UR-PR-08	SR-FR-01, SR-FR-03
UR-PO-01	SR-FR-16
UR-PO-02	SR-FR-16
UR-PO-03	SR-FR-16
UR-PO-04	SR-FR-16
UR-PO-05	–
UR-UI-01	SR-OR-MM-02
UR-UI-02	SR-OR-MM-02
UR-UI-03	–
UR-UI-04	SR-OR-SP-01
UR-PE-01	SR-OR-MM-01
UR-PE-02	SR-OR-OP-01
UR-PE-03	SR-FR-05
UR-PE-04	SR-OR-OP-01
UR-PE-05	SR-FR-13
UR-PE-06	SR-OR-MM-02
UR-AC-01	–
UR-CR-01	SR-FR-09, SR-FR-10
UR-CR-02	SR-FR-11
UR-CR-03	SR-FR-11
UR-CR-04	SR-FR-12
UR-CR-05	–

Continued on next page

Continued from previous page

UR	**SR**
UR-CR-06	SR-IR-SI-01, SR-IR-HI-01
UR-CR-07	–
UR-CR-08	SR-QR-05
UR-CR-09	SR-IR-CI-01
UR-CR-10	SR-IR-CI-01

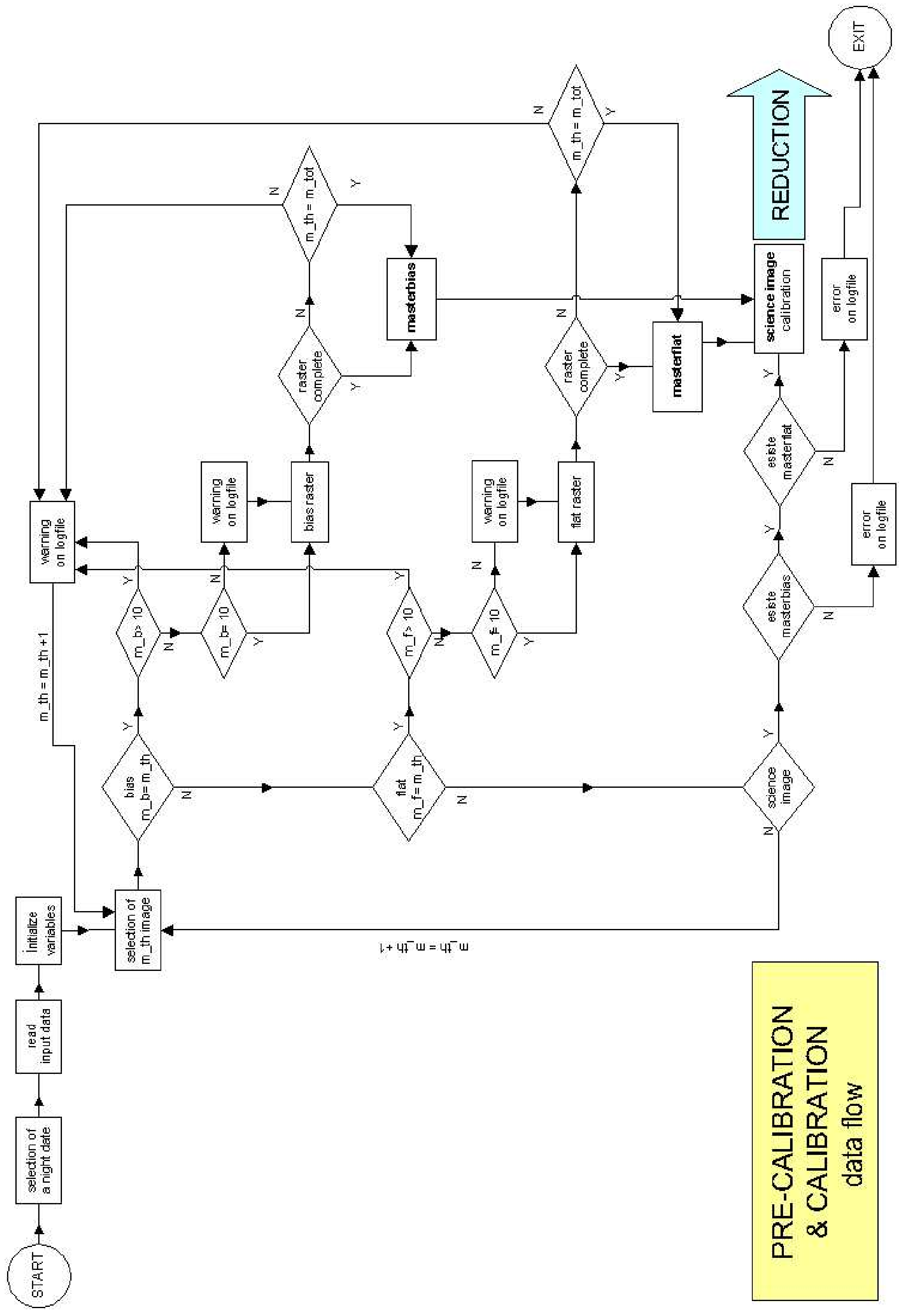

Figure C.2: General dataflow pre-calibration and calibration diagram.

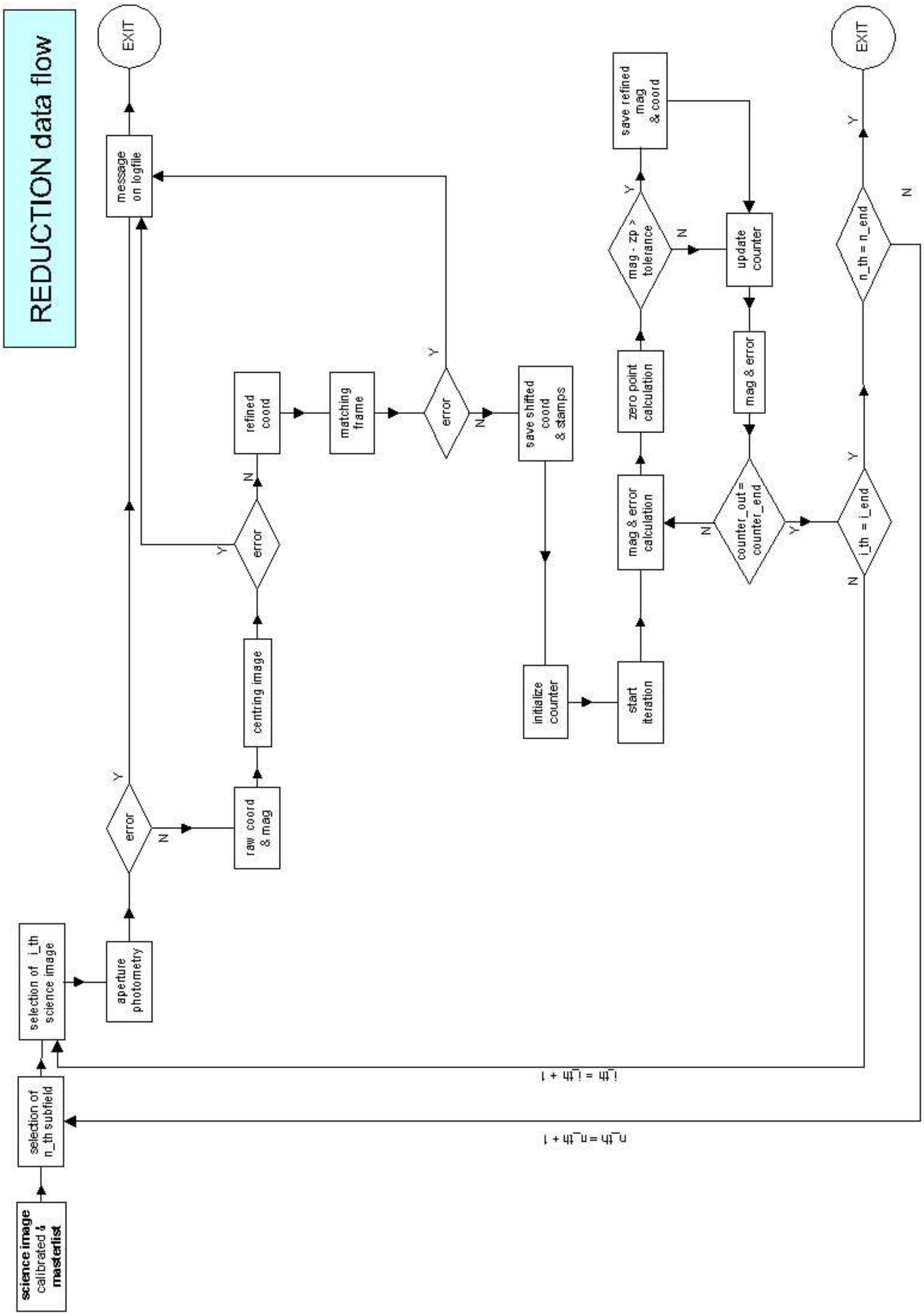

Figure C.3: General dataflow reduction diagram.

Appendix D

RATS Automatic Reduction Pipeline: Architectural Design Document (ADD)

Issue	Date	Section	Remarks
0.1	22/03/07	All	Creation of the document
0.2	31/03/07	All	First draft
0.4	14/04/07	All	Update after first draft revision
0.7	30/04/07	All	Update after second draft revision
0.9	10/05/07	All	Final draft revision
1.0	14/05/07	All	**Software review**

Table D.1: Change record for RATS–*ARP* ADD document.

D.1 Introduction

The italian project RATS (RAdial velocities and Transit Search) is a collaboration of different INAF Observatories (Padova, Catania, Napoli and Palermo), the Department of Astronomy and Physic of the University of Padova and ESA.
This first chapter of the Architectural Design Document (ADD) summarizes the purpose of this document. Also the definitions, acronyms and abbreviations used in this document are described in this section. The last two parts of this section contain references and an overview of the entire document.

D.1.1 Purpose of the document

The ADD provides a beginning of a solution – by means of component decomposition – for all software requirements as specified in the SRD ([RD3]) and defines an object model specifying the components and interfaces between components.

D.1.2 Scope of the software

RATS Automatic Reduction Pipeline (RATS–*ARP*) shall provide the lightcurves of stars in selected fields during a 5 years-long survey for the searching of transit of extrasolar giant planets. The software shall be built to work

with different scientific set up such as it is necessary for ground or space surveys of planetary transit. Moreover, the software provides tests for the adopted observing strategy and the management of scientific data.
The RATS–*ARP* shall support:

1. Detection of Extra Solar Planets (ESPs) that transit the disk of their parent star;
2. Detection of unknown Variable Stars (VSs);
3. Stellar flux measurements;
4. Automatic generation of stellar light curves;
5. False alarms (FA) reconnaissance;
6. Testing of spectroscopic follow up strategy (suspended);
7. Support for the simulation and definition of Top Level requirement for the FCU camera of WSO mission;
8. Improvement of planet formation mechanism knowledge (suspended);
9. Improvement of Solar System (SS) formation mechanism knowledge (suspended).

RATS–*ARP* software's benefits and goals are:

1. The software is extended to missions different from the RATS survey;
2. The strategy can be used for future mission planning;
3. Different data types can be used simultaneously;
4. The scientific data management can be used for future surveys planning;
5. Astrophysical parameters describing extrasolar transit planets will contribute to disentangle;
6. The planetary formation mechanism, to identify the environmental condition where these objects form or not and to have more hints about their physics.

D.1.3 Definitions, acronyms and abbreviations

Definitions, acronyms and abbreviations used in this document are listed below.

Applicable Document (AD)
Charge Coupled Device (CCD)
Central Processing Unit (CPU)
Database (DB)
European Space Agency (ESA)
Extrasolar Planet (ESP)
Extrasolar Planets (ESPs)
False Alarms (FA)
Field Camera Unit (FCU)
Flat Field (FF)
Field of view (FoV)
Full Width Half Maximum (FWHM)
Hardware (H/W)
Interface Description Language (IDL)
Julian Day (JD)
Not Available/Not Applicable (NA)
Operative System (OS)
Personal Computer (PC)
Point Spread Function (PSF)

Random Access Memory (RAM)

Radial Velocities and Transit Search (RATS)

RATS–Automatic Reduction Pipeline (RATS–ARP)

Reference Document (RD)

Software Requirements Document (SRD)

Solar System (SS)

Software (S/W)

To Be Defined (TBD)

To Be Written (TBW)

User Requirements Document (URD)

Universal Time (UT)

Variable Stars (VSs)

World Space Observatory UV (WSO-UV)

D.1.4 References

The following documents are relevant references for and applicable to the pipeline develop.

D.1.4.1 Referenced documents

[RD1] ESA Software Engineering Standards, ESA PSS-05-0 Issue 2 (BSSC), 1991

[RD2] V. Granata, User Requirement Document, RATS Automatic Reduction Pipeline, 2007

[RD3] V. Granata, Software Requirement Document, RATS Automatic Reduction Pipeline, 2007

D.1.4.2 Applicable documents

[AD1] ISIS, image subtraction package, http://www2.iap.fr/users/alard/package.html

[AD2] J. Rumbaugh, M. Blaha, W. Premerlani, F. Eddy, W. Lorensen, Object-oriented modelling and design, Prentice-Hall, 1991, ISBN 0-13-629841-9

D.1.5 Overview of the document

The structure of the document is as follows:

Section 2 summarizes the system context and design.

Section 3 provides a detailed description of the system context.

Section 4 provides an overview of the design technique used. In particular:

- subsection 4.1 describes and references the design method;
- subsection 4.2 gives the top level view of the system design.

Section 5 gives detailed top-level components information. In particular:

- subsection 5.1 describes type components;
- subsection 5.2 describes the components' purposes;
- subsection 5.3 describes the components' functionalities;
- subsection 5.4 lists the sub-components;
- subsection 5.5 describes the logical pre-conditions for using the component;

- subsection 5.6 describes the control and data-flow to and from the object;
- subsection 5.7 lists any resources required by the component;
- subsection 5.8 references any documentation necessary to understanding;
- subsection 5.9 describes the control and data-flow between subcomponents;
- subsection 5.10 gives an outline description of local data value.

Section 6 summarizes the feasibility study.

Section 7 gives a table cross referencing architectural components to software requirements.

D.2 System overview

The RATS *automatic reduction pipeline* to be designed and constructed is intend to be used for both the RATS and WSO-UV transit surveys. This software is necessary because reduction codes available to scientific community does not manage defocused images. It is also the intention of the RATS and WSO Team that this new software be more manageable, more easily extensible and more portable across on focus and defocused images. Please refer to the URD ([RD2]) for a more complete description of the background of this project.

D.3 System context

In the figure D.1 there is the description of interfaces with external components. For a complete description of the intended operating environment of the RATS and the pipeline, we refer to the URD ([RD2]) and the SRD ([RD3]) in which this environment is completely described. The system interfaces with the User through the H/W platform (keyboard, mouse and the screen) and with the printer through PostScript files.

D.4 System design

This section describes the method used for the decomposition of the system and gives a short description of the system components.

D.4.1 Design method

The design method used is object-oriented design. In particular we use the Object Modeling Technique (OMT) ([AD2]). The presented model is a decomposition view into components. A top-down approach is used to decompose the system.

D.4.2 System architecture

This section includes a description of the decomposition of the software to be developed into components for the purpose of modularization of the design. This description is given in the form of an OMT-style object diagram, in which the classes have been partitioned into 4 main layers. This partition has been chosen to bundle classes with a certain goal together and keep the interfaces between the different components as simple as possible.

D.4.2.1 H/W layer

The H/W layer includes the Schmidt telescope, the server and workstation PCs, the storage devices such as external hard disk and DVD/CD. It includes all access to the actual telescope configuration. All data capture information are provided to the rest of the program from this component and actual communication with the telescope and or images (or any other resource external to the software) takes place through this component. A scheme of this layer is shown in figure D.2.

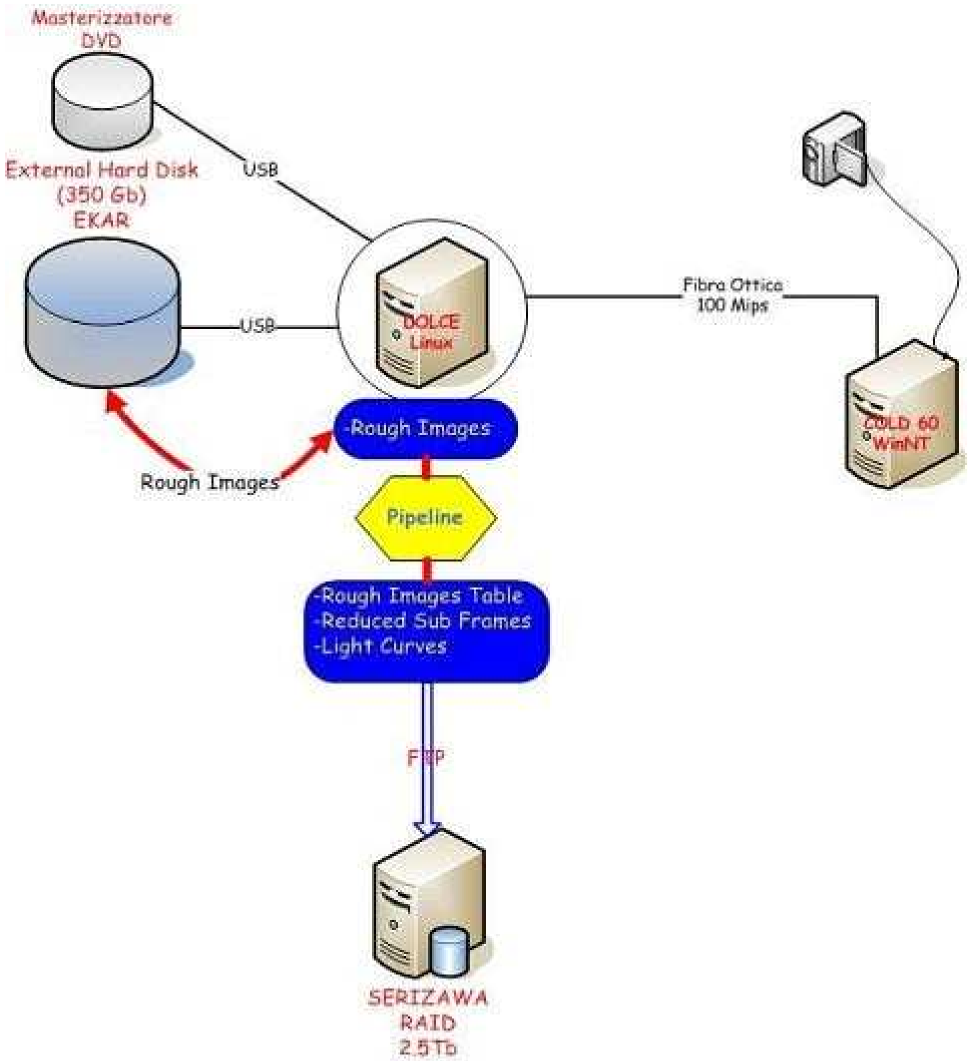

Figure D.1: S/W relationship with the external environment.

D.4.2.2 Off-line analysis layer

This layer includes all the ISIS procedure for data preparation in order to obtained from focused images the input masterlist for the RATS–*ARP*. This set of tools performs an interactive analysis. A scheme of this layer is shown in figure D.3.

D.4.2.3 Application layer

This is the core of RATS system. It contains the code necessary to compute the reduction to be executed. It is split up in an automatic calibration pipeline and a automatic reduction pipeline.
In the figures D.4 and D.5 both breakdowns are presented. Section D.4.2.5 of this document will specify the components in sufficient detail.

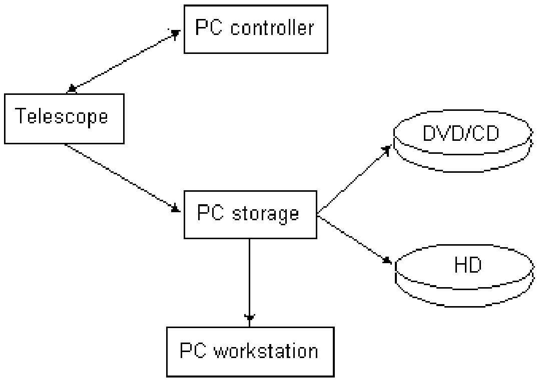

Figure D.2: Hardware layer for the software architecture.

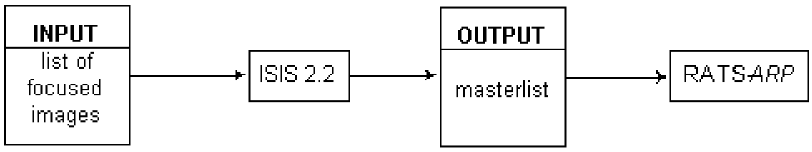

Figure D.3: Off-line analysis with ISIS 2.2 package.

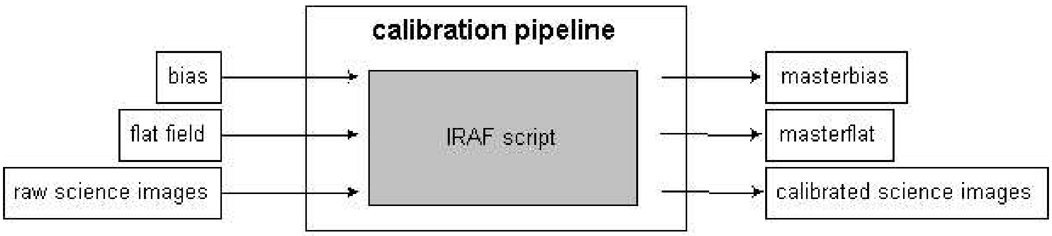

Figure D.4: Application layer: the calibration pipeline.

D.4.2.4 User Interface layer

This component is responsible for all the interfaces to the user of the RATS–*ARP* as well as the interpreter used to execute files. It takes care of monitoring and updating the reduction processes on screen, writing to a logfile and/or for the final User interfacing the access to a RATS-DB (TBD). A scheme of this layer is shown in figure D.6.

D.4.2.5 Decomposition description

Following the figures D.4 and D.5, the schematic list of subsystem decomposition and dependencies is:

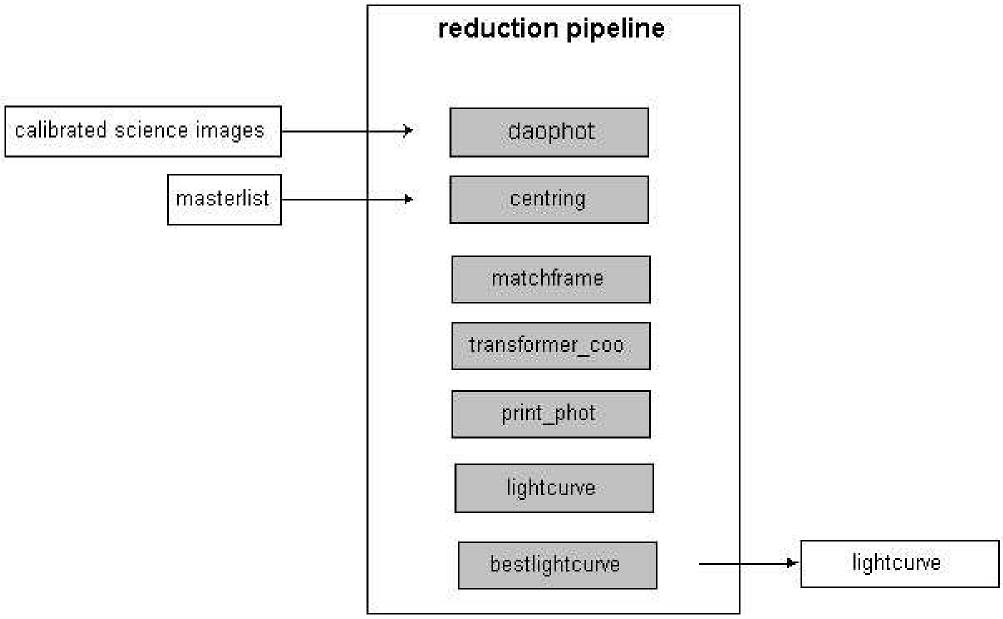

Figure D.5: Application layer: the reduction pipeline.

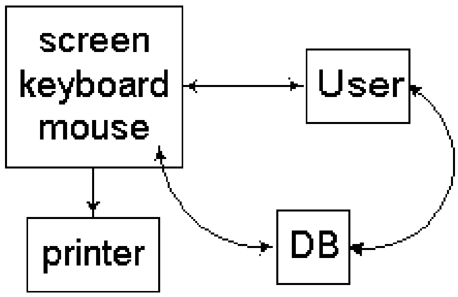

Figure D.6: User interface relationship.

- **calibration.csh:** pipeline
  - ▷ *calibra.cl:* IRAF script which perform calibration of raw science images.
- **procedura.csh:** reduction pipeline
  - ▷ *Daophot:* photometry
  - ▷ *centring:* centring images
  - ▷ *matchingframe:* frames match
    - – daomatch
    - – masterframe
      - > daomaster
  - ▷ *transformer-coo:* transformation of coordinates

- ▷ *lightcurve-creation:* lightcurves extractions and improvement

A detailed description of each of the component above can be found in the next section.

D.5 Components description

Complete descriptions of each pipeline's component have been included in this section. Each component has been given an unique identifier of the form ADDCn, with n a number in the range $[1; 9]$.

D.5.1 [ADDC1]: calibration.csh

D.5.1.1 Type

Pipeline.

D.5.1.2 Purpose

See subordinate components.

D.5.1.3 Function

Perform images calibration in order to obtain refined science images.

D.5.1.4 Subordinates

calibra.cl (ADDC2)

D.5.1.5 Dependencies

None.

D.5.1.6 Interfaces

It starts interactively, by a command line, when the Operator begins the reduction process of a night of observation.

D.5.1.7 Resources

See subcomponents and their descendants.

D.5.1.8 References

None.

D.5.1.9 Processing

See subordinate components.

D.5.1.10 Data

See subordinate components.

D.5.2 [ADDC2]: calibra.cl

D.5.2.1 Type

`IRAF` script.

D.5.2.2 Purpose

It reduces all the images acquired in a selected night of observation.

D.5.2.3 Function

Calibration of raw science images.

D.5.2.4 Subordinates

None.

D.5.2.5 Dependencies

None.

D.5.2.6 Interfaces

Called up by the parent.

D.5.2.7 Resources

No special or different requirements from [RD3].

D.5.2.8 References

[RD3].

D.5.2.9 Processing

- A masterbias is created from bias frames;
- a masterbias is subtracted from flat fields images;
- a masterflat is created from flat fields frames;
- raw science images are bias subtracted and divided by masterflat.

D.5.2.10 Data

- Masterbias
- Masterflat
- calibrated science images

D.5.3 [ADDC3]: procedura.csh

D.5.3.1 Type

Pipeline.

D.5.3.2 Purpose

See subordinate components.

D.5.3.3 Function

Performs automatic reduction in order to create lightcurve files.

D.5.3.4 Subordinates

- *Daophot* (ADDC4)
- *centring* (ADDC5)
- *matchframe.csh* (ADDC6)
- *transformer-coo* (ADDC7)
- *print-phot* (ADDC8)
- *lightcurve* (ADDC9)
- *bestlightcurves* (ADDC10)

D.5.3.5 Dependencies

ADDC1, ADDC2

D.5.3.6 Interfaces

It starts automatically when ADDC1 stops.

D.5.3.7 Resources

See subcomponents and their descendants.

D.5.3.8 References

None.

D.5.3.9 Processing

See subordinate components.

D.5.3.10 Data

See subordinate components.

D.5.4 [ADDC4]: daophot.f

D.5.4.1 Type

Executable.

D.5.4.2 Purpose

- It computes concentric aperture photometry.
- A separate sky value is determined for each source using specified inner and outer sky radii.
- Find positive brightness perturbations (i.e stars) in a 2 dimensional image and compute centroids and shape parameters

D.5.4.3 Function

For each science frame, this component performs the aperture photometry.

D.5.4.4 Subordinates

None.

D.5.4.5 Dependencies

A collection of images must exist.

D.5.4.6 Interfaces

A collection of images must exist.

D.5.4.7 Resources

No special or different requirements from [RD3].

D.5.4.8 References

[RD3].

D.5.4.9 Processing

- Find the raw coordinates of the stellar centroids;
- calculate an aperture magnitude of the defocused stars.

D.5.4.10 Data

- File.coo
- file.ap

D.5.5 [ADDC5]: centring.f

D.5.5.1 Type

Executable.

D.5.5.2 Purpose

It computes centroid coordinates of a stellar object.

D.5.5.3 Function

For each science frame, this component refines the calculation of coordinates.

D.5.5.4 Subordinates

None.

D.5.5.5 Dependencies

A collection of files with stellar coordinates must exist.

D.5.5.6 Interfaces

Called up by parent component.

D.5.5.7 Resources

No special or different requirements from [RD3].

D.5.5.8 References

[RD3].

D.5.5.9 Processing

Find the refined coordinates of the stellar centroids.

D.5.5.10 Data

File.coo

D.5.6 [ADDC6]: matchframe.csh

D.5.6.1 Type

Shell script.

D.5.6.2 Purpose

See subordinate components.

D.5.6.3 Function

For each science frame, this component find a match among the science frames that are shifted because of the different observing time.

D.5.6.4 Subordinates

- Daomatch
- masterframe.csh

D.5.6.5 Dependencies

A reference frame among all the science frames must exist.

D.5.6.6 Interfaces

Called up by parent component.

D.5.6.7 Resources

No special or different requirements from [RD3].

D.5.6.8 References

[RD3].

D.5.6.9 Processing

See subordinate components.

D.5.6.10 Data

See subordinate components.

D.5.7 [ADDC7]: daomatch.f

D.5.7.1 Type

Executable.

D.5.7.2 Purpose

It derives the shifts between the frames.

D.5.7.3 Function

This component combines the photometry from multiple science frames, finding the translation, rotation, and scaling solution between your different photometry files.

D.5.7.4 Subordinates

None.

D.5.7.5 Dependencies

A collection of aperture photometry related to each image must exist.

D.5.7.6 Interfaces

Called up by parent component.

D.5.7.7 Resources

No special or different requirements from [RD3].

D.5.7.8 References

[RD3].

D.5.7.9 Processing

Find the transformation (rotation and shifting) of coordinates of every stellar centroids compare to the reference frame.

D.5.7.10 Data

File.mch

D.5.8 [ADDC8]: masterframe.csh

D.5.8.1 Type

Shell script.

D.5.8.2 Purpose

See subordinate components.

D.5.8.3 Function

See subordinate components.

D.5.8.4 Subordinates

Daomaster.

D.5.8.5 Dependencies

See subordinate components.

D.5.8.6 Interfaces

Called up by parent component.

D.5.8.7 Resources

No special or different requirements from [RD3].

D.5.8.8 References

[RD3].

D.5.8.9 Processing

See subordinate components.

D.5.8.10 Data

See subordinate components.

D.5.9 [ADDC9]: daomaster.f

D.5.9.1 Type

Executable.

D.5.9.2 Purpose

It improves the offsets calculated by daomatch.

D.5.9.3 Function

It performs the actual file merging.

D.5.9.4 Subordinates

None.

D.5.9.5 Dependencies

A file.mch must exist in order to execute the merging.

D.5.9.6 Interfaces

Called up by parent component.

D.5.9.7 Resources

No special or different requirements from [RD3].

D.5.9.8 References

[RD3].

D.5.9.9 Processing

This component iteratively solves for zero-point shifts in the magnitude scales from image to image by essentially using all of the stable stars as "comparison" stars.

D.5.9.10 Data

A refined new-file.mch

D.5.10 [ADDC10]: transformer-coo.f

D.5.10.1 Type

Executable.

D.5.10.2 Purpose

It applies the improved offsets and recompute the unshifted coordinates.

D.5.10.3 Function

It performs an interpolation of coordinates values according to the transformation file.

D.5.10.4 Subordinates

None.

D.5.10.5 Dependencies

A file.mch must exist.

D.5.10.6 Interfaces

Called up by parent component.

D.5.10.7 Resources

No special or different requirements from [RD3].

D.5.10.8 References

[RD3].

D.5.10.9 Processing

Find the transformed coordinates.

D.5.10.10 Data

File with transformed coordinates.

D.5.11 [ADDC11]: lightcurve-creation

D.5.11.1 Type

Executable.

D.5.11.2 Purpose

For each star, it produces the file with the magnitude versus Julian Day.

D.5.11.3 Function

For a selected star, this component prints in a file the magnitude it has in each frame, calculate a zero point and iteratively refined the stellar magnitude.

D.5.11.4 Subordinates

None.

D.5.11.5 Dependencies

A masterlist must exist.

D.5.11.6 Interfaces

Called up by parent component.

D.5.11.7 Resources

No special or different requirements from [RD3].

D.5.11.8 References

[RD3].

D.5.11.9 Processing

Create the lightcurve files.

D.5.11.10 Data

File lightcurve.dat.

D.6 Feasibility and resource estimates

The following resources will be required (estimated) for the building, maintenance and operation of the software to be developed:

- a Pentium IV workstation with 1 GHz, 256 MB RAM, 50 GB free disk space at least, disk access time of 10 msec and a screen resolution of at least 1152 x 900 pixels;
- OS: Linux with Fedora 6.0 OS;
- `ISIS` packages;
- `DAOPHOT` (modified by S/W developer);
- `DAOMATCH` (Stetson's code);
- `DAOMASTER` (Stetson's code);
- `IRAF` code;
- `g77 Fortran 77` compiler.

All of these are described in the SRD ([RD3]).
At this point the project seems feasible, since most of the resources required, as described above, are available at the time of writing of this document.

D.7 SR vs. components traceability matrix

If a specific SR is fulfilled by more than one ADD component, the notation adopted in the second column of the table below is ADDCx-y-z-... where x-y-z-... are the number of the component involved.
If a specific SR is fulfilled by all the ADD components, the notation adopted in the second column of the table below is ADDC[1:11].
If a SR is related to H/W layer but is not correlated to a pipeline component, the notation adopted in the second column of the table below is H/WL.

Table D.2: Software Requirements *vs.* Architectural Components traceability matrix.

SR	Component(s)
SR-FR-01	ADDC1-2-3-4-5
SR-FR-02	ADDC1-2
SR-FR-03	ADDC1-2-3-4
SR-FR-04	ADDC1-2
SR-FR-05	ADDC1-2
SR-FR-06	ADDC1-2
SR-FR-07	ADDC1-2-3
SR-FR-07	ADDC6
SR-FR-09	ADDC5-6
SR-FR-10	ADDC4
SR-FR-11	ADDC4
SR-FR-12	ADDC6-7-8-9
SR-FR-13	ADDC1-2
SR-FR-14	ADDC5
SR-FR-15	ADDC3-4-5-6
SR-FR-16	H/WL
SR-FR-17	ADDC1-2
SR-IR-SI-01	H/WL
SR-IR-HI-01	H/WL
SR-IR-CI-01	H/WL
SR-OR-OP-01	ADDC1-3
SR-OR-MM-01	H/WL
SR-OR-MM-02	ADDC1-3

Continued on next page

Continued from previous page

SR	**Component(s)**
SR-OR-SP-01	ADDC1-3
SR-RR-PP-01	H/WL
SR-RR-RM-01	H/WL
SR-RR-DS-01	H/WL
SR-RR-DT-01	H/WL
SR-RR-SS-01	ADDC1-2
SR-VV-UT-01	ADDC[1:11]
SR-VV-UT-02	ADDC1-3
SR-VV-IT-01	ADDC[1:11]
SR-VV-IT-02	ADDC4-5-7-9-10-11
SR-POR-01	ADDC[1:11]
SR-QR-01	ADDC[1:11]
SR-QR-02	ADDC[1:11]
SR-QR-03	ADDC[1:11]
SR-QR-04	ADDC[1:11]
SR-QR-05	ADDC[1:11]
SR-MR-01	ADDC[1:11]
SR-MR-02	ADDC[1:11]
SR-MR-03	ADDC[1:11]

Appendix E

RATS Automatic Reduction Pipeline: Software User Manual (SUM)

Issue	Date	Section	Remarks
0.1	24/03/07	All	Creation of the document
0.2	31/03/07	All	First draft
0.4	15/04/07	All	Update after first draft revision
0.7	30/04/07	All	Update after second draft revision
0.9	05/05/07	All	Final draft revision
1.0	14/05/07	All	**Software review**

Table E.1: Change record for RATS–*ARP* SUM document.

E.1 Introduction

The italian project RATS (RAdial velocities and Transit Search) is a collaboration of different INAF Observatories (Padova, Catania, Napoli and Palermo), the Department of Astronomy and Physic of the University of Padova and ESA.
RATS–*ARP* has been developed in order to automatically obtain transit lightcurves for the RATS extrasolar planets survey.

E.1.1 Intended readership

This document is addressed to the User of RATS pipeline who is out to exploit RATS–*ARP* as scientific tool in order to identify and characterize candidate planetary transits.

E.1.2 Applicability statement

RATS–*ARP* software is released under GPL license and its use is duty-bound by the license itself. If the User does not accept one or more conditions, he cannot exploit the software.

E.1.3 Purpose

The scope of this document is to provide to the User the informations about installation, compiling and usage of RATS–*ARP* software.

E.1.4 How to use this document

This document is not intended to be a operating system tutorial. The knowledge of the User about the platform and compiler tools he is going to use for exploiting the pipeline is assumed.

E.1.5 Related documents

The related documents to this manual are:

- RATS–*ARP* User Requirements Document (URD)
- RATS–*ARP* Software Requirements Document (SRD)
- RATS–*ARP* Architectural and Design Document (ADD)
- RATS–*ARP* **SCD!** (SCD)

E.1.6 Definitions, acronyms and abbreviations

In the following text these acronyms are used:

Radial Velocities and Transit Search (RATS)

RATS–Automatic Reduction Pipeline (RATS–ARP)

User Requirements Document (URD)

Software Requirements Document (SRD)

Architectural and Design Document (ADD)

Software User Manual (SUM)

E.1.7 Problem reporting instructions

Problems in compiling and installation not considered in this document are to be pointed out via e-mail of the software's author.

E.1.8 Contacts

Author: Valentina Granata
e-mail: valentina.granata@unipd.it

E.2 Overview of the document

The structure of the document is as follows:

Section 3 provides the specific description of installing procedures.

Section 4 provides the specific instructions for software's usage. In particular:

- subsection 4.1 describes the functional requirements;
- subsection 4.2 describes cautions and warnings;
- subsection 4.3 describes procedures' modality;
- subsection 4.4 describes potential errors and causes.

Section 5 provides the definitions for reference usage. In particular:

- subsection 5.1 describes the functional requirements;
- subsection 5.2 describes the formal description;
- subsection 5.3 describes cautions and warnings;
- subsection 5.4 describes some input examples;
- subsection 5.5 describes potential errors and causes.

E.2.1 Hardware requirements

RATS–*ARP* has been developed for LINUX operational systems but, in principle any hardware restriction is contemplated. A few GB free disk space are required in order to allow the correct working of the pipeline, depending on the characteristics of images acquired. 256 MB RAM are the minimum requirements in order to speed up the software execution and minimize the disk access number.

E.2.2 Software requirements

RATS–*ARP* has been developed under Linux but, as the pipeline include `FORTRAN 77` codes and shell scripts, any restrictions on platform type have been detected: the software has been compiled and tested on Unix platform without any errors or functional problems. compiling tests have not been executed on Macintosh nor Windows platforms. In order to compile `FORTRAN 77` codes a g77 (GNU Fortran 77 compiler) open-source compiler is required. Up to now, g77 is based on GNU GCC project and different releases are available under Linux/Unix, Windows and Macintosh. Any other `FORTRAN 77` compiler (such as Intel Fortran Compiler, open source only for personal use under Linux) has been employed.
The User has to refer to specific compiler documentation for their correct usage.
Some bugs have been tested out with ISIS 2.1 version. ISIS2.2 is a slightly modified version which includes debugging and compatible with all versions of the compiler gcc, therefore any other following version will be suitable.
In the following, all the examples for the pipeline compiling refer to Linux platform, g77 compiler an ISIS 2.2 version.

E.3 Installation

After the User has obtained a RATS–*ARP* copy in a tar.bz2 package, he shall uncompress the archive in a suitable directory and shall compile the source codes inside. The files keep stored in rats-arp.tar.bz2 are:

- ▷ **INPUT files**:
  - photo.opt
  - daophot.opt
  - masterlist.als
- ▷ **EXECUTABLE files**:
  - *procedure.csh*
  - *daophot-mod.f*
  - *centring.f*
  - *matchframe.csh*
  - *masterframe.csh*
  - *transformer-coo.f*
  - *juliandate.csh*
  - *idlist.f*
  - *print-phot.f*

- *lightcurve.f*
- *lightcurve1.f*
- *bestlightcurve.f*
- *bestlightcurve1.f*

The file procedure.csh contains the calls to other executable files mentioned. In order to create all the executables, the User shall compile each Fortran file (*.f) as:

g77 -o executable sourcecode.f

The IRAF and ISIS2.2 packages' download and installation shall held by the User.

E.4 Instruction

In this section, the RATS–*ARP* functionality and its usage are described in detail.

- ▷ *photo.opt*
- ▷ *daophot.opt*
- ▷ *masterlist.als*

For detailed informations about the structure and format of each input files mentioned above, the User shall see following sections 5.1 and 5.2.
In order to use RATS–*ARP*, the User shall set all the executables and input files in the working directory together with .fits images acquired and launch the software: the execution is automatic and completely determined by the configuration selected by the User. A logfile shall be stored in the same directory, keeping track of the of the pipeline's steps: in this way, any scheme shall be displayed on the screen. The User can choose to avoid this logfile: in this way a control scheme shall be displayed. The magnitudes and coordinates of the potential candidate transits shall be stored on ASCII format files.
For detailed informations about the structure and format of each output file mentioned above, the User shall see following section E.5.5

E.4.1 Functional description

In order to use the RATS pipeline, the User shall determine the characteristics of instrumentation adopted to acquire the images. The input files are:

E.4.2 Procedures

RATS–*ARP* works only in a non-interactive mode: after compiling the executables and defining the input files, the User has only to launch the main executable. During the execution, the software shows on screen (standard output) or in a stored logfile messages and warnings about the pipeline progresses. A message informs the User the end of the reduction process.

E.5 References

In this section, the structure and format of input files are introduced. Finally, examples of some output file are shown.

E.5.1 Functional description

The *photo.opt* file contains the list of aperture radii used by `DAOPHOT` when performing aperture photometry, such as:

- on the 1^{st} row: the pixel value of the first aperture;

- on the 2^{nd} row: the pixel value of the second aperture;
- on the 3^{rd} row: the pixel value of the third aperture;
- on the 4^{th} row: the pixel value of the fourth aperture;
- on the 5^{th} row: the pixel value of the fifth aperture;
- on the 6^{th} row: the pixel value of the sixth aperture;
- on the 7^{th} row: the pixel value of the seventh aperture;
- on the 8^{th} row: the pixel value of the eighth aperture;
- on the 9^{th} row: the pixel value of the ninth aperture;
- on the 10^{th} row: the pixel value of the tenth aperture;
- on the 11^{th} row: the pixel value of the eleventh aperture;
- on the 12^{th} row: the pixel value of the twelfth aperture;
- on the 13^{th} row: the pixel value of inner radii of the sky annulus;
- on the 14^{th} row: the pixel value of the outer radii of the sky annulus.

It's important that User set the apertures in order to sample the PSF adequately, since it is these settings which will determine how accurate the model PSF created for the image is.

The *daophot.opt* file contains the list of parameters which optimize the reduction code `DAOPHOT` for the specific properties of the User's images, such as:

- on the 1^{st} row: the readout noise of detector;
- on the 2^{nd} row: the gain factor of the detector;
- on the 3^{rd} row: the radius of the circle within which the PSF is to be defined;
- on the 4^{th} row: the number of iteration to reduce the weight of discrepant pixels;
- on the 5^{th} row: the approximate Full Width Half Maximum;
- on the 6^{th} row: the fitting radius used in performing the profile fits;
- on the 7^{th} row: the lower level below the frame's mean sky values;
- on the 8^{th} row: the higher level above the frame's mean sky values;
- on the 9^{th} row: the significance threshold level of brightness;
- on the 10^{th} row: the degree of complexity with which the PSF is to be modeled;
- on the 11^{th} row: the value to decide weather to display results in real time or in a logfile;
- on the 12^{th} row: the value associated to the analytic first approximation to the PSF.

It's important that User set the parameters indicating only two alphanumeric characters. Each parameter identifier is followed by an equals sign and this is followed by a number.

The *masterlist.als* file contains the stellar characteristics of images acquired on focus, such as:

- header (2 rows);
- 2 blank rows;
- on the 1^{st} column: on the 1st column: the temporary stellar id;
- on the 2^{nd} column: on the 2nd column: the x stellar position (in pixel);
- on the 3^{rd} column: on the 3rd column: the y stellar position (in pixel);
- on the 4^{th} column: on the 4th column: the lower cut-off value of the admitting pixels;
- on the 5^{th} column: on the 5th column: the higher cut-off value of the admitting pixels;
- on the 6^{th} column: on the 6th column: the threshold in ADU for the detection of the stars;
- on the 7^{th} column: on the 7th column: the radius of the aperture No 1;
- on the 8^{th} column: on the 8th column: the parameter of the CCD camera "photons per ADU";
- on the 9^{th} column: on the 9th column: the parameter "Read noise".

Except the header and blank rows (4 rows in total), the total number of rows depends on the number of suitable stars detected on the focused images.

E.5.2 Formal description

The User shall find all the specific informations about the length and format of the CHARACTER variables in the RATS–*ARP* code.

E.5.3 Examples

E.5.4 Input files

In this section one example for each kind of input file are shown.

photo.opt

```
A1 = 3.
A2 = 4.
A3 = 5.
A4 = 6.
A5 = 7.
A6 = 8.
A7 = 9.
A8 = 0.
A9 = 0.
AA = 0.
AB = 0.
AC = 0.
IS = 10.
OS = 40.
```

daophot.opt

```
re = 5.000
ga = 1.65
psf = 13.580
ex = 9.000
fw = 5.
fi = 5.
lo = 3.000
hi = 55000.000
th = 3.000
va = 2.000
wa = -1.000
an = 6.000
```

masterlist.als

```
 NL    NX      NY      LOWBAD   HIGHBAD   THRESH    AP1     PH/ADU   RNOISE    FRAD
  1   2014    2045     -500.0   55000.0    17.68    3.00     1.08     5.00     4.01

  1  14.396  1030.730  18.2250   0.1400   99.9999  9.9999  18.4640   0.0841  99.9999  9.9999  -0.3895  1.0000
  2  15.335  1670.754  17.3870   0.0693   18.3300  0.0866  17.2900   0.0329  99.9999  9.9999  -0.4217  1.0610
  3  16.468    80.116  17.8660   0.1059   18.5950  0.1508  17.9670   0.0575  18.0920  0.0917  -0.3785  1.1630
  4  17.133  1676.314  17.0460   0.0531   18.0880  0.0712  17.0020   0.0267  17.0150  0.0278  -0.4127  1.0438
  5  18.081   538.893  16.0860   0.0274   16.9920  0.0295  15.8940   0.0136  16.1230  0.0156  -0.3582  1.3188
  6  19.129   647.673  18.1890   0.1343   99.9999  9.9999  18.3570   0.0768  18.4100  0.0834  -0.3833  1.0000
  7  21.511  1473.138  18.0310   0.1220   19.0790  0.2483  18.3110   0.0750  18.2280  0.0728  -0.4140  1.0000
  8  22.257  1231.996  99.9999   9.9999   99.9999  9.9999  19.3720   0.2856  18.9530  0.1645  -0.3550  1.0000
  9  22.563  1591.749  17.2620   0.0563   18.1530  0.0707  17.0660   0.0281  17.2320  0.0328  -0.4135  1.0000
```

E.5.5 Output file

In this section an example of output file is shown. The file name includes:

- the number of iteration performed in order to improve the stellar magnitude calculation (1^{st} digit);
- the point "." (2^{nd} digit)
- the string "*dat*" (from 3^{rd} to 5^{th});
- the number of star (from 6^{th} to 10^{th} digit)

6.dat02038

53420.02693287	1870.5970	498.6810	15.685	461.679	18.90	0.077
53420.02809028	1868.3020	501.3790	15.727	461.899	18.62	0.079
53420.02931713	1868.5610	497.6270	15.881	459.152	18.68	0.091
53420.03057870	1865.6430	503.1800	15.843	461.391	19.12	0.090
53420.03180556	1864.7160	502.8990	15.691	463.196	18.73	0.077
53420.03440972	1861.1540	508.6160	15.621	471.502	18.58	0.072
53420.03618056	1858.8790	504.7290	15.690	472.355	18.96	0.079
53420.03738426	1856.8690	511.6030	15.696	479.678	19.17	0.081
53420.03856481	1854.1230	510.8190	15.670	478.120	18.92	0.078

The final output contains 7 columns, allocated as follows:

- mean Julian day of the i^{th} image;
- x pixel coordinate on the i^{th} image;
- y pixel coordinate on the i^{th} image;
- stellar magnitude;
- sky value;
- error on sky value;
- error on magnitude.

E.6 Warnings and errors: possible causes

Lack and/or incompleteness of one or more file mentioned in the sections above shall cause the failure of the software: in these cases, an error message is recorded on logfile. Input values without any physical sense, can led to senseless results devoid of scientific benefits. Verification of configuration of input parameters is by the User.
The errors managed by the RATS–*ARP* are related to correct acquisition of input parameters and the resulting convergence in the reduction process. If some inconsistencies in input files reading or errors due to a non-convergence in the reduction process happened (such as, a bad formatting input file or a parameter missing), the software stops after giving informations to the User about the file corrupted with an error message on the screen (standard error output) or on logfile.
If some inconsistencies occurs but they do not compromise the results of the process, a warning message appears on the screen (standard error output) or on logfile and the software carries on.

A list of possible warning messages and their meaning is given in table E.2.
A list of possible error messages and their meaning is given in table E.3.

COD.	WARNING MESSAGE	MEANING
101	"There are more than 10 biases"	During the night, more the requested ([SRD]) 10 bias are acquired. All of them are used to create masterbias file.
102	"There are more than 10 flats"	During the night, more the requested ([SRD]) 10 flat are acquired. All of them are used to create masterflat file.
103	"Some bias frames missing"	During the night, less the requested ([SRD]) 10 bias are acquired. The bias frames available are used to create masterbias file.
104	"Some flat frames missing"	During the night, less the requested ([SRD]) 10 flat are acquired. The flat frames available are used to create masterflat file.
105	"Bias raster is not complete"	Bias raster is not complete. All the available bias frames are used to create masterbias file.
106	"Flat raster is not complete"	Flat raster is not complete. All the available flat frames are used to create masterflat file.

Table E.2: RATS–*ARP* warnings: messages and meaning.

COD.	ERROR MESSAGE	MEANING
601	"Masterbias not exists"	Masterbias does not exists. The science images calibration procedure cannot carry on. Failure and Exit.
602	"Masterflat not exists"	Masterflat does not exists. The science images calibration procedure cannot carry on. Failure and Exit.
603	"An error occurs in aperture photometry calculation"	An error occurs in aperture photometry calculation. The User shall check this step by himself. The procedure cannot carry on. Failure and Exit.
604	"An error occurs in the centring process"	An error occurs in the centring process. The User shall check this step by himself. The procedure cannot carry on. Failure and Exit.
605	"An error occurs in the matching of frames"	An error occurs in the matching frame process. The User shall check this step by himself. The procedure cannot carry on. Failure and Exit.

Table E.3: RATS–*ARP* errors: messages and meaning.

Appendix F

RATS Automatic Reduction Pipeline: code documentation

Issue	Date	Section	Remarks
0.1	24/03/07	All	Creation of the document
0.2	31/03/07	All	First draft
0.4	15/04/07	All	Update after first draft revision
0.7	30/04/07	All	Update after second draft revision
0.9	05/05/07	All	Final draft revision
1.0	14/05/07	All	**Software review**

Table F.1: Change record for RATS–*ARP* code documentation.

F.1 Introduction

The italian project RATS (RAdial velocities and Transit Search) is a collaboration of different INAF Observatories (Padova, Catania, Napoli and Palermo), the Department of Astronomy and Physic of the University of Padova and ESA. RATS–*ARP* has been developed in order to automatically obtain transit lightcurves for the RATS Extrasolar Planets survey.

F.2 Program description

In this section, all the RATS–*ARP* components are described. We present the mail shell script program in detail and summarizing the tasks of the pipeline with guidelines. In the following subsection, Stetson's DAOPHOT, DAOMATCH and DAOMASTER programs are not quoted because all rights are reserved and the code cannot be published without author's assent. The DAOPHOT version exploits in RATS–*ARP* has been slightly modified but only some warning messages has been included in this version. For this reason, we do not quoted this code all the same.
The flow diagram of the whole reduction pipeline is shown on page 230.

F.2.1 Pre-reduction: calibration.csh

```
#!/bin/csh -f
#-----------------------------------------------------------------------
# FILE NAME: calibration.csh
# PURPOSE: This shell script contains the IRAF script to perform
#          masterbias and masterflat creation and science images
#          calibration.
# AUTHOR:  Valentina Granata
# LAST REVISION: 26/03/07 (added header).
# This program is freeware.
#-----------------------------------------------------------------------

set bin = /home/RATS/executable/

rm biaslist flatlist fblist imagelist cimagelist
ls *B*.fits >> biaslist
ls *F*.fits >> flatlist
ls *O*.fits >> imagelist

# IRAF: flat, bias & correction of images
cl < calibra.cl << EOF >& logfile
logout
EOF
```

F.2.2 Reduction: reduction.csh

```
#-----------------------------------------------------------------------
# FILE NAME: reduction.csh
# PURPOSE: This shell script contains all the FORTRAN77 programs and
#          script needed to perform photometric analysis and lightcurve
#          determination.
# AUTHOR:  Valentina Granata
# LAST REVISION: 26/03/07 (added header).
# This program is freeware.
#-----------------------------------------------------------------------
#
#! /bin/csh -f
set bin = /home/RATS/executable/

#------------ parameter declaration ------------

set liste = `awk '{print $1}' "listaimm"`
set xmin   =   20
set xmax   = 2020
set ymin   =   20
set ymax   = 4170
set magmin =   10
set magmax =   18
set par   = `awk '{print $3}' "parametri"`
set nb = $#liste
set i = 1

rm -f dat*
#------------- julian date --------------------
rm -f MJD
```

```
    csh juliandate.csh

rm -f listamjd
awk '{print $3}' "MJD" >> 'listamjd'
set listemjd = `awk '{print $3}' "MJD"`
#------------- reading masterlist ------------
rm -f listaid_masterl
./idlist<<EOF
EOF
#---------------------------------------------
#              for i-th images
#---------------------------------------------
 while($i <= $nb)

         set fileroot = $liste[$i]

         rm -f $fileroot.coo
         rm -f $fileroot.ap
#--------------- daophot ---------------------
         echo ''
         echo 'Starting daophot ... '$fileroot
     $bin/daophot<<EOF >/dev/null
OPT

re = $par[1]
ga = $par[2]
psf =$par[3]
ex = $par[4]
fw = $par[5]
fi = $par[6]
lo = $par[7]
hi = $par[8]
th = $par[9]
va = $par[10]
wa = $par[11]
an = $par[12]

AT $fileroot

FI
1,1
$fileroot.coo
Y

PHOT
photo.opt
IS = 10.
OS = 40.

$fileroot.coo
$fileroot.ap

EXIT
EOF
#-------------- centering -------------------
rm -f find1.coo
```

```
cp -f $fileroot.coo find1.coo
rm -f coord.ap
rm -f picture
rm -f coord_new.ap
cp $fileroot.ap coord.ap
echo $fileroot > 'picture'
         echo 'centring is running ... '
./centring<<EOF >/dev/null
EOF
rm -f coord.ap
#--------------- matching frames --------------
rm -f $fileroot.ap
mv coord_new.ap $fileroot.ap
         echo 'matching frames ... '
    csh matchframe.csh<<EOF >/dev/null
EOF
#--------------- coordinate transf ------------
rm -f picture
         echo 'transformer_coo is running ... '
./transformer_coo<<EOF >/dev/null
EOF
head -3 $fileroot.coo > 'header'
cat 'coord_trasf' |  more >> 'header'
mv -f 'header' $fileroot.coo
rm -f coord_trasf
#--------------- daophot 2 --------------------
rm -f $fileroot.ap
        echo 'Starting daophot on centered stars ... '$fileroot
     $bin/daophot<<EOF >/dev/null
OPT
re = $par[1]
ga = $par[2]
psf =$par[3]
ex = $par[4]
fw = $par[5]
fi = $par[6]
lo = $par[7]
hi = $par[8]
th = $par[9]
va = $par[10]
wa = $par[11]
an = $par[12]

AT $fileroot

PHOT
photo.opt
IS = 10.
OS = 40.

$fileroot.coo
$fileroot.ap

EXIT
EOF
#--------------- printing photometry ----------
```

```
#
         set mjd = $listemjd[$i]
echo $mjd > 'juliandate'
rm -f photom.ap
rm -f listacurve
cp -f $fileroot.ap photom.ap
        echo 'print_phot is running ... '
./print_phot<<EOF
EOF
#
@ i += 1
end
#-----------------------------------------------
#                START CYCLE
#-----------------------------------------------
set nn = 5

rm -f listacurve
rm -f *lightcurve*.dat
rm -f 1.dat*
rm -f 2.dat*
rm -f 3.dat*
rm -f 4.dat*
rm -f 5.dat*
rm -f 6.dat*
        echo ''
set iter = 0
 while($iter <= $nn)

        echo 'lightcurve is running ... iteraction n. '$iter

if ($iter == 0) then
ls dat* >> listacurve
./lightcurve<<EOF
EOF
else
./lightcurve1<<EOF
$iter
EOF
endif

        echo 'bestlightcurve is running ... iteraction n. '$iter

if ($iter == 0) then
./bestlightcurve<<EOF
$iter
EOF
else
./bestlightcurve1<<EOF
$iter
EOF
endif
@ iter += 1
ls $iter.dat* > listacurve
end
```

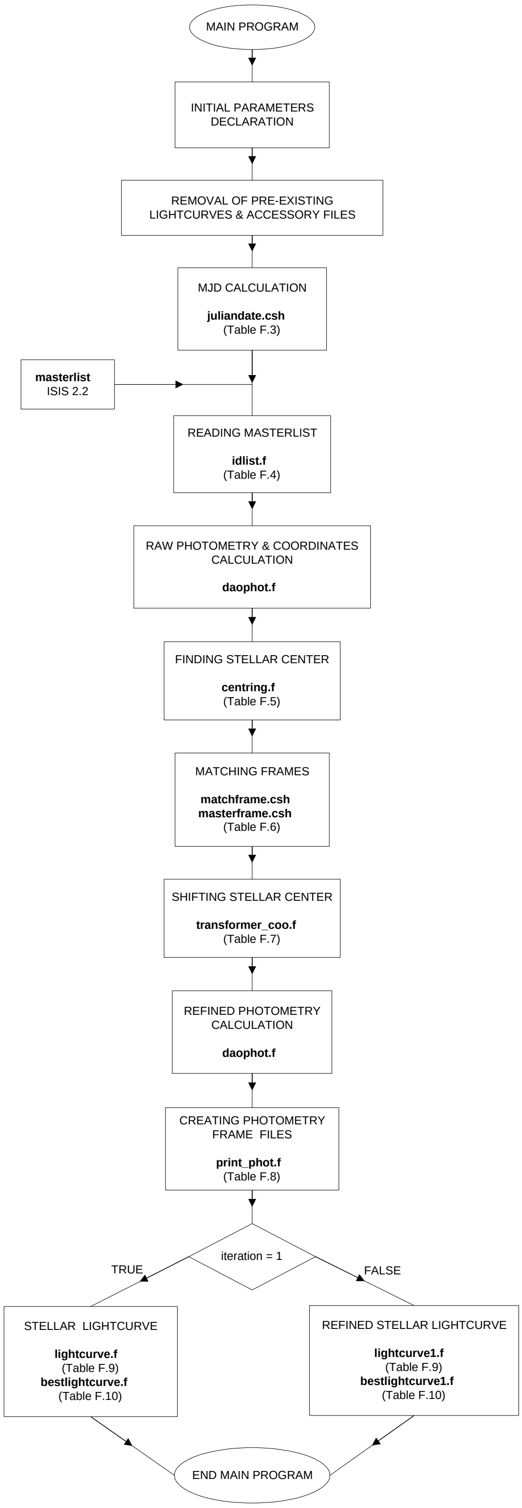

Figure F.1: Data flow for the main reduction program `reduction.csh`.

calibra.cl	
Programming language	`IRAF` script
Input file(s)	raw images
Output file(s)	masterbias, masterflat, calibrated images
Purpose	This script contains the IRAF tasks and parameters to perform masterbias and masterflat creation and science images calibration.
Author	Valentina Granata
Last revision	26/09/07 (added header)

Table F.2: `calibra.cl IRAF` script.

juliandate.csh	
Programming language	shell script
Input file(s)	science images
Output file(s)	list of images names
Purpose	This shell script performs julian day calculation from file naming.
Author	Valentina Granata
Last revision	26/09/07 (added header)

Table F.3: `juliandate.csh` shell script.

idlist.f	
Programming language	`FORTRAN77` executable
Input file(s)	masterlist
Output file(s)	*ad hoc* formatted masterlist
Purpose	This executable reads parameters from masterlist file.
Author	Valentina Granata
Last revision	26/09/07 (added header)

Table F.4: `idlist.f FORTRAN77` executable.

centring.f	
Programming language	FORTRAN77 executable
Input file(s)	raw aperture & coordinates files
Output file(s)	center coordinates files
Purpose	This executable performs coordinates determination for each stellar centroid
Author	Valentina Granata
Last revision	26/09/07 (added header)

Table F.5: `centring.f` `FORTRAN77` executable.

matchframe.csh & masterframe.csh	
Programming language	shell script
Input file(s)	center coordinates files
Output file(s)	shifted and matched frames
Purpose	The former shell script contains DAOMATCH program and shell scripts needed to perform matching among different frames, all referred to the first image taken as reference; the latter contains the DAOMASTER and FORTRAN77 programs needed to actually calculate the shift and rotation produced by time.
Author	Valentina Granata
Last revision	26/09/07 (added header)

Table F.6: `matchframe.csh` and `masterframe.csh` shell scripts.

transformer_coo.f	
Programming language	FORTRAN77 executable
Input file(s)	initial coordinates files
Output file(s)	shifted coordinates files
Purpose	This executable performs coordinates transformation for each stellar centroid.
Author	Valentina Granata
Last revision	26/09/07 (added header)

Table F.7: `transformer_coo.f` `FORTRAN77` executable.

print_phot.f	
Programming language	`FORTRAN77` executable
Input file(s)	refined photometry aperture files
Output file(s)	photometry files for each frame
Purpose	This executable prints on file photometric parameters such as: `x, y, mag, sky, ...`
Author	Valentina Granata
Last revision	26/09/07 (added header)

Table F.8: `print_phot.f FORTRAN77` executable.

lightcurve.f	
Programming language	`FORTRAN77` executable
Input file(s)	photometry files for each frame
Output file(s)	stellar lightcurve `ASCII` files
Purpose	This executable magnitude calculation at the first iteration.
Author	Valentina Granata
Last revision	26/09/07 (added header)

lightcurve1.f	
Programming language	`FORTRAN77` executable
Input file(s)	photometry files for each frame
Output file(s)	stellar lightcurve `ASCII` files
Purpose	This executable magnitude calculation if counter iteration is greater than 1.
Author	Valentina Granata
Last revision	26/09/07 (added header)

Table F.9: `lightcurve.f` and `lightcurve.f FORTRAN77` executables.

bestlightcurve.f	
Programming language	FORTRAN77 executable
Input file(s)	stellar lightcurve ASCII files
Output file(s)	refined lightcurve ASCII files
Purpose	This executable performs refined magnitude calculation and zero point determination at the first iteration.
Author	Valentina Granata
Last revision	26/09/07 (added header)

bestlightcurve1.f	
Programming language	FORTRAN77 executable
Input file(s)	stellar lightcurve ASCII files
Output file(s)	refined refined lightcurve ASCII files
Purpose	This executable performs refined magnitude calculation and zero point determination if counter iteration is greater than 1.
Author	Valentina Granata
Last revision	26/09/07 (added header)

Table F.10: `bestlightcurve.f` and `bestlightcurve1.f` `FORTRAN77` executables.

Bibliography

Adachi I., Hayashi C., Nakagawa K., 1976, Prog. Teor. Phys., 56, 1756

Alard C., Lupton R.H., 1998, ApJ, 503, 325

Alard C., 2000, A&AS, 144, 363

Alcock C. et al., 1993, Nature, 365, 621

Alencar S.H.P., Batalha C., 2002, ApJ, 571, 378

Alonso R. et al., 2004, ApJ., 613, L153

Artymowicz P., Lubow S.H., 1994, ApJ, 421, 655

Bakos G., Shporer A., Pal A., Torres G., Kovacs G., Latham D., Mazeh T., Ofir A., Noyes R., Sasselov D., Bouchy F., Pont F., Queloz D., Udry S., Esquerdo G., Sipocz B., Lazar J., 2007, ApJL (*submitted*)

Baraffe I., Chabrier G., Allard F., Hauschildt P.H., 2002, A&A, 382, 563

Baraffe I., Baraffe I., Chabrier G., Barman T.S., Allard F., Hauschildt P.H., 2003, A&A, 402, 701

Baranne A. et al., 1996, A&AS, 119, 373

Barbieri M., Marzari F., Scholl H., 2002, A&A, 396, 219

Barbieri M. et al., 2004, in *Stellar structure and habitable planet finding*, Proc. 2nd EDDINGTON workshop, ed. Favata F., Aigrain S., 538, 163

Barge P., Pellat R., 1993, Icarus, 104, 79

Bate M.R., Lubow S.H., Ogilvie G.I., Miller K.A., 2003, MNRAS, 341, 213

Benedict G.F., e al., 2002, ApJ, 581, L115

Bennet D.P., Rhie S.H., 1996, ApJ, 472, 660

Bennet D.P., Rhie S.H., 2002, ApJ, 574, 985

Benest D., 1988, A&A, 206, 143

Benest D., 1989, A&A, 223, 361

Benest D., 1993, Celestial Mechanics and Dynamical Astronomy, 56, 45

Benest D., 1996, A&A, 314, 983

Benest D., 2003, A&A, 400, 1103

Benz W., Asphaug E., 1999, Icarus, 142, 5

Beust, H., 2003, A&A 400, 1129.

Bodenheimer P., Pollack J.B., 1986, Icarus, 67, 391

Bodenheimer P., Hubickyj O., Lissauer J., 2000, Icarus, 67, 391

Bodenheimer P., Lin D.N.C., Mardling R.A., 2001, ApJ, 548, 466

Bodenheimer P., Lin D.N.C., 2002, *Annual Review of Earth and Planetary Sciences 30*, 113, 148

Bodenheimer P., Laughlin G., Lin D.N.C., 2003, ApJ, 592, 555

in *Scientific Detectors for Astronomy*, Amico P., Beletic J.W., J.E. Beletic eds., Kluwer Academic Publishers, 423

Bond I.A. et al., 2001, MNRAS, 327, 868

Bond, I. A., et al. 2004, ApJ, 606, L155

Borucki W.J., Summers A.L., 1984, Icarus, 58, 121

Boss A.P., 1988, in *Comments on Astrophysics*, 12, 169

Boss A.P., 1997, Science, 276, 1836

Boss A.P., 1998, ApJ, 503, 923

Boss, A., 2006, ApJ 641, 1148.

Bouchy F., Pont F., Santos N.C., Melo C., Mayor M., Queloz D., Udry S., 2004, A&A, 421, L13

Bouchy F. et al., 2005, A&A, 444, 15

Brown T.M., Kotak R., Horner S.D., Kennelly E.J., Korzennik S., Nisenson P., Noyes R.W., 1998, ApJS, 117, 563

Brown T.M., Charbonneau D., Gilliland R.L., Noyes R.W., Burrows A., 2001, ApJ, 552, 699

Brown T.M., 2003, ApJ, 593, L125

Burke C., McCulloghH P., Valenti J., Summers F., Stys J., Johns-Krull C., Janes K., Heasley J., Bissinger R., Foote C., Garcia-Melendo E., Gary B., Howell P., Masi F., Vanmuster T., 2007, BAAS, 39, no 1, 033.02

Burrows A. et al., 1997, ApJ, 491, 856

Burrows A., Sudarsky D., Hubbard W.B., 2003, ApJ, 594, 545

Butler R.P., Vogt S.S., Marcy G.W., Fischer D.A., Wright J.T., Henry G.W., Laughlin G., Lissauer J.J., 2004, ApJ, 617, 580

Cameron A.G.W., 1978, Moon & Planets, 18, 5

Campagnari A., 2005, in "*Accoppiamento a fibra ottica dello spettrografo Echelle di Asiago*", degree thesis at Padova University (private communication)

Chabrier G., Baraffe I., Allard F., Hauschildt P.H., 2000, ApJ, 542, 464

Chabrier G., Chabrier, G., Barman T., Barae I., Allard F., Hauschildt P.H., 2004, ApJ, 603, L53

Chambers J.E., Wetherill G.W., Boss A.P., 1996, Icarus, 119, 261.

Chambers J. E., Wetherill G. W., 1998, Icarus 136, 304

Chambers J.E., Quintana E.V., Duncan M.J., Lissauer J.J., AJ, 123, 2884

Charbonneau D., Brown T.M., Latham D.W., Mayor M., 2000, ApJ, 529, L45

Charbonneau D. et al., 2005, astro-ph/0503457

Chauvin G., Lagrange A.M., Dumas C., Zuckerman B., Mouillet D., Song I., Beuzit J.L., Lowrance P., 2004, A&A, 425, L29

Chauvin G., Lagrange A.M., Dumas C., Zuckerman B., Mouillet D., Song I., Beuzit J.L., Lowrance P., 2005, A&A, accepted (astroph/0504659)

Chen C. H., Kamp I., 2004, ApJ, 602, 985.

Claudi R.U. Cancian M., Barbieri M., Piotto G.P., Scuderi S., 2005, Mem. S.A.It. Suppl., 75, 282

Claudi R.U. et al., 2006, in *Astronomical telescopes and instrumentation*, SPIE conference, Orlando, in press

Cody A.M., Sasselov D.D., 2002, ApJ, 569, 451

Collier C.A., Bouchy F., Hebrard G., Maxted P., Pollaco D., Pont F., Skillen I., Smalley B., Street R., West R., Wilson D., Aigrain S., Christian D., Clarkson W., Enoch B., Evans A., Fitzsimmons A., Gillon M., Haswell C., Hebb L., Hellier C., Hodgkin S., Horne K., Irwin J., Kane S., Keenan F., Loelilet B., Lister T., Mayor M., Moutou C., Norton A., Osborne J., Parley N., Queloz D., Ryans R., Triaud A., Udry S., Wheatley P., 2006, MNRAS, 375, 951

Cox A.N., 2000, in *Allen's Astrophysical Quantities*, 4th edition, Springler

Cumming A., Marcy G.W., Butler R.P., 1999, ApJ, 526, 890

Cuzzi J., Weidenschilling S., 2006, in *Meteorites and the Early Solar System II*, D. S. Lauretta and H. Y. McSween Jr. (eds.), Arizona Univ. Press, Tucson, 353

Dalla Stella A., Marzari F., Barbieri M., Vanzani V., Ortolani S., 2005, 36th LPSC 2005, n. 1253

Deeg H.J., Garrido R., Claret A., 2001, New Astronomy, 6, 51

Delfosse X., Forveille T., Mayor M., Perrier C., Naef D., Queloz D., 1998, A&A, 338, L67

Desidera S., Barbieri M., 2007, A&A 462, 345

Dominik C., Tielens A., 1997, ApJ, 480, 647

Drake A.J., 2003, ApJ, 589, 1020

Duchene G., 1999, A&A, 248, 485

Dullemond C., Dominik C., 2005, A&A, 434, 971

Duncan M.J., Levison H.F., Lee M.H., 1998, AJ, 116, 2067

Duquennoy A., Mayor M., 1991, A&A, 248, 485

Eggenberger A., Udry S., Mayor M., 2003, in *ASP Conf. Ser. 294, Scientific Frontiers in Research on Extrasolar Planets*, ed. D. Denning & S. Seager, 43

Eggleton P., Kiseleva L., 1995, ApJ, 455, 640

ESA, PSS-05-0 Issue 2 (BSSC), 1991

Everhart E., 1985, in *Dynamics of comets: their origin and evolution*, Carusi A., Valsecchi G.B. (eds.), IAU Coll. Proceedings, 83, Reidel, Dordrecht, p.185

Fekel F.C., 1981, ApJ, 246, 879

Fisher D.A., Valenti J.A., 2005, ApJ, 622, 1012

Fischer D., Marcy G., Butler P., Sato B., Vogt S., Robinson S., Laughlin G., Henry G., Driscoll P., Takeda G., Wright J., Johnson J., 2007, arXiv:0704.1191v2

Fridlund M., Henning T., Lacoste H., 2003, in *Towards Other Earths: DARWIN/TPF and the Search for Extrasolar Terrestrial Planets*, ESA SP-539, ed. M. Fridlund, T. Henning, Noordwijk

Ford E.B., Kozinsky B., Rasio F.A., 2000, ApJ, 535, 385

Fortney J.J., Sudarsky D., Hubeny I., Cooper C.S., Hubbard W.B., Burrows A., Lunine J.I., 2003, ApJ, 589, 615

Gandolfi et al., 2005, Mem SAIt Suppl., 9, 180

Gaudi B.S., Seager S., Mallen-Ornelas G., 2005, ApJ, 623, 472

Ghez A.M., Neugebauer G., Matthews K., 1993, AJ, 106, 2005

Giampapa M., Crane E., Hott D., 1995, Icarus, 118, 199

Gillon M., Courbin F., Magain P., Borguet B., 2005, A&A, 442, 731

Goldreich P., Soter S., 1966, Icarus, 5, 375

Goldreich P., Ward W.R., 1973, ApJ, 183, 1051

Goldreich P., Tremaine S., 1980, ApJ, 241, 425

Gould A., Loeb A., 1992, Publ. Astr. Soc. Pac., 108, 465

Granata V., *Software Requirement Document (SRD)*, RATS Automatic Reduction Pipeline, 2007

Gratton R.G. et al., 2001, Experimental Astronomy, 12, 107

Gray D.F., 1997, Nature, 385, 795

Gray D.F., 1998, Nature, 391, 153

Graziani F., Black D. C., 1981, ApJ, 251, 337

Greenberg R., Wacher J.F., Hartmann W.L., Chapman C.R., 1978, Icarus, 35, 1

Greisen E.W., 1983, in *Non-linear coordinate systems in AIPS*, AIPS Memo, 27

Greisen E.W., Calabretta M., 1996, in *Representation of celestial coordinates in FITS* (*preprint*, available in PostScript form at `ftp://fits.cv.nrao.edu/fits/documents/wcs/wcs_all.ps`)

Guillot T., Burrows A., Hubbard W.B., Lunine J.L., Saumon D., 1996, ApJ, 459, L35

Guillot T., 1999, *A comparison of the interiors of Jupiter and Saturn*, Planetary and Space Science 47, 1183

Guillot T., Showman A.P., 2002, A&A, 385, 166

Haisch K.E., Lada E.A., Lada C.J., 2001, ApJ, 553, L153

Halbwachs J.L., Mayor M., Udry S., Arenou F., 2003, A&A, 397, 159

Hanisch R.J., Wells D.C., 1988, in "*World Coordinate System representations within the FITS format*"

Hansen B.M.S., 2002, in ASP Conf. Ser. 263, *Stellar Collisions, Mergers and their Consequences*, ed. M.M. Shara, San Francisco, 22

Harrington J., Deming D., Mattheus K., Richardson L., Rojo P., Wiedemann G., Zeehandelaar D., 2002, BAAS, 34, 30

Harten R.H., Grosbol P., Greisen E.W., Wells D.C., 1988, A&AS 73, 365

Hartmann J.D. et al., 2005, ApJ, 629, 881

Hatzes A.P., Cochran W.D., Endl M., McArthur B., Paulson D.B., Walker G.A.H., Campbell B., Yang S., 2003, ApJ, 599, 1383

Hayashi C., 1981, Prog. Theor. Phys. Suppl., 70, 35

Heggie D.C., 1975, MNRAS, 283, 566

Henry G.W., Marcy G.W., Butler R.P., Vogt S.S., 2000, ApJ, 529, L41

Heppenheimer T., 1978, A&A, 65, 421

Holman M.J., Wiegert P.A., 1999, ApJ, 117, 621

Holsapple K.A., 1994, P&SS, 42, 1067

Horne K. et al., in *First Eddington workshop on Stellar Structure and Habitable Planet Finding*, 2002, ed. F. Favata, I.W. Roxburgh, D. Galad-Enrquez, Noodwijk, 485, 137

Howell S.B., Merline W., 1995, in *New developments in array technology and applications, Davis Philip A.G., Janes K., Upgren A. eds., 371*

Howell S.B., Koehn B., Bowell E.L.G., Hoffman M., 1996, AJ, 112, 1302

Israelian G., 2003, in *Stars as Suns: Activity, Evolution and Planets*, IAUS 219, ed. A.K. Dupree, San Francisco, 57

Jha S., Charbonneau D., Garnavich P.M., Sullivan D.J., Sullivan T., Brown T.M., Tonry J.L., 2000, ApJ, 540, L45

Johns-Krull C., McCullough P., Burke C., Valenti J., Janes K., Bisinger R., Fleenor M., Foote C., Garcia-Melendo., Gary B., Howell P., Mallia F., Masi G., Prato L., Vanmuster T., 2007, BAAS, 39, no 1, 096.05

Kary D.M., Lissauer J.J., Greenzweig Y., 1993, Icarus, 106, 288

Kiseleva L., Aarseth S., Eggleton P., De al Fuente Marcos R., 1996, ASP Conf. S., 90, 433

Kohler R., Leinert C., 1998, A&A, 331, 977

Kokubo E., Ida S., 1998, Icarus, 131, 171

Kokubo E., Ida S., 2000, Icarus, 143, 15

Konacki M., Torres G., Jha S., Sasselov D.D., 2003a, Nature, 421, 507

Konacki M., Torres G., Sasselov D.D., Jha S. 2003c, ApJ, 597, 1076

Konacki M., et al. 2004, ApJ, 609, L37

Konacki M., Torres G., Sasselov D.D., Jha S., 2005, ApJ, 624, 372

Kortenkamp S.J., Wetherill G.W., 2000a, Icarus, 143, 60

Kortenkamp S.J., Wetherill G.W., 2000b, Lunar Plan. Sci. Conf., 31, abstract #1813.

Kortenkamp S.J., Kokubo E., Weidenschilling S.J., 2000, in *Origin of the Earth and Moon*, Canup R.M., Righter K., Eds., Arizona Univ. Press, Tucson), 85

Kortenkamp S., Wetherill G., Inaba S., 2001, Science, 293, 1127

Kortenkamp S.J., Weidenschilling S.J., Marzari F., 2006, 38^{th} DPS Meeting, Pasadena, CA, abstract #63.03

Kovacs G., Bakos G., Torres G., Sozzetti A., Latham D., Noyes R., Butler P., Marcy G., Fischer D., Fernandez J., Esquerdo G., Sasselov D., Stefanik R., Pal A., Lazar J., Sari P., 2007b, ApJ, 670, L41

Kroupa P., 1995, MNRAS, 277, 1491

Kubas D. et al., 2005, A&A, accepted, astro-ph/0502018

Kürster M., et al., 2003, A&A, 403, 1077

Lagrange A.M., Beust H., Udry S., Chauvin G., Mayor M., 2006, A&A, 459, 955

Larson R.B., 2001, in *IAU Symposium* n. 200, H. Zinnecker & R.D. Mathieu, Eds.

Laughlin G., Chambers J.E., 2002, AJ, 124, 592

Lissauer J.J., 1993, ARA&A, 31, 129

Lissauer J., Stewart G., 1993, in *Protostars and Planets III*, Arizona Univ. Press, Tucson, 1061

Lissauer J.J., 2004, in *Extrasolar planets: Today and Tomorrow*, ASP Conf. Series 321, ed. J.P. Beaulieu, A. Lecavelier des Etangs, C. Terquem, San Francisco, 271

Livio M., Pringle J.E., Saer R. A., 1992, MNRAS, 257, 15

Lorimer D.R., 2001, *Living Reviews in Relativity*, 4, 5

Lorimer D.R., Kramer M., 2005, *Handbook of Pulsar Astronomy*, Cambridge

Lubow S.H., Artymowicz P., 2000, in *Protostars and Planets IV*, 731.

Malmberg D., Davies M.B., Chambers J.E., 2007, MNRAS, 377, L1

Mao S., Paczyǹski B., 1991, ApJ, 374, L37

Marcy G.W., Butler R.P., Vogt S.S., Fischer D.A., Lissauer J.J., 1998, ApJ, 505, L14

Marcy G.W., Butler R.P., Fischer D.A., Vogt S.S., 2003, in *Scientific Frontiers in Research on Extrasolar Planets*, ASP Conf. Series 294, ed. D. Deming, S. Seager, San Francisco, 1

Marzari F., Davis D., Vanzani V., 1995, Icarus, 113, 168

Marzari F., Scholl H., 1998, Icarus, 131, 41

Marzari F., Scholl H., 2000, ApJ, 543, 328

Marzari F., Weidenschilling, S.J., 2002, Icarus, 156, 570

Marzari F., Weidenschilling S.J., Barbieri M., Granata V., 2005, ApJ, 618, 502

Marzari F., Thébault P., Scholl H., Kortenkamp S.J., arXiv:0705.3113v1

Marzari F., Barbieri M., 2007, A&A, 467, 347

Mathieu R.D., Ghez A.M., Jensen E.L.N., Simon M., 2000, in *Protostars and Planets IV*, ed. V. Mannings, A. P. Boss, & S. S. Russell (Tucson: Univ. of Arizona Press), 703

Mayer L., Quinn T., Wadsley J., Stadel J., Science, 298, 1756

Mayer L., Quinn T., Wadsley J., Stadel J., 2004, in *AAS/Division of Dynamical Astronomy Meeting*, 35

Mayor M., Queloz D., 1995, Nature, 378, 355

Mazeh T., Shahan J., 1979, A&A, 77, 145

Mazeh T. et al. 2000, ApJ, 532, L55

McArthur B.E., et al., 2004, ApJ, 614, L81

McCabe C., Duchene G., Ghez A.M., 2003, ApJ, 588, L113

McCullogh P., Stys J., Valenti J., Johns-Krull C., Janes K., Heasley J., Bye B., Dodd C., Fleming S., Pinnick A., Bissinger R., Gary B., Howell P., Vanmuster T., 2006, ApJ., 648, 1228

McMillan R.S., Hut P., Makino J., 1991, ApJ, 372, 111

Miller M.C., Hamilton D.P., 2001, ApJ, 550, 863

Mugrauer M., Neuhauser R., 2005, MNRAS 361, L15

Muterspaugh M.W., Lane B.F., Konacki M., Burke B.F., Colavita M.M., Kulkarni S.R., Shao M., 2006, A&A, 446, 723

Nelson A., 2000, ApJ, 537, 65

Neuhäuser R., Mugrauer M., Fukagawa M., Torres G., Schmidt T., 2007, astro-ph/0611427

Noyes R., Bakos G., Torres G., Pal A., Kovacs G., Latham D., Fernandez J., Fischer D., Butler P., Marcy G., Sipocz B., Esquerdo G., Sasselov D., Sato B., Stefanik R., Holman M., Lazar J., Papp I., Sari P., 2007, ApJL (*submitted*)

Öpik E.J., 1951, Proc. Irish Acad., 54, 165

Papaloizou J., Lin D.N.C., 1984, ApJ, 285, 818

Patience J. et al., 2002, ApJ, 581, 654

Pepe F., Mayor M., Galland F., Naef D., Queloz D., Santos N.C., Udry S., Burnet M., 2002, A&A, 388, 6327

Pilat-Lohinger E., Dvorak R., 2002, Celestial Mechanics and Dynamical Astronomy, 82, 143

Pilat-Lohinger E., Funk B., Dvorak R., 2003, A&A, 400, 1085

Phinney E.S., Hansen B.M.S., 1993, in ASP Conf. Ser. 36, *Planets around Pulsars*, ed. J.A. Phillips, S.E. Thorsett & S.R. Kulkarni, San Francisco, 371

Podsiadlowski P., Pringle J.E., Rees M.J., 1991, Nature, 352, 783

Pollack J.B., Hubickyj O., Bodenheimer P., Lissauer J.J., Podolak M., Greenzweig Y., 1996, Icarus, 124, 62

Pollaco D., Skillen I., Collier C.A., Loeillet B., Stempels H., Bouchy F., Gibson N., Hebb L., Hebrard G., Joshi Y., McDonald I., Smalley B., Smith A., Street R., Udry S., West R., Wilson D., Wheatley P., Aigrain S., Benn C., Bruce V., Christian D., Clarkson W., Enoch B., Evans A., Fitzsimmons A., Haswell C., Hellier C., Hickey S., Hodgkin S., Horne K., Hrudkova M., Irwin J., Kane S., Keenan F., Lister T., Maxted P., Mayor M., Moutou C., Norton A., Osborne J., Parley N., Pont F., Queloz D., Ryans R., Simpson E., 2007, MNRAS (*submitted*)

Pont F., Bouchy F., Queloz D., Santos N.C., Melo C., Mayor M., Udry S., 2004, A&A, 426, L15

Pont F., Melo C.H.F., Bouchy F., Udry S., Queloz D., Mayor M., Santos N.C., 2005, A&A, 433, L21

Pont F., 2005, astro-ph/0510846

Pont F. & ISSI Working Group on Transiting Planets, 2006, in *Transiting Extrasolar Planets Workshop*, Afonso C., Weldrake D. & Henning T. eds.

Queloz D., et al, 2000, A&A, 359, L13

Rabl G., Dvorak R., 1988, A&A, 191, 385

Rafikov R., 2003, AJ, 125, 942

Rafikov R., 2004, AJ, 128, 1348

Raghavan D., Henry T.J., Mason B.D., Subasavage J.P., Jao Wei-Chun, Beaulieu T.D., Hambly N.C., 2006, ApJ, 646, 523

Rasio F.A. Ford E.B., 1996, Science, 274, 954

Reipurth B., Zinnecker H., 1993, A&A, 278, 81

Reipurth B., 2000, AJ, 120, 3177

Rhie S.H., 2001, in *Gravitational Lensing: Recent Progress and Future Goals*, ASP Conf. Proc. 237, ed. T.G. Brainerd, C.S. Kochanek, San Francisco, 267

Rice, Armitage, 2003, ApJ, 598, L55

Richardson J., Harrington J., Seager S., Deming D., 2006, ApJ (*submitted*)

Rodriguez L.F., D'Alessio P., Wilner D.J., Ho P.T.P., Torrelles J.M., Curiel S., Gomez Y., Lizano S., Pedlar A., Canto J., Raga A.C., 1998, Nature, 395, 355

Rosenblatt F., 1971, Icarus, 14, 71

Rumbaugh J., Blaha M., Premerlani W., Eddy F., Lorensen W., *Object-oriented modelling and design*, Prentice-Hall, 1991, ISBN 0-13-629841-9

Saar S.H., Hatzes A., Cochran W., Paulson D., 2003, in *The Future of Cool-Star Astrophysics: 12th Cambridge Workshop on Cool Stars, Stellar Systems, and the Sun*, ed. A. Brown, G.M. Harper, T.R. Ayres, Colorado, 694

Safronov V.S., 1969, *Evolution of the Protoplanetary Cloud and Formation of the Earth and the Planets*, Israel program for scientific translation, TT-F 677

Sahu K., Casertano S., Bond H., Valenti J., Smith E., Minniti D., Zoccali M., Livio M., Panagia N., Piskunov N., Brown Th., Brown T., Renzini A., Rich R., Clarkson W., Lubow S., 2006, Nature, 443, 534

Santos N.C., Israelian G., Mayor M., Rebolo R., Udry S., 2002, A&A, 398, 363

Santos N.C., Israelian G., Mayor M., Rebolo R., Udry S., 2003a, A&A, 398, 363

Santos N.C., Israelian G., Mayor M., 2004, A&A, 415, 1153

Sato B. et al., 2005, ApJ, 633, 465

Savonije G.J., Papaloizou J.C.B., Lin D., 1994, MNRAS, 268, 13

Schneider J., Chevreton M., 1990, A&A, 232, 251

Schneider G. et al. 2005, AAS, 205, 1114

Scuderi S. et al., 2006, Mem SAIt Suppl., 9, 478

Seager S., Sasselov D.D., 2000, ApJ, 537, 916

Seager S., Mallen-Ornelas G., 2003, ApJ, 585, 1038

Shobbrook R.R., Herbison-Evans D., Johnston I.D., Lomb N.R., 1969, MNRAS, 145, 131

Showman A., Guillot T., 2002, A&A, 385, 166

Simkin S.M., 1974, A&A, 31, 129

Sirko E., Paczynski B., 2003, ApJ, 592, 1217

Sterzik M.F., Tokovinin A.A., 2002, A&A, 384, 1030

Stetson P.B., 1987, PASP, 99, 191

Stetson P.B., Harris W.E., 1988, AJ, 96, 909

Stetson P.B., 1992, JRASC, 86, 71

Stevens I.R., Rees M.J., Podsiadlowski P., 1992, MNRAS, 254, 19

Stewart G.R., Kaula W.M., 1980, Icarus, 44, 154

Strom S.E., Edwards S., Skrutskie M.F., 1993, in *Protostars and Planets III*, ed. E.H. Levy, J.I. Lunine, Tucson, 837

Strom S.E., Edwards S., Skrutskie M.F., in *Protostars and Planets III*, Arizona Univ. Press, Tucson, 837

Struve O., 1952, *The Observatory*, 72, 199

Thébault P., Brahic, A. 1998, P&SS, 47, 233

Thébault P., Beust H., 2001, A&A, 376, 621

Thébault P., Marzari F., Scholl H., 2002, A&A, 384, 594

Thébault P., Augereau J.C., Beust H., 2003, A&A, 408, 775

Thébault P., A&A, Marzari F., Scholl H., Turrini D., Barbieri M., 427, 1097

Thébault P., Marzari F., Scholl H., 2006, Icarus, 183, 193

Thommes E.W., Lissauer J.J., 2005, in *Astrophysics of Life: Proceedings of the Space Telescope Science Institute Symposium*, STScI symposium series 16, ed. M. Livio, I.N. Reid, W.B. Sparks, Cambridge, 41

Torres G., 2007a, ApJ, 654, 1095

Torres G., Bakos G., Kovacs G., Latham D., Fernandez J., Noyes R., Esquerdo G., Sozzetti A., Fischer D., Butler P., Marcy G., Stefanik R., Sasselov D., Lazar J., Papp I., Sari P., 2007b, ApJ, 666, L121

Udalski A. et al., 2002a, Acta Astronomica, 52, 1

Udalski A. et al., 2002b, Acta Astronomica, 52, 115

Udalski A., Szewczyk O., Zebrun K., Pietrzynski G., Szymanski M., Kubiak M., Soszynski I., Wyrzykowski L., 2002c, Acta Astronomica, 52, 317

Udalski A., 2003, Acta Astronomica, 53, 291

Udalski A., Szymanski M.K., Kubiak M., Pietrzynski G., Soszynski I., Zebrun K., Szewczyk O., Wyrzykowski L., 2004, Acta Astronomica, 54, 313

Udry S., Mayor M., Naef D., Pepe F., Queloz D., Santos N.C., Burnet M., 2002, A&A, 390, 267

Udry S., Mayor M., Santos N.C., 2003, A&A, 407, 369

Van Straten W., Bailes M., Britton M., Kulkarni S.R., Anderson S.B., Manchester R.N., Sarkissian J., 2001, Nature, 412, 158

Vidal-Madjar A., Lecavelier des Etangs A., Desert J.M., Ballester G., Ferlet R., Hebrard G., Mayor M., 2003, Nature, 422, 143

Vidal-Madjar A. et al., 2004, ApJ, 604, L69

Vogt S., Vogt S.S. et al., 1994, in *Proc. SPIE 2198, Instrumentation in Astronomy VIII*, ed. D.L. Crawford, E.R. Craine, 362

Vogt S., Marcy G.W., Butler R.P., Apps K., 2000, ApJ, 536, 902

Ward W.R., 1986, Icaurs, 67, 164

Watson A.J., Donahue T.M., Walker J.C., 1981, Icarus, 48, 150

Weidenschilling S.J., 1977, Astrophysics and Space Science, 51, 153

Weidenschilling S.J., 1980, Icarus, 44, 172

Weidenschilling S.J., Davis D.R., 1985, Icarus, 62, 16

Weidenschilling S.J. Marzari F., 1996, Nature, 384, 619

Weidenschilling S.J., Spaute D., Davis D.R., Marzari F., Ohtsuki K., Icarus 128, 429

Weidenschilling S.J., 2000, SSRv, 92, 295

Wells D.C., Greisen E.W., Harten R.H., 1981, A&AS, 44, 363

Wetherill G.W., Stewart G.R., 1989, Icarus, 77, 330

Wetherill G.W., Inaba S., 2000, SSRv, 92, 311

Whitmire D., Matese J., Criswell L., 1998, Icarus, 132, 196

Winn J., 2007, in *Extreme Solar Systems*, ASP. Conf. Ser., Fischer D., Rasio F., Thorsett S., Wolszczan A. eds

Wolszczan A., Frail D. A., 1992, Nature, 355, 145

Wolszczan A., 1994, Science, 264, 538

Konacki M., Maciejewski A.J., Wolszczan A., 1999, ApJ, 513, 471

Wolszczan A., Homan I.M., Konacki M., Anderson S.B., Xilouris K.M., 2000, ApJ, 540, L41

Konacki M., Wolszczan A., 2003b, ApJ, 591, L147

Wolszczan A., Konacki M., 2005, in *Planet Formation and Detection*, 2005, Winter Conference on Astrophysics, Aspen

Wuchterl G., Guillot T., Lissauer J.J., 2000, in *Protostars and planets IV*, ed. V. Mannings, A.P. Boss, S.S. Russell, Tucson, 1081

Youdin A., Shu F., 2002, ApJ, 580, 494

Youdin A., Chiang E., 2004, ApJ, 601, 1109

Zapatero Osorio M.R., Bejar V.J.S., Martn E.L., Rebolo R., Barrado, Navascues D., Bailer-Jones C.A.L., Mundt R., 2000, Science, 290, 103

Zucher S., Mazeh T., 2002, ApJ, 568, L113

Zucker S., Mazeh T., Santos N.C., Udry S., Mayor M., 2004, A&A, 426, 695